

The use of contrast-enhanced ultrasonography in the evaluation of feline renal perfusion

Emmelie Stock

Supervisors: Prof. Dr. Jimmy Saunders, Prof. Dr. Katrien Vanderperren

A dissertation submitted to Ghent University in partial fulfillment of the requirements for the
degree of Doctor of Veterinary Medicine.

Academic year: 2016-2017

This PhD was supported by a scientific research grant of the Special Research Fund of Ghent University.

The use of contrast-enhanced ultrasonography in the evaluation of feline renal perfusion

Emmelie Stock

Department of Medical Imaging and Small Animal Orthopaedics

Faculty of Veterinary Medicine

Ghent University

No part of this work may be reproduced in any form without permission of the author.

TABLE OF CONTENTS

<i>List of abbreviations</i>	9
CHAPTER I : GENERAL INTRODUCTION	12
1. Introduction	
2. The feline kidney	12
2.1. Anatomy	12
2.2. Physiology	14
2.3. Chronic kidney disease in cats	15
2.4. Hyperthyroidism and kidney disease in cats	18
3. Imaging of the kidney	20
3.1. Radiography	20
3.2. B-mode ultrasound	21
3.3. Renal perfusion imaging	23
3.3.1. Doppler ultrasound	23
3.3.2. Nuclear medicine	23
3.3.3. Computed tomography	25
3.3.4. Magnetic resonance imaging	25
4. Contrast-enhanced ultrasound	26
4.1. General	26
4.1.1. Ultrasound contrast agents	26
4.1.2. Imaging technique	27
4.1.3. Procedure	28
4.1.4. Safety	31
4.2. Contrast-enhanced ultrasound of the kidney	32
4.2.1. Normal kidney	32
4.2.2. Experimental animals	33
4.2.3. Human medicine	34
4.2.4. Veterinary medicine	36
5. Conclusion	38
6. References	39
CHAPTER II: SCIENTIFIC AIMS	52
CHAPTER III: QUANTITATIVE DIFFERENCES BETWEEN THE FIRST AND SECOND INJECTION IN CONTRAST-ENHANCED ULTRASONOGRAPHY OF FELINE KIDNEYS	
1. Abstract	56
2. Introduction	56
3. Materials and methods	57
4. Results	58
5. Discussion	61
6. References	64

CHAPTER IV: REPEATABILITY OF CONTRAST-ENHANCED ULTRASONOGRAPHY OF THE KIDNEYS IN HEALTHY CATS

1. Abstract	68
2. Introduction	68
3. Materials and methods	69
4. Results	71
5. Discussion	75
6. References	78

CHAPTER V: INFLUENCE OF ANESTHESIA AND SEDATION ON QUANTITATIVE CONTRAST-ENHANCED ULTRASONOGRAPHY OF THE HEALTHY FELINE KIDNEY

1. Abstract	82
2. Introduction	82
3. Materials and methods	83
4. Results	85
5. Discussion	87
6. References	90

CHAPTER VI: INFLUENCE OF AGEING ON CONTRAST-ENHANCED ULTRASOUND OF FELINE KIDNEYS IN HEALTHY CATS

1. Abstract	94
2. Introduction	94
3. Materials and methods	95
4. Results	97
5. Discussion	99
6. References	102

CHAPTER VII: EVALUATION OF FELINE RENAL PERFUSION AFTER ANGIOTENSIN-2 INFUSION WITH CONTRAST-ENHANCED ULTRASONOGRAPHY AND SCINTIGRAPHY

1. Abstract	106
2. Introduction	106
3. Materials and methods	108
4. Results	113
5. Discussion	116
6. References	119

CHAPTER VIII: EVALUATION OF RENAL PERFUSION IN HYPERTHYROID CATS BEFORE AND AFTER RADIOIODINE TREATMENT

1. Abstract	124
2. Introduction	124
3. Materials and methods	125
4. Results	128
5. Discussion	131
6. References	134

CHAPTER IX: ASSESSMENT OF RENAL PERFUSION IN CATS WITH CHRONIC KIDNEY DISEASE

1. Abstract	138
2. Introduction	138
3. Materials and methods	139
4. Results	142
5. Discussion	148
6. References	152

CHAPTER X: GENERAL DISCUSSION

1. Introduction	156
2. Quantitative differences between sequential injections	158
3. Repeatability	160
4. Influence of sedation and anesthesia	162
5. Influence of aging in healthy cats	163
6. Perfusion changes induced by angiotensin-II infusion	164
7. Renal perfusion evaluation in treatment of hyperthyroid cats	166
8. Cats with chronic kidney disease	167
9. Future perspectives	169
10. General conclusion	170
11. References	171

<i>Summary</i>	180
----------------	-----

<i>Samenvatting</i>	186
---------------------	-----

<i>Dankwoord</i>	192
------------------	-----

<i>Curriculum vitae</i>	200
-------------------------	-----

<i>Bibliography</i>	202
---------------------	-----

Publications in peer-reviewed scientific journals	202
---	-----

Research communications presented during scientific meetings	204
--	-----

List of abbreviations

^{99m}Tc	99m technetium
AT	Arrival time
AT II	Angiotensin II
AUC	Area-under-the-curve
BI	Baseline intensity
BOLD	Blood oxygen level dependency
CEUS	Contrast-enhanced ultrasound/ultrasonography
CKD	Chronic kidney disease
CNZ	Chronische nierziekte
CT	Computed tomography
CV	Coefficient of variation
DWI	Diffusion-weighted imaging
EDV	End diastolic velocity
EFRP	Effective renal plasma flow
FT	Fall time
GFR	Glomerular filtration rate
IM	Intramuscular
IRIS	International Renal Interest Society
IV	Intravenous
MAG ₃	Mercaptoacetyltriglycine
MI	Mechanical index
MRI	Magnetic resonance imaging
mTT	Mean transit time
OIH	Ortho-iodohippuric acid
Pa	Pascale
PAH	Para-aminohippuric acid
PE	Peak enhancement
PE*	Peak enhancement normalized to interlobar artery
PE _{A0}	Peak enhancement normalized to aorta
PI	Pulsatility index
PSV	Peak systolic velocity
RAAS	Renin-Angiotensin-Aldosterone system
RI	Resistive index
ROI	Region of interest
RT	Rise time
SBP	Systolic blood pressure
sCr	Serum creatinine
SDMA	Symmetric dimethylarginine
St Err	Standard error
T ₄	Thyroxine or tetraiodothyronine
Tc	Technetium
TSH	Thyroid stimulating hormone
TTP	Time-to-peak
UPC	Urine protein:creatinine ratio
US	Ultrasound/ultrasonography
USCA	Ultrasound contrast agent

USG	Urine specific gravity
Win	Wash-in rate
WiAUC	Wash-in area-under-the-curve
WiAUC*	Wash-in area-under-the-curve normalized to interlobar artery
W _{out}	Wash-out
WoAUC	Wash-out area-under-the-curve
WiPI	Wash-in perfusion index
WiR	Wash-in rate
WoR	Wash-out rate

CHAPTER 1

GENERAL INTRODUCTION

Adapted from:

Vanderperren K, Stock E, Pardon B, Saunders J. Contrast-enhanced ultrasound in sheep. *Small Ruminant Research*, 2017. *Accepted*.

1. Introduction

Chronic kidney disease (CKD) is a common disease in cats mainly affecting the elderly population.¹⁻³ Timely diagnosis may greatly improve life quality and expectancy; however diagnosing CKD in early stage of the disease process remains challenging.⁴

Contrast-enhanced ultrasonography (CEUS) is an emerging functional imaging technique. The use of intravenously administered microbubbles allows non-invasive evaluation of tissue perfusion.⁵

This introduction gives an overview of the anatomy and physiology of the feline kidney in normal and diseased states, imaging techniques available to study the kidney, and the current knowledge on the use of CEUS in renal imaging.

2. The feline kidney

2.1. *Anatomy*

The kidneys are paired bean-shaped organs located in the retroperitoneal space attached to the dorsal wall on either side of the spine. They consist of an outer cortex, an inner medulla and central renal pelvis, containing the renal hilus. The renal artery and vein, and ureters find their origin at the renal hilus.⁶ The functional unit of the kidney is the nephron, consisting of the renal corpuscle, where filtration occurs, and segments of the renal tubules, where absorption and secretion occurs, and collecting ducts.⁷ The renal corpuscle is composed of a coil of capillaries, the glomerulus and a surrounding capsule, Bowman's capsule, and is located in the renal cortex. In the cortex, the nephrons join a complex system of tubules and collecting ducts which traverse the kidney and end in the medullary collecting duct (Figure 1).

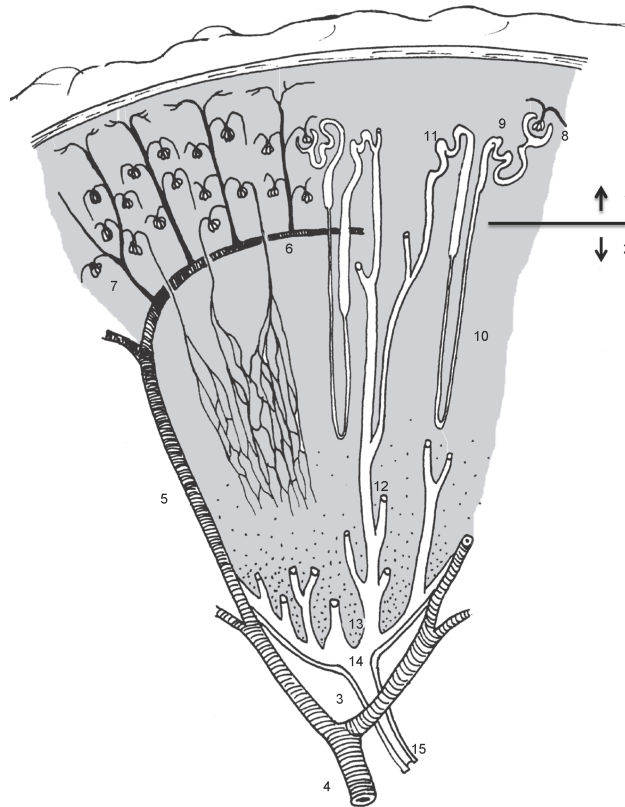


Figure 1. Internal architecture of the kidney. (Image courtesy of Prof. P. Simoens) (1.renal cortex 2.renal medulla 3.renal hilus 4.renal artery 5.interlobar artery 6.arcuate artery 7.interlobular artery 8.glomerulus 9.proximal tubule 10.Henle's loop 11.distal tubule 12.papillary duct 13.renal papilla 14.renal pelvis 15.ureter; the arteries are accompanied by veins)

The vascular system of the kidneys is rather complicated and closely related to the urine conducting system. The renal artery, originating from the abdominal aorta, divides at the hilus into the interlobar arteries, which are continued as the arcuate arteries running at the interface between cortex and medulla. The interlobular arteries originate from the arcuate arteries, radiate in a peripheral direction and mainly supply the renal cortex. The afferent arterioles, supplying the glomerular capillaries, arise from these interlobular arteries. Filtration takes place at the level of the glomerular capillaries, which are drained by the efferent arterioles. A second dense capillary network then arises; this contains the peritubular capillaries, which surround the cortical tubular elements, and the vasa recta, which continue towards the medulla. The term 'renal microvasculature' is used for the combination of the glomerular capillaries and the peritubular capillaries.⁸ Both the peritubular capillaries and vasa recta drain into the venous system. The renal vein finally drains into the caudal vena cava.^{6,9} Anatomical variations in the renal artery and vein are common. The most common anatomy for the renal artery is a single artery with bifurcation just

before the hilus, however a single renal artery without bifurcation is seen in about 4% of the cats. A double renal artery is only reported for the left kidney and occurs in 7% of the feline population. Similarly, a single renal vein with bifurcation is seen most often. Nevertheless, double or even triple renal veins are relatively common for the right kidney (respectively in 37 and 3% of the cats), and occur rarely at the left kidney. A single renal vein without bifurcation occurs in almost 20% of the cats.¹⁰ Figure 2 illustrates the vascular anatomy of the kidney.

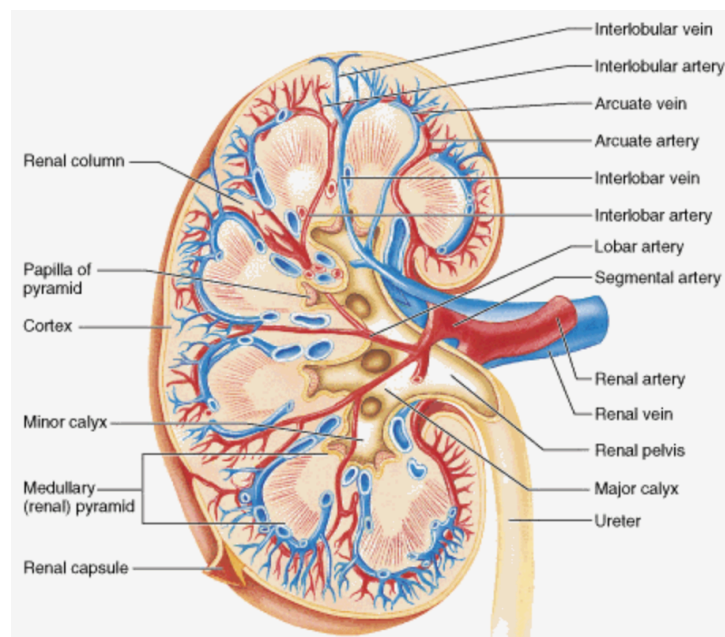


Figure 2. Pattern of distribution of the renal vessels within the kidney. (Copyright 2001 Benjamin Cummings, an imprint of Addison Wesley Longman, Inc)

2.2. Physiology

The kidneys are well-vascularized organs, receiving approximately 25% of the cardiac output.⁹ The high renal blood flow has a dual function: it provides blood for filtration and provides oxygen for the renal parenchyma. Therefore, a decrease in renal blood flow will cause ischemia and consequently alterations in renal function, as well as a decrease in glomerular filtration.^{7,9}

In order to maintain a stable glomerular filtration rate (GFR), the kidneys have the ability to keep a relatively constant renal blood flow despite changes in systemic blood pressure (renal autoregulation system). This is achieved by modulation of the systemic blood pressure and intravascular volume, intrinsic control of renal blood flow and glomerular capillary pressure.

The renin-angiotensin-aldosterone system (RAAS) provides a major contribution in this renal autoregulatory mechanism.^{7, 9} Renin is produced by the kidney in response to a decrease in perfusion pressure, often caused by hypotension. Renin aids in the transformation of angiotensinogen to angiotensin I, which in turn is converted into angiotensin II (AT II).⁷ AT II is the active form and causes vasoconstriction both inducing systemic hypertension and a decrease in renal blood flow. The efferent arteriole is more sensitive to the vasoconstrictive effects of AT II compared to the afferent arteriole.¹¹ Moreover, AT II stimulates the release of aldosterone and vasopressin, which enhances salt and water reabsorption, thereby increasing intravascular volume and thus improving renal perfusion.⁷ AT II also induces the production of vasodilative renal prostaglandins. The afferent arteriole is relatively more sensitive to these prostaglandins.^{7, 11} Both a systemic and a tissue-based or local RAAS system exist. The local RAAS appears to act in an autocrine manner to regulate organ function and is involved in pathological processes as CKD (discussed under 2.3). Two major receptor types for AT II are described. The type 1 receptor predominates and is present extra-renal as well as within the kidney. This receptor type mediates the classic effects of AT II, as described above. The type 2 receptor has a more limited distribution and generates effects opposed to those induced by the type 1 receptor.¹²

The 2 main systems responsible for the intrinsic control of renal blood flow are the myogenic reflex and the tubuloglomerular feedback. The myogenic reflex is responsible for alterations in the diameter of the afferent and efferent arteriole (vasoconstriction and vasodilation) in reaction to a change in intravascular pressure. The tubuloglomerular feedback system changes single nephron GFR based on the contents of the renal tubules.⁷

More than 90% of the renal blood flow supplies the cortex, only a minority supplies the medulla. Therefore, the medulla is already under normal circumstances poorly vascularized and more vulnerable to hypoxia.¹³ The kidneys tend to reduce the cortical blood flow and maintain medullary oxygen supply in cases of hypoxia.¹⁴

2.3. Chronic kidney disease in cats

CKD is a very common disease in cats, with an estimated prevalence of 1.6 to 50%^{1, 2} in the general feline population, increasing up to 30%³ or even 80%² in geriatric cats. It is defined as “structural and/or functional impairment of one or both kidneys that has been present for more than

approximately 3 months".¹⁵ CKD is a multifactorial pathophysiologic process resulting in progressive loss of nephrons in both number and function.¹⁶

Cats present with polyuria, polydipsia, progressive weight loss, muscle wasting, (partial) anorexia, halitosis and/or vomiting. These clinical signs occur when already a substantial decrease in renal function has occurred.⁴ The diagnosis is based on a combination of clinical signs, blood and urine exam. Azotemia, i.e. elevations in serum urea and creatinine concentrations will be noted on blood examination. However, these variables will only rise when approximately 70-75% of renal function is lost.¹⁷ A decreased urine specific gravity (USG) will be present in most cases, since the kidney gradually loses its ability to reabsorb water and thus concentrate the urine.⁴ Nevertheless, cats with CKD may retain their urinary concentrating ability despite being azotemic, in particular in early stages of the disease.¹⁸ A staging system has been proposed by the International Renal Interest Society (IRIS). This system is based on the patient's serum creatinine level, presence of proteinuria, measured by the urinary protein:creatinine ratio (UPC), and blood pressure. The serum creatinine (sCr) concentration determines the IRIS stage. Cats with a sCr < 140 $\mu\text{mol/L}$, which is still within laboratory reference interval, but presenting with another abnormality (e.g. abnormal renal imaging, decreased USG, renal proteinuria) are assigned to stage 1. Stage 2 includes cats with mild renal azotemia (140 – 250 $\mu\text{mol/L}$), stage 3 includes cats with moderate renal azotemia (251 – 440 $\mu\text{mol/L}$) and cats with severe renal azotemia (> 440 $\mu\text{mol/L}$) are assigned to stage 4.¹⁹

GFR measurement is considered the gold standard for evaluation of renal function. It can be calculated from urinary or plasma clearance of a marker. Commonly used markers are iohexol and creatinine.²⁰ Multiple samples must be obtained, making this technique labor-intensive, time-consuming and stressful for the patient, thereby limiting the practical use.²¹ Nevertheless, to overcome these limitations, limited sampling strategies have been described.^{21,22}

Recently, several new renal biomarkers have been investigated aiming to diagnose renal damage in early stage and to localize damage to the compartment of the kidney that is affected. Symmetric dimethylarginine (SDMA) is very recently introduced in veterinary medicine, and there is strong evidence for SDMA as an endogenous surrogate marker for GFR. More importantly, SDMA appears to detect a decrease in GFR prior to serum creatinine.²³ Fibroblast growth factor-23 has been shown to be an early indicator for the development of CKD in cats.²⁴ However, it is not available as a

routine diagnostic test. Cystatin C, a valuable renal marker in human medicine, has been shown to be a poor marker for GFR in cats.²⁵ Similarly, neutrophil gelatinase-associated lipocalin, a promising renal marker in dogs, seems to be of no value in cats.²⁶ Homocysteine, another promising marker in dogs, has not been evaluated in cats yet.²⁷

Urinary biomarkers have also been described, however only few of them have been investigated for the use in the diagnosis of feline CKD. Biomarkers which show potential for the diagnosis of CKD in cats are: albumin, retinol binding protein, Tamm-Horsfall protein, N-acetyl-beta-D-glucosaminidase, cauxin, neutrophil gelatinase-associated lipocalin and transforming growth factor beta-1.²⁶⁻²⁸

The pathophysiology of CKD is complex and still not completely understood. A primary, most often unknown insult initiates renal damage, which is followed by a sequence of functional and structural pathological changes finally resulting in a self-perpetuating process with progressive loss of functional nephrons.¹⁶ Several factors are believed to influence the occurrence of CKD in cats: genetic factors; other disease processes as periodontal disease, urinary tract infections, and infections with feline immunodeficiency virus; exposure to nephrotoxic drugs; episodes of prerenal azotemia or renal ischemia; previous general anesthesia; diet and vaccination.²⁹ In a study investigating iatrogenic unilateral ischemia in cats, acute epithelial necrosis was followed by chronic fibrosis, interstitial inflammation and tubular atrophy.³⁰ Independent of the underlying etiology, the most common histopathologic findings in cats with naturally occurring CKD are nonspecific tubulointerstitial inflammation, interstitial fibrosis and tubular atrophy.^{16, 29}

A reduction in functional nephrons will induce an adaptive response with elevation of the intraglomerular capillary pressure in order to increase the single nephron glomerular filtration rate of the surviving nephrons in an attempt to maintain GFR. However, this results in glomerular hypertrophy and intraglomerular hypertension, leading to cell injury, microaneurisms and finally segmental sclerosis and/or thrombosis of microvasculature.^{15, 16, 29}

Renal fibrosis starts in early stage of the disease process, and is correlated with renal function in both human and cats.³¹⁻³³ Fibrosis is a normal sequel of renal injury, however the process fails to terminate in CKD. The excessive fibrogenic response is characterized by accumulation of extracellular matrix, loss of renal microcirculation, infiltration of inflammatory cells, tubular atrophy, dilation and mineralization.^{16, 29, 31} The exact mechanism remains unclear, however several

profibrogenic factors have been recognized: transforming growth factor- β , AT II, endothelin-1, hyperphosphatemia, hypoxia, proteinuria.^{29,31}

The RAAS system is upregulated in early CKD.^{12,34} Increased levels of plasma renin, aldosterone, angiotensin I and AT II have been described in cats with experimentally induced CKD.³⁵ AT II concentrations are markedly higher in the kidney compared to the systemic circulation.^{12,29} AT II plays an important role in the progression of CKD. Due to its potent vasoconstrictive action it causes glomerular hypertension, decreased renal blood flow and subsequent renal hypoxia. Moreover, it increases the permeability of the glomerular filtration barrier thereby promoting proteinuria and the development of glomerulosclerosis. AT II has direct fibroproliferative actions and stimulates the production of inflammatory and fibrogenic factors as transforming growth factor- β and nuclear factor- $\kappa\beta$. The production of aldosterone by the adrenal gland is also stimulated by AT II. Aldosterone induces oxidative stress, inflammation and renal fibrosis.^{12,29,31}

The combination of these processes results in microvascular rarefaction and dysfunction, which is a central factor in CKD in both human and cats.^{8,30,36}

2.4. Hyperthyroidism and kidney disease in cats

Hyperthyroidism is another common disease in geriatric cats. The prevalence in a population of apparently healthy cats of over 9 years is reported to be 6%.³⁷ Hyperthyroidism is caused by the overproduction of active thyroid hormones by abnormally functioning thyroid tissue. In the majority of the patients a functional adenoma or hyperplasia is diagnosed, whereas thyroid carcinoma is reported only in a minority of the patients.³⁸ The underlying etiology causing hyperthyroidism remains currently unknown. As thyroid hormones have a broad range of effects on several body systems, clinical signs noticed in hyperthyroid cats are variable. The most typical clinical sign is weight loss with preserved to even increased appetite. Other signs include: hyperactivity, aggressiveness, altered behavior, muscle atrophy, polyuria/polydipsia, vomiting, diarrhea, tachypnea, tachycardia, heart murmurs.³⁹ The diagnosis is usually based on compatible clinical signs and increased serum total thyroxine (T4). Scintigraphy, using ^{99m}technetium (^{99m}Tc), is very useful in the work-up of hyperthyroid cats, as it provides both anatomic and functional information.⁴⁰

Treatment options include administration of radioactive iodine (¹³¹I), antithyroid drugs, special diet and surgery (thyroidectomy).³⁹ Radioiodine treatment is a permanent solution, which is safe and easy, non-invasive, and no anesthesia is required. Radioiodine treatment has been reported to be associated with longer survival times when compared to medical treatment.⁴¹ High success rates are reported after radioiodine treatment, ranging from 70% to 95%. However the definition of 'successful outcome' is variable.⁴² In a recent study, 66.5% of the cats had a normal T4 value 6 months after radioiodine treatment, 24% had a T4 value below reference limits and 9.5% had a T4 value above reference intervals.⁴³

The increased levels of thyroid hormones have important systemic and renal consequences. The hyperthyroid state induces decreased peripheral resistance by vasodilation of the peripheral vasculature. In consequence, the effective circulating volume decreases thereby stimulating the RAAS. Activation of the RAAS in its turn leads to sodium retention with resultant increase in blood volume. In addition, an increased heart rate and left ventricular contractility contribute to increased cardiac output. Furthermore, hyperthyroidism induces increased responsiveness, and upregulation of β -adrenergic receptors in cardiac and renal tissue. The combination of these processes leads to increased renal blood flow and consequently increased glomerular filtration rate.⁴⁴⁻⁴⁷

As both hyperthyroidism and CKD are common diseases in elderly cats, it is not surprising that both diseases often occur concurrently. The prevalence of concurrent CKD and hyperthyroidism prior to hyperthyroid treatment is approximately 14%⁴¹, even increasing to up to 40% post-treatment of hyperthyroidism.^{48, 49} Evaluation of renal function in hyperthyroid cats is therefore important. However, this has shown to be problematic. Clinical signs of both diseases overlap. Moreover, predicting post-treatment azotemia based on pre-treatment sCr is not reliable due to the increased GFR, lowering sCr, and decreased sCr due to reduction in muscle mass in hyperthyroid cats.⁴⁴ Proteinuria is often present in hyperthyroid cats but is not correlated with the development of azotemia after treatment.⁴⁴ USG is lower in hyperthyroid cats compared to healthy cats and also often remains lower post-treatment.^{50, 51} Pre-treatment measurement of GFR has some promise in predicting post-treatment azotemia, however great overlap with non-azotemic cats is present.^{44, 45} Whereas fibroblast growth factor 23 has shown promise for early diagnosis of CKD, it is not a good predictor for the development of post treatment azotemia in hyperthyroid cats.⁵² The use of SDMA

in hyperthyroid cats is currently under investigation. In conclusion, an ideal test to predict post-treatment azotemia is not available at this moment.

Treatment of hyperthyroidism results in a normalization in GFR and sCr.^{45, 50, 53, 54} A significant decrease in GFR is noted starting 1 week after ¹³¹I treatment and continuing up to 1 month after treatment.^{45, 54} Nevertheless, sCr may continue to increase up to 6 months after obtaining euthyroid state.⁴⁶

Cats developing post-treatment hypothyroidism have a higher risk of developing CKD and have shorter survival times, whereas no differences have been noticed in survival times between azotemic and non-azotemic cats obtaining euthyroid state after treatment. Iatrogenic hypothyroidism may occur up to 3 to 6 months post treatment.⁴⁹ It is important to differentiate iatrogenic hypothyroidism from euthyroid sick syndrome, in which a low total T4 occurs in patients with non-thyroidal illness as CKD.^{44, 49} The combination of low total T4 level with an elevated thyroid stimulating hormone (TSH) level is consistent with iatrogenic hypothyroidism, while normal TSH levels are present in cats with euthyroid sick syndrome.⁴⁶

3. Imaging of the kidney

3.1. Radiography

Abdominal radiographs are routinely made in veterinary practice. They allow assessment of renal size, shape and opacity. The kidneys are outlined by the retroperitoneal fat. Normal renal size in cats has been reported to be 2.4 to 3.0 times the length of the second lumbar vertebra. Kidneys should have homogeneous soft tissue opacity, however fat deposition in the renal pelvis can lead to a focal radiolucency. In cats with CKD, kidneys tend to be small and irregularly outlined. Abdominal radiographs also allow the assessment of the presence of radiopaque uroliths.⁵⁵

Excretory urography is obtained after intravenous administration of iodinated contrast medium, serial radiographs are made at several time points. Three renal phases are observed: (1) angiogram outlining the renal vasculature, (2) nephrogram with a diffusely increasing opacity of the renal parenchyma, and (3) pyelogram with filling of the renal pelvis and ureter. This technique is most useful for evaluation of the renal pelvis and ureter. Lesions of the renal parenchyma are more

difficult to diagnose. A poor or absent nephrogram will be seen in patients with renal dysfunction. It is important to notice that renal insufficiency is an important risk factor for contrast-medium-induced nephropathy, therefore, excretory urography is contra-indicated in these patients.⁵⁵

3.2. B-mode ultrasound

B-mode ultrasonography (US) is the most frequently used technique to assess the size, shape and internal architecture of kidneys. It has the advantages of being widely available, non-invasive and does not involve the use of ionizing radiation.

Normal kidneys are bean-shaped, smoothly outlined and well defined. Ultrasound textbooks mention kidney measurements in healthy cats ranging between 3.0 and 4.3 cm, however reference intervals vary and kidney dimensions are not widely studied in large populations of healthy cats.⁵⁶⁻

⁵⁹ The normal renal cortex has a uniform echogenicity, which is hypoechoic to the spleen (left kidney) and hypo- or isoechoic to the liver (right kidney). However, hyperechoic renal cortices have been reported in healthy cats, mainly in obese male cats. The renal medulla is hypo- to anechoic. The renal sinus, surrounding the renal pelvis, is hyperechoic due to the presence of fat and dense fibrous connective tissue. The renal pelvis is sometimes visible as a thin anechoic V-shaped line of 1-2mm wide.⁵⁸ A longitudinal and transverse B-mode ultrasound image of the kidney of a healthy cat is presented in Figure 3.

A thin hyperechoic line in the outer medulla, paralleling the corticomedullary junction, has been described in cats. This so called 'medullary rim sign' corresponds to calcium deposits in the lumen of the proximal tubules and has been described in healthy cats in and in conjunction with pathological conditions as acute tubular necrosis, pyogranulomatous vasculitis due to feline infectious peritonitis, chronic interstitial nephritis and renal calcification secondary to hypercalcemia.⁵⁸

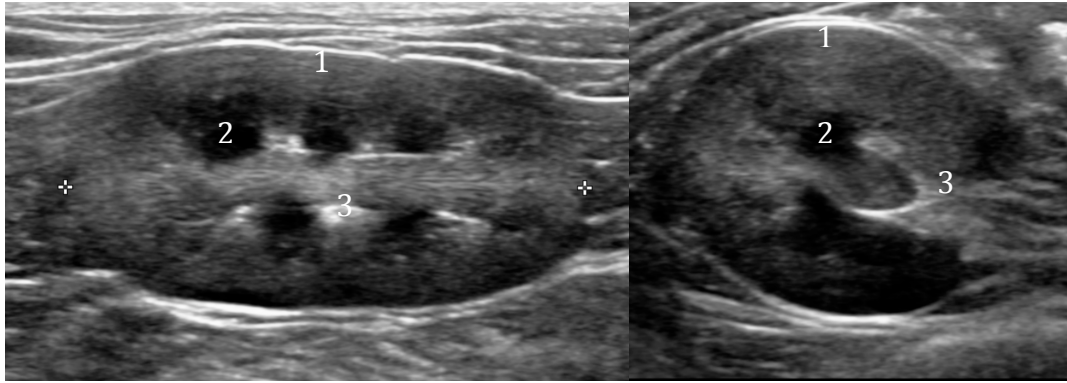


Figure 3. Longitudinal and transverse ultrasound image of a normal kidney, showing the cortex (1), medulla (2) and sinus (3).

Typical findings in cats with CKD are small, irregularly outlined kidneys, a decrease in corticomedullary differentiation and poorly discernible internal architecture.^{58,60} The echogenicity of cortex and medulla may be normal or hyperechoic (Figure 4).^{60,61} Small areas of mineralization may be observed in the renal parenchyma. These are deposits of calcium and phosphate and are associated with feline mineral and bone disease (previously 'renal secondary hyperparathyroidism').^{58,60} Unfortunately, ultrasonographic findings do not always correlate well with renal function.⁵⁸

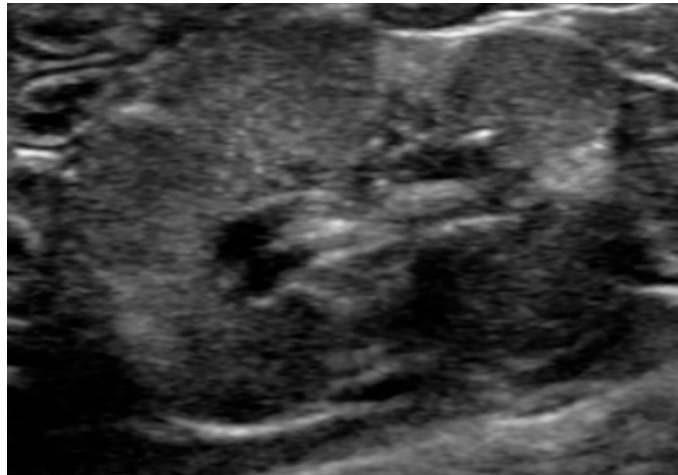


Figure 4. Ultrasound image of a kidney of a cat with CKD. The kidney is decreased in size, irregularly outlined, and several triangular hyperechoic lesions are present in the renal cortex (segmental cortical lesions).

3.3. Renal perfusion imaging

3.3.1. Doppler ultrasound

The use of pulsed-wave Doppler ultrasound of the interlobar or arcuate arteries allows the calculation of 2 indices: the resistive index (RI) and pulsatility index (PI). Both indices provide information about vascular resistance. The resistive index is the most used parameter, and is calculated as the ratio between the peak systolic velocity (PSV) and end-diastolic velocity (EDV); $RI = [PSV - EDV] / PSV$.⁶⁰ The RI mainly depends on the systemic blood pressure, glomerular filtration rate and renal blood flow.⁶² In animals with renal disease, RI increases due to increased vascular resistance, which reduces diastolic blood flow to a greater degree than systolic flow.⁶³⁻⁶⁵ In human medicine, RI is associated with prognosis of CKD⁶⁶, however a similar association has not been described in cats with CKD. Moreover, increase in RI is a non-specific finding as RI is also influenced by heart rate, urinary obstruction and hepatic function.^{60, 67} Additionally, Doppler is limited to evaluation of macroperfusion, as low-velocity flow in smaller vessels cannot be assessed.⁶⁰

3.3.2. Nuclear medicine

Two tracers are available for measurement of effective renal plasma flow (ERPF): ortho-iodohippuric acid (OIH) and mercaptoacetyltriglycine (MAG₃).^{68, 69}

OIH has a similar chemical structure to para-aminohippuric acid (PAH), which is the gold standard for measurement of renal plasma flow. It can be labeled with ¹³¹I or ¹²⁵I. ¹³¹I has the drawbacks that it has a long half-life, resulting in poor image quality and high patient radiation due to β-emission. ¹²⁵I has a shorter half-life and slightly better image quality, but is more expensive.⁶⁹

MAG₃ has biologic similarities to OIH, however the plasma clearance is lower. Still, a very high level of agreement is present between both tracers for humans and dogs.^{69, 70} In cats significant hepatic clearance occurs, which may interfere with calculation of ERPF.⁷¹ MAG₃ can be labeled with ^{99m}Tc, which is easily produced and results in superior image quality.⁶⁹ Sequential images obtained following ^{99m}Tc-MAG₃ administration are shown in Figure 5.

The relative blood flow to the kidneys can be assessed by calculating the K/A ratio and flow index. The K/A ratio is the ratio of the initial rise of the kidney curve to the arterial curve. The flow index is calculated as the area under the aortic curve divided by the area under the kidney curve. The area

under the aortic curve is calculated from initial upslope to point of peak activity, the area under the kidney curve is calculated for the same time interval. Normal values in people and dogs are described, whereas no information in cats is available.⁶⁹

The use of radioactive tracers is limited by equipment availability, cost and radioprotective considerations.

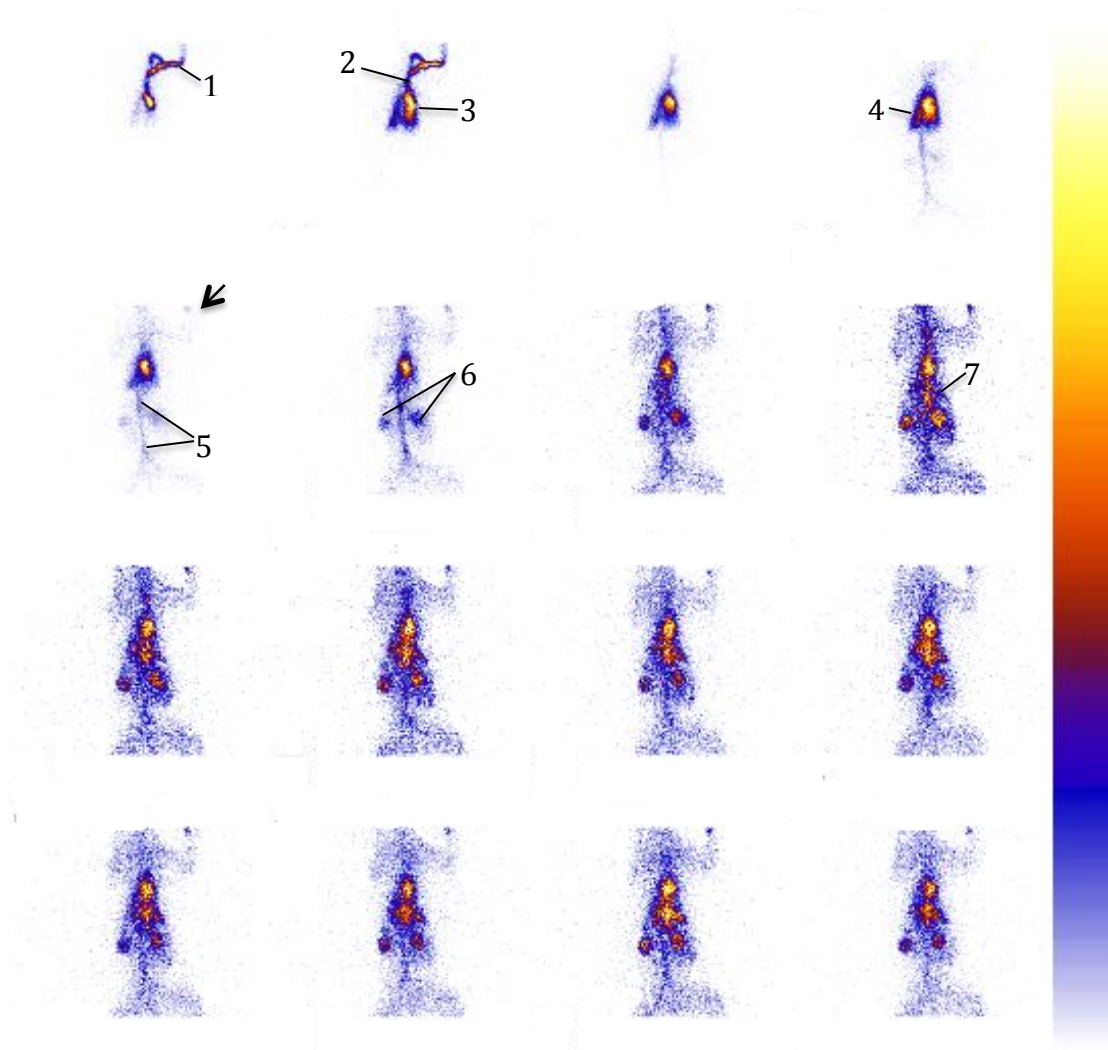


Figure 5. Dorsal images of a healthy cat following injection of $^{99m}\text{Tc-MAG}_3$. The frame rate is 1 frame per second, 2 frames are summed per image starting at 5s after IV injection (upper left) and ending at 36s (bottom right). The following structures are sequentially visualized: cephalic vein (1), cranial vena cava (2), heart (3), pulmonary parenchyma (4), abdominal aorta (5), kidneys (6), liver (7). The arrow indicates the injection site.

3.3.3. Computed tomography

The use of computed tomography (CT) dual-phase angiography has been used in cats to study vascular anatomy.¹⁰ In dogs, contrast-enhanced CT has been proven to be a feasible method to determine GFR.⁷² Only recently, quantitative contrast-enhanced CT has been described to determine the relative renal blood volume in experimental animals and people. Both studies showed a reduction of relative renal blood volume in patients with CKD and a correlation between relative renal blood volume and renal function and capillary rarefaction on histology was present.^{73, 74} Contrast-enhanced CT shows great potential for its use in the diagnosis of CKD, however the risk of radiocontrast nephropathy, need for anesthesia, high cost and involvement of ionizing radiation currently limit broader use. Approaches to reduced contrast toxicity are currently under evaluation: iodine-free contrast agents are being developed and novel renoprotective protocols will be evaluated.^{73, 74}

3.3.4. Magnetic resonance imaging

Renal blood volume and renal blood flow can be measured using high Tesla (≥ 3 Tesla) dynamic magnetic resonance imaging (MRI).⁷⁵

MRI has the advantages of high tissue contrast, multiplanar images capabilities and excellent spatial resolution. Still, small vessels may not be displayed well. Nephrogenic systemic fibrosis has been described in humans following administration of gadolinium-based contrast agents. It is a potentially life-threatening condition, mainly affecting patients with kidney dysfunction.^{76, 77} Therefore, functional unenhanced techniques have recently gained more attention.⁷⁶ Blood oxygen level dependency (BOLD) MRI provides the ability to noninvasively assess the state of intrarenal tissue oxygenation and is based on changing magnetic properties of blood with oxygenation level (hemoglobin is diamagnetic when oxygenated, paramagnetic when deoxygenated).^{76, 78} In diffusion-weighted imaging (DWI) the intrinsic motion of water molecules is used as contrast allowing studying capillary perfusion. Diffusion does not solely depend on capillary perfusion, but also on water diffusion in the extravascular space and tubular flow. A study in human medicine showed that DWI has promise to characterize renal disease.⁷⁹ Other non-contrast based functional

MRI techniques are diffusion tensor imaging and arterial spin labeling.⁷⁶ Research on the use of MRI to assess renal function is still limited and data in veterinary medicine are lacking.

4. Contrast-enhanced ultrasound

4.1. General

The addition of ultrasound contrast agent gives a new dimension to conventional ultrasonography. It allows real-time imaging of organ perfusion, up to a microvascular level.

4.1.1. Ultrasound contrast agents

Ultrasound contrast agent (USCA) consists of very small gas-filled microbubbles that are encapsulated by a shell. The microbubbles are 1-10 μm in diameter, which is in the size range of red blood cells. This allows the microbubbles to freely pass the lung capillaries without causing embolism. Furthermore, they cannot pass the vascular endothelium and thus remain strictly intravascular.^{5,80,81} Some USCAs (Sonazoid, Sonavist, Levovist) have a hepato/spleno-specific affinity in the late parenchymal phase that is probably due to pooling of the microbubbles in the hepatic sinusoids or due to phagocytosis by the Kupffer cells.⁸² The gas content of the microspheres is typically eliminated from the lungs by exhalation after 10 to 15 minutes, whereas shell components are filtered by the kidneys and eliminated by the liver.^{5,83}

There is a variety of commercially available microbubble contrast agents, which differ in their shell and gas core makeup. The selection of the shell material determines how easily the microbubbles are taken up by the immune system. A more hydrophilic material tends to be taken up more easily, which reduces the microbubble residence time in circulation, and thus limiting the imaging time. Secondly, the shell material affects also the microbubble mechanical elasticity: the more elastic the shell, the more acoustic energy it can withstand before bursting. Currently, microbubble shells are composed of albumin, galactose, lipid or polymers.⁸³

The gas core of the microbubbles is the most important part, because this determines the echogenicity. Microbubbles will compress, oscillate and reflect characteristic echoes under influence of an ultrasonic frequency field. Gas cores can be composed of air or heavy gases, e.g.,

perfluorocarbon or nitrogen. Inert gases (perfluor gases) with higher molecular weight provide advantages compared to air, because they dissolve more slowly in the blood, meaning a longer half-life, resulting in a longer lasting signal enhancement.⁵

The most commonly used USCAs in veterinary medicine are perflutren lipid microspheres (Definity; Lantheus, N. Billerica, USA) and phospholipid-stabilised sulfur hexafluoride microspheres (SonoVue; Bracco, Milan, Italy).⁸⁴ Figure 6 illustrates the composition of a typical SonoVue-microbubble.

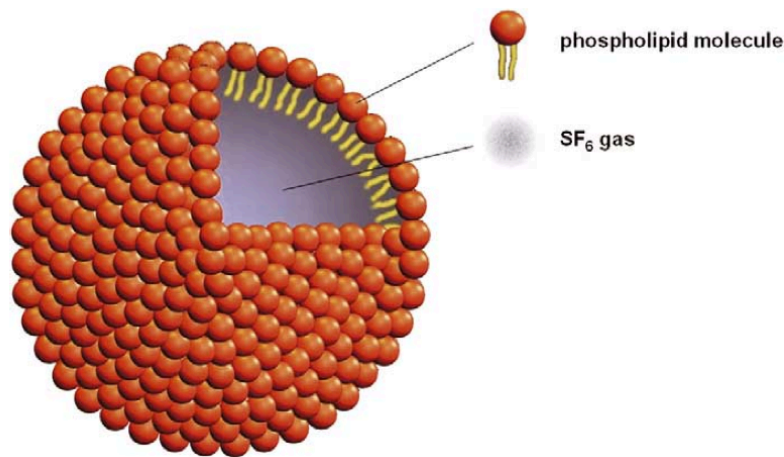


Figure 6. Composition of a microbubble (SonoVue®). (SF₆: sulfurhexafluoride; from: Greis, 2009)⁸¹

4.1.2. Imaging technique

Gas-containing microbubbles, which are mainly administered intravenously in the systemic circulation, have a high degree of echogenicity, because the acoustic difference between gas in the microbubbles and the blood is immense.⁵

Contrast-specific detection modes use the interaction of the microbubbles with ultrasound waves. This interaction depends on microbubble size, shell flexibility, transducer frequency and mechanical index (MI).⁸⁵⁻⁸⁷ The MI is basically conditioned by the acoustic power of the ultrasound beam. The acoustic power, measured in pascals (Pa), represents the energy of the sound beam acting on a target, e.g., a group of red cells or the contrast agent inside the blood stream. At very low acoustic power, oscillation of microbubbles is symmetrical and the change in size is equal in

both compression and expansion.⁸³ At low values of the acoustic power (30-70 kPa), microbubbles start to expand more than compress, and, thus, vibrate in a particular, non-linear manner, producing alternating contractions and relaxations, that way generating harmonic echoes. However, at high acoustic power (up to the order of MPa), microbubbles are 'broken' and an irregular, non-linear signal is generated.⁸³

The goal of contrast-specific imaging techniques is to separate the signal from the microbubbles from the signal caused by the surrounding tissue. Earlier techniques are based on filtering the harmonic signals: the fundamental frequency is blocked and only the harmonics are used to construct the image; complete separation of the signals from tissue and microbubbles is not obtained by this technique. Another approach is to transmit two pulses, with the second being reversed in phase from the first one; this technique is called 'pulse inversion'. Echoes from both pulses are summed to form the image; signals returning from tissues are opposite and cancel each other and are thus not displayed. Signals from non-linearly behaving microbubbles are summed.^{5,83}
⁸⁸ Nowadays, 'pulse-cancellation imaging' or 'Cadence Contrast Pulse Sequence' techniques are used. Multiple pulses of varying phase and amplitude are produced; these pulses are then processed to separate the signals from tissue and microbubbles.^{5,88}

4.1.3. Procedure

Generally, 2 models or types of imaging procedures exist in perfusion imaging using CEUS. The first is low-MI continuous imaging, following bolus kinetics. This is the most commonly used technique and also the technique used in this thesis, therefore, only this type will be further discussed. The second technique is called destructive imaging and follows flash-replenishment kinetics. Microbubbles are administered as a bolus or continuous infusion, at one point, they are destroyed by a high MI burst, then the scanner is switched back to low MI to allow refill of microbubbles in the area of interest.^{80,81}

Microbubbles are injected as a bolus into a peripheral vein using a catheter. The catheter size should be not smaller than 25 Gauge, as smaller sizes cause microbubble destruction. Variations in injection rate will have an impact on later quantification; therefore injection rate should be kept stable.^{89,90} Moreover, microbubbles are very sensitive to overpressure, which causes microbubble

destruction. Overpressure is present when the USCA suspension turns clearer in the syringe upon injection.⁹⁰ The use of a 3-way valve, allowing easy contrast injection immediately followed by saline flush, is recommended.^{90,91} The USCA should be administered as close to the vein as possible to minimize destruction in the non-biological environment and adherence to the tubing.⁹¹ The dosage should be chosen to obtain proper uniform enhancement while avoiding saturation/attenuation (shadowing) in deeper regions due to too high dosage.^{90,92} Dosages of 0.03 – 0.06 mL/kg are described for dogs and cats, mainly depending on the contrast agent used.⁹³⁻⁹⁵

Machine settings have a significant impact on the ultrasound signal. It is therefore of major importance to choose the settings correctly and keep them constant for all studies. As already discussed previously, the MI is the most important parameter. The MI should be kept low to avoid microbubble destruction, however too low MI will lead to a lack of penetration of the ultrasound beam and a weak contrast signal.⁹² The gain is a post-processing parameter, which has no influence on microbubble behavior; still, incorrect gain setting will result in poor image quality. The gain should be optimized to a pre-contrast level just suppressing any signal visible before contrast arrival.⁹² The time gain compensation should be kept constant in a linear matter.⁹⁰ The frame rate should be just high enough to avoid relevant gaps between subsequent imaging planes. High frame rates should be avoided as they increase the possibility of destroying the USCA.⁹² Some inconsistency exists on the optimal focus position. The energy distribution and thus microbubble destruction is highest at the level of the focus, despite this, image quality is optimal at the level of the focus. It is often advised to set the focus just distal to the area of interest.⁹²

One of the major challenges of CEUS is the presence of significant variability, caused by several factors: factors related to the patient, the contrast agent and machine settings. Factors related to machine settings are discussed earlier and can be minimized using proper study design. In contrast, factors related to the patient and contrast agent are more difficult to standardize.

Variations in the patient's blood pressure will have an effect on the mean size and resonance frequency of the microbubbles and hence the resulting signal.⁸⁹ Filtration of the microbubbles by the lungs has several effects on the bubbles: it will reduce the number of bubbles, mainly the number of larger bubbles, moreover diffusion of oxygen into the bubbles might occur. The latter is even more pronounced with animals under general anesthesia.⁹⁰ Thus, passage of the USCA through the lungs will mainly reduce the microbubble concentration and size.⁸⁹ Phagocytosis of

USCA in liver, spleen or lung might occur and thereby alter the concentration of freely flowing microbubbles elsewhere in the body.⁸⁹ The patient's body temperature will also influence microbubble concentration.^{89,90}

As discussed previously, the bubble composition and type will have a large influence on imaging characteristics. Additionally, inconsistencies within the same agent may be present. The way the agent is reconstituted (manual agitation) may induce significant variation in size and concentration.⁸⁹

A linear relationship is present between the USCA concentration and resulting enhancement. Therefore, quantification software can be used to correlate the CEUS signal to the quantity of microbubbles in the tissue of interest, which is a parameter for blood volume. The timing of contrast enhancement is correlated with the blood flow velocity.^{80,81} Typically, software is used to obtain a time-intensity curve from a region of interest (ROI), several parameters can be derived from this curves. After bolus injection, the curve has a characteristic dilution shape. There is a rapid increase in intensity followed by a decrease corresponding to elimination of contrast agent (wash-out). After this first phase, a second, recirculation phase, with a slow decrease is observed.⁵ Several perfusion parameters can be derived from this curve (Figure 7). Parameters related to blood volume are peak enhancement (PE), wash-in area-under-the-curve (WiAUC), wash-out area-under-the-curve (WoAUC) and total area-under-the-curve (AUC). The PE corresponds to the maximum contrast medium signal intensity. The WiAUC is calculated as the sum of all amplitudes inside the range from the beginning of the curve up to the time-to-peak (TTP). Similarly, WoAUC corresponds to the sum of all amplitudes inside the range from the TTP to the end of the descending curve. The other parameters, i.e. rise time (RT), mean transit time (mTT), TTP, wash-in rate (WiR), wash-in perfusion index (WiPI), fall time (FT), wash-out rate (WoR), are related to blood velocity. The WiR and WoR represent the slopes of respectively the ascending and descending curves. The RT corresponds to the time interval between the first arrival of contrast and the time of peak enhancement. The FT, in contrast, is the duration of contrast wash-out. mTT is the mean duration of complete contrast medium perfusion.

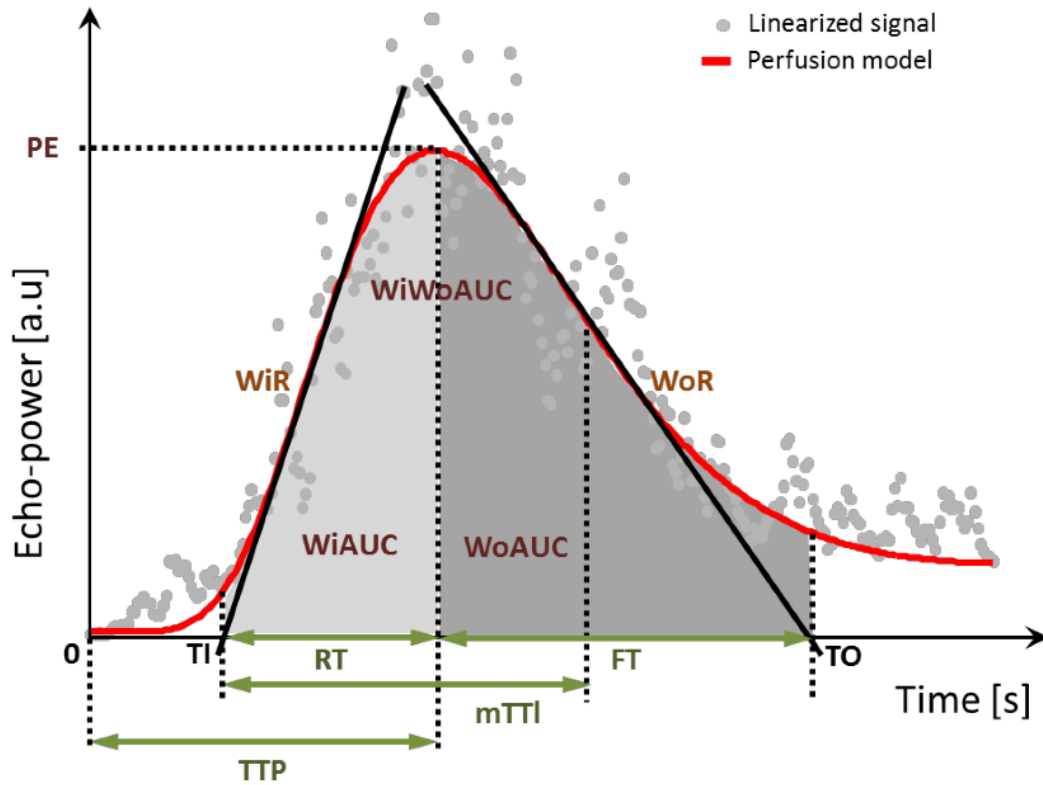


Figure 7. Typical time-intensity curve obtained after bolus injection of USCA, illustration the most important perfusion parameters (TI: point at which the maximum slope tangent intersects with the x-axis, TO: point at which the minimum slope intersects the x-axis; Copyright© 2015 Bracco Suisse SA)

4.1.4. Safety

USCA are very safe. The rate of adverse effects in humans is close to zero (1:10000) and significantly lower to what is reported for iodinated contrast agents (1-10/100).⁹² Adverse events reported in humans are dizziness, warmth, itching and nausea. More serious side effects as dyspnea, hypotension and decreased consciousness are extremely rare.⁹⁶ A large multicenter study including 411 dogs and 77 cats that underwent CEUS, only revealed mild and transient side effects in 0.9% (vomiting, syncope) of the dogs and 0% of the cats.⁸⁴ Moreover, in contrast to iodinated and gadolinium-based contrast agents, USCAs are not nephrotoxic and can safely be used in patients with renal impairment.^{92,97}

In experimental pigs, pseudo-anaphylaxis and secondary pulmonary hypertension in response to USCA administration has been reported.⁹⁸ Pigs developed more severe pulmonary hypertension compared to other species, which was likely attributable to thromboxane A₂ receptor activation and action of intravascular macrophages in pulmonary capillaries.⁹⁹ As in humans, it is possible

that animals with preexisting pulmonary hypertension or impaired cardiopulmonary function might be at increased risk for adverse events, resulting from injection of USCA, CEUS should be performed with caution in those animals.

On a cellular level, USCAs cause a variety of responses, as increased permeability for calcium ions, increased intracellular H₂O₂ levels, and decreased integrity of the cell wall. Rupture of glomerular capillaries, small petechiae on the surface of the kidney and transient hematuria have been noted in small rodents in studies using very high ultrasound frequencies, MI and exposure duration which do not correspond to clinical settings.^{100,101} Cell viability is not affected in a clinical setting.^{102,103}

Beside its extreme safeness, CEUS holds other important advantages for the use in routine clinical practice. It is relatively inexpensive, the equipment is widely available, exams can be performed in intensive care unit, sedation or anesthesia is only required in selected cases, there are no restrictions in performing serial examinations and there is a complete absence of ionizing radiation.

4.2. *Contrast-enhanced ultrasound of the kidney*

4.2.1. Normal kidney

The perfusion pattern obtained after bolus injection of USCA is similar between species.^{94,95,104-108} Typically 3 phases are observed: (1) an arterial phase, with fast enhancement of the renal artery and interlobar arteries, (2) a cortical phase with strong, homogeneous enhancement of the cortex, and (3) late phase, with gradual, less bright and more heterogeneous enhancement of the medulla (Figure 8). At peak medullary enhancement, there is a loss of clear delineation of cortex and medulla.¹⁰⁵ However, the medulla may also remain hypoechoic compared to the cortex.

The lower enhancement of the medulla is related to the vascular anatomy of the kidney. The medulla is significantly less vascularized compared to the cortex. Moreover, the microbubbles pass the cortical vasculature before reaching the medulla; therefore a portion of microbubbles is already destroyed by the time they reach the medulla.^{93,94}

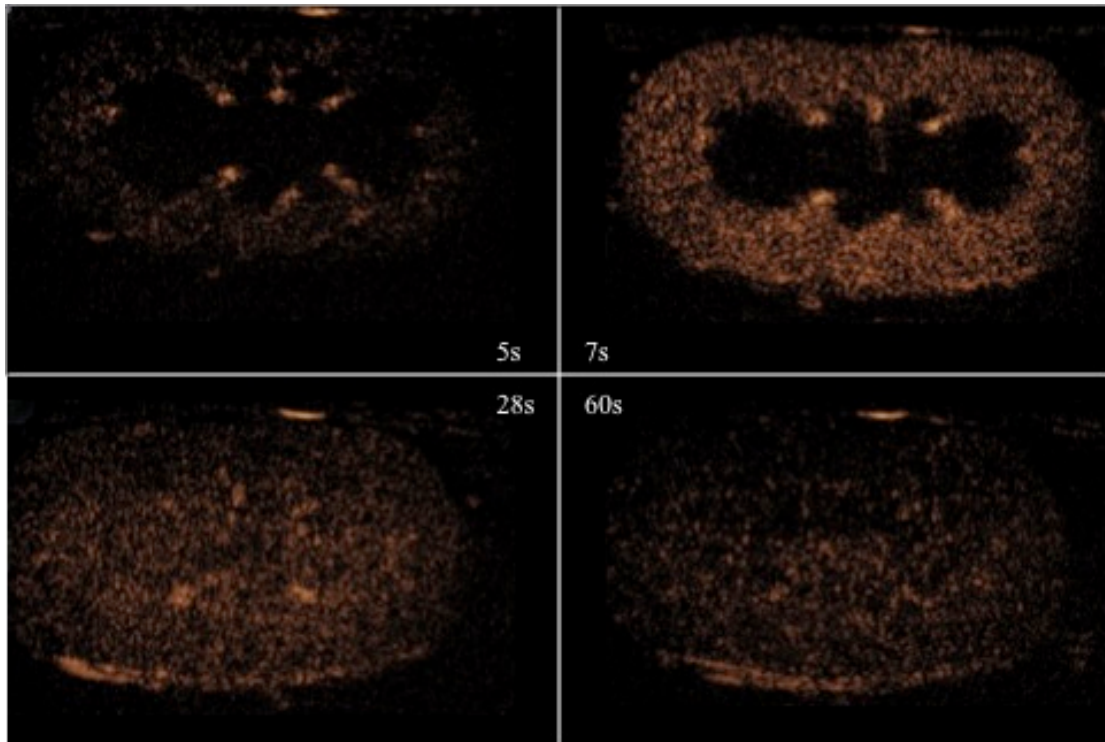


Figure 8. CEUS images of the kidney of a healthy cat showing the typical perfusion pattern. Early enhancement of the interlobar arteries (upper left), followed by bright and homogeneous enhancement of the cortex (upper right), corticomedullary phase (lower left), followed by a gradual wash-out (lower right).

4.2.2. Experimental animals

Contrast-enhanced ultrasound has been used in several studies in experimental animals. Only the studies with clinical relevance for small animal medicine will be briefly discussed.

Multiple studies have used experimental animals as a model for frequently occurring human disorders. Goto-Kakizaki rats are used as an animal model for type 2 diabetes with insulin resistance. Contrast-enhanced ultrasound of the kidneys of these rats revealed flattened time-intensity curves, with a longer time to peak. At 12-weeks age, slope rates of the curves further decreased and area under the curve increased. These changes were caused by insulin resistance-induced renal microvascular injury.¹⁰⁹

Dong et al. (2012) induced ischemic acute renal tubular necrosis in 30 rabbits. Contrast-enhanced ultrasound, blood exam and color Doppler flow imaging were performed 6 and 24 hours afterwards. At 6 hours, only CEUS was capable of detecting changes: area under the curve and time to peak were increased. Abnormalities were noted on blood exam after 24 hours, whereas no

significant changes were noted with color Doppler flow imaging.¹¹⁰

Similarly, in another study, cortical blood volume was significantly decreased in pig kidneys after an episode of systemic hypoxia. This was noted as decreased peak enhancement. Medullary blood volume remained unchanged, however, a decreased blood velocity was present.¹¹¹ This supports the hypothesis that the kidney down regulates the cortical blood flow in an attempt to protect the medulla from hypoxic injury.¹¹¹

4.2.3. Human medicine

Contrast-enhanced ultrasound is well established for its use in the diagnosis of renal pseudolesions (e.g. hypertrophy of Bertin columns and persistence of foetal lobatures). Benign lesions typically show a contrast enhancement that is similar to the surrounding normal parenchyma.¹⁰⁴ One of the most important applications of CEUS in nephrology, is the differentiation and classification of cystic lesions.¹⁰⁴ It is also commonly used in intensive care setting to detect renal parenchymal injuries and active bleeding, which is revealed by microbubble extravasation.^{104, 112} Additionally, CEUS is indicated for early diagnosis of acute pyelonephritis. In this case triangular areas of hypoperfusion are detected.¹¹³ Renal infarcts are typically seen as wedge-shaped regions without contrast-enhancement, whereas renal cortical ischemia is seen as the absence of enhancement of the interlobular vessels in the renal cortex.^{104, 114}

The majority of research in the field of renal CEUS focuses on the study of transplanted kidneys. Several authors have proven that CEUS is very useful for early assessment of graft dysfunction. Rejection is typically diagnosed as a decreased renal enhancement, which occurs even before changes are present on blood work, in estimated glomerular filtration and in resistive index.¹¹⁵⁻¹¹⁹ A simple index, time difference of the rise time between cortex and medulla, is established to predict acute rejection with a high degree of accuracy in a recent study.¹²⁰ Additionally, parametric images have been shown to aid in the diagnosis of acute rejection, as patients with rejection typically have heterogeneous contrast dynamics, in contrast to patients with normal transplant evolution with homogeneous contrast dynamics.¹²¹ Moreover, contrast-enhanced ultrasound is sensitive and specific to diagnose acute cortical necrosis.¹²² In this case a typical 'peripheral rim sign' is seen, representing the unenhanced renal cortex.¹²²

Studies on spontaneous, diffuse renal disorders are less numerous compared to the amount of research performed on transplant rejection. Nevertheless, this research area is of growing interest. Dong et al. (2014) revealed that renal enhancement in patients with early stage CKD is delayed and decreased. This is reflected by increased area under the curve, an increased slope of the ascending curve and decreased peak enhancement.¹⁰⁷ Similarly, in a study with 24 patients with various renal diseases (among them chronic glomerulonephritis, diabetic nephropathy and nephrosclerosis), the renal cortex of these patients was less strongly enhanced.¹²³ Another study on 85 patients with chronic kidney disease revealed similar results. There was a decreased enhancement of both cortex and medulla, which was reflected by significant changes in the calculated perfusion parameters: delayed rising, reduced peak enhancement, and accelerated decay. These changes were more severe with progressive renal dysfunction.¹²⁴ The latter observations are explained by the increased renal resistance noted in patients with chronic kidney disease.¹²⁴ Comparable results are obtained in a cohort of patients with diabetic kidney damage. Both the arrival time and time to peak were prolonged. The intensity increment and peak enhancement were decreased in comparison to healthy subjects. Interestingly, the area-under-the-curve tended to increase in patients with early stage kidney disease, whereas a decrease was observed in the patients with more advanced disease.¹²⁵ This can be explained by a hyperperfusion status in early stage diabetic nephropathy, progressing to a decreased vascularization when the disease progresses.¹²⁵

Moreover, a clear correlation was observed between CEUS parameters and other techniques to evaluate renal perfusion or renal function. Hosotani et al. (2002) revealed a positive correlation between CEUS and well-established techniques to measure renal plasma flow (PAH clearance and tc-99m MAG₃).¹²³ A strong positive correlation between area-under-the-curve and glomerular filtration rate was also determined.¹²⁵

CEUS has been proven to be a sensitive technique to detect changes in renal perfusion in response to various stimuli. These studies are extremely useful in the evaluation of the mechanism of action of several drugs, and in the assessment of pathophysiology of various disease processes. Imamura et al. (2013) found that diclofenac sodium, a non-selective non-steroidal anti-inflammatory drug, but not etodolac, a COX-2 selective non-steroidal anti-inflammatory drug, reduced renal blood flow measured with CEUS.¹²⁶ Valsartan, an angiotensin receptor blocker, could evoke an increased renal cortical perfusion after a single oral administration. This was seen as an increased blood velocity on CEUS, and confirmed with increased clearance of PAH.¹²⁷ In contrast, only a tendency towards

decreased peak enhancement was noted 1 hour after oral administration of captopril, an ACE-inhibitor. However, significant decreased peak enhancement was observed after infusion of angiotensin II in the same study. Contrast-enhanced ultrasonographic parameters correlated well with PAH-clearance.¹²⁸

A new research area on the use of CEUS in the intensive care unit is currently being developed. CEUS would be of great value in the early diagnosis of acute kidney injury and in the assessment of the impact of therapeutic interventions.¹²⁹ First results confirm that CEUS is a feasible and well-tolerated technique in critically-ill patients. A decrease in renal perfusion is observed within 24 hours after cardiac surgery.¹³⁰

4.2.4. Veterinary medicine

Studies on the use of CEUS in canine and feline nephrology are limited.

In cats, all studies have been performed on healthy subjects, describing the normal contrast-enhancement pattern.^{95,105,106}

Slightly more information is available in dogs. Quantitative analysis of normal perfusion in healthy dogs has been performed.^{94,131}

In correspondence with human medicine, CEUS appears to be a useful technique for differentiation between benign and malignant focal renal lesions. Malignant lesions are generally well vascularized. Large tortuous feeding vessels are detected in renal cell carcinomas (Figure 9). Smaller and less obvious arteries are seen in histiocytic sarcomas. Hemangiosarcoma metastases typically appear as non-enhancing nodules.¹³² In another study by the same author, the appearance of consecutive percutaneous renal biopsies was studied with CEUS. Contrast-enhanced ultrasound could detect more renal lesions compared to B-mode ultrasound. The lesions were hyperechoic immediately after biopsy, and turned hypoechoic within 30 minutes, corresponding with a thrombus developing after small hemorrhage. All kidneys regained normal appearance within 3 weeks.¹³³

Contrast-enhanced ultrasound was used to diagnose active renal hemorrhage in a young dog with spontaneous renal bleeding resulting in a hemoperitoneum.¹³⁴

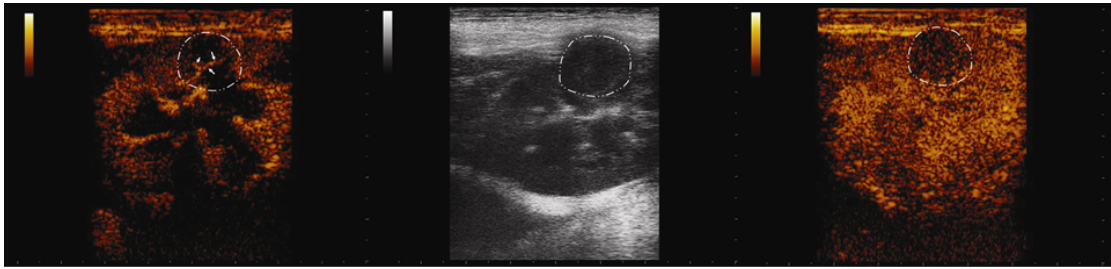


Figure 9. Ultrasound images of a renal carcinoma. B-mode US of a canine kidney with the presence of a hypoechoic mass (dotted line; middle image), CEUS during early phase allowing clear visualization of a tortuous vessel (left), and CEUS during late phase, showing early wash-out in the lesion compared to normal renal parenchyma. (From: Haers et al. 2010)¹³²

The effect of dexmedetomidine, a peripheral α -2 adrenoreceptor atagonist, on several abdominal organs among which the kidney, was examined with CEUS. Arrival time and time to peak were prolonged, whereas peak enhancement and wash-in were decreased in contrast to the control group. These changes could be attenuated with the addition of a peripheral α -2 adrenoreceptor antagonist, MK- 467.¹³⁵

Wei et al. (2001) were the first to prove the capability of CEUS to detect diffuse perfusion changes in canine kidneys. In a study on experimental dogs, renal perfusion was evaluated with CEUS and a digital flow meter, at baseline, after total renal blood flow was reduced with a renal artery stenosis or increased with intravenous infusion of dopamine. An excellent correlation was found between the CEUS parameters and the measurements obtained with the flow probe.¹³⁶ CEUS could also detect small perfusion changes in dogs with iatrogenically induced chronic ischemic renal disease. An ameroid constrictor was placed on the right renal artery of 5 healthy dogs. The earliest significant changes on CEUS occurred 4 weeks after surgery, there was an increase in peak enhancement and a delayed time to peak. The first significant changes on blood exam, elevation of sCr and urea, occurred only after 11 weeks. First changes on color Doppler flow imaging, RI and PSV, occurred even not before 12 weeks (PSV) and 14 weeks (RI).¹⁰⁷

An increase in renal blood volume parameters (PE and AUC) was seen in beagles with iatrogenic hypercortisolism compared to the control group. Glucocorticoids induce a decreased renal vascular resistance, renal vasodilation and plasma volume expansion and thereby increased renal blood flow. This was reliably measured with CEUS.⁹⁵

5. Conclusion

Renal disease is one of the most important health issues in cats. Important structural (decreased capillary number) and functional (vasoconstriction) loss of renal microvasculature occurs in CKD, resulting in decreased renal blood flow. The changes in renal vasculature are key feature in CKD independent of the initiating cause and play an important role in disease progression. Therefore, evaluation of renal perfusion using CEUS may deliver important new insights in the disease and its diagnosis.

6. References

1. Lund EM, Armstrong PJ, Kirk CA, Kolar LM, Klausner JS. Health status and population characteristics of dogs and cats examined at private veterinary practices in the United States. *Journal of the American Veterinary Medical Association*. 1999;214: 1336-1341.
2. Marino CL, Lascelles BDX, Vaden SL, Gruen ME, Marks SL. Prevalence and classification of chronic kidney disease in cats randomly selected from four age groups and in cats recruited for degenerative joint disease studies. *Journal of Feline Medicine and Surgery*. 2014;16: 465-472.
3. Lulich JP, Osborne CA, O'Brien TD, Polzin DJ. Feline Renal-Failure - Questions, Answers, Questions. *Compendium on Continuing Education for the Practicing Veterinarian*. 1992;14: 127-152.
4. Polzin JP. Chronic kidney disease. In: Bartges J, Polzin JP (eds): *Nephrology and Urology of Small Animals*. Chichester: Wiley-Blackwell, 2011;433-471.
5. Haers H, Saunders JH. Review of clinical characteristics and applications of contrast-enhanced ultrasonography in dogs. *Journal of the American Veterinary Medical Association*. 2009;234: 460-470.
6. Budras KD, McCarthy PH, Fricke W, Richter R. *Anatomy of the dog*. Hannover, Germany: Schlütersche, 2007.
7. Klein BG. *Cunningham's Textbook of Veterinary Physiology*. In: Verlander JW (ed): *Renal physiology*. Missouri, USA: Saunders, 2012.
8. Jen KY, Haragsim L, Laszik ZG. Kidney microvasculature in health and disease. *Cardiorenal Syndromes in Critical Care*. 2011;169: 51-72.
9. Regan MC, Young LS, Geraghty J, Fitzpatrick JM. Regional renal blood flow in normal and disease states. *Urological Research*. 1995;23: 1-10.
10. Caceres AV, Zwingenberger AL, Aronson LR, Mai W. Characterization of normal feline renal vascular anatomy with dual-phase CT angiography. *Veterinary Radiology & Ultrasound*. 2008;49: 350-356.
11. Itkin RJ. Effects of the renin-angiotensin system on the kidneys. *Compendium on Continuing Education for the Practicing Veterinarian*. 1994;16: 753-763.
12. Siragy HM, Carey RM. Role of the Intrarenal Renin-Angiotensin-Aldosterone System in Chronic Kidney Disease. *American Journal of Nephrology*. 2010;31: 541-550.
13. Evans RG, Eppel GA, Anderson WP, Denton KM. Mechanisms underlying the differential control of blood flow in the renal medulla and cortex. *Journal of Hypertension*. 2004;22: 1439-1451.

14. Brezis M, Rosen S. Mechanisms of Disease - Hypoxia of the Renal Medulla - Its Implications for Disease. *New England Journal of Medicine*. 1995;332: 647-655.
15. Polzin DJ. Chronic kidney disease. In: Ettinger SJ, Feldman EC (eds): *Textbook of veterinary internal medicine: diseases of the dog and the cat* Missouri: Saunders Elsevier, 2010;1990 - 2020.
16. Brown CA, Elliott J, Schmiedt CW, Brown SA. Chronic Kidney Disease in Aged Cats: Clinical Features, Morphology, and Proposed Pathogeneses. *Veterinary Pathology*. 2016;53: 309-326.
17. Finco DR, Brown SA, Vaden SL, Ferguson DC. Relationship between plasma creatinine concentration and glomerular filtration rate in dogs. *Journal of Veterinary Pharmacology and Therapeutics*. 1995;18: 418-421.
18. Paepe D, Daminet S. Feline CKD: Diagnosis, staging and screening - what is recommended? *Journal of Feline Medicine and Surgery*. 2013;15 Suppl 1: 15-27.
19. IRIS kidney. 2017 [cited; Available from: <http://www.iris-kidney.com>]
20. Braun JP, Lefebvre HP. Kidney function and damage. In: Kaneko JJH, Harvey JW, Bruss ML (eds): *Clinical biochemistry of domestic animals*. London: Elsevier, 2008;485-582.
21. Finch NC, Heiene R, Elliott J, Syme HM, Peters AM. A single sample method for estimating glomerular filtration rate in cats. *Journal of Veterinary Internal Medicine*. 2013;27: 782-790.
22. Paepe D, Lefebvre HP, Concordet D, van Hoek I, Croubels S, Daminet S. Simplified methods for estimating glomerular filtration rate in cats and for detection of cats with low or borderline glomerular filtration rate. *Journal of Feline Medicine and Surgery*. 2015;17: 889-900.
23. Hall JA, Yerramilli M, Obare E, Yerramilli M, Jewell DE. Comparison of Serum Concentrations of Symmetric Dimethylarginine and Creatinine as Kidney Function Biomarkers in Cats with Chronic Kidney Disease. *Journal of Veterinary Internal Medicine*. 2014;28: 1676-1683.
24. Finch NC, Geddes RF, Syme HM, Elliott J. Fibroblast growth factor 23 (FGF-23) concentrations in cats with early nonazotemic chronic kidney disease (CKD) and in healthy geriatric cats. *Journal of Veterinary Internal Medicine*. 2013;27: 227-233.
25. Ghys LF, Paepe D, Lefebvre HP, Reynolds BS, Croubels S, Meyer E, et al. Evaluation of Cystatin C for the Detection of Chronic Kidney Disease in Cats. *Journal of Veterinary Internal Medicine*. 2016;30: 1074-1082.
26. Wang IC, Hsu WL, Wu PH, Yin HY, Tsai HJ, Lee YJ. Neutrophil Gelatinase-Associated Lipocalin in Cats with Naturally Occurring Chronic Kidney Disease. *Journal of Veterinary Internal Medicine*. 2017;31: 102-108.

27. Hokamp JA, Nabity MB. Renal biomarkers in domestic species. *Vet Clin Pathol.* 2016;45: 28-56.
28. Habenicht LM, Webb TL, Clauss LA, Dow SW, Quimby JM. Urinary cytokine levels in apparently healthy cats and cats with chronic kidney disease. *Journal of Feline Medicine and Surgery.* 2013;15: 99-104.
29. Jepson RE. Current Understanding of the Pathogenesis of Progressive Chronic Kidney Disease in Cats. *Veterinary Clinics of North America: Small Animal Practice.* 2016;46: 1015-1048.
30. Schmiedt CW, Brainard BM, Hinson W, Brown SA, Brown CA. Unilateral Renal Ischemia as a Model of Acute Kidney Injury and Renal Fibrosis in Cats. *Veterinary Pathology.* 2016;53: 87-101.
31. Lawson J, Elliott J, Wheeler-Jones C, Syme H, Jepson R. Renal fibrosis in feline chronic kidney disease: known mediators and mechanisms of injury. *Veterinary Journal.* 2015;203: 18-26.
32. Yabuki A, Mitani S, Fujiki M, Misumi K, Endo Y, Miyoshi N, et al. Comparative study of chronic kidney disease in dogs and cats: Induction of myofibroblasts. *Research in Veterinary Science.* 2010;88: 294-299.
33. Chakrabarti S, Syme HM, Brown CA, Elliott J. Histomorphometry of Feline Chronic Kidney Disease and Correlation With Markers of Renal Dysfunction. *Veterinary Pathology.* 2013;50: 147-155.
34. Mitani S, Yabuki A, Sawa M, Chang HS, Yamato O. Intrarenal distributions and changes of Angiotensin-converting enzyme and Angiotensin-converting enzyme 2 in feline and canine chronic kidney disease. *Journal of Veterinary Medical Science.* 2014;76: 45-50.
35. Watanabe T, Mishina M. Effects of benazepril hydrochloride in cats with experimentally induced or spontaneously occurring chronic renal failure. *Journal of Veterinary Medical Science.* 2007;69: 1015-1023.
36. Ballermann BJ, Obeidat M. Tipping the balance from angiogenesis to fibrosis in CKD. *Kidney International Supplements.* 2014;4: 45-52.
37. Wakeling J, Elliott J, Syme H. Evaluation of predictors for the diagnosis of hyperthyroidism in cats. *Journal of Veterinary Internal Medicine.* 2011;25: 1057-1065.
38. Naan EC, Kirpensteijn J, Kooistra HS, Peeters ME. Results of thyroidectomy in 101 cats with hyperthyroidism. *Veterinary Surgery.* 2006;35: 287-293.
39. Scott-Moncrieff JC. Feline hyperthyroidism. In: Feldman EC, Nelson RW, Reusch C, Scott-Moncrieff JC, Behrend E (eds): *Canine and feline endocrinology.* St Louis, Missouri, USA: Saunders Elsevier, 2015;136-195.

40. Daniel GB, Neelis DA. Thyroid scintigraphy in veterinary medicine. *Seminars in Nuclear Medicine*. 2014;44: 24-34.
41. Milner RJ, Channell CD, Levy JK, Schaer M. Survival times for cats with hyperthyroidism treated with iodine 131, methimazole, or both: 167 cases (1996-2003). *Journal of the American Veterinary Medical Association*. 2006;228: 559-563.
42. Volckaert V, Vandermeulen E, Daminet S, Saunders JH, Peremans K. Hyperthyroidism in cats Part II: scintigraphic diagnosis and radioiodine treatment. *Vlaams Diergeneeskundig Tijdschrift*. 2016;85: 265-273.
43. Volckaert V, Vandermeulen E, Dobbeleir A, Duchateau L, Saunders JH, Peremans K. Effect of thyroid volume on radioiodine therapy outcome in hyperthyroid cats. *Journal of Feline Medicine and Surgery*. 2016;18: 144-149.
44. van Hoek I, Daminet S. Interactions between thyroid and kidney function in pathological conditions of these organ systems: A review. *General and Comparative Endocrinology*. 2009;160: 205-215.
45. van Hoek I, Lefebvre HP, Peremans K, Meyer E, Croubels S, Vandermeulen E, et al. Short- and long-term follow-up of glomerular and tubular renal markers of kidney function in hyperthyroid cats after treatment with radioiodine. *Domestic Animal Endocrinology*. 2009;36: 45-56.
46. Vaske HH, Schermerhorn T, Grauer GF. Effects of feline hyperthyroidism on kidney function: a review. *Journal of Feline Medicine and Surgery*. 2016;18: 55-59.
47. Langston CE, Reine NJ. Hyperthyroidism and the kidney. *Clinical Techniques in Small Animal Practice*. 2006;21: 17-21.
48. Slater MR, Geller S, Rogers K. Long-term health and predictors of survival for hyperthyroid cats treated with iodine 131. *Journal of Veterinary Internal Medicine*. 2001;15: 47-51.
49. Williams TL, Elliott J, Syme HM. Association of iatrogenic hypothyroidism with azotemia and reduced survival time in cats treated for hyperthyroidism. *Journal of Veterinary Internal Medicine*. 2010;24: 1086-1092.
50. Becker TJ, Graves TK, Kruger JM, Braselton WE, Nachreiner RF. Effects of methimazole on renal function in cats with hyperthyroidism. *Journal of the American Animal Hospital Association*. 2000;36: 215-223.

51. Graves TK, Olivier NB, Nachreiner RF, Kruger JM, Walshaw R, Stickle RL. Changes in renal function associated with treatment of hyperthyroidism in cats. *American Journal of Veterinary Research*. 1994;55: 1745-1749.
52. Williams TL, Elliott J, Syme HM. Calcium and phosphate homeostasis in hyperthyroid cats: associations with development of azotaemia and survival time. *Journal of Small Animal Practice*. 2012;53: 561-571.
53. Adams WH, Daniel GB, Legendre AM, Gompf RE, Grove CA. Changes in renal function in cats following treatment of hyperthyroidism using ¹³¹I. *Veterinary Radiology & Ultrasound*. 1997;38: 231-238.
54. Boag AK, Neiger R, Slater L, Stevens KB, Haller M, Church DB. Changes in the glomerular filtration rate of 27 cats with hyperthyroidism after treatment with radioactive iodine. *Veterinary Record*. 2007;161: 711-715.
55. Seiler G. The kidneys and ureters. In: Thrall DE (ed): *Textbook of veterinary diagnostic radiology*. St Louis, Missouri, USA: Saunders Elsevier, 2013;705-725.
56. Walter PA, Feeney DA, Johnston GR, Fletcher TF. Feline renal ultrasonography: quantitative analyses of imaged anatomy. *American Journal of Veterinary Research*. 1987;48: 596-599.
57. Debruyne K, Paepe D, Daminet S, Combes A, Duchateau L, Peremans K, et al. Renal dimensions at ultrasonography in healthy Ragdoll cats with normal kidney morphology: correlation with age, gender and bodyweight. *Journal of Feline Medicine and Surgery*. 2013;15: 1046-1051.
58. Debruyne K, Haers H, Combes A, Paepe D, Peremans K, Vanderperren K, et al. Ultrasonography of the feline kidney. Technique, anatomy and changes associated with disease. *Journal of Feline Medicine and Surgery*. 2012;14: 794-803.
59. Paepe D. Screening for early feline chronic kidney disease. Limitations of currently available tests and possible solutions. Ghent University, Belgium, 2014.
60. d'Anjou MA, Penninck D. Kidneys and ureters. In: Penninck D, M.A. dA (eds): *Atlas of small animal ultrasonography*. Oxford: Wiley Blackwell, 2015;331-362.
61. Drost WT, Henry GA, Meinkoth JH, Woods JP, Lehenbauer TW. Quantification of hepatic and renal cortical echogenicity in clinically normal cats. *American Journal of Veterinary Research*. 2000;61: 1016-1020.
62. Novellas R, Espada Y, De Gopegui RR. Doppler ultrasonographic estimation of renal and ocular resistive and pulsatility indices in normal dogs and cats. *Veterinary Radiology & Ultrasound*. 2007;48: 69-73.

63. Novellas R, Ruiz de Gopegui R, Espada Y. Assessment of renal vascular resistance and blood pressure in dogs and cats with renal disease. *Veterinary Record*. 2010;166: 618-623.
64. Tipisca V, Murino C, Cortese L, Mennonna G, Auletta L, Vulpe V, et al. Resistive index for kidney evaluation in normal and diseased cats. *Journal of Feline Medicine and Surgery*. 2015;18: 471-475.
65. Rivers BJ, Walter PA, Polzin DJ, King VL. Duplex Doppler estimation of intrarenal Pourcelot resistive index in dogs and cats with renal disease. *Journal of Veterinary Internal Medicine*. 1997;11: 250-260.
66. Sugiura T, Wada A. Resistive index predicts renal prognosis in chronic kidney disease. *Nephrology Dialysis Transplantation*. 2009;24: 2780-2785.
67. Novellas R, de Gopegui RR, Espada Y. Increased renal vascular resistance in dogs with hepatic disease. *Veterinary Journal*. 2008;178: 257-262.
68. Vandermeulen E, De Sadeleer C, Dobbeleir A, Ham HR, Vermeire ST, van Bree H, et al. Nuclear medicine: investigation of renal function in small animal medicine. *Vlaams Diergeneeskundig Tijdschrift*. 2011;80: 105-114.
69. Daniel GB, Mitchell SK, Mawby D, Sackman JE, Schmidt D. Renal nuclear medicine: A review. *Veterinary Radiology & Ultrasound*. 1999;40: 572-587.
70. Lora-Michiels M, Anzola K, Amaya G, Solano M. Quantitative and qualitative scintigraphic measurement of renal function in dogs exposed to toxic doses of gentamicin. *Veterinary Radiology & Ultrasound*. 2001;42: 553-561.
71. Drost WT, McLoughlin MA, Mattoon JS, Lerche P, Samii VF, DiBartola SP, et al. Determination of extrarenal plasma clearance and hepatic uptake of technetium-99m-mercaptoacetyltriglycine in cats. *American Journal of Veterinary Research*. 2003;64: 1076-1080.
72. O'Dell-Anderson KJ, Twardock R, Grimm JB, Grimm KA, Constable PD. Determination of glomerular filtration rate in dogs using contrast-enhanced computed tomography. *Veterinary Radiology & Ultrasound*. 2006;47: 127-135.
73. von Stillfried S, Apitzsch JC, Ehling J, Penzkofer T, Mahnken AH, Knuchel R, et al. Contrast-enhanced CT imaging in patients with chronic kidney disease. *Angiogenesis*. 2016;19: 525-535.
74. Ehling J, Babickova J, Gremse F, Klinkhammer BM, Baetke S, Knuechel R, et al. Quantitative Micro-Computed Tomography Imaging of Vascular Dysfunction in Progressive Kidney Diseases. *Journal of the American Society of Nephrology*. 2016;27: 520-532.

75. Grenier N, Quaia E, Prasad PV, Juillard L. Radiology imaging of renal structure and function by computed tomography, magnetic resonance imaging, and ultrasound. *Seminars in Nuclear Medicine*. 2011;41: 45-60.
76. Herget-Rosenthal S. Imaging Techniques in the Management of Chronic Kidney Disease: Current Developments and Future Perspectives. *Seminars in Nephrology*. 2011;31: 283-290.
77. Durand E, Chaumet-Riffaud P, Grenier N. Functional renal imaging: new trends in radiology and nuclear medicine. *Seminars in Nuclear Medicine*. 2011;41: 61-72.
78. Artunc F, Rossi C, Boss A. MRI to assess renal structure and function. *Current Opinion in Nephrology and Hypertension*. 2011;20: 669-675.
79. Notohamiprodo M, Reiser MF, Sourbron SP. Diffusion and perfusion of the kidney. *European Journal of Radiology*. 2010;76: 337-347.
80. Cosgrove D, Lassau N. Imaging of perfusion using ultrasound. *European Journal of Nuclear Medicine and Molecular Imaging*. 2010;37: S65-S85.
81. Greis C. Ultrasound contrast agents as markers of vascularity and microcirculation. *Clinical Hemorheology and Microcirculation*. 2009;43: 1-9.
82. Forsberg F, Goldberg BB, Liu JB, Merton DA, Rawool NM, Shi WT. Tissue-specific US contrast agent for evaluation of hepatic and splenic parenchyma. *Radiology*. 1999;210: 125-132.
83. Correas JM, Bridal L, Lesavre A, Mejean A, Claudon M, Helenon O. Ultrasound contrast agents: properties, principles of action, tolerance, and artifacts. *European Radiology*. 2001;11: 1316-1328.
84. Seiler GS, Brown JC, Reetz JA, Taeymans O, Bucknoff M, Rossi F, et al. Safety of contrast-enhanced ultrasonography in dogs and cats: 488 cases (2002-2011). *Journal of the American Veterinary Medical Association*. 2013;242: 1255-1259.
85. Greis C. Technology overview: SonoVue (Bracco, Milan). *European Radiology*. 2004;14 Suppl 8: P11-15.
86. Emmer M, van Wamel A, Goertz DE, de Jong N. The onset of microbubble vibration. *Ultrasound in Medicine and Biology*. 2007;33: 941-949.
87. Uhlendorf V, Scholle FD, Reinhardt M. Acoustic behaviour of current ultrasound contrast agents. *Ultrasonics*. 2000;38: 81-86.
88. Kollmann C. New sonographic techniques for harmonic imaging-underlying physical principles. *European Journal of Radiology*. 2007;64: 164-172.

89. Tang MX, Mulvana H, Gauthier T, Lim AKP, Cosgrove DO, Eckersley RJ, et al. Quantitative contrast-enhanced ultrasound imaging: a review of sources of variability. *Interface Focus*. 2011;1: 520-539.
90. Hyvelin JM, Tardy I, Arbogast C, Costa M, Emmel P, Helbert A, et al. Use of Ultrasound Contrast Agent Microbubbles in Preclinical Research Recommendations for Small Animal Imaging. *Investigative Radiology*. 2013;48: 570-583.
91. O'Brien R, Seiler G. Clinical applications of contrast ultrasound In: Penninck D, d'Anjou MA (eds): *Atlas of small animal ultrasonography* Oxford, UK: John Wiley and Sons, 2015;481 - 493.
92. Dietrich CF, Ignee A, Hocke M, Schreiber-Dietrich D, Greis C. Pitfalls and Artefacts using Contrast Enhanced Ultrasound. *Zeitschrift Fur Gastroenterologie*. 2011;49: 350-356.
93. Haers H, Daminet S, Smets PMY, Duchateau L, Aresu L, Saunders JH. Use of quantitative contrast-enhanced ultrasonography to detect diffuse renal changes in Beagles with iatrogenic hypercortisolism. *American Journal of Veterinary Research*. 2013;74: 70-77.
94. Waller KR, O'Brien RT, Zagzebski JA. Quantitative contrast ultrasound analysis of renal perfusion in normal dogs. *Veterinary Radiology & Ultrasound*. 2007;48: 373-377.
95. Schweiger H, Ohlerth S, Gerber B. Contrast-enhanced ultrasound of both kidneys in healthy, non-anaesthetized cats. *Acta Veterinaria Scandinavica*. 2015;57: 57-80.
96. Piscaglia FB, L. The safety of Sonovue (R) in abdominal applications: Retrospective analysis of 23188 investigations. *Ultrasound in Medicine and Biology*. 2006;32: 1369-1375.
97. Leinonen MR, Raekallio MR, Vainio OM, Sankari S, O'Brien RT. The effect of contrast-enhanced ultrasound on the kidneys in eight cats. *Veterinary Journal*. 2011;190: 109-112.
98. Grauer SE, Pantely GA, Xu JP, Ge SP, Giraud GD, Shiota T, et al. Myocardial imaging with a new transpulmonary lipid-fluorocarbon echo contrast agent: Experimental studies in pigs. *American Heart Journal*. 1996;132: 938-945.
99. Bramos D, Tsirikos N, Kottis G, Pamboucas C, Kostopoulou V, Trika C, et al. The acute effect of an echo-contrast agent on right ventricular dimensions and contractility in pigs. *Journal of Cardiovascular Pharmacology*. 2008;51: 86-91.
100. Miller DL, Dou CY, Wiggins RC. Contrast-Enhanced Diagnostic Ultrasound Causes Renal Tissue Damage in a Porcine Model. *Journal of Ultrasound in Medicine*. 2010;29: 1391-1401.
101. Williams AR, Wiggins RC, Wharram BL, Goyal M, Dou C, Johnson KJ, et al. Nephron injury induced by diagnostic ultrasound imaging at high mechanical index with gas body contrast agent. *Ultrasound in Medicine and Biology*. 2007;33: 1336-1344.

102. Juffermans LJM, van Dijk A, Jongenelen CAM, Drukarch B, Reijerkerk A, de Vries HE, et al. Ultrasound and Microbubble-Induced Intra- and Intercellular Bioeffects in Primary Endothelial Cells. *Ultrasound in Medicine and Biology*. 2009;35: 1917-1927.
103. Jimenez C, de Gracia R, Aguilera A, Alonso S, Cirugeda A, Benito J, et al. In Situ Kidney Insonation With Microbubble Contrast Agents Does Not Cause Renal Tissue Damage in a Porcine Model. *Journal of Ultrasound in Medicine*. 2008;27: 1607-1615.
104. Granata A, Zanolli L, Insalaco M, Valentino M, Pavlica P, Di Nicolo PP, et al. Contrast-enhanced ultrasound (CEUS) in nephrology: Has the time come for its widespread use? *Clinical and Experimental Nephrology*. 2014.
105. Kinns J, Aronson L, Hauptman J, Seiler G. Contrast-enhanced ultrasound of the feline kidney. *Veterinary Radiology & Ultrasound*. 2010;51: 168-172.
106. Leinonen MR, Raekallio MR, Vainio OM, Ruohoniemi MO, Biller DS, O'Brien RT. Quantitative contrast-enhanced ultrasonographic analysis of perfusion in the kidneys, liver, pancreas, small intestine, and mesenteric lymph nodes in healthy cats. *American Journal of Veterinary Research*. 2010;71: 1305-1311.
107. Dong Y, Wang WP, Cao J, Fan P, Lin X. Early assessment of chronic kidney dysfunction using contrast-enhanced ultrasound: a pilot study. *British Journal of Radiology*. 2014;87: 1-7.
108. Yi K, Ji S, Kim J, Yoon J, Choi M. Contrast-enhanced ultrasound analysis of renal perfusion in normal micropigs. *Journal of Veterinary Science*. 2012;13: 311-314.
109. Ma F, Yadav GP, Cang YQ, Dang YY, Wang CQ, Liu B, et al. Contrast-enhanced ultrasonography is a valid technique for the assessment of renal microvascular perfusion dysfunction in diabetic Goto-Kakizaki rats. *Nephrology*. 2013;18: 750-760.
110. Dong Y, Wang WP, Cao JY, Fan PL, Lin XY. Quantitative evaluation of acute renal failure in rabbits with contrast-enhanced ultrasound. *Chinese Medical Journal*. 2012;125: 652-656.
111. Brabrand K, de Lange C, Emblem KE, Reinholt FP, Saugstad OD, Stokke ES, et al. Contrast-Enhanced Ultrasound Identifies Reduced Overall and Regional Renal Perfusion During Global Hypoxia in Piglets. *Investigative Radiology*. 2014;49: 540-546.
112. Valentino M, Ansaloni L, Catena F, Pavlica P, Pinna AD, Barozzi L. Contrast-enhanced ultrasonography in blunt abdominal trauma: considerations after 5 years of experience. *Radiologia Medica*. 2009;114: 1080-1093.

113. Mitterberger M, Pinggera GM, Colleselli D, Bartsch G, Strasser H, Steppan I, et al. Acute pyelonephritis: comparison of diagnosis with computed tomography and contrast-enhanced ultrasonography. *Bju International*. 2008;101: 341-344.
114. Siracusano S, Bertolotto M, Ciciliato S, Valentino M, Liguori G, Visalli F. The current role of contrast-enhanced ultrasound (CEUS) imaging in the evaluation of renal pathology. *World Journal of Urology*. 2011;29: 633-638.
115. Benozzi L, Cappelli G, Granito M, Davoli D, Favali D, Montecchi MG, et al. Contrast-Enhanced Sonography in Early Kidney Graft Dysfunction. *Transplantation Proceedings*. 2009;41: 1214-1215.
116. Fischer T, Muhler M, Kroncke TJ, Lembcke A, Rudolph J, Diekmann F, et al. Early postoperative ultrasound of kidney transplants: evaluation of contrast medium dynamics using time-intensity curves. *Rofo*. 2004;176: 472-477.
117. Kay DH, Mazonakis M, Geddes C, Baxter G. Ultrasonic microbubble contrast agents and the transplant kidney. *Clinical Radiology*. 2009;64: 1081-1087.
118. Lebkowska U, Janica J, Lebkowski W, Malyszko J, Lebkowski T, Leoniuk J, et al. Renal Parenchyma Perfusion Spectrum and Resistive Index (RI) in Ultrasound Examinations With Contrast Medium in the Early Period After Kidney Transplantation. *Transplantation Proceedings*. 2009;41: 3024-3027.
119. Schwenger V, Zeier M. Contrast-enhanced sonography as early diagnostic tool of chronic allograft nephropathy. *Nephrology Dialysis Transplantation*. 2006;21: 2694-2696.
120. Jin YJ, Yang C, Wu SD, Zhou S, Ji ZB, Zhu TY, et al. A Novel Simple Noninvasive Index to Predict Renal Transplant Acute Rejection by Contrast-Enhanced Ultrasonography. *Transplantation*. 2015;99: 636-641.
121. Fischer T, Fillmonow S, Rudolph J, Morgera S, Budde K, Slowinski T, et al. Arrival time parametric imaging: A new ultrasound technique for quantifying perfusion of kidney grafts. *Ultraschall in Der Medizin*. 2008;29: 418-423.
122. Fernandez CP, Ripolles T, Martinez MJ, Blay J, Pallardo L, Gavela E. Diagnosis of Acute Cortical Necrosis in Renal Transplantation by Contrast-Enhanced Ultrasound: a Preliminary Experience. *Ultraschall in Der Medizin*. 2013;34: 340-344.
123. Hosotani Y, Takahashi N, Kiyomoto H, Ohmori K, Hitomi H, Fujioka H, et al. A new method for evaluation of split renal cortical blood flow with contrast echography. *Hypertension Research*. 2002;25: 77-83.

124. Tsuruoka K, Yasuda T, Koitabashi K, Yazawa M, Shimazaki M, Sakurada T, et al. Evaluation of renal microcirculation by contrast-enhanced ultrasound with sonazoid (TM) as a contrast agent. *International Heart Journal*. 2010;51: 176-182.
125. Ma F, Cang YQ, Zhao BZ, Liu YY, Wang CQ, Liu B, et al. Contrast-enhanced ultrasound with SonoVue could accurately assess the renal microvascular perfusion in diabetic kidney damage. *Nephrology Dialysis Transplantation*. 2012;27: 2891-2898.
126. Imamura H, Hata J, Iida A, Manabe N, Haruma K. Evaluating the effects of diclofenac sodium and etodolac on renal hemodynamics with contrast-enhanced ultrasonography: a pilot study. *European Journal of Clinical Pharmacology*. 2013;69: 161-165.
127. Kishimoto N, Mori Y, Nishiue T, Nose A, Kijima Y, Tokoro T, et al. Ultrasound evaluation of valsartan therapy for renal cortical perfusion. *Hypertension Research*. 2004;27: 345-349.
128. Schneider AG, Hofmann L, Wuerzner G, Glatz N, Maillard M, Meuwly JY, et al. Renal perfusion evaluation with contrast-enhanced ultrasonography. *Nephrology Dialysis Transplantation*. 2012;27: 674-681.
129. Schneider A, Johnson L, Goodwin M, Schelleman A, Bellomo R. Bench-to-bedside review: Contrast enhanced ultrasonography - a promising technique to assess renal perfusion in the ICU. *Critical Care*. 2011;15: 157.
130. Schneider AG, Goodwin MD, Schelleman A, Bailey M, Johnson L, Bellomo R. Contrast-enhanced ultrasound to evaluate changes in renal cortical perfusion around cardiac surgery: a pilot study. *Critical Care*. 2013;17: 138.
131. Bahr A, Wrigley R, Salman M. Quantitative evaluation of Imagent (R) as an abdominal ultrasound contrast medium in dogs. *Veterinary Radiology & Ultrasound*. 2000;41: 50-55.
132. Haers H, Vignoli M, Paes G, Rossi F, Taeymans O, Daminet S, et al. Contrast Harmonic Ultrasonographic Appearance of Focal Space-Occupying Renal Lesions. *Veterinary Radiology & Ultrasound*. 2010;51: 516-522.
133. Haers H, Smets P, Pey P, Piron K, Daminet S, Saunders JH. Contrast Harmonic Ultrasound Appearance of Consecutive Percutaneous Renal Biopsies in Dogs. *Veterinary Radiology & Ultrasound*. 2011;52: 640-647.
134. Gerboni GM, Capra G, Ferro S, Bellino C, Perego M, Zanet S, et al. The use of contrast-enhanced ultrasonography for the detection of active renal hemorrhage in a dog with spontaneous kidney rupture resulting in hemoperitoneum. *Journal of Veterinary Emergency and Critical Care*. 2015;25: 751-758.

135. Restitutti F, Laitinen MR, Raekallio MR, Vainionpaa M, O'Brien RT, Kuusela E, et al. Effect of MK-467 on organ blood flow parameters detected by contrast-enhanced ultrasound in dogs treated with dexmedetomidine. *Veterinary Anaesthesia and Analgesia*. 2013;40: E48-E56.
136. Wei K, Le E, Bin JP, Coggins M, Thorpe J, Kaul S. Quantification of renal blood flow with contrast-enhanced ultrasound. *Journal of the American College of Cardiology*. 2001;37: 1135-1140.

CHAPTER II

SCIENTIFIC AIMS

Chapter II Scientific aims

Chronic kidney disease is a very common pathology in companion animals, especially in cats. Nevertheless, early diagnosis remains challenging. Vascular changes play an important role in the pathophysiology and occur early in the disease process.

Contrast-enhanced ultrasound is a functional imaging technique that allows non-invasive assessment of macro- and microperfusion. It is extremely safe, allowing its use in geriatric patients and patients suffering from renal disease. Studies in human medicine show great potential for the diagnosis of diffuse renal disorders. However, data in veterinary medicine are limited. Up to date only few studies have described the normal perfusion pattern of the kidney in healthy cats, whereas data on pathological conditions are lacking.

Therefore, the final goal of this thesis was to assess the potential of CEUS as a tool to evaluate feline renal perfusion.

Specific objectives of this thesis were:

1. To determine if significant differences in renal perfusion parameters are present between the first and second injection of contrast agent.

Few studies have stated that the first injection of microbubbles may lead to more variable and lower enhancement of the studied organ and should thus not be used for evaluation, whereas others mention no significant difference between subsequent injections.

2. To determine the variation of the perfusion parameters obtained with CEUS of the kidney in a population of healthy cats

Contrast-enhanced ultrasound is inherently very sensitive to variation, which may complicate its diagnostic capabilities. Knowledge on the existing variation for the different perfusion parameters in healthy cats is therefore required.

3. To determine the influence of anesthesia or sedation on renal perfusion parameters.

Contrast-enhanced ultrasound can be performed on conscious animals, however sedation or anesthesia may be required in uncooperative patients. As most

Chapter II Scientific aims

anesthetic agents have cardiovascular effects, an influence on contrast-enhanced ultrasound is assumed.

4. To investigate the effect of age on CEUS parameters

Aging causes a decrease in renal plasma flow and an increase in renal vascular resistance in people. However, the influence of aging on feline renal perfusion has not been studied.

5. To assess the capabilities of CEUS to detect changes in renal perfusion after infusion of AT II.

To date it is unclear if CEUS is capable of detecting relatively small perfusion changes in cats. AT II is a potent renal vasoconstrictor that is often upregulated in patients with renal disease.

6. To describe renal perfusion parameters of cats with CKD and compare them with those from healthy cats

Few human studies have described a decreased perfusion in people with CKD, however the perfusion pattern and changes in perfusion parameters in cats with CKD remain unknown.

7. To investigate renal perfusion of hyperthyroid cats, before and after radioiodine treatment

Changes in renal hemodynamics play an important role in functional renal changes in cats with hyperthyroidism. CEUS allows evaluation of renal perfusion and may therefore deliver important insights in renal function in hyperthyroid cats.

CHAPTER III

QUANTITATIVE DIFFERENCES BETWEEN SEQUENTIAL INJECTIONS

Adapted from:

Stock E., Vanderperren K., Haers H., Duchateau L., Hesta M., Saunders J.H. Quantitative differences between the first and second injection of contrast agent in contrast-enhanced ultrasonography of feline kidneys and spleen. *Ultrasound in Medicine and Biology* 2017; **43**: 500-504.

1. Abstract

Contrast-enhanced ultrasound is a valuable and safe technique for the evaluation of organ perfusion. Repeated injections of ultrasound contrast agents are often administered during the same imaging session. However, it remains unclear if quantitative differences are present between the consecutive microbubble injections. Therefore, the first and second injection of contrast agent for the left renal cortex, renal medulla and the splenic parenchyma in healthy cats, were compared. A lower peak enhancement and area-under-the-curve were observed for the first injection of contrast agent in the feline kidney, both for the renal cortex and medulla, and spleen. Moreover, for the renal cortex, the time-intensity curve was steeper after the second injection. Findings from the current study demonstrate that a second injection of contrast agent provides stronger enhancement. The exact mechanism behind our findings remains unclear, however saturation of the lung macrophages is believed to play an important role.

2. Introduction

Contrast-enhanced ultrasonography (CEUS) allows real-time visualization of macro- and microvascularization. Creating time-intensity curves and calculating several perfusion parameters allows quantification of tissue perfusion. The technique is extremely safe and can be performed in patients with renal impairment.^{1,2} CEUS shows great potential for evaluation and diagnosis of various renal disorders in human and veterinary medicine.^{3,4}

Repeated injections of contrast agent are most often required in CEUS studies for different reasons. The first injection is sometimes used to optimize image settings. Multiple lesions may also be present, urging for several injections of contrast agent to be able to study all of them. In the assessment of diffuse renal disorders, both kidneys must be imaged. Additionally, patient motion during the study may induce the need for multiple injections of contrast agent. Some authors already mentioned that tissue enhancement after the first injection of microbubbles is subjectively less bright in comparison with subsequent contrast agent injections.^{3,5,6} A study on CEUS of liver and aorta in human subjects confirmed this finding quantitatively.⁷ In contrast, no significant differences were found between the first and second injection of contrast agent in mice liver and tumor tissue. However, a tendency towards a higher peak enhancement after consecutive microbubble injections was noted.⁸ Thus far, it remains unclear if there are significant differences

between the first and second injection of contrast agent. Nevertheless, it is of major importance to know if differences are present between both injections as this could influence study results.

Therefore, the purpose of this study was to compare several perfusion parameters in the left kidney and spleen in healthy cats between the first and second contrast injection. The hypothesis is that the second injection of contrast agent will result in an increased enhancement of both the left kidney and the spleen; this will mainly be reflected by an increased peak enhancement and area-under-the-curve.

3. Materials and methods

The experiments were approved by the Local Ethical Committee of Ghent University (EC2014/38). Seven healthy purpose-bred laboratory cats with a mean \pm standard error age of 4.7 ± 0.9 years and mean \pm standard error body weight of 3.1 ± 0.2 kg were used. All cats were female neutered. The cats were judged healthy based on physical examination, hematology, routine biochemistry, urinalysis and abdominal ultrasound. The kidneys had a normal size and appearance on B-mode ultrasound.

A 22-Gauge catheter was placed in the cephalic vein. All cats were anesthetized with propofol (Propovent®, Abbott Lab, Berkshire, UK), 6 mg/kg intravenous, maintained with additional boluses of 1 mg/kg on effect.

A commercial contrast agent (Sonovue®, Bracco, Milan, Italy) was administered at 0.15 mL per bolus, immediately followed by a 1 mL saline bolus. A three-way stopcock was used to avoid delay between the contrast agent and the saline flush. The same person performed the injections in a standardized way. The cats received 2 consecutive injections, with approximately 10 minutes between the two injections. In-between the injections, the microbubbles were destroyed by setting the acoustic power at the highest value and scanning the caudal abdominal aorta, liver and spleen for approximately 2 minutes.

A linear array transducer of 5-7.5 MHz on a dedicated ultrasound machine (MyLab 30 CV, Esaote, Genoa, Italy), equipped with CnTI-contrast tuned imaging technology, was used. Machine settings were kept constant between the injections. A mechanical index of 0.09 was applied. The gain setting was adapted to a value just suppressing signals before arrival of contrast agent (55-58%). An image clip of 120 s at a frame rate of 7.5 frames per second was recorded for every injection. Imaging was started simultaneously with the contrast agent injection.

The kidney was consistently imaged in a longitudinal plane. The spleen was imaged simultaneously with the left kidney.

Quantitative analysis was performed using an image analysis program (Image J, US National Institutes of Health, Bethesda, Md). The data were not linearized before quantification. Mean pixel intensity was measured every second from 0s to 70s, every 2 seconds from 70s to 90s and every 4 seconds from 90s to 120s. A circular region of interest (ROI) was drawn in the renal cortex and medulla at approximately the same location (ventral aspect of the renal cortex, central aspect of the renal medulla). The size of the ROI was kept constant (5 mm diameter). A ROI containing the complete visualized part of the spleen, was drawn for the splenic parenchyma. Care was taken to avoid large vessels. The mean pixel intensity values were used to create time-intensity curves. The curves were analyzed for blood flow parameters representing blood volume (baseline intensity (BI), peak enhancement (PE), area-under-curve (AUC)) and blood velocity (arrival time (AT), time-to-peak (TTP), wash-in/out (W_{in}/W_{out})). W_{out} was not calculated for the spleen, as only the first part of the wash-out occurred within the time the clip was captured (120 s). BI was defined as the intensity measured the first 3 seconds after contrast agent injection. AT was set at the point where the curve reached a value at least 5 mean pixel intensity values higher than BI. W_{in} was calculated from data points between 10% higher than BI and 90% of PE; W_{out} from points between 90% of PE and T=120s (end of the study). PE and AUC were corrected for the BI.

Statistical test selection and analysis was performed by one of the authors (LD). The statistical analysis was based on a mixed model with cat as random effect and sequence (first or second injection) as fixed effect, using F-tests at the 5% significance level (SAS Version 9.4, SAS Institute Inc, Cary, NC).

4. Results

Subjectively, a lower enhancement was seen for the first injection compared to the second injection (Figure 1).

AUC was significantly higher for the second injection compared to the first injection for both the renal cortex ($P = 0.01$) and medulla ($P = 0.04$). The PE was also higher for the second injection; this was only significant for the renal cortex ($P = 0.009$) while a trend was present for the renal medulla ($P = 0.055$). Additionally, for the renal cortex, the W_{in} ($P = 0.01$) and W_{out} ($P = 0.006$) were less steep for the first injection compared to the second. No significant differences were present

Chapter III Quantitative differences between sequential injections

between the first and second injection for AT (cortex: $P = 0.4$; medulla: $P = 0.3$) and TTP (cortex: $P = 0.3$; medulla: $P = 0.08$).

Similarly, the PE ($P = 0.007$) and AUC ($P = 0.008$) in the splenic parenchyma were significantly higher for the second injection compared to the first.

The BI was consistently comparable for the first and second injection.

Time-intensity curves, comparing the first and second injection, are represented by Figure 2.

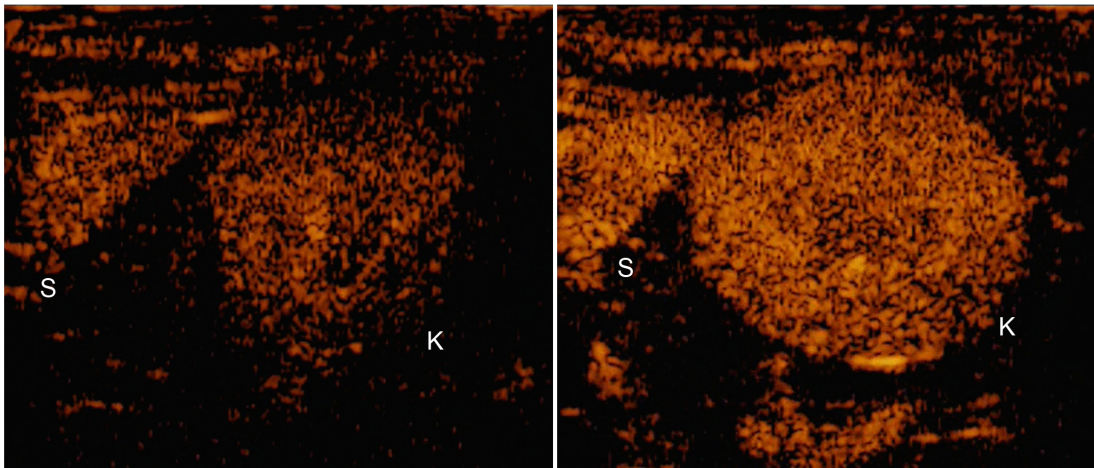


Figure 1. Contrast-enhanced ultrasound images of the spleen (S) and left kidney (K) of a cat, illustrating a lower enhancement after the first injection of contrast agent (left) compared to the second injection (right). Both images are obtained 30 s after contrast injection.

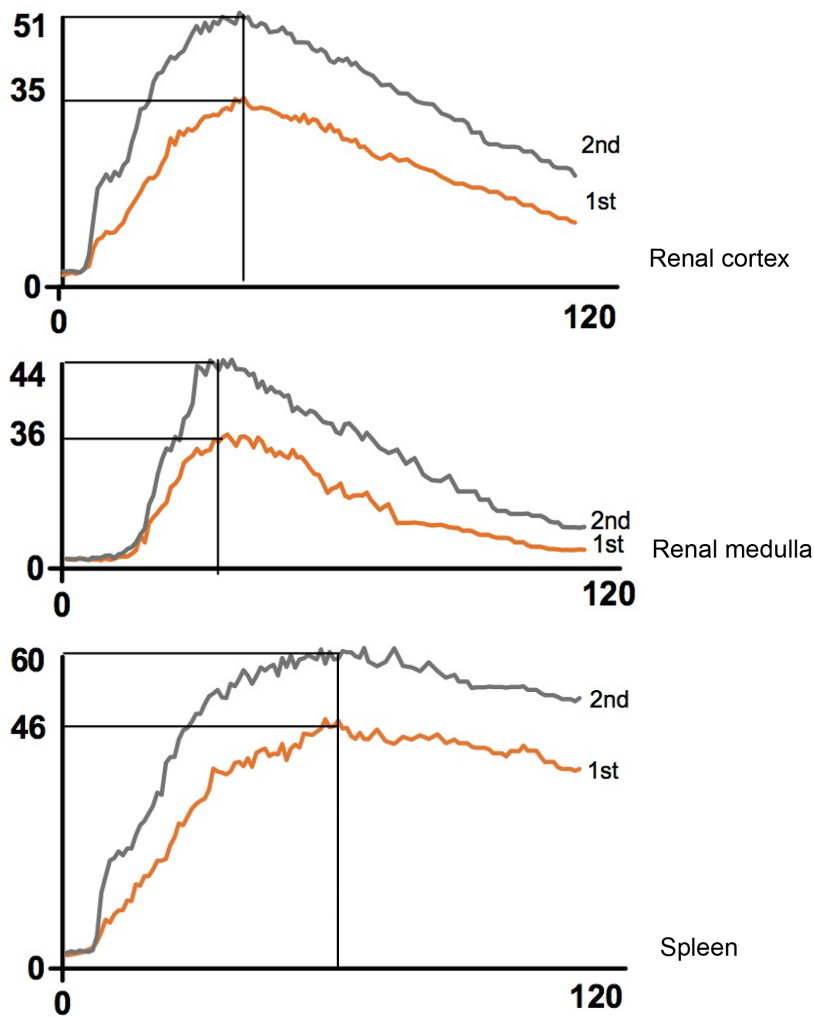


Figure 2. Mean time-intensity curves calculated from the renal cortex, renal medulla and spleen demonstrating a lower peak enhancement, lower area-under-the-curve for the first injection of microbubbles. The time (in seconds, s) is displayed on the horizontal axis, the intensity (in arbitrary units, a.u.) on the vertical axis; 1st: first injection of microbubbles, 2nd: second injection of microbubbles within the same imaging session.

5. Discussion

In the present study, significant differences were observed between the first and second injection of ultrasound contrast agent. The most reproducible differences between the two injections were a higher PE and AUC for the second injection, seen in the renal cortex, renal medulla and splenic parenchyma. For the renal cortex, the wash-in and wash-out were also steeper after the second injection.

In agreement with our results, a tendency towards a higher PE after consecutive microbubble injections was also noted in a recent study in mice tumors.⁸ However, in this study, the opposite effect, i.e. a decreasing PE after consecutive injections, was observed in the liver.⁸ This might be due to short-term accumulation in liver Kupffer cells. In a human study, an increased PE and AUC were noted in the liver after the second injection of microbubbles.⁷

There were no significant differences in BI between the first and second injection, indicating that no residual microbubbles were remaining in tissue of interest before the second injection. In between the injections, the remaining microbubbles were destroyed by setting the acoustic power at the highest value and scanning the caudal abdominal aorta, liver and spleen for approximately 2 minutes. We avoided applying ultrasound waves of relatively high acoustic power on the kidney, as this could potentially cause capillary rupture.^{9,10}

Rix et al. (2014) observed an increased heart rate after the first injection of microbubbles, which coincides with a faster circulation. This explains the faster W_{in} . Moreover, an elevated heart rate and decreased TTP might result in a concentrated microbubble bolus, resulting in a higher PE.⁸ In humans, it was found that injections of relatively low volumes of phospholipid solutions might result in complement activation-related pseudo-allergy, causing a transient increase in heart rate and pulse pressure.¹¹ The heart rate was not measured in our study. But in another study of our research group, we did not observe a change in heart rate after consecutive contrast agent injections in healthy cats (unpublished results). Moreover, no effects on AT and TTP are present in the current study. It should be noted that the volume of the saline itself might cause an accelerated circulation in mice.⁸

In mice, short-term accumulation of microbubbles in the liver sinusoids and spleen might also explain the higher PE in tumors.⁸ It is unlikely that hepatic and splenic accumulation of contrast agent would explain the higher PE in the current study as the majority of the microbubbles in the liver and spleen were destroyed by scanning these organs using high acoustic power. Moreover, it

can be assumed that the low volume of contrast agent does not result in liver saturation in cats. In humans, injection of 1.2 – 1.4 mL microbubble solution does not result in liver saturation.¹²

Another explanation for the stronger enhancement after the second injection might be saturation of the lung macrophages by the microbubbles.⁷ This would allow more microbubbles to pass the lung and finally reach the systemic circulation. In pigs, administration of microbubbles resulted in an acute, transient and dose-dependent right ventricular dilatation, increased pulmonary pressure and increased fractional shortening.¹³ This could be caused by transient hypoxic pulmonary vasoconstriction. Pigs are known to develop severe pulmonary hypertension, which is likely to be caused by activation of pulmonary macrophages. Also in dogs, increased pulmonary vascular resistance and pulmonary artery pressure was seen after administration of high doses of Levovist.¹⁴ No significant hemodynamic changes were observed at clinical, weight-adjusted doses in these dogs. The exact etiology of the effects on the pulmonary vascularization in these dogs remains unclear, transient pulmonary vasoconstriction might be a possible explanation.¹⁴

The last explanation that may be raised is a local effect caused by a vascular mediator. An interaction could be present between the contrast agent and the endothelium, moreover, the influence of the ultrasound waves on microbubbles could reinforce this effect. The combination of both could cause local activation of vasodilative substances. Well-perfused organs as the kidneys and neoplastic tissues might therefore be more sensitive to this effect.

Several factors may influence the presence and extent of differences between the first and second injection of contrast agent. First, the type of contrast agent may be an important factor. It is known that great differences are present in the extent and duration of phagocytosis by the reticuloendothelial system depending on the type of contrast agent.¹⁵ Generally, SonoVue shows a low uptake by Kupffer cells in contrast to other types of microbubbles, as Sonazoid, Optison and Levovist.¹⁶ Moreover, the species may play an important role. As previously mentioned, pigs are prone to develop extensive pulmonary hypertension after activation of lung macrophages. To our knowledge, no information is available on this phenomenon in cats. Finally, the organ of interest may influence the results, as suggested in the murine study of Rix (2014), which showed contrasting results in tumor tissue compared to the liver. In the latter study, PE in tumor tissue tended to increase after repeated microbubble injections, whereas the PE in the liver decreased steadily.⁸

Our study has some limitations. Cardiovascular parameters were not measured regularly throughout the study. However, data of other studies performed by our research group in feline

patients, revealed no significant changes in heart rate, blood pressure, respiratory rate after the first injection of contrast agent. The assessment of heart rate, blood pressure and even more interesting, pulmonary artery pressure and the pressures in the different cardiac chambers would deliver important information to distinguish between the possible causes for the low enhancement after the first injection. Body temperature was also not measured. It is known that hypothermia alters the blood flow and ultimately the distribution of contrast agent.¹⁷ However, it is very unlikely that the cats would develop hypothermia, since the study duration was very short (15-20 minutes) and they were only superficially anesthetized. Moreover, only the first and second injections of contrast agent were studied. It would be interesting to have information about the subsequent injections of contrast agent. It remains unknown if differences are present between the second injection and following injections of contrast agent. Last, we do not know how long this effect lasts. In other words, it is unclear if the same findings would be present, if a second imaging session would be performed in the same animal several hours later.

In conclusion, we demonstrated clear differences in renal perfusion parameters between the first and second injection of contrast agent of the left kidney and spleen in cats. Less bright enhancement is achieved by the first injection. Unfortunately, we were not able to distinguish between the possible explanations for these findings. Activation/saturation of the lung macrophages is the most plausible explanation. Further research is necessary to clarify the mechanism of our findings and investigate if similar phenomena are present in other species and different organs. Our findings have important implications: the first injection should not be compared quantitatively to the second injection; additionally it is recommended to use the second injection for further analysis as it provides better enhancement.

6. References

1. Piscaglia FB, L. The safety of Sonovue (R) in abdominal applications: Retrospective analysis of 23188 investigations. *Ultrasound in Medicine and Biology*. 2006;32: 1369-1375.
2. Seiler GS, Brown JC, Reetz JA, Taeymans O, Bucknoff M, Rossi F, et al. Safety of contrast-enhanced ultrasonography in dogs and cats: 488 cases (2002-2011). *Journal of the American Veterinary Medical Association*. 2013;242: 1255-1259.
3. Haers H, Daminet S, Smets PMY, Duchateau L, Aresu L, Saunders JH. Use of quantitative contrast-enhanced ultrasonography to detect diffuse renal changes in Beagles with iatrogenic hypercortisolism. *American Journal of Veterinary Research*. 2013;74: 70-77.
4. Granata A, Zanoli L, Insalaco M, Valentino M, Pavlica P, Di Nicolo PP, et al. Contrast-enhanced ultrasound (CEUS) in nephrology: Has the time come for its widespread use? *Clinical and Experimental Nephrology*. 2015;19: 606-615.
5. Pey P, Vignoli M, Haers H, Duchateau L, Rossi F, Saunders JH. Contrast-enhanced ultrasonography of the normal canine adrenal gland. *Veterinary Radiology & Ultrasound*. 2011;52: 560-567.
6. Salwei RM, O'Brien RT, Matheson JS. Characterization of lymphomatous lymph nodes in dogs using contrast harmonic and power Doppler ultrasound. *Veterinary Radiology & Ultrasound*. 2005;46: 411-416.
7. Skrok J. Markedly increased signal enhancement after the second injection of Sonovue compared to the first - a quantitative normal volunteer study. 12th European symposium on ultrasound contrast imaging. Rotterdam, the Netherlands, 2007.
8. Rix A, Palmowski M, Gremse F, Palmowski K, Lederle W, Kiessling F, et al. Influence of Repetitive Contrast Agent Injections on Functional and Molecular Ultrasound Measurements. *Ultrasound in Medicine and Biology*. 2014;40: 2468-2475.
9. Miller DL, Dou CY, Wiggins RC. Contrast-Enhanced Diagnostic Ultrasound Causes Renal Tissue Damage in a Porcine Model. *Journal of Ultrasound in Medicine*. 2010;29: 1391-1401.
10. Williams AR, Wiggins RC, Wharram BL, Goyal M, Dou C, Johnson KJ, et al. Nephron injury induced by diagnostic ultrasound imaging at high mechanical index with gas body contrast agent. *Ultrasound in Medicine and Biology*. 2007;33: 1336-1344.
11. Szebeni J. Complement mediated hypersensitivity to nanomedicines. *Molecular Immunology*. 2011;48: 1715-1715.

Chapter III Quantitative differences between sequential injections

12. Weskott HP. Emerging roles for contrast-enhanced ultrasound. *Clinical Hemorheology and Microcirculation*. 2008;40: 51-71.
13. Bramos D, Tsirikos N, Kottis G, Pamboucas C, Kostopoulou V, Trika C, et al. The acute effect of an echo-contrast agent on right ventricular dimensions and contractility in pigs. *Journal of Cardiovascular Pharmacology*. 2008;51: 86-91.
14. Schwarz KQ, Bezante GP, Chen X, Phillips D, Schlieff R. Hemodynamic effects of microbubble echo contrast. *Journal of the American Society of Echocardiography*. 1996;9: 795-804.
15. Tang MX, Mulvana H, Gauthier T, Lim AKP, Cosgrove DO, Eckersley RJ, et al. Quantitative contrast-enhanced ultrasound imaging: a review of sources of variability. *Interface Focus*. 2011;1: 520-539.
16. Yanagisawa K, Moriyasu F, Miyahara T, Yuki M, Iijima H. Phagocytosis of ultrasound contrast agent microbubbles by Kupffer cells. *Ultrasound in Medicine and Biology*. 2007;33: 318-325.
17. Hyvelin JM, Tardy I, Arbogast C, Costa M, Emmel P, Helbert A, et al. Use of Ultrasound Contrast Agent Microbubbles in Preclinical Research Recommendations for Small Animal Imaging. *Investigative Radiology*. 2013;48: 570-583.

CHAPTER IV

REPEATABILITY OF CONTRAST-ENHANCED ULTRASONOGRAPHY OF THE KIDNEYS IN HEALTHY CATS

Adapted from:

Stock E., Duchateau L., Volckaert V., Polis I., Saunders J.H.*, Vanderperren K.* (* shared senior authorship). Repeatability of contrast-enhanced ultrasonography of the kidneys in healthy cats.

Ultrasound in Medicine and Biology. *Under revision.*

1. Abstract

Contrast-enhanced ultrasound (CEUS) has the ability to image and quantify tissue perfusion. It holds great potential for the use in the diagnosis of various diffuse renal diseases in both human and veterinary medicine. Nevertheless, the technique is known to have an inherent relatively high variability, related to various factors associated with the patient, the contrast agent and machine settings. Therefore, the aim of this study was to assess week-to-week intra- and inter-cat variation of several perfusion parameters obtained with contrast-enhanced ultrasound of both kidneys of 12 healthy cats. Repeatability was determined by calculating the coefficient of variation (CV). The CEUS parameters with the lowest variation for the renal cortex were time-to-peak (CV 6.0%), rise time (CV 13%), fall time (CV 19%) and mean transit time (24 %). Intensity-related parameters and parameters related to the slope of the time-intensity curve had a CV of > 35%. Lower repeatability was present for perfusion parameters derived from the renal medulla compared to the renal cortex. Normalization to the interlobar artery did not cause a reduction in variation. In conclusion, time-related parameters for the cortex show a reasonable repeatability, whereas poor repeatability is present for intensity-related parameters and parameters related to in- and outflow of contrast agent. Poor repeatability is also present for all perfusion parameters for the renal medulla, except for time-to-peak, which has a good repeatability.

2. Introduction

CEUS allows assessment of tissue perfusion in a wide variety of clinical conditions. It enhances the diagnostic accuracy of B-mode ultrasound by adding the use of an intravenously administered contrast agent. The contrast agent is composed of microbubbles consisting of a high molecular weight gas encapsulated by a stabilizing shell.¹ The technique has several advantages: it is extremely safe, without nephro- or hepatotoxicity, and does not use ionizing radiation.¹⁻³ Contrast-enhanced ultrasound shows great potential for the diagnosis of diffuse renal disorders. Quantitative CEUS has shown to be useful in the diagnosis of humans with renal transplant rejection, diabetic nephropathy and chronic renal disease.⁴⁻⁸ In dogs, CEUS is capable of measuring perfusion changes in iatrogenically induced ischemic renal disease and iatrogenic hypercortisolism.^{9, 10} Our research group demonstrated the utility of CEUS to detect renal vasoconstriction induced by angiotensin II infusion in cats.¹¹

Chapter IV Repeatability

The major challenge in CEUS is the relatively high degree of variability, which originates from several factors related to the patient, the contrast agent, machine settings and the operator.¹² Machine settings and, to a lesser extent operator dependent factors, can be controlled. However, contrast agent composition and patient factors such as blood pressure, heart rate and respiratory rate cannot be controlled. It is of major importance to know the magnitude of these variations in and between healthy subjects to estimate to what extent quantification of the feline kidney perfusion with CEUS is reliable, before the technique can be used for the diagnosis of disease in patients. Therefore, this repeatability study is designed to determine normal inter- and intra-individual variation in healthy cats.

3. Materials and methods

Twelve healthy European Shorthair cats, 9 female neutered and 3 male neutered cats, were included with the permission of the local ethical committee of Ghent University (EC 2014/148). The mean \pm standard error age of the cats was 6.9 ± 0.8 years. Their mean \pm standard error weight was 3.3 ± 0.1 kg. The cats were healthy based on physical examination, blood pressure measurement, complete blood count and serum biochemical analysis, urinalysis and abdominal ultrasound. In all cats, both kidneys had a normal size and appearance on ultrasound. The cats were free from medication for at least 2 months and received the same, commercial food at least 2 months prior to the study and during the study period.

CEUS of both feline kidneys was performed at 3 time points within a 7-day interval. At every time point a 22-Gauge catheter was placed in one of the cephalic veins. Anesthesia was induced with a bolus of propofol (Propovet 10 mg/mL; Abbott Laboratories), 4-8 mg/kg intravenously, given to effect, and maintained with additional boluses (1 mg/kg) as necessary. The hair was clipped over the ventrolateral portion of the abdomen. Alcohol and coupling gel were applied to the skin. The ultrasound exams were performed with the cat in dorsal recumbency.

The left kidney (for the 1st and 2nd injection) and the right kidney (for the 3rd injection) were centered on the screen and imaged in a longitudinal plane. The transducer was manually positioned by the same person during each imaging procedure and was maintained at the same position during the CEUS examination.

Chapter IV Repeatability

Sulfur hexafluoride-filled microbubbles (Sonovue®, Bracco, Italy), provided in a commercially available kit, were reconstituted according to the manufacturer's guidelines. The contrast agent was used within a time interval of 6 hours. Before each injection, the suspension was rehomogenized by gently agitating the vial from top to bottom. A 0.05 mL/kg bolus of ultrasound contrast agent was manually administered intravenously over approximately 3s, followed by injection of a 1.5 mL saline bolus. A three-way stopcock was used to avoid any delay between the injection of contrast agent and saline. The same person performed the injection in all cats. Three to 4 injections of contrast were performed: the first one was not used for further quantification since this injection often results in lower enhancement.¹³ Between subsequent injections, to avoid artifacts, remnant microbubbles were destroyed by setting the acoustic power at the highest level and scanning the caudal abdominal aorta, external and internal iliac arteries for 2 minutes.

All examinations were performed using a linear transducer of 12-5 MHz on a dedicated machine (iU22, Philips, Bothell, WA) with contrast-specific software. Basic technical parameters were: a single focus placed directly under the kidney, persistency off, mechanical index 0.09, dynamic range C50, gain 85%, side-by-side imaging. These settings were repeated during each injection. All studies were digitally registered as a movie clip at a rate of 7 frames per second, and this during 90 seconds.

The movie clips were exported as DICOM and analyzed using specialized computer software (VueBox®, Bracco Suisse SA, Switzerland) for objective quantitative analysis. Analyses were based on linearized video data. Six regions-of-interest (ROIs) were manually drawn: 1 on an interlobar artery, 3 in the renal cortex, and 2 in the renal medulla. ROI-placement is illustrated in Figure 1. The ROIs for the cortex and medulla were identical in size (4 mm for the cortex, 3 mm for the medulla) and shape and drawn at approximately the same depth. For every ROI, the software determined mean pixel intensities and created a time-intensity curve. Time-intensity curves were analyzed for blood flow parameters representing blood volume (peak enhancement (PE), wash-in area under the curve (WiAUC), wash-out area under the curve (WoAUC) and total area under the curve (AUC)) and blood velocity (rise time (RT), mean transit time (mTT), time to peak (TTP), wash-in rate (WiR), wash-in perfusion index (WiPI), fall time (FT), wash-out rate (WoR)). The values for the 3 ROIs for the cortex and 2 ROIs for the medulla were averaged. Peak enhancement and WiAUC for the cortex and medulla were normalized to values from the interlobar artery (PE* and WiAUC*).

Statistical analyses were performed with SAS (SAS version 9.4, SAS Institute Inc.). The analysis was based on a random effects model using restricted maximum likelihood to estimate the variance components. Three variance components were estimated, v_1 corresponding to the variation between repeated measurements on the same kidney, v_2 to the extra variation when considering observations of the two kidneys of the same cat and v_3 to the extra variation when considering observations of different cats. The variance components were used to determine 95% reference intervals for repeated observations on the same kidney and for repeated observations on kidneys of different cats. Furthermore, the coefficient of variation (CV), defined as the ratio of the standard deviation over the mean, was determined for the within cat repeated observations.

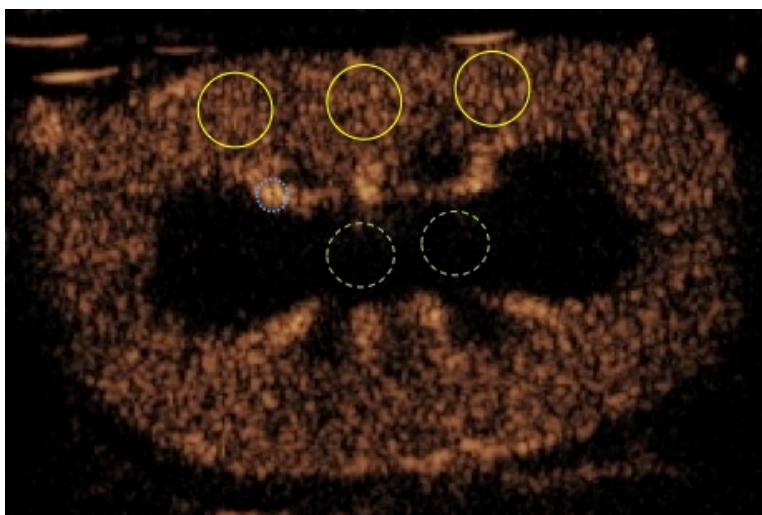


Figure 1. Contrast-enhanced ultrasound image of the left kidney of a cat illustrating the position of the regions-of-interest in the renal cortex (yellow___), renal medulla (green ---) and interlobar artery (blue +++). The image was obtained at peak cortical enhancement (10 s after contrast injection).

4. Results

The weight of cats remained stable and no remarkable events were reported during the study period. The contrast agent was well tolerated by all cats and no side effects were noticed.

An overview of the variation for the different perfusion parameters is given in Tables 1-3 and Figure 2. As shown in Tables 2 and 3, the CEUS parameters with the lowest CV were those related to the blood velocity: TTP, RT and FT. Variation was greater for the medulla (42% for FT, 26% for RT and 13% for TTP) compared to the renal cortex (19% for FT, 13% for RT and 6% for TTP). Mean transit

time (mTT), a parameter for mean duration of complete contrast medium perfusion, showed reasonable variation for the renal cortex (24%), whereas high CV was noted for the medulla (83%). Parameters related to the slope of the time-intensity curve showed moderate variation, which was consistently greater for the medulla. Parameters related to the signal intensity showed the highest variation. Coefficients of variation for PE were 41% and 46% for the renal cortex and medulla respectively, even increasing to 63% for the interlobar artery. Consequently, normalizing PE to the interlobar artery, did not reduce variance, but in contrast caused a clear increase in CV with values for PE* of 56% for the cortex and 67% for the medulla. Similar results were obtained for the AUC with CV values varying between 37% and 45% for the cortex and medulla. Similarly, normalizing WiAUC to the interlobar artery caused an increase in CV.

The extra variation due to different kidneys of the same cat is small, and close to zero for the renal cortex. The extra variation added by considering different cats is relatively small in respect to the variation due to repeated measurements on the same cat.

Variable	v_1	v_2	v_3	v_1	v_2	v_3
	Renal cortex			Renal medulla		
PE	700064.11	0.00	94321.97	17877.34	1335.34	13291.83
PE*	67.38	0.60	4.10	2.24	0.42	0.94
WiAUC	3044906.72	0.00	1164708.92	1101109.68	364418.44	831708.58
WiAUC*	80.48	0.00	1.22	39.45	1.95	23.43
AUC	15666348.73	0.00	6126522.55	10022876.60	2528158.89	3937022.34
WoAUC	4944824.02	0.00	1947085.66	4967136.51	1058428.79	1114792.93
mTT	45.71	0.19	61.58	6536.44	4760.97	0.00
RT	0.25	0.02	0.23	20.38	5.62	4.95
TTP	0.41	0.10	1.64	15.58	3.99	10.69
FT	0.98	0.07	0.46	188.20	59.25	40.89
WiR	128608.35	0.00	7729.98	314.54	12.50	149.32
WiPI	259793.99	0.00	35450.72	6812.22	529.70	5058.44
WoR	70551.60	0.00	2535.62	133.48	7.31	46.34

Table 1. The estimated variance components explaining the variation of different perfusion parameters of feline kidneys using contrast-enhanced ultrasound. v_1 stands for the variation between repeated measurements on the same kidney, v_2 for the extra variation when considering observations of the two kidneys of the same cat and v_3 for the extra variation when considering observations of different cats. (PE = peak enhancement; PE* = normalized peak enhancement; WiAUC = wash-in area-under-the curve; WiAUC* = normalized WiAUC; AUC = total area-under-the-curve; WoAUC = wash-out area-under-the-curve; mTT = mean transit time; RT = rise time; TTP = time-to-peak; FT = fall time; WiR = wash-in rate; WiPI = wash-in perfusion index; WoR = wash-out rate)

Variable	Mean \pm St Err	Within cat 95% reference interval	Between cat 95% reference interval	CV
PE	2042.44 \pm 165.68	[369.05 – 3715.84]	[259.88 – 3825.01]	41.0%
PE*	14.65 \pm 1.50	[0.00 – 32.07]	[0.00 – 31.63]	56.0%
WIAUC	4637.91 \pm 426.88	[1147.98 – 8127.84]	[534.44 – 8741.38]	37.6%
WIAUC*	19.19 \pm 1.53	[1.25 – 37.14]	[1.12 – 37.27]	46.7%
AUC	10718.00 \pm 974.03	[2802.30 – 18634.59]	[1381.88 – 20055.01]	36.9%
WoAUC	6080.53 \pm 548.25	[1633.14 – 10527.92]	[830.04 – 11331.02]	36.6%
mTT	27.94 \pm 2.53	[14.41 – 41.46]	[7.20 – 48.67]	24.4%
RT	3.82 \pm 0.16	[2.82 – 4.82]	[2.41 – 5.23]	13.1%
TTP	11.09 \pm 0.39	[9.82 – 12.37]	[8.16 – 14.03]	5.7%
FT	5.21 \pm 0.26	[3.22 – 7.19]	[2.75 – 7.66]	19.0%
WiR	733.03 \pm 65.12	[15.79 – 1450.27]	[0.00 – 1471.51]	48.9%
WiPI	1248.77 \pm 101.12	[229.37 – 2268.17]	[162.04 – 2335.50]	40.8%
WoR	499.95 \pm 46.72	[0.00 – 1031.18]	[0.00 – 1040.64]	53.1%

Table 2. The mean \pm standard error (St Err) and the within and between cat 95% reference interval and CV (coefficient of variation) for the within cat repeated observations for the perfusion values of the renal cortex of feline kidneys using contrast-enhanced ultrasound. (PE = peak enhancement; PE* = normalized peak enhancement; WIAUC = wash-in area-under-the curve; WIAUC* = normalized WIAUC; AUC = total area-under-the-curve; WoAUC = wash-out area-under-the-curve; mTT = mean transit time; RT = rise time; TTP = time-to-peak; FT = fall time; WiR = wash-in rate; WiPI = wash-in perfusion index; WoR = wash-out rate)

Variable	Mean \pm St Err	Within cat 95% reference interval	Between cat 95% reference interval	CV
PE	292.09 \pm 40.92	[24.68 – 559.50]	[0.00 – 652.67]	45.9%
PE*	2.24 \pm 0.40	[0.00 – 5.23]	[0.00 – 6.03]	67.0%
WIAUC	2783.10 \pm 342.25	[684.42 – 4881.77]	[0.00 – 5814.43]	37.7%
WIAUC*	12.14 \pm 1.53	[0.00 – 24.71]	[0.00 – 28.25]	51.7%
AUC	7679.05 \pm 851.75	[1347.27 – 14010.84]	[0.00 – 15800.15]	41.2%
WoAUC	4900.04 \pm 529.83	[442.63 – 9357.46]	[0.00 – 10244.33]	45.5%
mTT	96.91 \pm 19.06	[0.00 – 258.60]	[0.00 – 309.48]	83.4%
RT	17.15 \pm 1.11	[8.12 – 26.18]	[6.02 – 28.27]	26.3%
TTP	30.54 \pm 1.23	[22.65 – 38.44]	[19.54 – 41.54]	12.9%
FT	32.83 \pm 3.39	[5.39 – 60.27]	[0.00 – 66.79]	41.8%
WiR	28.7719 \pm 4.67	[0.00 – 64.24]	[0.00 – 72.42]	61.6%
WiPI	182.48 \pm 25.27	[17.40 – 347.55]	[0.00 – 405.19]	45.2%
WoR	15.23 \pm 2.81	[0.00 – 38.33]	[0.00 – 42.59]	75.9%

Table 3. The mean \pm standard error (St Err) and the within and between cat 95% reference interval and CV (coefficient of variation) for the within cat repeated observations for the perfusion values of the renal medulla of feline kidneys using contrast-enhanced ultrasound. (PE = peak enhancement; PE* = normalized peak enhancement; WIAUC = wash-in area-under-the curve; WIAUC* = normalized WIAUC; AUC = total area-under-the-curve; WoAUC = wash-out area-under-the-curve; mTT = mean transit time; RT = rise time; TTP = time-to-peak; FT = fall time; WiR = wash-in rate; WiPI = wash-in perfusion index; WoR = wash-out rate)

Chapter IV Repeatability

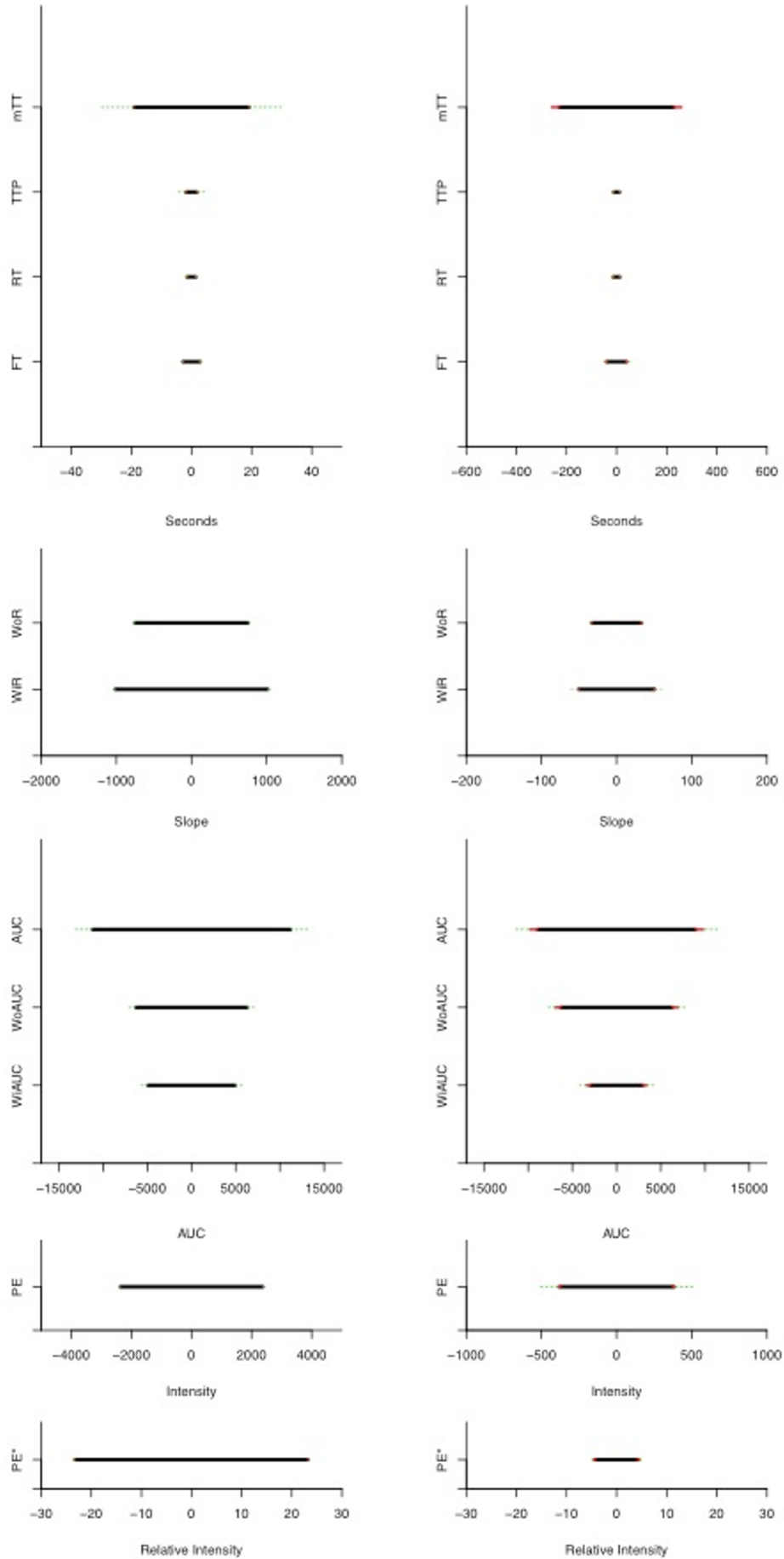


Figure 1. The 95% intervals for a difference between two observations for different perfusion parameters of feline kidneys using contrast-enhanced ultrasound for the cortex (left) and medulla (right). The thick bar corresponds to the 95% interval of the difference between two observations from the same kidney, same cat. The medium bar corresponds to the additional width of the 95% reference interval when considering two different kidneys of the same cat, and the narrow and dotted bar to the additional width of the 95% reference interval when considering two kidneys of different cats. (PE = peak enhancement; PE*=normalized peak enhancement; WiAUC = wash-in area-under-the curve; AUC = total area-under-the-curve; WoAUC = wash-out area-under-the-curve; mTT = mean transit time; RT = rise time; TTP = time-to-peak; FT = fall time; WiR = wash-in rate; WoR = wash-out rate)

5. Discussion

Contrast-enhanced ultrasound is associated with a relatively high degree of variability, which may cause diagnostic uncertainty. However, the causes of this high variability have not yet been completely understood, and can be related to several factors such as the operator, scanner settings, patient related factors and the contrast agent. Careful study design standardizing image acquisition and data processing may reduce variability. However, the variation caused by physiological patient factors and the contrast agent cannot be controlled. Therefore, the repeatability, referring to the variation in serial measurements performed on the same subject under comparable conditions¹⁴, as well as intersubject variation of several perfusion parameters were investigated in this study. In an effort to minimize variation, machine settings were standardized, the same operator performed the ultrasound, the injection and quantification were also performed by one person, and measurements were made within a reasonably short period of time.

The highest variation in this study was related to the intensity parameters reflecting blood volume. The CV for PE for the renal cortex (41%) was higher compared to those previously reported in mice and rat kidneys, ranging from 10% - 25% for manual injections for the renal cortex.¹⁵⁻¹⁷ Nevertheless, higher values for the CV for PE were reported in a study using CEUS for assessing cerebral perfusion in humans (47-53%).¹⁸ The CV for AUC (36-38%) was similar to the one reported in other studies in rodents.^{15, 16} Again, lower repeatability was found in the human study on cerebral perfusion (CV 64-65%). The variation for time related parameters has only been reported in one study on mice kidneys. In our study the CV for TTP was lower, whereas the CV for WoR and mTT was slightly higher compared to the murine study.¹⁵ Similar values for CV were obtained for WiR.¹⁵ No

Chapter IV Repeatability

results have previously been published on variation of any parameter for the renal medulla or interlobar artery.

There is no clear cut-off value for CV defining adequate repeatability. CV values of 10-15% for successive injections of contrast agent in the same imaging session in the same animal, in rodent kidneys are proposed by one study.¹⁷ However, these values are set arbitrarily. Moreover, higher CV's are to be expected when considering different imaging sessions and inter-subject variation. The CV for measurement of glomerular filtration in cats, the gold standard for evaluation of renal function, is reported to be up to 20%.¹⁹

PE is the most critical parameter in terms of variation because it is influenced by many different factors. One of these is the concentration of microbubbles present in the contrast agent. This is influenced by the production process, the way the agent is reconstituted, the mode of administration and physical and physiological factors in the environment.^{12, 20, 21} Moreover, the acoustic window, and uncontrollable patient-related factors such as blood pressure, heart rate, filtration of the microbubbles by the lungs, and phagocytosis by the reticuloendothelial system will also induce variation.^{12, 17} Therefore, it has been proposed to remove part of this variation by normalization with neighboring 'normal' tissue as a reference.^{12, 22} However, when imaging the feline kidney in a standardized longitudinal plane it is impossible to consistently include other tissues such as the spleen for the left kidney, the liver for the right kidney or the abdominal aorta, as this would interfere with the standardized imaging plane of the kidneys in some cats. The interlobar arteries are always in the imaging plane, and were thus chosen as reference tissue. However, the variance in PE is higher for the interlobar artery compared to the remainder of the kidney. Interlobar arteries are small structures and may be inconsistently imaged, moreover they are highly susceptible to motion artifact from breathing. Drawing a ROI surrounding a structure of this size is challenging and may be susceptible to inter- and intra-observer variability. Moreover, under pathological conditions, as chronic kidney disease the flow within the interlobar artery could be affected and therefore not serve as normal reference tissue. The abdominal aorta could be used as reference tissue, although it should be imaged separately urging an additional administration of contrast. It could remove part of the variation induced by microbubble concentration and some patient factors. Nevertheless, the acoustic window will be different. Larger variations in blood pressure exist in larger arteries and may therefore induce additional variation.¹²

Two main approaches are used to measure renal perfusion using CEUS: bolus kinetics and flash-replenishment kinetics. For the bolus method, a single bolus of ultrasound contrast medium is

Chapter IV Repeatability

administered intravenously and a curve representing the acoustic intensity over time is obtained. Flash-replenishment kinetics are based on the reappearance of ultrasound contrast agent after complete destruction of the microbubbles by a flash of high mechanical intensity. An infusion of contrast agent is most often used for this technique.²³ The different methods have their associated limitations and measure different perfusion parameters. A lower variation is suspected to result from flash-replenishment kinetics, however no supporting data are currently available. A manual bolus injection was performed in this study, as this is the most commonly used method in clinical imaging procedures. Increasing the injection time causes both an increase in TTP and a decrease in PE and WiR.²⁴ A commercially available bolus-injection system has recently been introduced. Controlled injections performed by this system improved reproducibility for TTP, WiR and WoR, whereas PE and AUC were not significantly different between manual and controlled injections.¹⁵ Repeatability for the TTP in this study was relatively good, whereas low repeatability was present for the WiR and WoR. Controlled injection might therefore aid in the improvement of the repeatability of these 2 parameters.

The discrepancy between the values for cortex and medulla is likely to be related with the specific anatomic and physiologic characteristics of the medullary blood supply. The medulla only receives 10% of the total renal blood flow.^{25,26} The medullary blood supply directly diverges from the cortical supply and is derived exclusively from the juxtamedullar glomeruli. Discrepancies exist between the inner and outer medulla, as the outer medulla receives approximately 40% of the cortical blood flow, whereas the inner medulla receives 10%.²⁶ However, outer and inner medulla cannot strictly be delineated on ultrasound images, therefore ROI placement is likely to be inconsistent in both medullary regions, hence increasing variability. Moreover, subtle changes in total and cortical renal blood flow, may induce larger changes in the medullary blood flow due to redistribution between juxtamedullar and cortical glomeruli.²⁶

In conclusion, this study shows that intensity-related parameters and parameters related to the slope of the time-intensity curve show moderate to high variation in healthy cats and may therefore be a complicating factor in the diagnostic capabilities of CEUS. Relatively good repeatability is present for time-derived parameters. It would be interesting to investigate if normalization to the abdominal aorta and using a bolus-injection system could reduce variation. Moreover, destruction-reperfusion techniques may be less susceptible to variation, although no data are available at the moment.

6. References

1. Haers H, Saunders JH. Review of clinical characteristics and applications of contrast-enhanced ultrasonography in dogs. *Journal of the American Veterinary Medical Association*. 2009;234: 460-470.
2. Dietrich CF, Ignee A, Hocke M, Schreiber-Dietrich D, Greis C. Pitfalls and Artefacts using Contrast Enhanced Ultrasound. *Zeitschrift Fur Gastroenterologie*. 2011;49: 350-356.
3. Seiler GS, Brown JC, Reetz JA, Taeymans O, Bucknoff M, Rossi F, et al. Safety of contrast-enhanced ultrasonography in dogs and cats: 488 cases (2002-2011). *Journal of the American Veterinary Medical Association*. 2013;242: 1255-1259.
4. Dong Y, Wang WP, Cao J, Fan P, Lin X. Early assessment of chronic kidney dysfunction using contrast-enhanced ultrasound: a pilot study. *British Journal of Radiology*. 2014;87: 1-7.
5. Ma F, Cang YQ, Zhao BZ, Liu YY, Wang CQ, Liu B, et al. Contrast-enhanced ultrasound with SonoVue could accurately assess the renal microvascular perfusion in diabetic kidney damage. *Nephrology Dialysis Transplantation*. 2012;27: 2891-2898.
6. Tsuruoka K, Yasuda T, Koitabashi K, Yazawa M, Shimazaki M, Sakurada T, et al. Evaluation of renal microcirculation by contrast-enhanced ultrasound with sonazoid (TM) as a contrast agent. *International Heart Journal*. 2010;51: 176-182.
7. Fischer T, Fillmonow S, Rudolph J, Morgera S, Budde K, Slowinski T, et al. Arrival time parametric imaging: A new ultrasound technique for quantifying perfusion of kidney grafts. *Ultraschall in Der Medizin*. 2008;29: 418-423.
8. Kay DH, Mazonakis M, Geddes C, Baxter G. Ultrasonic microbubble contrast agents and the transplant kidney. *Clinical Radiology*. 2009;64: 1081-1087.
9. Dong Y, Wang WP, Cao JY, Fan PL, Lin XY. Quantitative evaluation of contrast-enhanced ultrasonography in the diagnosis of chronic ischemic renal disease in a dog model. *Plos One*. 2013;8: e70377.
10. Haers H, Daminet S, Smets PMY, Duchateau L, Aresu L, Saunders JH. Use of quantitative contrast-enhanced ultrasonography to detect diffuse renal changes in Beagles with iatrogenic hypercortisolism. *American Journal of Veterinary Research*. 2013;74: 70-77.
11. Stock E, Vanderperren K, Bosmans T, Dobbeleir A, Duchateau L, Hesta M, et al. Evaluation of feline renal perfusion with contrast-enhanced ultrasonography and scintigraphy. *Plos One*. 2016;11: e0164488.

Chapter IV Repeatability

12. Tang MX, Mulvana H, Gauthier T, Lim AK, Cosgrove DO, Eckersley RJ, et al. Quantitative contrast-enhanced ultrasound imaging: a review of sources of variability. *Interface Focus*. 2011;1: 520-539.
13. Stock E, Vanderperren K, Haers H, Duchateau L, Hesta M, Saunders JH. Quantitative differences between the first and second injection of contrast agent in contrast-enhanced ultrasonography of feline kidneys and spleen. *Ultrasound in Medicine and Biology*. 2017;43: 500-504.
14. Bartlett JW, Frost C. Reliability, repeatability and reproducibility: analysis of measurement errors in continuous variables. *Ultrasound Obstetrics & Gynecology*. 2008;31: 466-475.
15. Dizeux A, Payen T, Barrois G, Le Guillou Buffello D, Bridal SL. Reproducibility of Contrast-Enhanced Ultrasound in Mice with Controlled Injection. *Molecular Imaging Biology*. 2016;18: 651-658.
16. Stapleton S, Goodman H, Zhou YQ, Cherin E, Henkelman RM, Burns PN, et al. Acoustic and kinetic behaviour of definity in mice exposed to high frequency ultrasound. *Ultrasound in Medicine and Biology*. 2009;35: 296-307.
17. Hyvelin JM, Tardy I, Arbogast C, Costa M, Emmel P, Helbert A, et al. Use of Ultrasound Contrast Agent Microbubbles in Preclinical Research Recommendations for Small Animal Imaging. *Investigative Radiology*. 2013;48: 570-583.
18. Vinke EJ. Development of a contrast enhanced ultrasound technique for the measurement of cerebral blood flow in patients with acute brain injury at the intensive care unit (Thesis). University of Twente, The Netherlands 2015.
19. Finch N. Measurement of glomerular filtration rate in cats: methods and advantages over routine markers of renal function. *Journal of Feline Medicine and Surgery*. 2014;16: 736-748.
20. Mulvana H, Stride E, Hajnal JV, Eckersley RJ. Temperature Dependent Behavior of Ultrasound Contrast Agents. *Ultrasound in Medicine and Biology*. 2010;36: 925-934.
21. Talu E, Powell RL, Longo ML, Dayton PA. Needle size and injection rate impact microbubble contrast agent population. *Ultrasound in Medicine and Biology*. 2008;34: 1182-1185.
22. Payen TG, A.; Lamuraglia, M.; Lucidarme, O.; Arditi, M.; Le Guillou, D.; Bridal, SL. . Choice and normalization of contrast ultrasound parameters for detection of anti-angiogenic response. *IEEE International Ultrasonics Symposium*. Orlando, 2011;1486 - 1489.
23. Cosgrove D, Lassau N. Imaging of perfusion using ultrasound. *European Journal of Nuclear Medicine and Molecular Imaging*. 2010;37: S65-S85.

Chapter IV Repeatability

24. Palmowski M, Lederle W, Gaetjens J, Socher M, Hauff P, Bzyl J, et al. Comparison of conventional time-intensity curves vs. maximum intensity over time for post-processing of dynamic contrast-enhanced ultrasound. *European Journal of Radiology*. 2010;75: e149-153.
25. Regan MC, Young LS, Geraghty J, Fitzpatrick JM. Regional renal blood flow in normal and disease states. *Urological Research*. 1995;23: 1-10.
26. Evans RG, Eppel GA, Anderson WP, Denton KM. Mechanisms underlying the differential control of blood flow in the renal medulla and cortex. *Journal of Hypertension*. 2004;22: 1439-1451.

CHAPTER V
INFLUENCE OF ANESTHESIA AND SEDATION ON QUANTITATIVE
CONTRAST-ENHANCED ULTRASONOGRAPHY OF THE HEALTHY FELINE
KIDNEY

Adapted from:

Stock E., Vanderperren K., Van der Vekens E., Haers H., Duchateau L., Polis I., Hesta M., Saunders J.H.
The effect of anesthesia with propofol and sedation with butorphanol on quantitative contrast-
enhanced ultrasonography of the healthy feline kidney. *The Veterinary Journal* 2014, 202; 637 –
639.

1. Abstract

Contrast-enhanced ultrasonography of the left kidney was performed in 6 healthy adult purpose-bred cats, using a commercial contrast agent (Sonovue, Bracco). A cross-over design was used to compare 3 protocols: awake, butorphanol (Dolorex, MSD AH; 0.4 mg/kg IM), and propofol (Propovet, Abbott Lab; 3.5-7.7 mg/kg IV boluses on effect). Time-intensity curves were created from 2 regions-of-interest drawn in the renal cortex. The curves were analyzed for blood flow parameters representing blood volume (baseline intensity, peak enhancement, area-under-curve) and blood velocity (arrival time, time-to-peak, wash-in/out) using a mixed model with cat as random effect.

There was no difference in the subjective enhancement pattern between the 3 protocols. No significant effect of butorphanol compared to awake cats was observed in any of the perfusion parameters. Propofol induced a significant increase in arrival time, time-to-peak and wash-in compared to awake and butorphanol sedated cats.

Sedation with butorphanol has favorable cardiovascular properties without significant influence on renal perfusion parameters but its sedative properties are often insufficient in healthy cats. Propofol causes a decrease in renal blood velocity.

2. Introduction

Contrast-enhanced ultrasonography (CEUS) is an imaging modality improving the diagnostic accuracy of ultrasonography (US). Ultrasound contrast agents (USCAs) are gas-filled microbubbles, encapsulated by a stabilizing shell which have a diameter of 1-8 μm and are administered intravenously (IV). As they do not cross the endothelium, they are strict blood pool agents, able to improve the visualization of the perfusion and vascularization of the organ of interest.¹ The CEUS technique and the USCAs are extremely safe and well tolerated.²

CEUS has become established as a reliable method for the differential diagnosis of focal hepatic and splenic lesions in small animal patients.³⁻⁷ It has been described for the characterization of focal renal lesions in dogs.⁸ Promising results have been achieved with quantitative CEUS to evaluate tissue perfusion. Quantitative CEUS is able to detect changes in renal blood flow in dogs undergoing hydrocortisone treatment.⁹ The perfusion of kidneys, liver, pancreas, small intestines and lymph nodes has been studied in healthy cats.¹⁰⁻¹³

Quantitative information about renal perfusion can be valuable in the diagnosis of diffuse renal disorders. As up to 30% of the older cats suffer from renal disease, accurate and early diagnosis is of major importance in veterinary medicine.¹⁴ Renal perfusion parameters in healthy cats are established, but these results are achieved in sedated or anesthetized cats.^{11,12} However, anesthetic and sedative agents may affect renal blood flow and thereby altering the perfusion variables measured with CEUS.¹⁵

Therefore, the objectives of this study are (1) to evaluate the renal perfusion pattern of healthy cats and (2) to compare the renal perfusion patterns of healthy cats that were imaged awake, sedated with butorphanol and anesthetized with propofol.

3. Materials and methods

Six purpose-bred laboratory cats with mean \pm standard error age of 3.2 ± 0.4 years and mean \pm standard error weight of 3.6 ± 0.3 kg, were studied. Five cats were female neutered, 1 was male neutered. The cats were healthy based on physical examination, Doppler blood pressure measurement, complete blood count and serum biochemical analysis, urinalysis (sediment, dipstick, specific gravity, urinary protein:creatinine ratio) and abdominal US. The kidneys had a normal size and appearance on US. The study protocol was approved by the Local Ethical Committee of Ghent University (EC2013/36).

A 22-Gauge catheter was placed in the cephalic vein. The cats were scanned six times during a three-week period with three different protocols, with a minimum of two days wash-out period between each protocol. The cats were randomly assigned to a sequence of the three different protocols. A cross-over design with 2 periods with each 3 sequences was used. One protocol was assigned to each sequence within the period. In the first protocol the cats were awake and only manual restraint was applied. In the second protocol the cats were sedated with butorphanol 0.4 mg/kg IM (Dolorex, MSD AH). After administration of butorphanol, a period of 15 – 20 minutes in a calm environment was respected. In the third protocol, anesthesia was induced with a bolus of propofol (Propovet, Abbott Laboratories) 3.5-7.7 mg/kg IV given to effect and maintained with 0-3 additional boluses as necessary. The mean \pm standard error total dose of propofol was $8.6 \text{ mg/kg} \pm 0.9$. Propofol was administered over a 30 seconds period, followed by a bolus of 2 mL sterile NaCl-solution.

The hair was clipped over the ventrolateral portion of the abdomen. Alcohol and coupling gel were applied on the skin. The US exams were performed with the cats in dorsal recumbency. A conventional US examination of the abdomen was performed prior to the CEUS study. For CEUS, the left kidney was centered on the screen and was imaged in a dorsal plane. The transducer was manually positioned by the same person during each imaging procedure and was maintained at the same position during the CEUS examination. All cats received three bolus injections of contrast medium (Sonovue, Bracco), 0.15 mL for each injection, followed by a 1 mL saline bolus. A three-way stopcock was used to avoid any delay between the injection of USCA and saline. The first injection of USCA was performed and the kidney was imaged for two minutes. Thereafter, to destroy residual or trapped microbubbles prior to the next injection, the cranial abdomen was scanned with maximal acoustic pressure. This avoided enhancement artefacts and took approximately five minutes. The microbubble injection procedure was repeated with a second and a third injection. All examinations were performed using a linear transducer of 12-5 MHz on a dedicated machine (iU22 xMATRIX, Philips) with contrast-specific software. A single focus, placed underneath the kidney was used. The mechanical index was set at 0.09. For the gain setting, we started with a nearly anechoic image, representing nearly full suppression of fundamental signal. The gain was optimized during the first injection to reach uniform brightness of the image. These settings were repeated during the second and third injection. All studies were digitally registered as a movie clip at a rate of 10 frames per second.

The clips were analyzed using specialized computer software (QLab, Philips) for qualitative and quantitative analysis. Two ovoid regions-of-interest (ROIs) of approximately 4 mm diameter were manually drawn in the renal cortex, at the same location in each cat, as is shown in Figure 1. For every ROI, the software determined mean pixel intensities and created a time-intensity curve. Time-intensity curves were analyzed for blood flow parameters representing blood volume (baseline intensity (BI), peak enhancement (PE), area-under-curve (AUC)) and blood velocity (arrival time (AT), time-to-peak (TTP), wash-in/out or up/downslope (W_{in}/W_{out})).

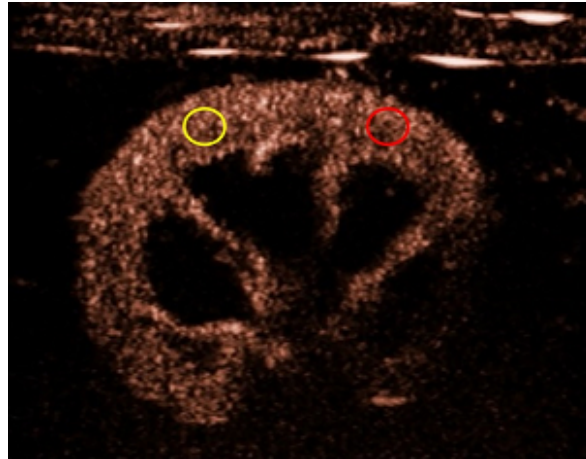


Figure 1. Contrast-enhanced image of the left kidney with 2 ovoid regions-of-interest drawn in the renal cortex.

To compare the three protocols with respect to the different blood flow parameters, a mixed model with protocol and injection sequence as categorical fixed effects and cat and time period nested in cat as random effects was used (SAS Version 9.3). The F-test at the 5% significance level was performed to assess the effect of sedation/anesthesia protocol on the values of the various parameters of renal blood flow obtained with CEUS. The Bonferroni's adjustment technique was used for multiple comparisons and adjusted P-values are reported.

4. Results

The subjective enhancement pattern of the left kidney was similar in all cats, with the different protocols. Microbubbles were first imaged in the renal artery, followed by variable enhancement of the interlobar arteries. There was a uniform, rapid enhancement of the renal cortex followed by a slower enhancement of the renal medulla. Contrast enhancement in the medulla was more heterogeneous and remained hypoechoic throughout W_{in} and W_{out} compared to the cortex.

Mean \pm standard error values of the renal blood flow parameters for the different protocols are summarized in Table 1. The time-intensity curves are represented in Figure 2. Significant effects were found for AT, TTP and W_{in} . Anesthesia with propofol resulted in a significant ($P < 0.001$) increase in AT and TTP, compared to sedation with butorphanol and awake cats. W_{in} was significantly ($P = 0.0382$) slower in cats that received propofol compared to cats sedated with butorphanol and awake cats. No significant effects between the three protocols were found for BI, PI, W_{out} and AUC. All perfusion parameters obtained during sedation with butorphanol were comparable with the perfusion parameters obtained for awake cats.

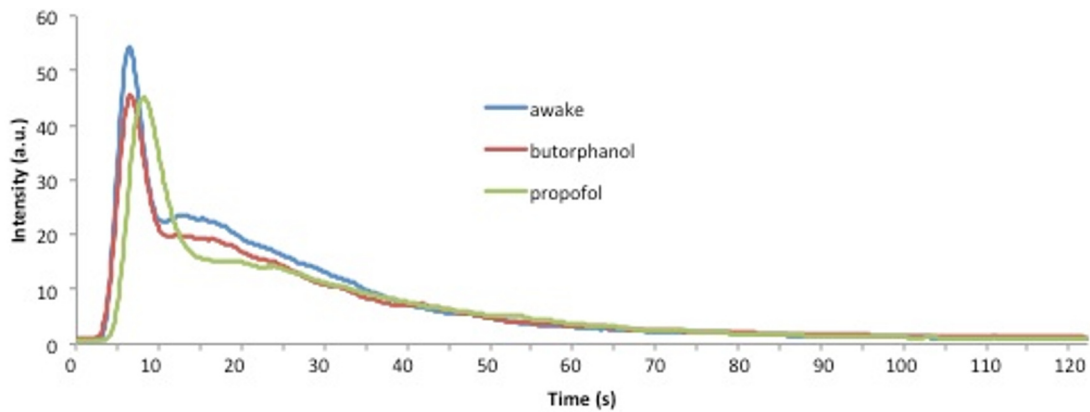


Figure 2. Mean time-intensity curves calculated from the renal cortex in awake cats, cats sedated with butorphanol and anesthetized with propofol. Signal intensity, expressed in arbitrary units (a.u.), is displayed on the y-axis and time, in seconds (s), on the x-axis.

Perfusion parameter	Awake	Butorphanol	Propofol
BI	0.77 ± 0.19	1.20 ± 0.18	0.69 ± 0.18
PE	60.66 ± 5.08	53.73 ± 4.88	51.47 ± 4.88
AT	3.83 ± 0.41	3.85 ± 0.40	5.14 ± 0.40 ^a
TTP	6.19 ± 0.40	6.18 ± 0.40	7.90 ± 0.40 ^a
W _{in}	27.55 ± 2.12	23.94 ± 2.05	19.93 ± 2.05 ^b
W _{out}	-0.45 ± 0.04	-0.39 ± 0.04	-0.39 ± 0.04
AUC	792.80 ± 139.74	695.55 ± 136.90	722.42 ± 136.90

Table 1. Means and standard errors of perfusion parameters calculated from the renal cortex in awake cats, cats sedated with butorphanol and anesthetized with propofol. ^a value represents a significant (P<0,05) effect in respect to awake and butorphanol group; ^bvalue represents a significant (P<0,05) effect in respect to awake group (BI base intensity, PE peak enhancement, AT arrival time, TPP time-to-peak, W_{in} wash-in, W_{out} wash-out, AUC area-under-curve)

None of the cats had adverse reactions during or after contrast medium administration. In the awake group, it was sometimes difficult to retain the cats immobile during two minutes resulting in motion artifacts and rejection of clips for further quantitative assessment (2/24). Administration of butorphanol resulted in a low level of sedation, not improving patient cooperation. Hence, it did not result in a reduction of motion artifacts or rejection rate of clips (2/24). Injection of propofol resulted in a superficial anesthesia of variable duration. This greatly improved the ease of performing the contrast study and resulted in complete rejection of motion artifact (except

breathing artifact). Therefore, all clips in the propofol group could be used for quantitative analysis.

5. Discussion

The kidney is a well-vascularized organ that receives 20-25% of the cardiac output. Renal autoregulatory mechanisms ensure a relatively constant renal blood flow over a wide range of perfusion pressures.¹⁶ Renal blood flow can be maintained constant for mean arterial blood pressures between 80 and 180 mmHg, although even within this range several extrinsic and intrinsic forces can cause the autoregulatory mechanism to fail which results in alterations of renal blood flow.¹⁵ Perfusion parameters obtained with CEUS are not only determined by renal blood flow but also by the systemic circulation, since the bubbles are transported by the venous and arterial circulation from the injection site to the kidney.

In this study, quantitative perfusion parameters were only determined for the renal cortex. Renal perfusion is well reflected by its cortical perfusion as more than 90% of the blood entering the kidney goes to the cortex. The blood flow in the medulla is lower and more variable compared to the cortical blood flow.¹⁶

The subjective enhancement pattern of the kidney obtained in this study was similar to previous descriptions.^{11,12} In this study, no subjective enhancement differences were observed between the protocols. Anesthesia with butorphanol and propofol induced an increase in the heterogeneity of the spleen in cats, which is related to the anesthesia-induced splenic congestion.¹⁷ Congestion following anesthesia is not observed in the renal parenchyma. Despite the absence of effect on subjective enhancement pattern, there were clear differences in the quantitative perfusion parameters between the propofol-group and the other groups.

Three studies have described CEUS perfusion parameters of the feline kidney. All of them used commercial second-generation contrast agent different from the present study (Definity, Lantheus).^{11,12,18} Kinns et al. (2010) only determined TTP in cats sedated with hydromorphone and midazolam (n=1) or anesthetized with isoflurane (n=7).¹¹ The TTP (13 ± 3.2 s) was markedly higher than the TTP in all our 3 protocols. Other studies were performed on cats premedicated with atropine, sedated with acepromazine and morphine and anesthetized with diazepam and ketamine.^{12, 18} The time-related parameters (AT and TTP) were comparable with our findings in awake cats and cats sedated with butorphanol and lower compared to the values obtained in the

cats anesthetized with propofol. In contrast, there were great differences between their values for BI, PI, W_{in} and W_{out} compared to our results. A higher BI, lower PI, a slower W_{in} and a faster W_{out} were observed. Leinonen *et al.* (2010, 2011a) always used the first or second contrast-injection for quantification.^{12,18} The contrast parameters in our study resulted from the mean of the second and third injection. This could explain the higher PI and the effect on W_{in}/W_{out} , although not the influence on BI. Several technical parameters influence the perfusion parameters. It is therefore important to standardize the imaging protocol and machine settings when performing CEUS studies and to be very careful with extrapolation of results.

Butorphanol is an opiate with agonistic effects on the κ -receptor and only minor effects on the μ -receptor, explaining its analgesic and sedative properties with minor cardiovascular effects.¹⁹ There were no significant differences in the perfusion parameters obtained after sedation with butorphanol compared with awake cats. Nevertheless, the variable and low sedation level make it of limited use for sedation of healthy cats. Butorphanol is still a valuable sedative agent for the use in cats in a poor general condition or suffering from severe cardiovascular disease.

Propofol is an anesthetic agent acting by enhancing the GABA-receptors in the central nervous system. In contrast to butorphanol, propofol has well-known cardiovascular influences. The combined effect of a depression of the baroreceptor response and central sympathetic depression induces a decrease in cardiac output and systemic vascular resistance resulting in a depression of systolic and diastolic blood pressure.²⁰ In dogs, induction with propofol caused decreased arterial blood pressure and systemic vascular resistance, although no effect on cardiac output and renal blood flow was noted.²¹ The hemodynamic effects of propofol depend on the dose and the plasma level.²⁰ Systemic blood pressure and heart rate was not measured in this study due to practical constraints. There was a significant delay in blood velocity parameters such as AT and TTP, the effect on W_{in} was less pronounced but still significant. A decrease of blood velocity is likely to be caused by systemic hypotension. Our findings correspond with a previous study on the feline spleen, in which an increase in AT was seen after anesthesia with butorphanol and propofol.¹⁷ In contrast, propofol anesthesia caused a reduction in TTP without a change in W_{in} when performing CEUS of the liver in dogs.²² This finding was explained by an increased hepatic arterial blood flow, which has been described after induction of anesthesia with propofol in dogs.²¹ A shorter TTP from time of contrast reaching the kidney was also noted in dogs receiving propofol and isoflurane compared to awake dogs.²³ This was a non-randomized, non-controlled study with only 2 dogs imaged awake and 6 dogs under anesthesia.

Other commercially available sedative agents for cats, which were not studied in this experiment, are dexmedetomidine and alfaxalone. Dexmedetomidine is an α -2 adrenergic agonist which can be administered IV and IM, and results in deep sedation with muscle relaxation. The pronounced side-effects as bradycardia, decrease in cardiac output, increase in peripheral vascular resistance and respiratory depression are a major drawback for use in CEUS studies.²⁴ Dexmedetomidine caused a pronounced increase in AT and TTP in the canine spleen, kidney and small intestine. In the kidney, additionally, a decreased PI and W_{in} were found.²⁵ MK-467, a non-commercially available peripheral α -2 adrenoceptor antagonist, showed to be capable of altering these effects without reducing the sedative properties. The addition of MK-467 seems very promising for the use of dexmedetomidine in CEUS examinations. Currently, studies in cats are lacking, moreover, the agent is not registered for use in veterinary medicine in Europe.

Alfaxalone is a more recent anesthetic agent that can be used for sedation in cats. It can be administered IV, IM or even SC, but IM injection is painful. It has similar cardiovascular effects compared to propofol. Moreover, the quality of recovery is poor with excitement, hyperreactivity and ataxia.^{26,27}

In conclusion, contrast-enhanced ultrasonography can be performed in awake cats, although sedation or anesthesia is required for uncooperative patients. Butorphanol has no significant influence on CEUS parameters, but its sedative properties are often insufficient. Propofol causes a significant delay in AT and TTP and has an effect on W_{in} .

6. References

1. Haers H, Saunders JH. Review of clinical characteristics and applications of contrast-enhanced ultrasonography in dogs. *Journal of the American Veterinary Medical Association*. 2009;234: 460-470.
2. Seiler GS, Brown JC, Reetz JA, Taeymans O, Bucknoff M, Rossi F, et al. Safety of contrast-enhanced ultrasonography in dogs and cats: 488 cases (2002-2011). *Journal of the American Veterinary Medical Association*. 2013;242: 1255-1259.
3. Nakamura K, Takagi S, Sasaki N, Kumara WRB, Murakami M, Ohta H, et al. Contrast-Enhanced Ultrasonography for Characterization of Canine Focal Liver Lesions. *Veterinary Radiology & Ultrasound*. 2010;51: 79-85.
4. Nakamura K, Sasaki N, Murakami M, Bandula Kumara WR, Ohta H, Yamasaki M, et al. Contrast-enhanced ultrasonography for characterization of focal splenic lesions in dogs. *Journal of Veterinary Internal Medicine*. 2010;24: 1290-1297.
5. O'Brien RT, Iani M, Matheson J, Delaney F, Young K. Contrast harmonic ultrasound of spontaneous liver nodules in 32 dogs. *Veterinary Radiology & Ultrasound*. 2004;45: 547-553.
6. Ohlerth S, Dennler M, Ruefli E, Hauser B, Poirier V, Siebeck N, et al. Contrast harmonic imaging characterization of canine splenic lesions. *Journal of Veterinary Internal Medicine*. 2008;22: 1095-1102.
7. Rossi F, Leone VF, Vignoli M, Laddaga E, Terragni R. Use of contrast-enhanced ultrasound for characterization of focal splenic lesions. *Veterinary Radiology & Ultrasound*. 2008;49: 154-164.
8. Haers H, Vignoli M, Paes G, Rossi F, Taeymans O, Daminet S, et al. Contrast Harmonic Ultrasonographic Appearance of Focal Space-Occupying Renal Lesions. *Veterinary Radiology & Ultrasound*. 2010;51: 516-522.
9. Haers H, Daminet S, Smets PMY, Duchateau L, Aresu L, Saunders JH. Use of quantitative contrast-enhanced ultrasonography to detect diffuse renal changes in Beagles with iatrogenic hypercortisolism. *American Journal of Veterinary Research*. 2013;74: 70-77.
10. Diana A, Specchi S, Baron Toaldo M, Chiochetti R, Laghi A, Cipone M. Contrast-enhanced ultrasonography of the small bowel in healthy cats. *Veterinary Radiology & Ultrasound*. 2011;52: 555-559.
11. Kinns J, Aronson L, Hauptman J, Seiler G. Contrast-enhanced ultrasound of the feline kidney. *Veterinary Radiology & Ultrasound*. 2010;51: 168-172.

12. Leinonen MR, Raekallio MR, Vainio OM, Ruohoniemi MO, Biller DS, O'Brien RT. Quantitative contrast-enhanced ultrasonographic analysis of perfusion in the kidneys, liver, pancreas, small intestine, and mesenteric lymph nodes in healthy cats. *American Journal of Veterinary Research*. 2010;71: 1305-1311.
13. Rademacher N, Ohlerth S, Scharf G, Lalahova D, Sieber-Ruckstuhl N, Alt M, et al. Contrast-Enhanced Power and Color Doppler Ultrasonography of the Pancreas in Healthy and Diseased Cats. *Journal of Veterinary Internal Medicine*. 2008;22: 1310-1316.
14. Lulich JP, Osborne CA, O'Brien TD, Polzin DJ. Feline Renal-Failure - Questions, Answers, Questions. *Compendium on Continuing Education for the Practicing Veterinarian*. 1992;14: 127-152.
15. Greene SA, Grauer GF. *Veterinary anesthesia and analgesia*. Iowa, USA: Wiley Blackwell, 2007.
16. Regan MC, Young LS, Geraghty J, Fitzpatrick JM. Regional renal blood flow in normal and disease states. *Urological Research*. 1995;23: 1-10.
17. Leinonen MR, Raekallio MR, Vainio OM, O'Brien RT. Effect of anaesthesia on contrast-enhanced ultrasound of the feline spleen. *Veterinary Journal*. 2011;190: 273-277.
18. Leinonen MR, Raekallio MR, Vainio OM, Ruohoniemi MO, O'Brien RT. The effect of the sample size and location on contrast ultrasound measurement of perfusion parameters. *Veterinary Radiology & Ultrasound*. 2011;52: 82-87.
19. Hosgood G. Pharmacologic features of butorphanol in dogs and cats. *Journal of the American Veterinary Medical Association*. 1990;196: 135-136.
20. Short CE, Bufalari A. Propofol anesthesia. *Veterinary Clinics of North America: Small Animal Practice*. 1999;29: 747-778.
21. Wouters PF, Van de Velde MA, Marcus MA, Deruyter HA, Van Aken H. Hemodynamic changes during induction of anesthesia with etanalone and propofol in dogs. *Anesthesia and Analgesia*. 1995;81: 125-131.
22. Nyman HT, Kristensen AT, Kjelgaard-Hansen M, McEvoy FJ. Contrast-enhanced ultrasonography in normal canine liver. Evaluation of imaging and safety parameters. *Veterinary Radiology & Ultrasound*. 2005;46: 243-250.
23. Waller KR, O'Brien RT, Zagzebski JA. Quantitative contrast ultrasound analysis of renal perfusion in normal dogs. *Veterinary Radiology & Ultrasound*. 2007;48: 373-377.

Chapter V Influence of sedation and anesthesia

24. Biermann K, Hungerbuhler S, Mischke R, Kastner SB. Sedative, cardiovascular, haematologic and biochemical effects of four different drug combinations administered intramuscularly in cats. *Veterinary Anaesthesia and Analgesia*. 2012;39: 137-150.
25. Restitutti F, Laitinen MR, Raekallio MR, Vainionpaa M, O'Brien RT, Kuusela E, et al. Effect of MK-467 on organ blood flow parameters detected by contrast-enhanced ultrasound in dogs treated with dexmedetomidine. *Veterinary Anaesthesia and Analgesia*. 2013;40: E48-E56.
26. Muir W, Lerche P, Wiese A, Nelson L, Pasloske K, Whittem T. The cardiorespiratory and anesthetic effects of clinical and supraclinical doses of alfaxalone in cats. *Veterinary Anaesthesia and Analgesia*. 2009;36: 42-54.
27. Ramoo S, Bradbury LA, Anderson GA, Abraham LA. Sedation of hyperthyroid cats with subcutaneous administration of a combination of alfaxalone and butorphanol. *Australian Veterinary Journal*. 2013;91: 131-136.

CHAPTER VI
INFLUENCE OF AGEING ON CONTRAST-ENHANCED ULTRASOUND OF FELINE KIDNEYS
IN HEALTHY CATS

Adapted from:

Stock E., Paepe D., Daminet S., Duchateau L., Saunders J.H.*, Vanderperren K.* (*shared senior authorship). Influence of ageing on quantitative contrast-enhanced ultrasound of the kidneys in healthy cats. *Veterinary Record. Under revision.*

1. Abstract

The degenerative effects of ageing on the kidneys have been extensively studied in humans. However, only recently interest has been addressed to renal ageing in veterinary medicine. Contrast-enhanced ultrasound is a relatively new technique allowing non-invasive evaluation of renal perfusion in conscious cats. Renal perfusion parameters were obtained in 43 healthy cats ageing 1 to 16 years old, and the cats were divided in 4 age categories: 1-3 years, 3-6 years, 6-10 years and > 10 years. Routine renal parameters as serum creatinine, serum urea, urine specific gravity, urinary protein:creatinine ratio, and systolic blood pressure were also measured. No significant differences in any of the perfusion parameters were observed among the different age categories. A trend towards a lower peak enhancement and wash-in area-under-the-curve with increasing age, suggestive for a lower blood volume, was detected when comparing the cats > 10 years with the cats between 1 and 3 years. Additionally, no significant age-effect was observed for the serum and urine parameters, whereas a higher blood pressure was observed in healthy cats between 3-6 years and > 10 years.

2. Introduction

Renal ageing has been a hot topic in human research for several years, whereas it has only recently gained interest in veterinary medicine.^{1, 2} The population of senior and geriatric cats has been increasing in the past years.³⁻⁵ Consequently, effects of ageing on animal health have grown more interest and more attention is paid to health screening in elderly cats.⁶

In people, ageing is associated with structural changes accompanied by progressive deterioration of renal function. A reduction in renal mass and glomerular number is present in elderly people, paralleled by an increased percentage of sclerotic glomeruli.¹ Moreover, glomerular filtration rate (GFR) and renal plasma flow decrease with age, whereas renal vascular resistance increases.^{1, 7, 8} The reduction in renal blood flow is believed to be primary and precede the changes in GFR and renal morphology.⁸ This decline appears to be a part of the normal physiologic process of cellular and organ senescence.¹ Information on the influence of ageing on renal morphology and function in veterinary medicine is limited. An age-related decrease in GFR have been described in small breed dogs.⁹ In one study, a lower GFR was present in older cats compared to young cats as measured with the exogenous creatinine clearance test however, no age-effect was present when GFR was

measured with exo-iohexol, endo-iohexol and chromium-51 ethylenediaminetetraacetic acid.^{9,10} A higher serum creatinine concentration (sCr) has been found in elderly cats.^{6,9,11}

Contrast-enhanced ultrasound (CEUS) is a functional imaging technique that allows evaluation of tissue perfusion through the use of intravenously injected contrast agent. The ultrasound contrast agent is composed of millions of microbubbles, which are tiny gas filled spheres, stabilized by an outer shell. These microbubbles have a size similar to those of red blood cells; consequently they do not pass the endothelium and remain strictly intravascular.^{12,13} Promising results have been obtained with CEUS for the evaluation of diffuse renal disorders in both human and veterinary medicine.¹⁴⁻¹⁸

The objective of this study was to determine the effect of age on several perfusion parameters obtained with CEUS of the kidneys in healthy cats divided in 4 age groups. The hypothesis was that ageing would be associated with a decline in renal blood volume and a higher vascular resistance seen as a decrease in slope of the time-intensity curve.

3. Materials and methods

Healthy cats of ≥ 1 year were included. The cats were divided into 4 age groups: group 1 (1-3 years), group 2 (3-6 years), group 3 (6-10 years) and group 4 (> 10 years). Ten to 12 cats were included in each group. Cats were considered healthy if no significant abnormalities were reported in the history, nor detected on physical examination, complete blood count, serum biochemistry profile, thoracic radiographs, and abdominal ultrasound. Cats with both sCr $> 161.8 \mu\text{mol/L}$ ¹¹ and urine specific gravity < 1.035 were excluded. Only cats free of any medication for at least 2 months were included.

The study protocol was approved by the local ethical committee of the Faculty of Veterinary Medicine, Ghent University, Belgium (EC2015/68) and the Deontological Committee of the Belgian Federal Agency for the Safety of the Food Chain. All owners were informed about the study and gave their written consent.

A routine physical exam, including non-invasive measurement of the systolic blood pressure (SBP) by Doppler ultrasonic technique, was performed in all cats. Thyroid palpation was performed in all cats ≥ 6 years. Five mL of blood was collected by jugular venipuncture. Blood work consisted of

complete blood count and serum biochemistry, including total thyroxine (T4) level in cats of ≥ 6 years. Five to 10 mL of urine was collected by ultrasound-guided cystocentesis. Urinalysis included sediment analysis as described in Paepe et al.(2013)⁶, urine specific gravity (USG), urinary protein:creatinine ratio (UPC), dipstick, and urine culture. Thoracic radiographs (left-right lateral and ventrodorsal projections) and complete abdominal ultrasound were performed.

For the administration of ultrasound contrast agent, a 22-Gauge indwelling catheter was placed in the cephalic vein. The hair was clipped over the ventrolateral aspect of the abdomen and coupling gel was applied to the skin. The ultrasound examinations were performed with the unsedated cat manually restrained in dorsal recumbency. The kidney of interest was centered on the screen and was imaged in a longitudinal plane using dual-screen (simultaneous display of conventional B-mode and contrast-mode image). The transducer was manually positioned during each imaging procedure and was maintained at the same position during the CEUS examination.

The contrast agent (Sonovue®, Bracco, Italy), 0.05 mL/kg, was injected IV (bolus injection over +/- 3 s) followed by injection of 1.5 mL saline bolus. A three-way stopcock was used to avoid any delay between the injection of contrast agent and saline. The same person performed the injection in a standardized way. Three to 4 injections of contrast were performed: two for the left kidney, one for the right kidney and one for the caudal abdominal aorta in 14 cats. Between subsequent injections, to avoid artifacts, remnant microbubbles were destroyed by setting the acoustic power at the highest level and scanning the caudal aspect of the abdominal aorta for approximately 2 minutes.

All examinations were performed using a linear transducer of 12-5 MHz on a dedicated machine (iU22, Philips) equipped with contrast-specific software. Basic technical parameters were a single focus placed under the kidney, persistency off, mechanical index 0.09, high dynamic range setting (C50), timer started at the beginning of the injection, gain 85% (corresponding to a nearly dark/anechoic image before USCA administration). The settings were repeated during each injection. All studies were digitally registered as a movie clip at a rate of 9 frames per second, during 90 seconds.

The clips were exported in DICOM format and analyzed using specialized computer software (VueBox®, Bracco Suisse SA, Geneva, Switzerland) for objective quantitative analysis. Six regions-of-interest (ROIs) were manually drawn: 3 in the renal cortex, 2 in the renal medulla and 1 on an interlobar artery. The ROI's were similar in size and drawn at the same depth for every region (4

mm diameter for the cortex, 3 mm diameter for the medulla and 1-1.5 mm diameter for the interlobar artery). For every ROI, the software determined mean pixel intensity as a function of time creating a time-intensity curve. Time-intensity curves were analyzed for peak enhancement (PE), wash-in area under the curve (WiAUC), rise time (RT), mean transit time (mTT), time to peak (TTP), wash-in rate (WiR), wash-in perfusion index (WiPI; WiAUC/RT), wash-out area under the curve (WoAUC), total area under the curve (AUC), fall time (FT), and wash-out rate (WoR). The values for the 3 ROIs in the renal cortex and 2 ROIs in the renal medulla were averaged. Peak enhancement, for the cortex and medulla were normalized to the values obtained for the interlobar artery (PE*) and the aorta (PE_{A0}).

Statistical analyses were performed with SAS (SAS version 9.4, SAS Institute Inc.). Perfusion parameters obtained with CEUS, sCr, serum urea, USG, UPC and, SBP were compared among the different age groups, using a linear fixed effects model with age as categorical fixed effect. A global significance level of 5% was used and adjusted P-values (Tukey's multiple comparisons technique) were calculated for pairwise comparisons.

4. Results

Forty-three cats were included: 41 domestic short- or longhaired cats, and 2 Ragdoll cats. The mean \pm standard error age of the total population was 6.5 ± 0.6 years, with 10 cats group 1, 11 cats in group 2, 12 cats in group 3 and 10 cats in group 4. The mean \pm standard error body weight was 4.0 ± 0.1 kg, with the body condition score ranging from 4/9 to 8/9. No significant abnormalities were seen on thoracic x-rays and routine abdominal ultrasound. The kidneys of all cats were normal in size (3.0 – 4.6 cm), had a smooth, regular outline and a normal internal architecture.¹⁹

Systolic blood pressure, sCr, serum urea, USG and UPC are summarized in Table 1. No significant differences for sCr, serum urea, USG and UPC were observed among the different age groups. A significantly higher SBP was present in group 2 compared to group 1 (P=0.043), and in group 4 compared to group 1 (P=0.005). Six cats in the total population had SBP > 160 mmHg, 1 cat in group 2, 1 cat, in group 3 and 4 cats in group 4.

Variables	Group 1 (n=10)	Group 2 (n=11)	Group 3 (n=12)	Group 4 (n=10)	Reference values
Blood pressure (mmHg)	122.0 ± 7.6 ^a	152.0 ± 7.6 ^b	142.5 ± 6.1	159.4 ± 6.7 ^{ab}	
sCr (µmolL ⁻¹)	107.5 ± 7.1	109.5 ± 7.1	103.9 ± 6.2	117.8 ± 7.1	64.5 – 161.8
Serum urea (mmolL ⁻¹)	8.9 ± 0.5	7.7 ± 0.5	7.6 ± 0.4	8.3 ± 0.5	6.2 – 12.7
USG	1.049 ± 0.003	1.046 ± 0.003	1.050 ± 0.003	1.043 ± 0.003	
UPC	0.11 ± 0.02	0.11 ± 0.02	0.18 ± 0.02	0.16 ± 0.02	< 0.40

Table 1. Baseline characteristics for the included cats divided into 4 age groups.

The data are expressed as mean ± standard error. Groups with the same letter differ significantly from each other (group 1 = 1 to 3 years; group 2 = 3 to 6 years; group 3 = 6 to 10 years; group 4 = > 10 years; SBP = systolic blood pressure; sCr = serum creatinine; USG = urine specific gravity; UPC = urinary protein:creatinine ratio)

No significant differences between the age groups were present for any of the perfusion parameters obtained with CEUS. However, a tendency towards a lower PE (P=0.078) and WiAUC (P=0.078) for the renal cortex were present when comparing group 1 and 4.

The CEUS parameters for the renal cortex and medulla are summarized in Table 2. Figure 1 illustrates the normal perfusion pattern of the kidney in healthy cats.

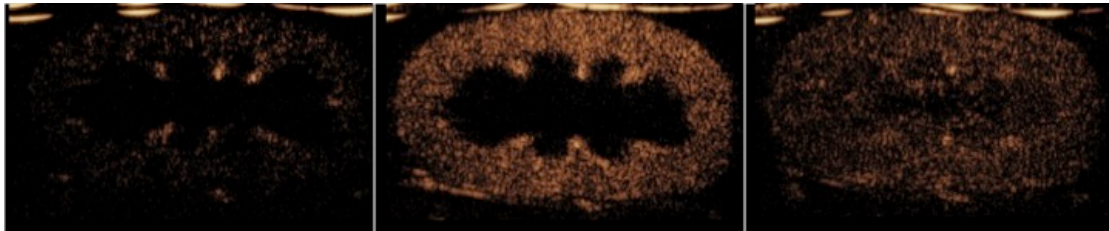


Figure 1. Sequential CEUS images demonstrating the normal perfusion pattern obtained with contrast-enhanced ultrasound of the kidney in healthy cats. Early enhancement of the interlobar arteries (5 s), followed by peak cortical enhancement (7 s) and a late corticomedullary phase (20 s).

Variable, by location	Group 1 (n=10)	Group 2 (n=11)	Group 3 (n=12)	Group 4 (n=10)
Renal cortex				
PE	2355.14 ± 294.54	1917.34 ± 298.90	1459.44 ± 258.33	1303.77 ± 303.47
PE*	30.45 ± 4.35	30.82 ± 4.35	26.74 ± 3.71	24.58 ± 4.71
PE _{A0}	13.18 ± 3.50	9.84 ± 4.79	4.81 ± 5.35	2.80 ± 10.78
WiAUC	3780.25 ± 414.94	2765.83 ± 420.67	2471.70 ± 363.92	2297.94 ± 426.65
RT	2.74 ± 0.12	2.53 ± 0.12	2.85 ± 0.11	2.95 ± 0.13
mTT	19.00 ± 1.98	23.09 ± 2.01	21.90 ± 1.74	22.65 ± 2.05
TTP	7.60 ± 0.28	7.17 ± 0.28	7.87 ± 0.25	8.05 ± 0.28
WiR	1186.28 ± 181.47	1094.59 ± 184.29	699.69 ± 159.16	606.15 ± 187.24
WiPI	1440.90 ± 179.61	1174.22 ± 182.27	893.89 ± 157.53	799.12 ± 185.06
WoAUC	4993.57 ± 520.00	3693.11 ± 527.27	3333.16 ± 456.07	3099.85 ± 534.85
FT	3.81 ± 0.21	3.49 ± 0.22	3.94 ± 0.19	4.10 ± 0.22
WoR	793.18 ± 138.91	751.03 ± 141.38	462.15 ± 121.83	508.60 ± 143.99
Renal medulla				
PE	209.49 ± 222.25	203.36 ± 216.32	191.75 ± 188.58	152.66 ± 228.69
PE*	2.88 ± 0.69	3.62 ± 0.68	2.89 ± 0.59	3.06 ± 0.73
PE _{A0}	0.90 ± 0.20	1.06 ± 0.27	0.92 ± 0.32	0.65 ± 0.67
WiAUC	1167.18 ± 369.43	2288.19 ± 363.53	1721.03 ± 317.68	1498.01 ± 375.62
RT	14.96 ± 1.52	19.36 ± 1.50	16.08 ± 1.31	16.70 ± 1.55
mTT	103.20 ± 31.59	121.79 ± 31.09	111.21 ± 27.17	113.83 ± 32.12
TTP	25.98 ± 1.69	30.01 ± 1.66	27.42 ± 1.45	26.25 ± 1.72
WiR	25.53 ± 189.59	17.20 ± 184.53	21.66 ± 160.87	15.74 ± 195.08
WiPI	130.63 ± 135.99	128.58 ± 132.36	120.53 ± 115.39	96.74 ± 139.93
WoAUC	2904.03 ± 629.50	4799.73 ± 629.50	3158.24 ± 542.59	2698.69 ± 676.65
FT	29.63 ± 3.78	39.17 ± 3.78	31.11 ± 3.25	29.67 ± 4.08
WoR	13.19 ± 153.90	8.28 ± 153.90	11.32 ± 130.59	8.07 ± 168.59

Table 2. Perfusion parameters obtained with CEUS of healthy cats divided into 4 age groups. The data are expressed as mean ± standard error. (group 1 = 1 to 3 years; group 2 = 3 to 6 years; group 3 = 6 to 10 years; group 4 = > 10 years; PE = peak enhancement; PE* = peak enhancement normalized to interlobar artery; PE_{A0} = peak enhancement normalized to the aorta; WiAUC = wash-in area-under-the curve; RT = rise time; mTT = mean transit time; TTP = time-to-peak; WiR = wash-in rate; WiPI = wash-in perfusion index; WoAUC = wash-out area-under-the-curve;; FT = fall time; WoR = wash-out rate)

5. Discussion

To our knowledge, this is the first study assessing the age-effect on renal perfusion in healthy cats. No significant changes in renal perfusion parameters were noticed in this study. However a tendency towards a lower PE and WiAUC was present in elderly cats, indicating a decrease in renal blood volume with age. This corresponds to the findings in human studies, where a reduction in renal blood flow is considered to be a typical functional finding with increasing age.^{1, 7, 8, 20} Moreover, the renal blood flow reduction in elderly people is believed to be primary and leading to a reduction in GFR and morphologic renal changes.⁸ In humans, age-related changes involve mainly

the renal cortex whereas the medulla is usually unaffected corresponding to the findings in our study.⁸ Typical morphological changes in elderly people are increased glomerular sclerosis, reduction in glomerular volume, decrease area and hyalinization of afferent arterioles, and tubulointerstitial fibrosis.^{1,7,8,21} Similarly in ageing dogs, glomerulosclerosis, interstitial fibrosis and lipofuscin accumulation have been described.^{2,22} In contrast, no vascular morphologic changes were present in aged beagles.²² In dogs, structural changes in ageing kidneys may be clinically silent and not associated with functional deterioration as reported in humans.² A lower GFR was detected in geriatric small breed dogs, whereas no decline was seen in ageing large breed dogs.⁹ Variable results are found for sCr in dogs, however no clinical significant changes were noticed as sCr remained within normal reference intervals in all dogs.^{9,23} No age-related differences in several urinary markers as urinary albumin:creatinine ratio, urinary C-reactive protein:creatinine ratio, urinary retinol binding protein:creatinine ratio and urinary N-acetyl-beta-D-glucosaminidase:creatinine ratio, are reported in healthy dogs.²⁴ Research in ageing cats is even more limited. An age-effect on GFR was only reported in one study using an exogenous creatinine clearance test, whereas no age-effect was seen in other studies.^{9,10} Higher sCr and serum urea is has been described in geriatric cats.^{6,11} However, in our study, no age-effect on sCr was noted.

Age-related effects on time-based parameters or parameters related to the slope of the time-intensity curve were not observed in this study. Renal resistance is reported to increase in ageing people, commonly noted as an increase in intrarenal Doppler indices.²⁵ Nevertheless, a significant age-effect on the resistive index was also not detected in a study on 24 healthy cats.²⁶

A significantly higher SBP was present in group 4 compared to group 1. The blood pressure in group 2 was also higher compared to group 1. An age effect on SBP has previously been described in several studies in cats.^{6,11,27} Efforts were made to reduce stress-related hypertension due to the 'white coat effect', however single SBP measurements as done in this study are not sufficient to diagnose hypertension.²⁸ An underlying cause for hypertension was not found by the basic work-up included in this study. Further work-up and serial assessment of SBP was beyond the scope of our study.

The main limitation of this study is the low number of cats in each group, and even more the low number of geriatric cats.

Chapter VI Influence of ageing in healthy cats

In conclusion, no significant age-related effects on renal perfusion parameters obtained with CEUS were detected in this study. However, a tendency towards lower PE and WiAUC, indicative for a lower blood volume, was present in geriatric cats. Further studies including a larger number of geriatric cats are needed to confirm these findings and determine the clinical relevance of these findings.

Acknowledgements

The authors want to thank Bracco Suisse SA (Geneva, Switzerland) for their scientific support on the use of VueBox® and Medvet (Antwerp, Belgium) for the laboratory analyses.

6. References

1. Esposito C, Plati A, Mazzullo T, Fasoli G, De Mauri A, Grosjean F, et al. Renal function and functional reserve in healthy elderly individuals. *Journal of Nephrology*. 2007;20: 617-625.
2. Cianciolo RE, Benali SL, Aresu L. Aging in the canine Kidney. *Veterinary Pathology*. 2016;53: 299-308.
3. Laflamme DP, Abood SK, Fascetti AJ, Fleeman LM, Freeman LM, Michel KE, et al. Pet feeding practices of dog and cat owners in the United States and Australia. *Journal of the American Veterinary Medical Association*. 2008;232: 687-694.
4. Lund EM, Armstrong PJ, Kirk CA, Kolar LM, Klausner JS. Health status and population characteristics of dogs and cats examined at private veterinary practices in the United States. *Journal of the American Veterinary Medical Association*. 1999;214: 1336-1341.
5. Lawler DF, Evans RH, Chase K, Eilersieck M, Li Q, Larson BT, et al. The aging feline kidney: a model mortality antagonist? *Journal of Feline Medicine and Surgery*. 2006;8: 363-371.
6. Paepe D, Verjans G, Duchateau L, Piron K, Ghys L, Daminet S. Routine health screening: findings in apparently healthy middle-aged and old cats. *Journal of Feline Medicine and Surgery*. 2013;15: 8-19.
7. Fliser D, Zeier M, Nowack R, Ritz E. Renal functional reserve in healthy elderly subjects. *Journal of the American Society of Nephrology*. 1993;3: 1371-1377.
8. Hollenberg NK, Adams DF, Solomon HS, Rashid A, Abrams HL, Merrill JP. Senescence and the renal vasculature in normal man. *Circulation Research*. 1974;34: 309-316.
9. Miyagawa Y, Takemura N, Hirose H. Assessments of factors that affect glomerular filtration rate and indirect markers of renal function in dogs and cats. *Journal of Veterinary Medical Science*. 2010;72: 1129-1136.
10. van Hoek I, Vandermeulen E, Duchateau L, Lefebvre H, Croubels S, Peremans K, et al. Comparison and reproducibility of plasma clearance of exogenous creatinine, exo-iohexol, endo-iohexol and ⁵¹Cr-EDTA in young adult and aged healthy cats. *Journal of Veterinary Internal Medicine*. 2007;21: 950-958.
11. Ghys LF, Paepe D, Duchateau L, Taffin ER, Marynissen S, Delanghe J, et al. Biological validation of feline serum cystatin C: The effect of breed, age and sex and establishment of a reference interval. *Veterinary Journal*. 2015;204: 168-173.

12. Haers H, Saunders JH. Review of clinical characteristics and applications of contrast-enhanced ultrasonography in dogs. *Journal of the American Veterinary Medical Association*. 2009;234: 460-470.
13. Ohlerth S, O'Brien RT. Contrast ultrasound: General principles and veterinary clinical applications. *Veterinary Journal*. 2007;174: 501-512.
14. Dong Y, Wang WP, Cao J, Fan P, Lin X. Early assessment of chronic kidney dysfunction using contrast-enhanced ultrasound: a pilot study. *British Journal of Radiology*. 2014;87: 1-7.
15. Dong Y, Wang WP, Cao JY, Fan PL, Lin XY. Quantitative evaluation of contrast-enhanced ultrasonography in the diagnosis of chronic ischemic renal disease in a dog model. *Plos One*. 2013;8: e70377.
16. Hosotani Y, Takahashi N, Kiyomoto H, Ohmori K, Hitomi H, Fujioka H, et al. A new method for evaluation of split renal cortical blood flow with contrast echography. *Hypertension Research*. 2002;25: 77-83.
17. Tsuruoka K, Yasuda T, Koitabashi K, Yazawa M, Shimazaki M, Sakurada T, et al. Evaluation of renal microcirculation by contrast-enhanced ultrasound with sonazoid (TM) as a contrast agent. *International Heart Journal*. 2010;51: 176-182.
18. Haers H, Daminet S, Smets PMY, Duchateau L, Aresu L, Saunders JH. Use of quantitative contrast-enhanced ultrasonography to detect diffuse renal changes in Beagles with iatrogenic hypercortisolism. *American Journal of Veterinary Research*. 2013;74: 70-77.
19. Debruyne K, Haers H, Combes A, Paepe D, Peremans K, Vanderperren K, et al. Ultrasonography of the feline kidney. Technique, anatomy and changes associated with disease. *Journal of Feline Medicine and Surgery*. 2012;14: 794-803.
20. Davies DF, Shock NW. Age changes in glomerular filtration rate, effective renal plasma flow, and tubular excretory capacity in adult males. *Journal of Clinical Investigation*. 1950;29: 496-507.
21. Yoon HE, Kim EN, Kim MY, Lim JH, Jang IA, Ban TH, et al. Age-Associated Changes in the Vascular Renin-Angiotensin System in Mice. *Oxidative Medicine and Cellular Longevity*. 2016: 6731093.
22. Smets PM, Lefebvre HP, Aresu L, Croubels S, Haers H, Piron K, et al. Renal function and morphology in aged Beagle dogs before and after hydrocortisone administration. *Plos One*. 2012;7: e31702.

Chapter VI Influence of ageing in healthy cats

23. Lowseth LA, Gillett NA, Gerlach RF, Muggenburg BA. The effects of aging on hematology and serum chemistry values in the beagle dog. *Veterinary Clinical Pathology*. 1990;19: 13-19.
24. Smets PMY, Meyer E, Maddens BEJ, Duchateau L, Daminet S. Urinary Markers in Healthy Young and Aged Dogs and Dogs with Chronic Kidney Disease. *Journal of Veterinary Internal Medicine*. 2010;24: 65-72.
25. Terry JD, Rysavy JA, Frick MP. Intrarenal Doppler: characteristics of aging kidneys. *Journal of Ultrasound in Medicine*. 1992;11: 647-651.
26. Tipisca V, Murino C, Cortese L, Mennonna G, Auletta L, Vulpe V, et al. Resistive index for kidney evaluation in normal and diseased cats. *Journal of Feline Medicine and Surgery*. 2015;18: 471-475.
27. Sansom J, Rogers K, Wood JL. Blood pressure assessment in healthy cats and cats with hypertensive retinopathy. *American Journal of Veterinary Research*. 2004;65: 245-252.
28. Brown S, Atkins C, Bagley R, Carr A, Cowgill L, Davidson M, et al. Guidelines for the identification, evaluation, and management of systemic hypertension in dogs and cats. *Journal of Veterinary Internal Medicine*. 2007;21: 542-558.

CHAPTER VII
EVALUATION OF FELINE RENAL PERFUSION AFTER ANGIOTENSIN-II
INFUSION WITH CONTRAST-ENHANCED ULTRASONOGRAPHY AND
SCINTIGRAPHY

Adapted from:

Stock E, Vanderperren K, Bosmans T, Dobbeleir A, Duchateau L, Hesta M, Lybaert L, Peremans K, Vandermeulen E, Saunders J. Evaluation of feline renal perfusion with contrast-enhanced ultrasonography and scintigraphy. PLoS ONE 2016, 11: e0164488.

1. Abstract

Contrast-enhanced ultrasound (CEUS) is an emerging technique to evaluate tissue perfusion. Promising results have been obtained in the evaluation of renal perfusion in health and disease, both in human and veterinary medicine. Renal scintigraphy using ^{99m}Tc -Mercaptoacetyltriglycine (MAG_3) is another non-invasive technique that can be used to evaluate renal perfusion. However, no data are available on the ability of CEUS or ^{99m}Tc - MAG_3 scintigraphy to detect small changes in renal perfusion in cats. Therefore, both techniques were applied in a normal feline population to evaluate detection possibilities of perfusion changes by angiotensin II (AT II).

Contrast-enhanced ultrasound using a bolus injection of commercially available contrast agent and renal scintigraphy using ^{99m}Tc - MAG_3 were performed in 11 healthy cats after infusion of 0.9% NaCl (control) and AT II.

AT II induced changes were noticed on several CEUS parameters. Mean peak enhancement, wash-in perfusion index and wash-out rate for the entire kidney decreased significantly after AT II infusion. Moreover, a tendency towards a lower wash-in area-under-the curve was present. Renal scintigraphy could not detect perfusion changes induced by AT II.

This study shows that CEUS is able to detect changes in feline renal perfusion induced by AT II infusion.

2. Introduction

Chronic kidney disease is of major importance in both human and veterinary medicine with a prevalence of 13% in people and even up to 50% in randomly selected cats, increasing to 68.8% in cats with degenerative joint disease.¹⁻³ It is a progressive disorder with often an unclear etiology. Early diagnosis is essential as intervention in early stage of the disease process may provide better life expectancy and quality of life.⁴ The assessment of renal perfusion is an important component in the evaluation of kidney disease as these renal perfusion changes occur early in the disease process.⁵

However, performing an accurate, noninvasive measurement of renal perfusion is challenging. The gold standard to estimate renal plasma flow is determination of para-amino hippuric acid (PAH) clearance, although this is technically laborious and requires specific equipment, limiting the use in clinical circumstances.⁶

Renal perfusion can also be evaluated using radioactive tracers: OIH and MAG_3 . Both tracers have high first-pass extraction rate, but do not reach an extraction rate of 100%, thus the term 'effective renal plasma flow' (ERPF) is used.⁷ OIH has a similar chemical structure to PAH, and can be bound to ^{123}I or ^{131}I . Although the disadvantage is poor quality images compromising quantification, the tracer is still useful for blood clearance techniques.⁷ MAG_3 can be labeled with $^{99\text{m}}\text{Tc}$, making it a good tracer for imaging procedures.⁷ Despite its 30% lower clearance compared to OIH, high agreement between both tracers was found in both humans and dogs.^{8,9} Significant hepatic uptake of MAG_3 is noted in cats, requiring camera-based investigation as it allows distinction of the separate organs.¹⁰ Some limitations are associated with the use of radioactive tracers, including costs, involvement of radiation, and limited equipment availability.

CEUS is a functional ultrasound technique that allows assessment of both macro- and microcirculation. Ultrasound contrast agent consists of tiny gas-filled bubbles (microbubbles) that have a rheology similar to red blood cells after intravenous injection.¹¹ It is an extremely safe, cost-effective technique, which does not involve the use of ionizing radiation.^{12,13} The rate of adverse effects is close to zero, and, in contrast to iodinated contrast agents used in computed tomography or gadolinium-based contrast agent used in magnetic resonance imaging, no nephrotoxicity is involved, allowing safe use in geriatric and pediatric patients and patients with renal insufficiency.¹² Several studies in human medicine have shown promising results for the use of CEUS in the diagnosis of diffuse renal disorders, such as early assessment of chronic kidney dysfunction, diabetic kidney damage, and rejection of renal transplants.¹⁴⁻¹⁸ In dogs, CEUS was proven to be useful for the early detection of iatrogenic chronic ischemic renal disease and to detect diffuse renal changes in beagles with iatrogenic hypercortisolism.^{19,20} Nevertheless, it remains unclear if small changes in renal perfusion can be detected using a bolus injection of ultrasound contrast agent in cats.

The objective of this study was to investigate the ability of CEUS and renal scintigraphy using $^{99\text{m}}\text{Tc}$ - MAG_3 to detect changes in renal perfusion of healthy cats at baseline and during infusion of AT II (an arterial vasoconstrictor).

3. Materials and methods

Animals

The study was carried out in strict accordance with the recommendations of the European Convention for the Protection of Vertebrate Animals used for Experimental and other Scientific Purposes. The protocol was approved by the Ethical Committee of the Faculty of Veterinary Medicine of Ghent University (EC2014/38). All efforts were made to minimize suffering. During the experiments, the cats were continuously monitored by experienced veterinarians to assess basic clinical parameters and signs of discomfort. Since suffering was limited and no detrimental effect on further life quality was present, the cats are further kept as experimental animals.

Eleven healthy purpose-bred European Shorthair cats (Charles River Laboratories (30/3202), France and Lab of animal nutrition (LA2400378), Ghent university, Belgium) without any history of cardiovascular, renal or endocrine disease were included. They were judged healthy based on physical examination and non-invasive Doppler blood pressure measurement, hematology, biochemistry profile, urinalysis, and abdominal ultrasound. Both kidneys of all cats had a normal size and appearance on ultrasound. The mean \pm standard error age of the cats 5.29 ± 0.4 years, with a mean \pm standard error body weight of 3.53 ± 0.2 kg; body condition score 4-5/9). Eight cats were female, 3 were male, and all of them were neutered. The cats were housed indoor in stable groups of 10 cats, with free access to water, and fed a standard dry food twice a day.

Study design

The cats were premedicated with butorphanol (Dolorex, 10 mg/ml, MSD animal health) 0.2 mg/kg IV, 20 minutes before anesthesia induction. Anesthesia was induced with propofol (Propovet®, 10 mg/ml, Abbott Laboratories) IV given to effect (6.30 ± 1.13 mg/kg), until endotracheal intubation could be performed. Anesthesia was maintained with isoflurane vaporized in 100% oxygen, using a non-rebreathing system, to reach an end tidal isoflurane percentage of 1.2 – 1.4%.

All the subjects received a vasoconstrictor (AT II) and a control treatment (0.9% sodium chloride), in a randomized order, with a washout period of 14 days. Vasoconstriction was obtained with an infusion of AT II at a rate of 2 ng/kg/min using a syringe pump (Perfusor Space, BBraun, Germany) for the total duration of the CEUS study and renal scintigraphy. Cats undergoing control treatment

Chapter VII Perfusion changes induced by angiotensin II infusion

received an infusion of sterile 0.9% sodium chloride at the same rate and total volume as the AT II infusion. Infusion was started 5 minutes after the start of the inhalation anesthesia. On each study day, renal perfusion was evaluated using CEUS and MAG_3 scintigraphy, started 15 minutes after initiation of the intravenous infusion of AT II or 0.9% sodium chloride. The imaging techniques were performed in a randomized order.

Blood pressure (non-invasive Doppler measurement), heart rate, peripheral arterial oxygen saturation, end tidal isoflurane and carbon dioxide concentrations were closely monitored.

Preparation AT II

A stock solution (1000 $\mu\text{g}/\text{mL}$) was prepared by adding 1 mg of anhydrous AT II (Sigma-Aldrich, USA) to 1 mL of sterile 0.9% sodium chloride solution. This solution was filtered through a 0.22 μm filter (Steriflip Vacuum Filtration System with millipore Express PLUS membrane, Millipore Corporation, Belgium), aliquoted into sterile cryovials (100 μL per vial), and stored at -80°C . On the study day, 1 aliquot was thawed on ice and serially diluted in sterile 0.9% NaCl solution to produce solutions with final concentration of 0.1 $\mu\text{g}/\text{mL}$.

Contrast-enhanced ultrasound

The hair was clipped over the ventrolateral aspect of the abdomen. Alcohol and coupling gel were applied to the skin. The US exams were performed with the cat in dorsal recumbency.

The left kidney was centered on the screen and imaged in a longitudinal plane. The transducer was manually positioned by the same person during each imaging procedure and was maintained at the same position during the CEUS examination.

A 0.15 mL bolus of sulfur hexafluoride-filled microbubbles (Sonovue[®], Bracco, Italy) was injected into a 22-Gauge indwelling catheter in the cephalic vein. The same person performed the bolus injection in a standardized way in all cats. The ultrasound contrast agent was injected over approximately 3 seconds followed by injection of 1 mL saline bolus. A three-way stopcock was used to minimize delay between the injection of microbubbles and saline. Three injections of contrast were performed: the first injection was not used for further evaluation. Between subsequent injections, remnant microbubbles were destroyed in the caudal abdominal aorta by setting the acoustic power at the highest level during 2 minutes.

All examinations were performed using a linear transducer of 12-5 MHz on a dedicated machine (iU22, Philips, Bothell, WA) with contrast-specific software. Basic technical parameters were a high dynamic range setting (50 dB), single focus placed directly under the kidney, persistency off, mechanical index 0.09, timer started at the beginning of the injection. For the gain setting, we started with a nearly dark/anechoic image, representing nearly full suppression of fundamental signal (gain: 85 %). These settings were repeated during each injection. All studies were digitally registered as a movie clip at a rate of 7 frames per second, during 90 seconds.

The clips were analyzed using specialized computer software (VueBox®, Bracco Suisse SA, Switzerland) for objective quantitative analysis. Six regions-of-interest (ROIs) were manually drawn: 1 on an interlobar artery, 3 in the renal cortex, 2 in the renal medulla, and a ROI containing the entire kidney (Figure 1). The ROIs for the cortex and medulla were identical in size for every clip and drawn at approximately the same depth. For every ROI, the software determined mean pixel intensities proportional to contrast-agent concentration and created a time-intensity curve. Time-intensity curves were analyzed for peak enhancement (PE), wash-in area under the curve (WiAUC), rise time (RT), mean transit time (mTT), time to peak (TTP), wash-in rate (WiR), wash-in perfusion index (WiPI; $WiAUC/RT$), wash-out area under the curve (WoAUC), total area under the curve (AUC), fall time (FT), and wash-out rate (WoR). Parameters related to blood volume are PE, WiAUC, WoAUC and AUC. The PE corresponds to the maximum contrast medium signal intensity. The WiAUC is calculated as the sum of all amplitudes inside the range from the beginning of the curve up to the TTP. Similarly, WoAUC corresponds to the sum of all amplitudes inside the range from the TTP to the end of the descending curve. The other parameters, i.e. RT, mTT, TTP, WiR, WiPI, FT, WoR, are related to blood velocity. The WiR and WoR represent the slopes of respectively the ascending and descending curves. The RT corresponds to the time interval between the first arrival of contrast and the time of peak enhancement. The FT, in contrast, is the duration of contrast wash-out. Mean transit time is the mean duration of complete contrast medium perfusion. The values for the 3 ROIs in the renal cortex and 2 ROIs in the renal medulla were averaged. Peak enhancement, and WiAUC for the cortex, medulla and entire kidney were normalized to the values obtained for the interlobar artery.

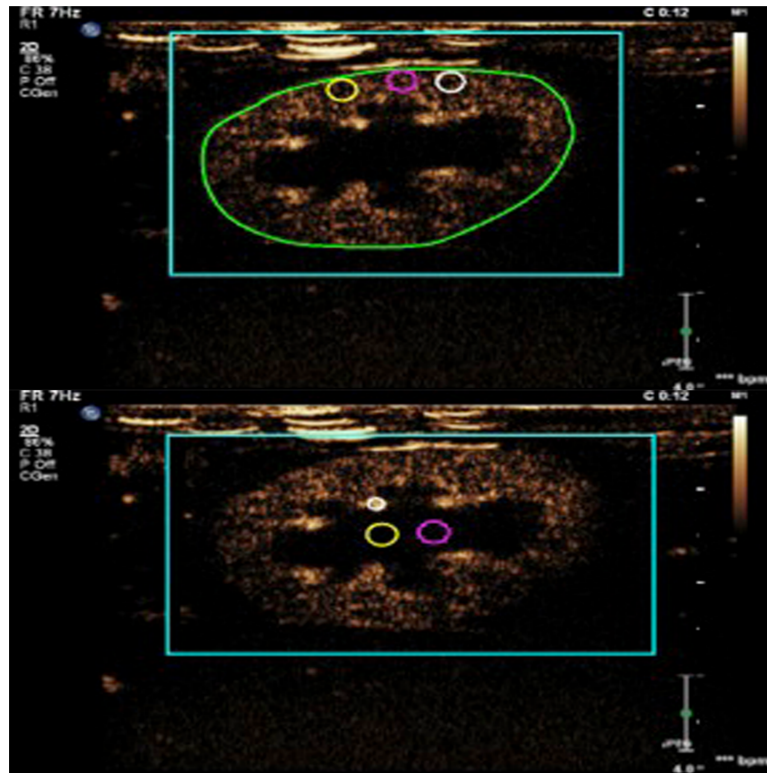


Fig 1. Contrast-enhanced longitudinal image of the left kidney of a cat. Note the ROIs drawn around the entire kidney, in the renal cortex (upper image), renal medulla and centered on an interlobar artery (lower image).

Scintigraphy

The cats received 124 to 137 MBq (136.18 ± 7.44 MBq) of $^{99m}\text{Tc-MAG}_3$ intravenously via the cephalic vein catheter, followed by a 1 mL bolus of sterile saline flush, using the 3-way stopcock.

The images were acquired using a gamma camera fitted with a low energy, high-resolution collimator. The cats were positioned in dorsal recumbency with the camera centered dorsal to the kidneys for dynamic imaging (matrix 128x128). Dynamic scanning started simultaneously with intravenous injection of the radiopharmaceutical. The dynamic protocol consisted of 60 frames at 1 second per frame, followed by 120 frames at 4 seconds per frame.

A 30 second static image of the full and empty syringe was performed. The net amount of injected radioactivity was determined by subtracting the amount of radioactivity in the syringe before and after injection measured in a dose calibrator.

Image frames from the dynamic acquisition for the first 30 seconds were summed. Regions of interest were manually drawn around the left and the right kidney, and the aorta at the level of the kidneys. Equally sized background ROIs were drawn caudal to the kidneys, excluding major

vascular structures and the lower urinary tract (Figure 2). The regions of interest were applied to each frame and time-activity curves for the ROIs were generated. The kidney activity was background corrected. No depth correction was applied. A mathematical analysis program (Microsoft Excell) was used to determine the slopes of the kidney and aortic uptake curves.

The K/A ratio was the ratio of the initial rise of each kidney curve to the initial rise of the arterial curve, using the following formula⁷:

$$\text{K/A ratio} = \frac{\text{slope of the kidney curve}}{\text{slope of the aortic curve}}$$

The flow index was calculated by using the following formula⁷:

$$\text{Flow index} = \frac{\text{Area under the aortic curve}}{\text{Area under the kidney curve}}$$

The area under the aortic curve was calculated from initial upslope to the point of peak activity. The area under the kidney curve was calculated for the same time interval.

Statistical analysis

A mixed model with period and treatment as categorical fixed effects and cat as random effect was used (SAS Version 9.3). Analysis for the CEUS parameters was performed per location. The F-test at the 5% significance level was used to assess the effect of AT II infusion on the values of the various parameters of renal blood flow obtained with CEUS and MAG₃. Correlations between perfusion parameters obtained with CEUS and renal scintigraphy were calculated using Pearson correlation coefficients.

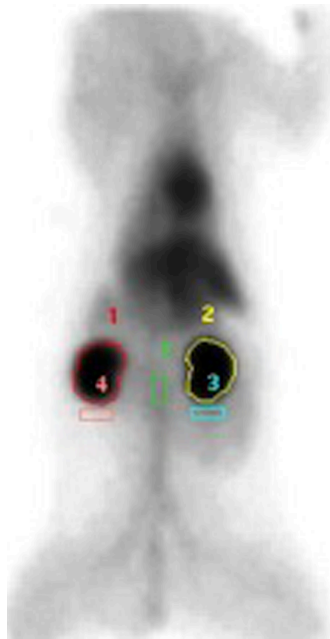


Fig 2. Summed dynamic dorsal images from a cat injected with $^{99m}\text{Tc-MAG}_3$. Note the ROIs drawn on both kidneys with the rectangular background placed caudal to the kidneys and a rectangular ROI drawn on the aorta at the level of the kidneys.

4. Results

General

AT II infusion, administration of SonoVue® and $^{99m}\text{Tc-MAG}_3$ were well tolerated and no adverse effects were noticed. Good quality images were obtained with both imaging techniques in all study subjects.

The mean systolic blood pressure during the procedure was 88 ± 22 mmHg (ranging from 63 to 132 mmHg) for the AT II treatment and 72 ± 8 mmHg (ranging from 60 – 82 mmHg) for the placebo treatment. There was a statistically significant increase ($P=0.03$) in systolic blood pressure with infusion of AT II whereas no influence of AT II infusion was noted on the heart rate.

Contrast-enhanced ultrasound

A mean decrease of 26.1% ($P=0.04$) in PE for the entire kidney and a 19.7 % ($P=0.12$) decrease for the renal cortex was noticed with infusion of AT II compared to control treatment. However, only the results for the entire kidney reached statistical significance.

Although not significant, a tendency for a lower AUC was observed after AT II infusion for the entire kidney and renal cortex, with the effect being most prominent for WiAUC. A 23.2% ($P=0.08$) reduction in WiAUC was noted for the entire kidney, while a 21.3% ($P=0.15$) reduction was present

Chapter VII Perfusion changes induced by angiotensin II infusion

for the renal cortex. Similarly, a reduction of 18.8% ($P=0.20$) for the entire kidney and 21.9% ($P=0.18$) for the renal cortex for the WoAUC and a reduction of 20.7% ($P=0.14$; entire kidney) and 21.8% ($P=0.14$; renal cortex) in total AUC were present. None of the results reached statistical significance.

Furthermore, AT II infusion induced a significant reduction in WiPI ($P=0.04$) and WoR ($P=0.02$) for the entire kidney.

The results of PE and WiAUC normalized to the interlobar artery (PE* and WiAUC*) were in accordance with PE and WiAUC, i.e. a decrease of these parameters was observed with AT II infusion. However, none of these results reached statistical significance (P-values ranging between 0.34 and 0.22).

No changes were observed in any of the perfusion parameters for the renal medulla and the time-related parameters for the renal cortex.

Graphs demonstrating the influence of AT II on the most important perfusion parameters can be consulted in Figure 3.

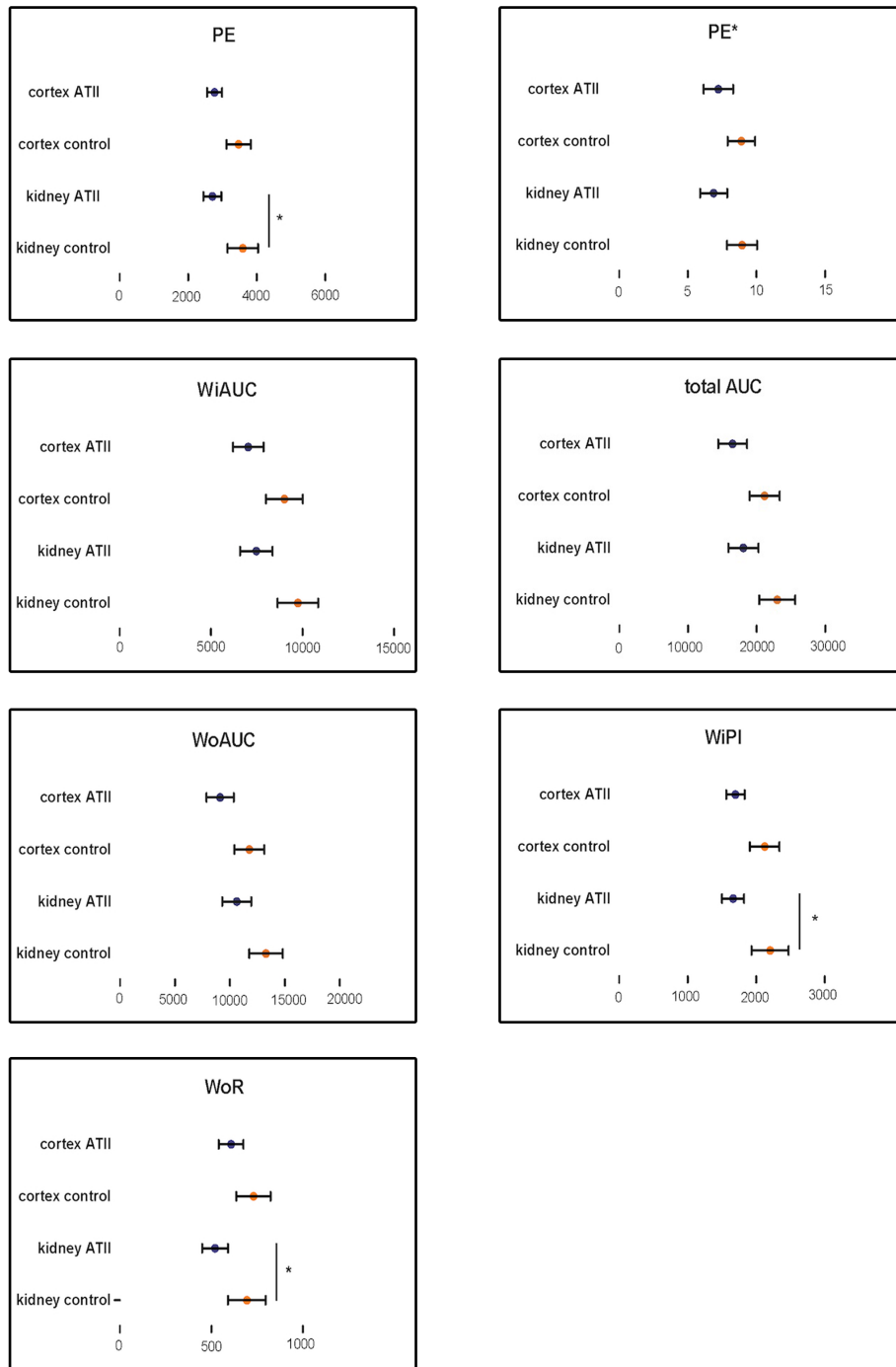


Fig 3. Changes in CEUS parameters induced by angiotensin II (AT II) presented as means +/- standard error. * p value < 0.05. From left to right, top to bottom: peak enhancement (PE), ratio of peak enhancement with interlobar artery (PE*), wash-in area-under-the-curve (WiAUC), total area-under-the-curve (total AUC), wash-out area-under-the-curve (WoAUC), wash-in perfusion index (WiPI) and wash-out-rate (WoR). All parameters are expressed in arbitrary units.

Renal scintigraphy

A negligible effect of AT II was noticed on the flow index for the left kidney (4% decrease, $P=0.52$), while a 26% ($P=0.19$) decrease was noted for the right kidney. K/A ratio decreased by 16% ($P=0.22$) for the left kidney and 11% ($P=0.50$) for the right kidney (Figure 4). However, none of the parameters reached statistical significance when comparing AT II infusion with control treatment.

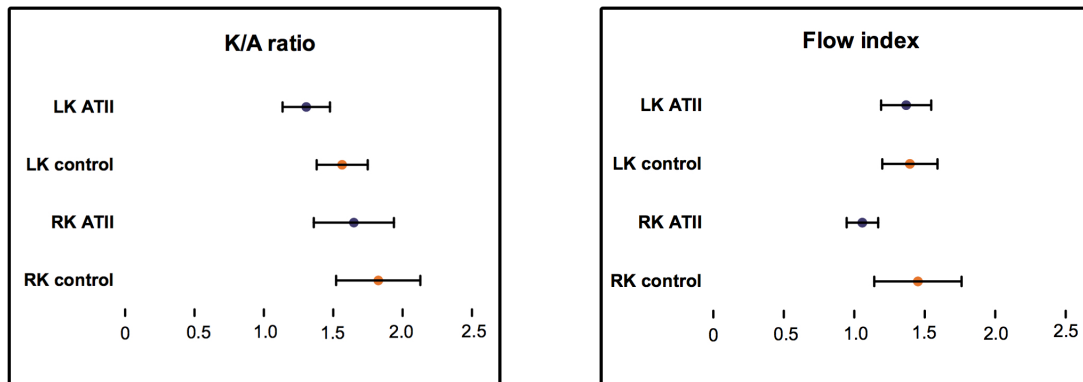


Fig 4. Changes in scintigraphic perfusion parameters induced by angiotensin II (ATII) presented as means +/- standard error. LK: left kidney, RK: right kidney.

No association was observed between the perfusion variables obtained with CEUS and those obtained with renal scintigraphy.

5. Discussion

In this study, we have shown that CEUS is capable of detecting perfusion changes induced by AT II infusion in healthy cats. We found a significant decrease in PE and a tendency towards a lower WiAUC compared to control measurements. Moreover a significant reduction in WiPI and WoR was noticed with AT II infusion.

The physiologic effects of AT II can easily explain the AT II-induced decrease in renal blood volume, noticed as a decrease in PE and AUC. AT II is a potent vasoconstrictor, causing an increased systemic blood pressure and even more important, an increased renal perfusion pressure. The latter is achieved by vasoconstriction of both the afferent and efferent glomerular arterioles.^{21, 22} Consequently, AT II causes dose-dependent decreases in total and cortical renal blood flow.^{22, 23} The efferent arteriole is more sensitive to the vasoconstrictive effects of AT II compared to the afferent arteriole.²⁴ Additionally, a decreased WiPI and WoR were noted after AT II infusion. WiPI is

calculated as a ratio of WIAUC and RT. The reduction in WoR corresponds to slower outflow of contrast medium.

In our study, infusion of AT II did not alter any of the perfusion parameters for the renal medulla. Studies performed on rats using invasive laser Doppler perfusion monitoring, report an inconsistent effect of angiotensin on the medullary blood flow varying from no influence to an increase in medullary blood flow.^{23, 25, 26} The exact etiology remains unclear: a higher concentration of vasodilatory substances as prostaglandins, kinins and nitrogen oxide in the renal medulla, may likely cause this phenomenon.^{23, 26}

Our results are in accordance with a study in humans where a dose-dependent decrease in perfusion index of the renal cortex was observed with CEUS after infusion of AT II. The changes in perfusion index paralleled those in estimated renal plasma flow measured with PAH-clearance techniques.²⁷ In a recent study in sheep, a very heterogeneous and inconsistent response on CEUS parameters was noticed after infusion of AT II. The only significant finding was an increase in mean transit time, corresponding with a delayed replenishment, caused by a high dose AT II infusion.²⁸ In both the human and sheep study, CEUS was performed using continuous infusion of contrast agent followed by several destruction-refilling sequences, whereas in our study a bolus injection was performed. Therefore, different perfusion parameters are obtained in our study compared to the human and sheep study, and thus exact comparison of the results is not possible.

The discrepancy between the flow index for the left and right kidney is most likely related to inclusion of liver activity in the ROI for the right kidney. Variable hepatic uptake of ^{99m}Tc-MAG₃ has been described in cats.¹⁰ The anatomic location of the right kidney close to the caudate lobe of the liver complicates complete exclusion of liver activity within the renal ROI.

We did not observe an association between any of the CEUS parameters and values obtained with ^{99m}Tc-MAG₃ scintigraphy. Perfusion changes induced by AT II did not reach statistical significance with renal scintigraphy. In a study with human patients with various renal diseases, a significant correlation was present between ERPF determined by PAH-clearance, ERPF determined by ^{99m}Tc-MAG₃ scintigraphy and decline ratio obtained with CEUS. However, no association was seen between the peak enhancement obtained with CEUS, scintigraphy and PAH-clearance. Contrast-enhanced ultrasound in the latter study was performed using a combination of harmonic power Doppler and intermittent imaging during a continuous infusion of contrast agent.²⁹ A strict comparison between CEUS and renal scintigraphy is impossible because with CEUS regional blood flow is determined on a microvascular level while total renal blood flow on a macrovascular level

is assessed using renal scintigraphy. Moreover, both techniques only deliver relative perfusion parameters, as no formulas exist to calculate effective or estimated renal plasma flow derived from these techniques in cats. Different perfusion parameters are calculated from both techniques, further complicating a comparison. Furthermore, there is a high heterogeneity in the parameters that are determined by CEUS. The assessed parameters depend on the injection procedure: different parameters are calculated using continuous infusing of contrast-agent compared by bolus injection.

This study has some limitations. Although there is a gold standard for global renal plasma flow evaluation (PAH), there is not one for microperfusion. Laser Doppler probes have been used in rats for evaluation of global renal perfusion as well as cortical and medullary perfusion.^{23,25,26} However, the technique has not been described in cats and is due to its invasiveness unethical to use. Renal scintigraphy using ^{99m}Tc-MAG₃ is the only non-invasive technique available for evaluation of perfusion in cats. Data on the use of renal scintigraphy in cats is limited and no formula is established to determine ERPF as available in dogs and human.⁷

Second, anesthesia might suppress the effect of AT II. Therefore, the response of the anesthetized cats in this study might differ from the response that would be seen in conscious cats. We choose to anesthetize the cats to eliminate the variable and unpredictable variations in blood pressure caused by stress. In a murine study, barbiturate anesthesia was found to decrease baseline arterial pressure, however it did not alter the response to AT II.³⁰ In sheep, isoflurane anesthesia reduced the hypertensive response to AT II both in magnitude and duration, however the reduction in renal blood flow was similar to conscious animals.³¹

In conclusion, this study demonstrates that CEUS is a potentially valuable technique to detect changes in feline renal perfusion after infusion of AT II. These perfusion changes were not depicted by renal scintigraphy. Further research is warranted to determine the value of CEUS for diagnosis of naturally occurring diffuse renal pathology.

Acknowledgements

The authors want to thank Bracco Suisse SA (Geneva, Switzerland) for their scientific support on the use of VueBox® and Medvet (Antwerp, Belgium) for the laboratory analyses.

6. References

1. Coresh J, Selvin E, Stevens LA, Manzi J, Kusek JW, Eggers P, et al. Prevalence of chronic kidney disease in the United States. *Journal of the American Medical Association*. 2007;298: 2038-2047.
2. Marino CL, Lascelles BDX, Vaden SL, Gruen ME, Marks SL. Prevalence and classification of chronic kidney disease in cats randomly selected from four age groups and in cats recruited for degenerative joint disease studies. *Journal of Feline Medicine and Surgery*. 2014;16: 465-472.
3. Lulich JP, Osborne CA, O'Brien TD, Polzin DJ. Feline Renal-Failure - Questions, Answers, Questions. *Compendium on Continuing Education for the Practicing Veterinarian*. 1992;14: 127-152.
4. Bartges JW. Chronic Kidney Disease in Dogs and Cats. *Veterinary Clinics of North America Small Animal Practice*. 2012;42: 669-692.
5. Regan MC, Young LS, Geraghty J, Fitzpatrick JM. Regional renal blood flow in normal and disease states. *Urological Research*. 1995;23: 1-10.
6. Osbaldiston GW, Fuhrman W. The clearance of creatinine, inulin, para-aminohippurate and phenosulphothalein in the cat. *The Canadian Journal of Comparative Medicine*. 1970;34: 138-141.
7. Daniel GB, Mitchell SK, Mawby D, Sackman JE, Schmidt D. Renal nuclear medicine: A review. *Veterinary Radiology & Ultrasound*. 1999;40: 572-587.
8. Taylor A, Ziffer JA, Steves A, Eshima D, Delaney VB, Welchel JD. Clinical Comparison of I-131 Orthoiodohippurate and the Kit Formulation of Tc-99m Mercaptoacetyltriglycine. *Radiology*. 1989;170: 721-725.
9. Itkin RJ, Krawiec DR, Twardock AR, Gelberg HB. Quantitative Renal Scintigraphic Determination of Effective Renal Plasma-Flow in Dogs with Normal and Abnormal Renal-Function, Using Tc-99m-Mercaptoacetyltriglycine. *American Journal of Veterinary Research*. 1994;55: 1660-1665.
10. Drost WT, McLoughlin MA, Mattoon JS, Lerche P, Samii VF, DiBartola SP, et al. Determination of extrarenal plasma clearance and hepatic uptake of technetium-99m-mercaptoacetyltriglycine in cats. *American Journal of Veterinary Research*. 2003;64: 1076-1080.
11. Haers H, Saunders JH. Review of clinical characteristics and applications of contrast-enhanced ultrasonography in dogs. *Journal of the American Veterinary Medical Association*. 2009;234: 460-470.

12. Dietrich CF, Ignee A, Hocke M, Schreiber-Dietrich D, Greis C. Pitfalls and Artefacts using Contrast Enhanced Ultrasound. *Zeitschrift Fur Gastroenterologie*. 2011;49: 350-356.
13. Seiler GS, Brown JC, Reetz JA, Taeymans O, Bucknoff M, Rossi F, et al. Safety of contrast-enhanced ultrasonography in dogs and cats: 488 cases (2002-2011). *Journal of the American Veterinary Medical Association*. 2013;242: 1255-1259.
14. Dong Y, Wang WP, Cao J, Fan P, Lin X. Early assessment of chronic kidney dysfunction using contrast-enhanced ultrasound: a pilot study. *British Journal of Radiology*. 2014;87: 1-7.
15. Ma F, Cang YQ, Zhao BZ, Liu YY, Wang CQ, Liu B, et al. Contrast-enhanced ultrasound with SonoVue could accurately assess the renal microvascular perfusion in diabetic kidney damage. *Nephrology Dialysis Transplantation*. 2012;27: 2891-2898.
16. Tsuruoka K, Yasuda T, Koitabashi K, Yazawa M, Shimazaki M, Sakurada T, et al. Evaluation of renal microcirculation by contrast-enhanced ultrasound with sonazoid (TM) as a contrast agent. *International Heart Journal*. 2010;51: 176-182.
17. Fischer T, Muhler M, Kroncke TJ, Lembcke A, Rudolph J, Diekmann F, et al. Early postoperative ultrasound of kidney transplants: Evaluation of contrast medium dynamics using time-intensity curves. *Rofo*. 2004;176: 472-477.
18. Kay DH, Mazonakis M, Geddes C, Baxter G. Ultrasonic microbubble contrast agents and the transplant kidney. *Clinical Radiology*. 2009;64: 1081-1087.
19. Haers H, Daminet S, Smets PMY, Duchateau L, Aresu L, Saunders JH. Use of quantitative contrast-enhanced ultrasonography to detect diffuse renal changes in Beagles with iatrogenic hypercortisolism. *American Journal of Veterinary Research*. 2013;74: 70-77.
20. Dong Y, Wang WP, Cao JY, Fan PL, Lin XY. Quantitative evaluation of contrast-enhanced ultrasonography in the diagnosis of chronic ischemic renal disease in a dog model. *Plos One*. 2013;8: e70377.
21. Klein BG. *Cunningham's Textbook of Veterinary Physiology*. In: Verlander JW (ed): Renal physiology. Missouri, USA: Saunders, 2012.
22. Evans RG, Head GA, Eppel GA, Burke SL, Rajapakse NW. Angiotensin II and neurohumoral control of the renal medullary circulation. *Clinical and Experimental Pharmacology and Physiology*. 2010;37: e58-69.
23. Badzynska B, Grzelec-Mojzesowicz M, Dobrowolski L, Sadowski J. Differential effect of angiotensin II on blood circulation in the renal medulla and cortex of anaesthetised rats. *Journal of Physiology*. 2002;538: 159-166.

Chapter VII Perfusion changes induced by angiotensin II infusion

24. Itkin RJ. Effects of the renin-angiotensin system on the kidneys. *Compendium on Continuing Education for the Practicing Veterinarian*. 1994;16: 753-763.
25. Nobes MS, Harris PJ, Yamada H, Mendelsohn FAO. Effects of angiotensin on renal cortical and papillary blood flows measured by laser-Doppler flowmetry. *American Journal of Physiology*. 1991;261: F998-F1006.
26. Walker LL, Rajaratne AA, Blair-West JR, Harris PJ. The effects of angiotensin II on blood perfusion in the rat renal papilla. *Journal of Physiology*. 1999;519 Pt 1: 273-278.
27. Schneider AG, Hofmann L, Wuerzner G, Glatz N, Maillard M, Meuwly JY, et al. Renal perfusion evaluation with contrast-enhanced ultrasonography. *Nephrology Dialysis Transplantation*. 2012;27: 674-681.
28. Schneider AG, Calzavacca P, Schelleman A, Huynh T, Bailey M, May C, et al. Contrast-enhanced ultrasound evaluation of renal microcirculation in sheep. *Intensive Care Medicine Experimental*. 2014;2: 33.
29. Hosotani Y, Takahashi N, Kiyomoto H, Ohmori K, Hitomi H, Fujioka H, et al. A new method for evaluation of split renal cortical blood flow with contrast echography. *Hypertension Research*. 2002;25: 77-83.
30. Chapman BJ, Brooks DP, Munday KA. Half-life of angiotensin II in the conscious and barbiturate-anaesthetized rat. *British Journal of Anaesthesia*. 1980;52: 389-393.
31. Lee WB, Ismay MJ, Lumbers ER. Mechanisms by Which Angiotensin-II Affects the Heart-Rate of the Conscious Sheep. *Circulation Research*. 1980;47: 286-292.

CHAPTER VIII

EVALUATION OF RENAL PERFUSION IN HYPERTHYROID CATS BEFORE AND AFTER RADIOIODINE TREATMENT

Adapted from:

Stock E., Daminet S., Paepe D., Buresova E., Vandermeulen E., Smets P., Duchateau L., Saunders J.H.*, Vanderperren K.* (*shared senior authorship). Evaluation of renal perfusion in hyperthyroid cats before and after radioiodine treatment. *Journal of Veterinary Internal Medicine*. *Under revision*.

1. Abstract

Hyperthyroidism and renal disease are among the most important health issues in geriatric cats. Both diseases often occur concurrently and mutually influence each other, with hyperthyroidism possibly masking underlying renal disease. As changes in renal perfusion play an important role in functional renal changes in hyperthyroid cats, investigation of renal perfusion may deliver novel insights. Contrast-enhanced ultrasound (CEUS) is a safe and non-invasive technique that allows evaluation of tissue perfusion. In this study, renal perfusion is assessed with CEUS in 42 hyperthyroid cats, before and after radioiodine treatment.

An increase in several time-related perfusion parameters was observed after radioiodine treatment, indicating a decreased blood velocity upon resolution of the hyperthyroid state. Further, a small post-treatment decrease in peak enhancement was present in the renal medulla, suggesting a lower medullary blood volume.

In conclusion, CEUS shows a higher cortical and medullary blood velocity and higher medullary blood volume in hyperthyroid cats before radioactive treatment in comparison with 1-month control.

2. Introduction

Both hyperthyroidism and renal disease are common pathologies in elderly cats, and unsurprisingly these pathologies often occur concurrently. The prevalence of cats suffering from both diseases has been reported to be approximately 14%.¹ The incidence of azotemia occurring shortly after treatment of hyperthyroidism even reaches 40% suggesting unmasking of pre-existing impaired renal function.¹⁻³

A complex relationship exists between the thyroid glands and the kidneys. In cats with hyperthyroidism, increased thyroxin levels induce decreased vascular resistance as well as increased cardiac output, leading to increased renal blood flow, and subsequently increased glomerular filtration rate (GFR).⁴ Treatment of hyperthyroidism inversely results in a decrease in GFR 1 month after treatment, whereas GFR is found to be stable between 1 and 6 months post treatment.^{2, 5} Importantly, predicting changes in renal function before treatment of hyperthyroidism is complicated. Routine renal variables as serum creatinine (sCr), serum urea, urine specific gravity (USG) and proteinuria are insensitive since they are strongly influenced by

the hyperthyroid state of the cat.⁴ Pre-treatment measurement of GFR shows promise in predicting post-treatment azotemia, however great overlap exists with cats that remain non-azotemic.^{2, 4} Therefore, an ideal test to predict post-treatment azotemia is not available at this moment.

Renal blood flow plays a fundamental role in the functional renal changes present in hyperthyroid cats, hence evaluation of renal perfusion could deliver important new insights in renal function in hyperthyroid cats.⁴ CEUS is a functional imaging modality that allows assessment of macro- and microperfusion through the use of an intravenously administered contrast agent. The contrast agent consists of gas-filled microbubbles stabilized by an outer phospholipid shell and have approximately the size of red blood cells. Consequently, they do not cross the endothelium after intravenous administration and act as blood pool agents. Major advantages associated with CEUS are its excellent safety profile allowing the use in geriatric patients and patients suffering from renal disease, the non-invasiveness, the absence of ionizing radiation and relatively short imaging times.⁶

The objective of this study was to evaluate renal perfusion using CEUS in hyperthyroid cats, before and after radioiodine treatment. The hypothesis was that a higher renal perfusion, both a higher blood velocity and higher blood volume, would be present before radioiodine treatment compared to the 1-month control.

3. Materials and methods

Fifty-one client-owned hyperthyroid cats presented for radioiodine treatment at the Faculty of Veterinary Medicine of Ghent University (Belgium) were included in the study with the permission of the local ethical committee of Ghent University (EC 2015/67). Owners signed an informed consent prior to inclusion.

Inclusion criteria were a diagnosis of hyperthyroidism based on clinical signs, increased serum total thyroxine (T4) concentration and increased pertechnetate uptake in one or both thyroid glands on scintigraphic scan. Cats with concurrent systemic disease, including pre-existing overt renal disease or with hemodynamic significant cardiac disease, defined as severe left atrial dilation, signs of congestive heart failure or significant arrhythmias, were excluded. Anti-thyroid treatment, either medication (methimazole, carbimazole) or diet (Hill's prescription Y/D), was

ceased at least 10 days prior to radioiodine treatment. Cats maintained their original, commercial diet throughout the study period.

The cats were evaluated on the day of radioiodine treatment and 1 month after treatment. Pre-treatment evaluation included a thorough physical exam, standard two-view thoracic x-rays (lateral and ventrodorsal projections), abdominal ultrasound, CEUS of the kidneys and cardiac ultrasound. Post-treatment evaluation included physical examination, CEUS of the kidneys and cardiac ultrasound. A complete blood count, serum biochemistry profile including serum total T₄, and complete urinalysis (USG, urinary pH, urinary protein:creatinine ratio (UPC), sediment examination⁷ and bacterial culture) were performed at both occasions. At both occasions systolic blood pressure was measured by Doppler ultrasonic technique, following the consensus statement of the American College of Veterinary Internal Medicine.⁸

In 10 cats, GFR was measured with a plasma exogenous creatinine clearance test. This was performed one day prior to radioiodine treatment and repeated 1 day prior to the post-treatment exam. A limited sampling strategy, minimally impacting the reliability of the GFR estimate, was used, as previously described.⁹ Briefly, 40.0 mg/kg creatinine was administered intravenously and blood samples were taken in EDTA tubes before and 5, 30, 60, 120, 180, 360 and 600 minutes after injection. The borderline GFR cut-off value was defined as 1.7 mL/min/kg, the lower GFR cut-off value as 1.2 mL/min/kg.⁹

CEUS procedure

A 22-Gauge indwelling catheter was placed in the cephalic vein. Anesthesia was induced with a bolus of propofol (Propofol®, Abbott Laboratories) 3.5-7.7 mg/kg IV given to effect and maintained with 0-3 additional boluses as necessary.

The hair was clipped over the ventrolateral aspect of the abdomen and coupling gel was applied to the skin. The ultrasound examinations were performed with the cat in dorsal recumbency. The kidney of interest was centered on the screen and was imaged in a longitudinal plane using dual-screen (simultaneous display of conventional B-mode and contrast-mode image). The transducer was manually positioned during each imaging procedure and was maintained at the same position during the CEUS examination.

The contrast agent (Sonovue®, Bracco, Italy), 0.05 mL/kg, was injected IV (bolus injection over +/- 3 s) followed by injection of 1.5 mL saline bolus. A three-way stopcock was used to avoid any delay between the injection of contrast agent and saline. The same person performed the injection in a standardized way. Three to four injections of contrast were performed: two for the left kidney, one for the right kidney and one for the abdominal aorta in 13 cats. Between subsequent injections, to avoid artifacts, remnant microbubbles were completely destroyed by setting the acoustic power at the highest level and scanning the caudal aspect of the abdominal aorta for approximately 2 minutes.

All examinations were performed using a linear transducer of 12-5 MHz on a dedicated machine (iU22, Philips) with contrast-specific software. Basic technical parameters were a single focus placed under the kidney, persistency off, mechanical index 0.09, high dynamic range setting (C50), timer started at the beginning of the injection, gain 85% (corresponding to a nearly dark/anechoic image before contrast administration). The settings were repeated during each injection. All studies were digitally registered as a movie clip at a rate of 9 frames per second, during 90 seconds.

The clips were exported in DICOM format and analyzed using specialized computer software (VueBox®, Bracco Suisse SA, Geneva, Switzerland) for objective quantitative analysis. Six regions-of-interest (ROIs) were manually drawn: 3 in the renal cortex, 2 in the renal medulla and 1 on an interlobar artery. If the abdominal aorta was included, 3 ROIs were drawn in the middle of the aortic lumen. The ROIs were similar in size and drawn at the same depth for every region. Care was taken to avoid including cystic lesions and focal parenchymal lesions within the ROI. For every ROI, the software determined mean pixel intensity as a function of time and created a time-intensity curve. Time-intensity curves were analyzed for peak enhancement (PE), wash-in area under the curve (WiAUC), rise time (RT), mean transit time (mTT), time to peak (TTP), wash-in rate (WiR), wash-in perfusion index (WiPI; WiAUC/RT), wash-out area under the curve (WoAUC), total area under the curve (AUC), fall time (FT), and wash-out rate (WoR). The PE corresponds to the maximum contrast medium signal intensity. The WiAUC is calculated as the sum of all amplitudes inside the range from the beginning of the curve up to the TTP. Similarly, WoAUC corresponds to the sum of all amplitudes inside the range from the TTP to the end of the descending curve. The other

parameters, i.e. RT, mTT, TTP, WiR, WiPI, FT, WoR, are related to blood velocity. The WiR and WoR represent the maximum and minimum slopes of the time-intensity curves. The RT corresponds to the time interval between the first arrival of contrast and the time of peak enhancement. The FT, in contrast, is the duration of contrast wash-out. Mean transit time is the mean duration of complete contrast medium perfusion. The values for the 3 ROIs in the renal cortex, 2 ROIs in the renal medulla, and the 2 ROIs in aorta were averaged. Peak enhancement for the cortex and medulla was normalized to the values obtained for the interlobar artery (PE*) and abdominal aorta (PE_{AO}).

Statistical analysis

Analyses were based on a linear mixed model with cat and kidney nested in cat as random effects and treatment (pre/post radioiodine treatment) as a categorical fixed effect (SAS version 9.4). Analyses were done separately for the renal cortex and medulla. Correlations between perfusion parameters and heart rate, blood pressure, total T4, serum sCr, and GFR were calculated for the renal cortex and medulla using Spearman correlation coefficients (ρ). A difference was considered statistically significant if $P < 0.05$.

4. Results

In total 9 cats were excluded from the study: 4 cats because of an additional pathology (suspected pulmonary neoplasia $n=1$, intestinal lymphoma $n=1$, severe cardiomegaly and left atrial dilation $n=1$, second-degree atrioventricular block $n=1$), 4 cats due to aggressive behavior and 1 cat was lost for follow-up. For the 42 remaining cats, no significant abnormalities were noted on thoracic radiographs or abdominal ultrasound. Alterations seen on echocardiography were compatible with hyperthyroidism and improved or remained stable after treatment.

The median age at time of inclusion was 12 years 9 months (range 7y5m to 16y7m).

Of the 42 cats included, 27 (64%) had a post-treatment total T4 value within the normal reference interval, and 15 (36%) showed a total T4 value below. None showed a total T4 value above the normal reference interval at 1 month after radioiodine therapy. Two cats (4.8 %) developed post-treatment azotemia, one of them had total T4 level below the reference range 1 month post-treatment. Additionally, 1 cat with normal sCr levels had decreased post-treatment GFR and one cat

with normal sCr had borderline GFR. An overview of the baseline characteristics of the cats, before and after radioiodine treatment is provided in Table 1.

Variables	Pre-treatment	Post-treatment	P-value
Body weight (kg)	3.8 ± 0.1	4.1 ± 0.1	< 0.001
Heart rate (bpm)	209.4 ± 4.2	169.7 ± 4.4	< 0.001
Blood pressure (mmHg)	161.2 ± 4.6	162.7 ± 4.9	0.793
Total T4	114.6 ± 4.3	13.0 ± 4.3	< 0.001
sCr (μmolL ⁻¹)	65.3 ± 4.1	109.6 ± 4.1	< 0.001
Serum urea (mmolL ⁻¹)	8.7 ± 0.5	10.4 ± 0.5	< 0.001
USG	1.044 ± 0.001	1.037 ± 0.001	< 0.001
UPC	0.71 ± 0.05	0.23 ± 0.05	< 0.001
GFR (mL/kg/min)	3.9 ± 0.3	2.5 ± 0.3	0.003

Table 1. Clinical parameters before and after radioiodine treatment provided as mean ± standard error (bpm beats per minute; T4 thyroxine; sCr serum creatinine; USG urine specific gravity; UPC urinary protein:creatinine ratio; GFR glomerular filtration rate)

Both kidneys had a normal appearance on B-mode ultrasonography in 27 cats, including 1 of the 2 cats developing post-treatment azotemia. Two cats had a unilateral small kidney (< 3 cm), with a subjectively decreased corticomedullary definition, 1 of these developed post-treatment azotemia, whereas the other did not. Three other cats showed a mildly decreased corticomedullary definition in normal-sized kidneys. Three cats had a mildly irregular renal outline, 5 had segmental cortical lesions and 4 had small cystic lesions, none of these cats developed post-treatment azotemia. One cat, without post-treatment azotemia, had mild bilateral pyelectasia without signs of obstruction, this improved post-treatment. Eight cats had bilateral hyperechoic renal cortices, all of them were male castrated, suggesting fat infiltration.¹⁰

No significant side effects of the sonographic contrast material were noted. However, 1 cat showed mild and transient tachypnea after the first injection of contrast agent during the pre-treatment evaluation, which resolved spontaneously within 10 minutes.

Several perfusion parameters showed significant changes between pre- and post-treatment values. A comparison between the perfusion parameters before and after radioiodine treatment is provided in Table 2. Moreover, representative time-intensity curves are provided in Figure 1.

Variable, by location	Pre-treatment	Post-treatment	P-value
Renal cortex			
PE	2193.27 ± 147.85	2146.47 ± 147.85	0.771
PE*	20.09 ± 1.48	19.06 ± 1.49	0.557
PE ^{A0}	9.89 ± 1.23	8.54 ± 1.11	0.31
WiAUC	3566.26 ± 270.32	4864.32 ± 270.32	< 0.001
RT	2.79 ± 0.10	3.79 ± 0.10	< 0.001
mTT	24.36 ± 1.60	28.73 ± 1.60	0.011
TTP	7.83 ± 0.22	9.91 ± 0.22	< 0.001
WiR	1119.38 ± 85.46	793.75 ± 85.46	0.008
WiPI	1342.53 ± 90.26	1317.72 ± 90.26	0.801
WoAUC	4830.39 ± 368.63	6767.46 ± 368.63	< 0.001
AUC	8396.54 ± 636.37	11632.00 ± 636.37	< 0.001
FT	3.87 ± 0.17	5.46 ± 0.17	< 0.001
WoR	755.90 ± 62.89	501.47 ± 62.89	0.004
Renal medulla			
PE	308.93 ± 25.14	270.59 ± 25.52	0.093
PE*	3.01 ± 0.26	2.37 ± 0.26	0.044
PE ^{A0}	1.40 ± 0.23	1.10 ± 0.21	0.30
WiAUC	2530.39 ± 202.54	2512.68 ± 205.86	0.935
RT	14.01 ± 0.66	16.25 ± 0.68	0.001
mTT	68.36 ± 10.93	87.84 ± 11.19	0.196
TTP	24.58 ± 0.76	30.99 ± 0.77	< 0.001
WiR	36.90 ± 3.83	27.40 ± 3.88	0.004
WiPI	194.04 ± 15.64	168.53 ± 15.87	0.075
WoAUC	4403.78 ± 363.00	3974.35 ± 370.89	0.259
AUC	6949.01 ± 560.01	6442.36 ± 572.20	0.387
FT	25.54 ± 1.32	26.80 ± 1.35	0.386
WoR	18.98 ± 2.26	15.28 ± 2.30	0.072

Table 2. Mean ± standard error values of renal perfusion parameters in hyperthyroid cats before and 1 month after radioiodine treatment. (PE peak enhancement, PE* peak enhancement normalized to interlobar artery, PE_{A0} peak enhancement normalized to abdominal aorta, WiAUC wash-in area-under-the-curve, RT rise time, mTT mean transit time, TTP time-to-peak, WiR wash-in rate, WiPI wash-in perfusion index, WoAUC wash-out area-under-the-curve, AUC total area-under-the-curve, FT fall time, WoR wash-out rate)

The RT (P<0.001), mTT (P=0.011), TTP (P<0.001) and FT (P<0.001) for the renal cortex increased significantly post-treatment. In parallel with this, the WiR (P=0.008) and WoR (P=0.004) decreased. A post-treatment increase was also seen for the WiAUC (P<0.001), WoAUC (P<0.001) and total AUC (P<0.001) for the renal cortex. Similarly, for the renal medulla, RT (P=0.001) and TTP (P<0.001) increased post-treatment, whereas WiR (P=0.004) decreased. Moreover, a significant post-treatment decrease in normalized PE (PE*; P=0.044) was noticed for the medulla.

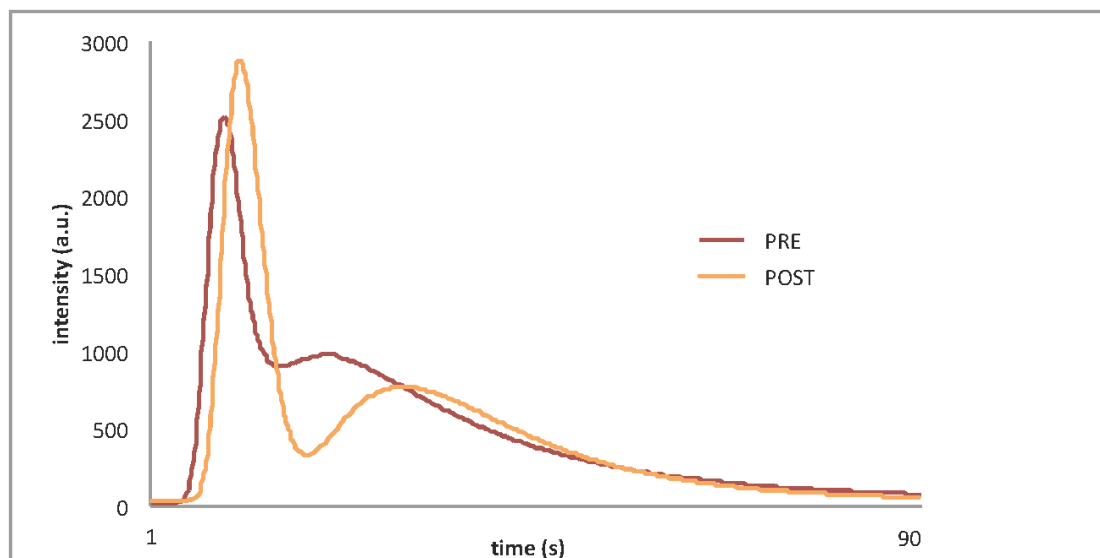


Figure 1. Representative time-intensity curves for the renal cortex of a hyperthyroid cat before (pre) and 1 month after (post) radioiodine treatment.

Significant negative correlations were present between the heart frequency and RT in the cortex ($\rho=-0.46$; $P<0.001$) and TTP for both cortex ($\rho=-0.42$; $P=0.001$) and medulla ($\rho=-0.39$; $P=0.003$), meaning that shorter TTP and RT, and thus higher renal blood velocity, are present as heart frequency increases. Similarly, significant negative correlations were present between the total T4 and cortical RT ($\rho=-0.60$; $P<0.001$), TTP ($\rho=-0.59$; $P<0.001$) and FT ($\rho=-0.57$; $P<0.001$), and medullary TTP ($\rho=-0.48$; $P<0.001$). Moreover, a positive correlation was present between sCr and cortical ($\rho=0.68$; $P<0.001$) and medullary ($\rho=0.41$; $P=0.001$) TTP, and cortical FT ($\rho=0.52$; $P<0.001$). Negative correlations were found between GFR and cortical TTP ($\rho=-0.51$; $P=0.021$), cortical RT ($\rho=-0.53$; $P=0.002$), cortical FT ($\rho=-0.50$; $P=0.024$) and medullary RT ($\rho=-0.62$; $P=0.004$) and FT ($\rho=-0.68$; $P=0.001$).

However, significant correlations were also present between heart frequency and sCr ($\rho=-0.48$; $P<0.001$), heart frequency and GFR ($\rho=0.47$; $P=0.042$), heart frequency and total T4 ($\rho=0.59$; $P<0.001$), total T4 and sCr ($\rho=-0.71$; $P<0.001$), total T4 and GFR ($\rho=0.61$; $P=0.004$), complicating the interpretation.

5. Discussion

Multiple studies have been investigating routine urine and serum renal markers and GFR in hyperthyroid cats before and after treatment.^{2, 3, 5, 11-14} This is the first study focusing on renal perfusion where we showed that CEUS was capable to detect significant changes in renal blood

flow before and after radioiodine treatment. A faster inflow of contrast agent, reflected by lower RT and TTP, was present during the hyperthyroid state pre-treatment. Similarly, a faster outflow (FT) was present. Consequently, the mTT, time of duration of contrast enhancement, was shorter. WiR and WoR, representing the slope of respectively the inflow and outflow phase of the time-intensity curve, were higher in the pre-treatment phase. The combination of these findings indicates a higher velocity of renal blood flow in hyperthyroid cats, which decreases significantly 1 month after ¹³¹I treatment. Similar changes were present for the renal medulla. The changes in CEUS parameters can in part be attributed to the decreased systemic vascular resistance that is present in hyperthyroidism. Thyroid hormones induce increased nitric oxide levels in the renal cortex and medulla, resulting in vasodilation. Additionally, an increased number of beta-adrenergic receptors is present in the renal cortex during the hyperthyroid state.⁴ Secondly, it should be mentioned that the ultrasound contrast agent is injected intravenously and hence 'travels' in the systemic circulation before reaching the kidney. Therefore, the higher heart rate and cardiac output in hyperthyroid cats will have reinforced the effects on renal blood velocity. This is also reflected by the moderate negative correlations between heart rate and several time-based perfusion parameters.

The AUC of the renal cortex significantly increased after radioiodine treatment. The AUC is influenced by both the height of the time-intensity curve (intensity, represented by the PE) and the width of the curve (time, represented by several time-based parameters, most importantly mTT). No significant changes were observed in PE after radioiodine treatment; therefore, the change in AUC can be attributed to the longer duration of contrast enhancement after radioiodine treatment. While most of the previously mentioned data were obtained in the renal cortex, little is known about the microvascular alterations accompanying hyperthyroidism in the renal medulla. This study showed a small, but significant decrease in normalized PE (PE*) for the renal medulla after radioiodine treatment indicating a larger blood volume in the renal medulla during the hyperthyroid state. It is known that the hyperthyroid state induces an increased renal blood flow, resulting from a combination of increased cardiac output, decreased vascular resistance, overall increased blood volume, and upregulation of beta-adrenergic receptors in the renal cortex.^{4,15} A higher estimated renal blood flow in hyperthyroid cats has been described by Adams et al. (1997). In the latter study, total renal blood flow was measured using a radionuclide based technique (¹³¹I ortho-iodo-hippurate).¹⁶ Nevertheless, no significant changes were observed in PE for the renal cortex in our study, although they were expected. This is most likely caused by the high variability

and consequently broad 95% confidence intervals for this parameter.^{17,18} The intensity measured on CEUS images, and thus the PE, is strongly influenced by several factors. Uncontrollable patient-related factors as filtration by the lungs and phagocytosis by the reticuloendothelial system will influence the final microbubble concentration in the renal parenchyma.^{19,20}

Only 4.8% of the cats in this study developed post-treatment azotemia, which is considerably lower than the 17% - 39% reported in literature.^{1,2,12,13} The percentage of cats having low total T4 one month after radioiodine treatment (36%) was similar to the values reported in literature (24%-51%).^{11,21,22} Iatrogenic hypothyroidism is well-known to contribute to the development of renal dysfunction.²² On the other hand, CKD can induce euthyroid sick syndrome with suppression of the serum total T4 levels. Measurement of thyroid-stimulating hormone (TSH) allows differentiation between iatrogenic hypothyroidism and euthyroid sick syndrome. The combination of low total T4 and elevated TSH is consistent with iatrogenic hypothyroidism.^{4,15} However, TSH concentration is also influenced by the radioiodine treatment, TSH concentration is reported to be within normal reference interval 3 months after radioiodine treatment.²² Therefore, TSH was not measured in this study.

Due to the low number of cats developing CKD after radioiodine treatment in this study it was not possible to assess the predictive value of CEUS for the development of post-treatment azotemia. Longer follow-up might have allowed identification of slightly more cats developing CKD, however significant changes in renal function are reported to occur within 4 weeks after treatment and not thereafter.^{2,5}

In conclusion, CEUS allowed assessment of renal perfusion in hyperthyroid cats before and after radioiodine treatment. A significant reduction in both cortical and medullary blood velocity was noted 1 month after radioiodine treatment. However, no significant decrease in cortical blood volume could be detected. Further research is warranted to investigate the diagnostic capabilities of CEUS in the assessment of renal perfusion in hyperthyroid cats and investigate its predictive value for the development of post-treatment azotemia.

Acknowledgements

The authors want to thank Bracco Suisse SA (Geneva, Switzerland) for their scientific support on the use of VueBox® and Idexx laboratories.

6. References

1. Milner RJ, Channell CD, Levy JK, Schaer M. Survival times for cats with hyperthyroidism treated with iodine 131, methimazole, or both: 167 cases (1996-2003). *Journal of the American Veterinary Medical Association*. 2006;228: 559-563.
2. van Hoek I, Lefebvre HP, Peremans K, Meyer E, Croubels S, Vandermeulen E, et al. Short- and long-term follow-up of glomerular and tubular renal markers of kidney function in hyperthyroid cats after treatment with radioiodine. *Domestic Animal Endocrinology*. 2009;36: 45-56.
3. Slater MR, Geller S, Rogers K. Long-term health and predictors of survival for hyperthyroid cats treated with iodine 131. *Journal of Veterinary Internal Medicine*. 2001;15: 47-51.
4. van Hoek I, Daminet S. Interactions between thyroid and kidney function in pathological conditions of these organ systems: A review. *General and Comparative Endocrinology*. 2009;160: 205-215.
5. Boag AK, Neiger R, Slater L, Stevens KB, Haller M, Church DB. Changes in the glomerular filtration rate of 27 cats with hyperthyroidism after treatment with radioactive iodine. *Veterinary Record*. 2007;161: 711-715.
6. Haers H, Saunders JH. Review of clinical characteristics and applications of contrast-enhanced ultrasonography in dogs. *Journal of the American Veterinary Medical Association*. 2009;234: 460-470.
7. Paepe D, Verjans G, Duchateau L, Piron K, Ghys L, Daminet S. Routine health screening: findings in apparently healthy middle-aged and old cats. *Journal of Feline Medicine and Surgery*. 2013;15: 8-19.
8. Brown S, Atkins C, Bagley R, Carr A, Cowgill L, Davidson M, et al. Guidelines for the identification, evaluation, and management of systemic hypertension in dogs and cats. *Journal of Veterinary Internal Medicine*. 2007;21: 542-558.
9. Paepe D, Lefebvre HP, Concordet D, van Hoek I, Croubels S, Daminet S. Simplified methods for estimating glomerular filtration rate in cats and for detection of cats with low or borderline glomerular filtration rate. *Journal of Feline Medicine and Surgery*. 2015;17: 889-900.
10. Debruyne K, Haers H, Combes A, Paepe D, Peremans K, Vanderperren K, et al. Ultrasonography of the feline kidney. Technique, anatomy and changes associated with disease. *Journal of Feline Medicine and Surgery*. 2012;14: 794-803.

11. Adams WH, Daniel GB, Legendre AM, Gompf RE, Grove CA. Changes in renal function in cats following treatment of hyperthyroidism using ¹³¹I. *Veterinary Radiology & Ultrasound*. 1997;38: 231-238.
12. Becker TJ, Graves TK, Kruger JM, Braselton WE, Nachreiner RF. Effects of methimazole on renal function in cats with hyperthyroidism. *Journal of the American Animal Hospital Association*. 2000;36: 215-223.
13. Graves TK, Olivier NB, Nachreiner RF, Kruger JM, Walshaw R, Stickle RL. Changes in renal function associated with treatment of hyperthyroidism in cats. *American Journal of Veterinary Research*. 1994;55: 1745-1749.
14. Riensche MR, Graves TK, Schaeffer DJ. An investigation of predictors of renal insufficiency following treatment of hyperthyroidism in cats. *Journal of Feline Medicine and Surgery*. 2008;10: 160-166.
15. Vaske HH, Schermerhorn T, Grauer GF. Effects of feline hyperthyroidism on kidney function: a review. *Journal of Feline Medicine and Surgery*. 2015.
16. Adams WH, Daniel GB, Legendre AM. Investigation of the effects of hyperthyroidism on renal function in the cat. *Can J Vet Res*. 1997;61: 53-56.
17. Vinke EJ. Development of a contrast enhanced ultrasound technique for the measurement of cerebral blood flow in patients with acute brain injury at the intensive care unit (Thesis). University of Twente, The Netherlands 2015.
18. Gauthier TP, Averkiou MA, Leen EL. Perfusion quantification using dynamic contrast-enhanced ultrasound: the impact of dynamic range and gain on time-intensity curves. *Ultrasonics*. 2011;51: 102-106.
19. Tang MX, Mulvana H, Gauthier T, Lim AKP, Cosgrove DO, Eckersley RJ, et al. Quantitative contrast-enhanced ultrasound imaging: a review of sources of variability. *Interface Focus*. 2011;1: 520-539.
20. Hyvelin JM, Tardy I, Arbogast C, Costa M, Emmel P, Helbert A, et al. Use of Ultrasound Contrast Agent Microbubbles in Preclinical Research Recommendations for Small Animal Imaging. *Investigative Radiology*. 2013;48: 570-583.
21. Volckaert V, Vandermeulen E, Dobbeleir A, Duchateau L, Saunders JH, Peremans K. Effect of thyroid volume on radioiodine therapy outcome in hyperthyroid cats. *Journal of Feline Medicine and Surgery*. 2016;18: 144-149.

22. Williams TL, Elliott J, Syme HM. Association of iatrogenic hypothyroidism with azotemia and reduced survival time in cats treated for hyperthyroidism. *Journal of Veterinary Internal Medicine*. 2010;24: 1086-1092.

CHAPTER IX

ASSESSMENT OF RENAL PERFUSION IN CATS WITH CHRONIC KIDNEY DISEASE

Adapted from:

Stock E., Paepe D., Daminet S., Vandermeulen E., Duchateau L., Saunders J.H.*, Vanderperren K.* (* shared senior authorship). Contrast-enhanced ultrasound for the assessment of renal perfusion in cats with chronic kidney disease. *Journal of Veterinary Internal Medicine*. *Under revision*.

1. Abstract

Contrast-enhanced ultrasound (CEUS) is an emerging, functional imaging technique allowing non-invasive assessment of tissue perfusion. Human studies show that the technique holds great potential to be used in the diagnosis of chronic kidney disease (CKD). However, data in veterinary medicine are currently lacking. This study evaluates the diagnostic capabilities of CEUS in client-owned cats with CKD (n=14) in comparison with healthy control cats (n=43).

In cats with CKD, longer time-to-peak and shorter mean transit times were observed for the renal cortex. In contrast, a shorter time-to-peak and rise time were seen for the renal medulla. The findings for the renal cortex indicate a decreased blood velocity and shorter total duration of enhancement, likely caused by increased vascular resistance in CKD. An increased blood velocity in the renal medulla has not been described before, and may be due to a different response to regulatory factors in cortex and medulla.

In conclusion, CEUS was capable of detecting perfusion changes in cats with CKD. Further research is warranted to assess the diagnostic capabilities of CEUS in early stage of the disease process.

2. Introduction

CKD is one of the most commonly diagnosed diseases in elderly cats. The prevalence has been reported to be approximately 1-3% in the general feline population, even increasing to 30% in geriatric cats.¹⁻³ Renal disease is reported to be the cause of death in 14-17% of senior and geriatric cats.⁴ A primary, often unidentified trigger, initiates renal damage and nephron loss, which finally results in self-perpetuating renal injury and progressive renal disease.⁵ The most common histologic findings in cats with CKD are tubulointerstitial lesions as tubular atrophy, interstitial inflammation and fibrosis.⁶ Diagnosis in early stage of the disease progress allows timely initiation of supportive therapy and slows the disease progress.⁷ Prompt diagnosis remains challenging. The diagnosis is most often based on elevations of serum urea and creatinine concentrations combined with a low urine specific gravity. These changes are unfortunately only present when already a substantial portion of renal function is lost. Measurement of glomerular filtration rate (GFR) provides more accurate assessment of renal function, but requires multiple blood samples, limiting its use in routine clinical practice.^{8,9} Therefore, the search for improved noninvasive diagnostic methods for early renal disease is still ongoing.

Renal function is closely related to renal perfusion; hence evaluation of renal perfusion could yield new information about kidney function and improve diagnosis. Performing an accurate and non-invasive measurement of renal perfusion is challenging. Dynamic high-field magnetic resonance imaging, contrast-enhanced computed tomography or renal scintigraphy can be used to assess renal perfusion. In practice, clinical application of those techniques is limited by relatively high costs, limited availability, long examination times and exposure to ionizing radiation.^{10,11} Doppler ultrasound allows calculation of perfusion indices providing information about vascular resistance. These indices are elevated in animals with renal disease, but are relatively unspecific as they are influenced by multiple non-renal factors.¹²⁻¹⁴ Moreover, Doppler ultrasound is limited to evaluation of macroperfusion since low-velocity flow in smaller vessels cannot be assessed.¹²

Contrast-enhanced ultrasound (CEUS) is an emerging technique using microbubbles to enhance detection of tissue perfusion up to a microvascular level. These bubbles are gas-filled spheres stabilized by an outer shell. They have a size similar to those of red blood cells and thus remain strictly in the blood pool after intravenous injection. CEUS has been shown to be a promising technique for the early diagnosis of renal disease in humans, however data in veterinary medicine are lacking.^{15,16}

The aim of this study was to evaluate the efficacy of CEUS in the diagnosis of CKD in cats. The hypothesis is that CEUS would be a practical, non-invasive technique to detect perfusion changes in cats with CKD.

3. Materials and methods

The study was performed with approval of the local ethical committee of the Faculty of Veterinary Medicine, Ghent University, Belgium and the deontological committee of the Belgian Federal Agency for the Safety of the Food Chain (EC2015-68). All owners gave their full informed consent to participate in the study.

Subjects

Fourteen cats with CKD and 43 healthy control cats were included. The diagnosis of CKD was made prior to inclusion and was based on the presence of compatible clinical signs and laboratory findings i.e. increased serum creatinine (> 161.8 $\mu\text{mol/L}$)¹⁷ and decreased urine specific gravity (< 1.035). Cats with significant concurrent systemic disease, hyperthyroidism, and urinary tract

obstructions leading to postrenal azotemia were excluded. The CKD cats were subdivided into 4 stages according to the classification of the International Renal Interest Society (IRIS) classification.¹⁸ Cats with lack of significant abnormalities in history, on physical examination, thoracic radiographs, abdominal ultrasound, complete blood count, biochemistry, and urinalysis were defined as 'healthy'. All medication or nutritional supplements, except for phosphorus binders in the CKD group, were withdrawn at least 14 days prior to inclusion.

Study design

A routine physical exam, including non-invasive measurement of the blood pressure by Doppler ultrasonic technique, assessment of body weight, body condition score on a 9-point scale and muscle condition score¹⁹, cervical palpation for scoring the thyroid gland size (in cats > 6 years)²⁰, cardiac and lung auscultation, abdominal palpation, peripheral lymph node palpation, evaluation of the color and refill of the mucous membranes, was performed in all cats. Blood work consisted of complete blood count and serum biochemistry, including total thyroxine (T4) level in cats of 6 years and older. Urinalysis included urine specific gravity (USG), sediment analysis (as described in Paepe et al. (2013))²¹, urinary protein: creatinine ratio (UPC), dipstick, and bacterial urine culture. Thoracic radiographs (left-right lateral and ventrodorsal projections) and complete abdominal ultrasound were performed.

CEUS procedure

A 22-Gauge indwelling catheter was placed in the cephalic vein.

The hair was clipped over the ventrolateral portion of the abdomen and coupling gel was applied to the skin. The ultrasound exams were performed with the cat in dorsal recumbency. The kidney of interest was centered on the screen and was imaged in a longitudinal plane using dual-screen (simultaneous display of conventional B-mode and contrast-mode image). The transducer was manually positioned during each imaging procedure and was maintained at the same position during the CEUS examination.

The contrast agent (Sonovue®, Bracco, Italy), 0.05 mL/kg, was injected IV (bolus injection over +/- 3 s) followed by injection of 1.5 mL saline bolus. A three-way stopcock was used to avoid any delay between the injection of contrast agent and saline. The same person performed the injection in a standardized way in all cats. Three injections of contrast were performed: two for the left kidney

and one for the right kidney. The first injection was not used for further analysis.²² Between subsequent injections, to avoid artifacts, remnant microbubbles were completely destroyed by setting the acoustic power at the highest level and scanning the caudal aspect of the abdominal aorta for approximately 2 minutes.

All examinations were performed using a linear transducer of 12-5 MHz on a dedicated machine (IU22, Philips) with contrast-specific software. Basic technical parameters were a single focus placed under the kidney, persistency off, mechanical index 0.09, high dynamic range setting (C50), timer started at the beginning of the injection, gain (85%, corresponding to a nearly dark/anechoic image before USCA administration). The settings were repeated during each injection. All studies were digitally registered as a movie clip at a rate of 9 frames per second, during 90 seconds.

The clips were analyzed using specialized computer software (VueBox®, Bracco Research, Switzerland) for objective quantitative analysis. Six regions-of-interest (ROIs) were manually drawn: 3 in the renal cortex, 2 in the renal medulla and 1 on an interlobar artery. The ROIs were similar in size and drawn at the same depth for every region. Cystic lesions and focal parenchymal lesions were not included in the ROIs. For every ROI, the software determined mean pixel intensity and created a time-intensity curve. Time-intensity curves were analyzed for peak enhancement (PE), wash-in area under the curve (WiAUC), rise time (RT), mean transit time (mTT), time to peak (TTP), wash-in rate (WiR), wash-in perfusion index (WiPI; $WiAUC/RT$), wash-out area under the curve (WoAUC), total area under the curve (AUC), fall time (FT), and wash-out rate (WoR). Parameters related to blood volume are PE, WiAUC, WoAUC and AUC. The PE corresponds to the maximum contrast medium signal intensity. The WiAUC is calculated as the sum of all amplitudes inside the range from the beginning of the curve up to the TTP. Similarly, WoAUC corresponds to the sum of all amplitudes inside the range from the TTP to the end of the descending curve. The other parameters, i.e. RT, mTT, TTP, WiR, WiPI, FT, WoR, are related to blood velocity. The WiR and WoR represent the maximum and minimum slopes of time-intensity curve. The RT corresponds to the time interval between the first arrival of contrast and the time of peak enhancement. The FT, in contrast, is the duration of contrast wash-out. Mean transit time is the mean duration of complete contrast medium perfusion. The values for the 3 ROIs in the renal cortex and 2 ROIs in the renal medulla were averaged. Peak enhancement for the cortex, and medulla was normalized to the values obtained for the interlobar artery (PE*).

Statistical analysis

Statistical analyses were performed using statistical software (SAS version 9.4). A linear mixed model with cat as random effect and health status (CKD/healthy) as categorical fixed effect was used. Age-group was also incorporated in the model as a categorical fixed effect to adjust in age between CKD and healthy cats. Age-groups were defined as: group 1 (1-3 years), group 2 (3-6 years), group 3 (6-10 years) and group 4 (> 10 years). Correlations between perfusion parameters and renal size, IRIS stage, serum creatinine (sCr), USG and UPC were calculated for the renal cortex and medulla using Spearman correlation coefficients (ρ). A difference was considered statistically significant if $P < 0.05$.

4. Results

Breed distribution consisted of 9 domestic short- or longhaired cats and 5 purebred cats (2 Ragdoll cats, 2 Bengals, and 1 British Shorthair) for the group of CKD cats and 41 domestic short- or longhaired cats and 2 purebred cats (2 ragdolls) for the healthy cats. The mean \pm standard error age for the CKD group was 9.3 ± 1.4 years, and 6.5 ± 0.6 years for the healthy group. The mean \pm standard error body weight for the CKD group was 4.2 ± 0.3 kg, and for the healthy group 4.0 ± 0.1 kg. Six cats had CKD IRIS stage 2, one of them was proteinuric (UPC > 0.4). Eight cats had CKD IRIS stage 3, of which 2 cats with proteinuria.

Systolic blood pressure, sCr, serum urea, USG and UPC are summarized in Table 1.

Variables	Control group (n=43)	CKD group (n=14)	P-value
Blood pressure (mmHg)	144.3 ± 3.6	141.0 ± 5.9	0.632
sCr (μmolL^{-1})	$110.4 \pm 5.2^*$	$278.1 \pm 9.3^*$	< 0.001
Serum urea (mmolL^{-1})	$8.2 \pm 0.4^*$	$18.8 \pm 0.7^*$	< 0.001
USG	$1.048 \pm 0.001^*$	$1.021 \pm 0.002^*$	< 0.001
UPC	$0.13 \pm 0.03^*$	$0.34 \pm 0.05^*$	0.004

Table 1. Baseline characteristics for CKD and healthy cats presented as mean \pm standard errors. (sCr serum creatinine concentrations, USG urine specific gravity, UPC urinary protein: creatinine ratio)

All healthy cats had a normal size and appearance of their kidneys on B-mode ultrasonography. For the CKD group, renal size was < 3.0 cm for one or both kidneys in 6 cats, 7 cats had segmental cortical lesions in one or both kidneys, an irregular outline for one of both kidneys was observed in 10 cats, and corticomedullary definition was decreased in all cats. One cat showed mild unilateral

pyelectasia, and another cat mild bilateral pyelectasia, without signs of ureteral obstruction. A single large cyst deforming the renal cortex was present in one cat, whereas few small cortical cystic lesions were detected in both kidneys in another, domestic shorthaired cat. None of the cats was diagnosed with polycystic kidney disease.

The contrast agent and the imaging procedure were well tolerated by all cats and no side effects were noticed.

Qualitative analysis of the CEUS images showed heterogeneous cortical enhancement in all cats with segmental cortical lesions.

Quantitative CEUS demonstrated significant differences between CKD and healthy cats in several perfusion parameters for the renal cortex and medulla (Table 2 and Figures 1-3). The mTT for the renal cortex, a parameter for mean duration of complete contrast medium perfusion, was approximately 4 s shorter in cats with CKD compared to healthy cats ($P=0.028$). The TTP for the cortex was longer in the CKD group ($P=0.003$). In contrast, for the medulla, the TTP decreased for the CKD patients ($P=0.003$), associated with a shorter RT ($P=0.001$) and FT ($P=0.04$)

Variable, by location	CKD	Healthy	P-value
Renal cortex			
PE	1635.12 ± 269.59	1779.16 ± 151.24	0.643
PE*	19.24 ± 3.96	27.72 ± 2.01	0.065
WiAUC	2751.49 ± 385.53	2869.57 ± 216.27	0.791
RT	3.01 ± 0.12	2.77 ± 0.06	0.068
mTT	17.63 ± 1.62	21.84 ± 0.91	0.028
TTP	8.75 ± 0.29	7.71 ± 0.16	0.003
WiR	800.61 ± 161.92	904.15 ± 90.84	0.580
WiPI	1000.53 ± 164.59	1089.36 ± 92.33	0.640
WoAUC	3606.29 ± 487.55	3830.47 ± 273.50	0.690
AUC	6357.95 ± 871.83	6700.00 ± 489.07	0.733
FT	4.12 ± 0.20	3.83 ± 0.11	0.199
WoR	523.94 ± 118.77	638.30 ± 66.65	0.405
Renal medulla			
PE	208.71 ± 203.82	276.83 ± 99.06	0.766
PE*	3.65 ± 0.70	3.02 ± 0.36	0.433
WiAUC	1653.36 ± 349.31	1892.97 ± 172.91	0.542
RT	11.23 ± 1.45	16.69 ± 0.71	0.001
mTT	50.48 ± 28.14	111.03 ± 13.89	0.060
TTP	20.16 ± 1.66	27.37 ± 0.82	0.003
WiR	4.69 ± 173.44	93.23 ± 84.29	0.649
WiPI	130.85 ± 124.72	172.68 ± 60.62	0.765
WoAUC	2934.74 ± 592.16	3519.01 ± 300.48	0.387
AUC	4570.11 ± 921.83	5446.80 ± 467.50	0.404
FT	23.25 ± 3.76	32.05 ± 1.90	0.043
WoR	0.00 ± 141.21	70.26 ± 70.48	0.631

Table 2. Table 2. Mean ± standard error values of renal perfusion parameters obtained by contrast-enhanced ultrasound for cats suffering from CKD and healthy cats. (PE peak enhancement, PE* normalized PE, WiAUC wash-in area-under-the-curve, RT rise time, mTT mean transit time, TTP time-to-peak, WiR wash-in rate, WiPI wash-in perfusion index, WoAUC wash-out area-under-the-curve, AUC total area-under-the-curve, FT fall time, WoR wash-out rate)

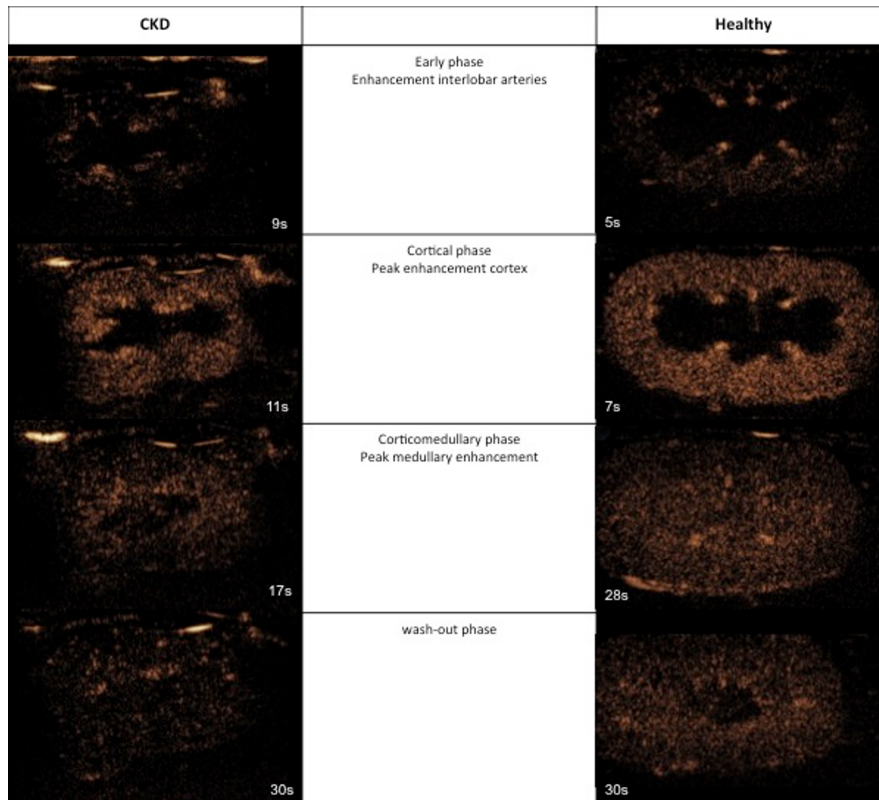


Figure 1. Representative serial contrast ultrasound images of a cat suffering from chronic kidney disease (left) and a healthy cat (right). The enhancement starts later in the CKD cat compared to the healthy cat and is of shorter duration.

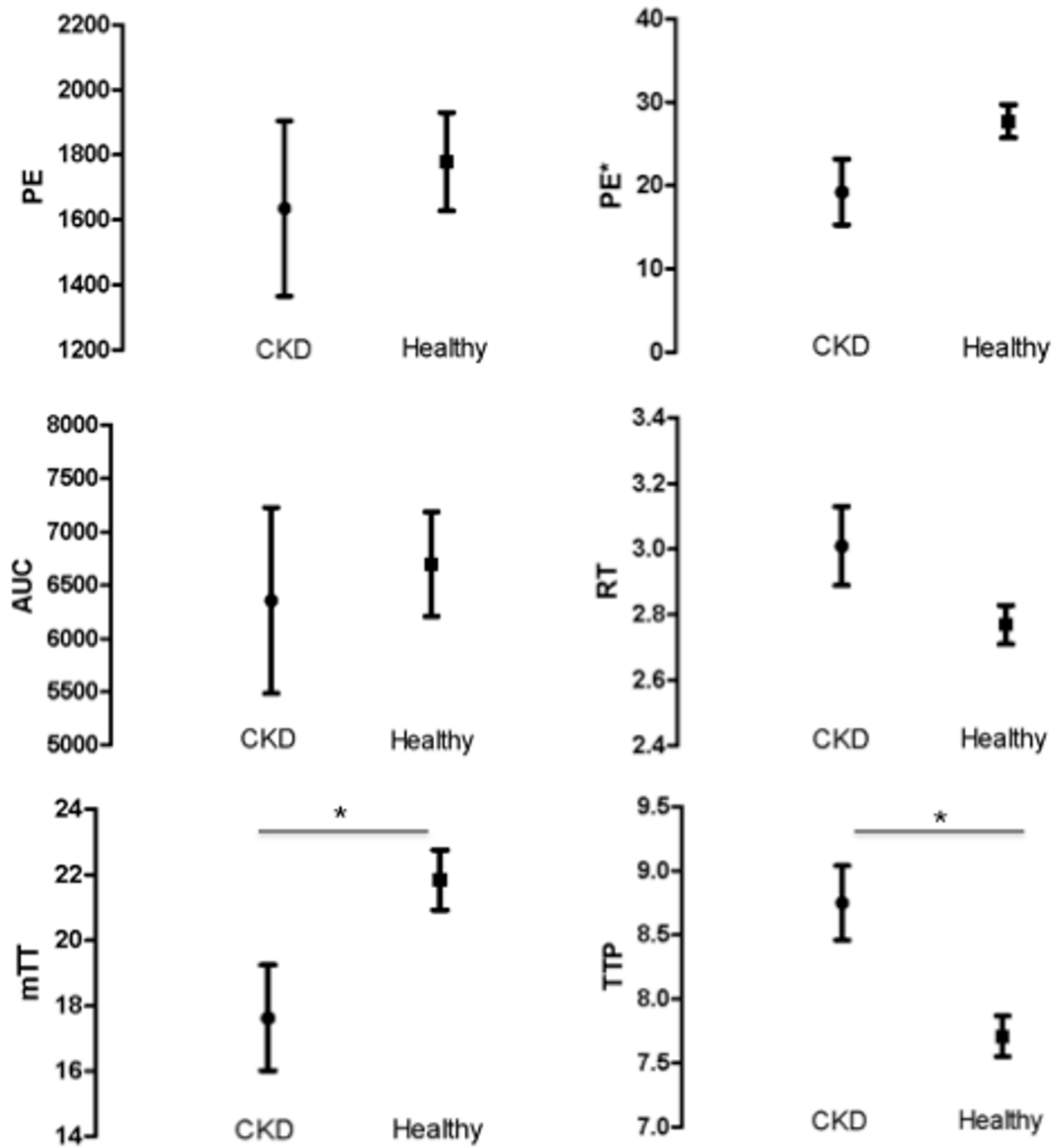


Figure 2. Differences in PE, PE*, AUC, RT, TTP, mTT from the renal cortex between cats with CKD and healthy cats, presented as mean \pm standard error. * P-value < 0.05. (PE peak enhancement, PE* normalized peak enhancement, AUC total area-under-the-curve, RT rise time, mTT mean transit time, TTP time-to-peak)

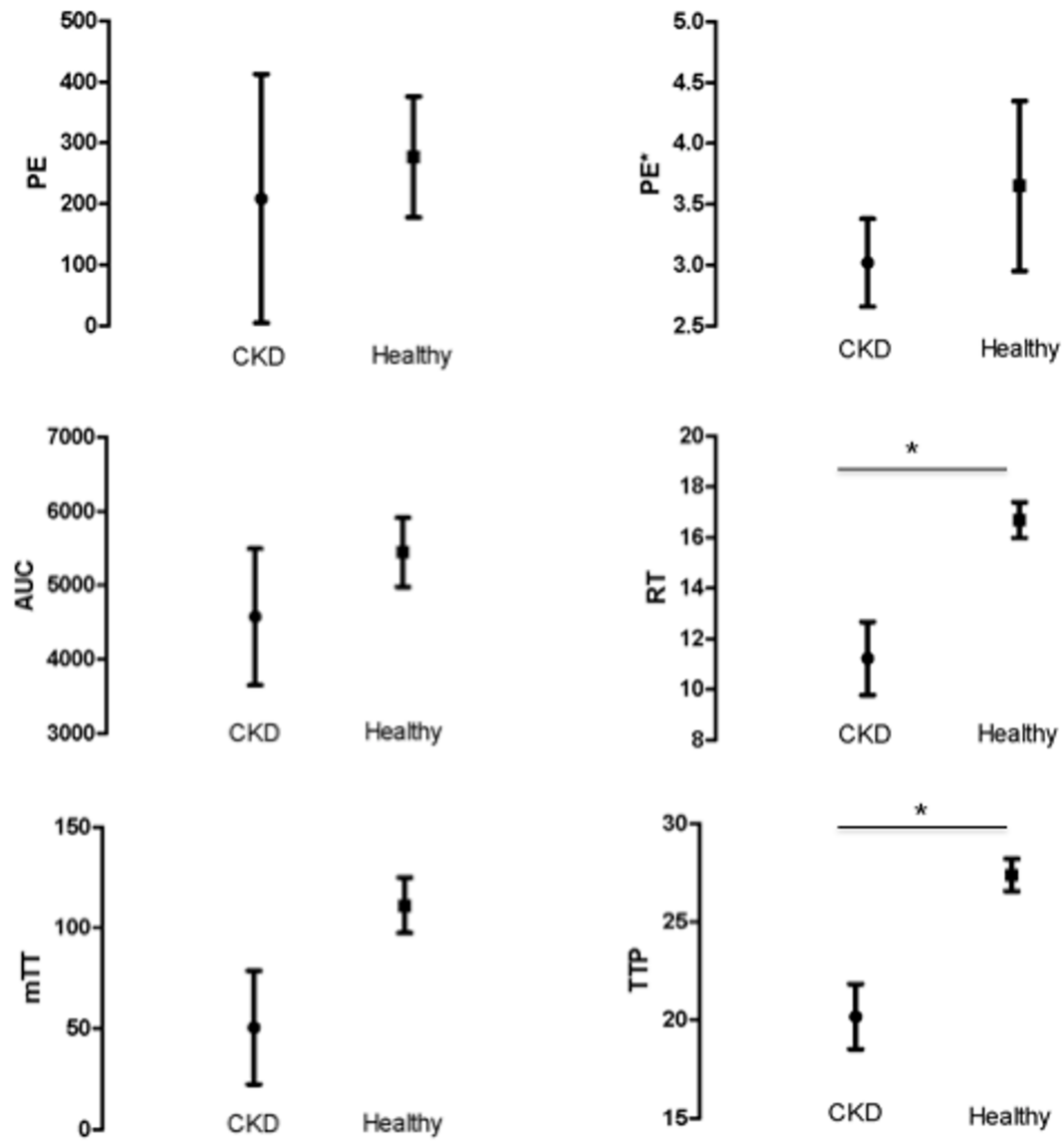


Figure 3. Differences in in PE, PE*, AUC, RT, TTP, mTT from the renal medulla between cats with CKD and healthy cats, presented as mean \pm standard error. * P-value < 0.05. (PE peak enhancement, PE* normalized peak enhancement, AUC total area-under-the-curve, RT rise time, mTT mean transit time, TTP time-to-peak)

For the renal cortex and medulla, significant correlations were present between the mTT and TTP and IRIS stage, and renal size. Additionally, significant correlations were present between the RT for the renal medulla and sCr, IRIS stage, USG and renal size. For the renal medulla, mTT and TPP were also significantly correlated to sCr, USG and renal size. Urine specific gravity was significantly correlated to medullary RT, mTT and TTP and to cortical PE*. Additionally, a significant correlation was present for the cortical PE* and IRIS stage. Spearman correlation coefficients and P-values are summarized in Table 3 and 4.

Variable pair	ρ (P)
IRIS stage – mTT	-0.29 (0.03)
IRIS stage – TTP	0.32 (0.02)
IRIS stage – PE*	-0.37 (0.005)
Renal size – mTT	0.30 (0.02)
Renal size –TTP	-0.30 (0.02)
USG – PE*	0.10 (0.02)

Table 3. Correlations between IRIS stage, renal size, USG, and renal perfusion parameters for the renal cortex. (mTT mean transit time, TTP time-to-peak, PE* normalized peak enhancement)

Correlation	ρ (P)
sCr – mTT	-0.38 (0.004)
sCr – TTP	-0.43 (0.001)
sCr - RT	- 0.46 (0.003)
IRIS stage – mTT	-0.38 (0.005)
IRIS stage – TTP	-0.47 (0.003)
IRIS stage – RT	-0.41 (0.002)
Renal size – mTT	0.43 (0.001)
Renal size –TTP	0.33 (0.01)
Renal size - RT	0.41 (0.001)
USG –mTT	0.45 (0.005)
USG – TTP	0.37 (0.006)
USG – RT	0.31 (0.02)

Table 4. Correlations between IRIS stage, renal size, USG, and renal perfusion parameters for the renal medulla. (sCr serum creatinine, IRIS international renal interest society, USG urine specific gravity, mTT mean transit time, TTP time-to-peak, RT riste time)

5. Discussion

This is the first study describing quantitative perfusion parameters of kidneys in cats with CKD, using CEUS.

Chronic kidney disease is one of the most important health issues in elderly cats.² Tubular atrophy, tubulointerstitial inflammation and fibrosis are the most common histologic abnormalities in cats with CKD.⁶ Histologic studies in human and rodent kidneys have shown that tubulointerstitial lesions are associated with damage to the renal arterioles and arteries, and distortion and loss of peritubular capillaries.²³ Tubulointerstitial fibrosis impairs renal blood flow and increases renal vascular resistance.^{23,24} Renal capillary rarefaction is considered a central mechanism in initiation and progression of CKD in people and rodents.^{25, 26} Moreover, the renin-angiotensin system is activated in CKD leading to higher renal tissue concentrations of angiotensin II compared to plasma concentrations. As angiotensin II is a potent vasoconstrictor, the combination of these

changes is likely to decrease renal blood flow in patients with CKD, resulting in decreased blood volume and decreased blood velocity. A recent study using CT angiography to evaluate renal blood volume and vascular anatomy in people showed a 41% reduction in cortical renal blood volume in patients with CKD compared to healthy subjects. CKD patients also showed reduction in luminal diameters of segmental arteries. Moreover, cortical renal blood volume decreased during progression of CKD and was correlated with a decline in GFR.²⁶ Medullary blood volume values were more variable and did not correlate with GFR.²⁶

The most striking findings of our study were a shorter mTT time, indicating shorter enhancement, and an increased TTP for the renal cortex. The longer TTP suggests a decreased blood velocity. These findings correspond to previous studies in human medicine, in which a decreased TTP was also described in patients with CKD of various origin and patients with diabetic nephropathy.^{27, 28} A decreased TTP was also an early finding in dogs in which ischemic renal disease was induced by placing an ameroid constrictor around the renal artery.²⁹

The PE, a parameter for the intensity of enhancement, reflects the blood volume entering the kidney and is hence expected to be decreased in patients with CKD. Previous studies on CEUS in humans with CKD reported a decrease in PE^{15, 16, 27, 28}, however a significant decrease in PE was not present in this study. Close inspection of the results in the human studies shows that a great degree of overlap in PE for patients with CKD and healthy subjects.^{15, 16, 27, 28} A relatively low number of feline patients with CKD were included in our study; significance might have been achieved by including a higher number of patients. Moreover, PE is known to suffer from an inherently high variability, as it is susceptible to many influencing factors.^{30, 31} Variation may be attributed to the contrast agent itself (amount and physical properties of the microbubbles), uncontrollable patient-factors as blood pressure, heart rate, filtration of the bubbles by the lungs and phagocytosis by the reticuloendothelial system and the manual injection procedure.

Changes in AUC have also been described in humans with CKD, whereas no significance was obtained in our study. Both an increase as a decrease in AUC has been described in people with CKD. Ma et al. (2012) observed an increase in AUC in early stage diabetic nephropathy, whereas a decrease was noticed in advanced stages.²⁸ An increase in AUC was reported in 41 humans with CKD, whereas a decrease was reported in the canine study with iatrogenic ischemic renal disease.¹⁵
²⁹ The variable effects on AUC may be explained by the fact that AUC is influenced by the PE, as well as the slope of the time-intensity curve. The AUC is composed of 2 parts: an initial part relating to

inflow of contrast and a descending part related to the outflow of contrast medium. Moreover, AUC may be influenced by the stage and progression of CKD.

The decreased TTP and RT for the renal medulla in CKD patients in this study were not completely expected. Only one study has described CEUS of the medulla in people with CKD. In the human study, findings for the medulla paralleled those from the cortex, thus showing delayed time to peak.²⁷ Still, it has been described that the vascular anatomy and physiology of the renal medulla differs importantly from those of the cortex. The renal medulla makes up less than 30% of the total renal volume but only receives 10% of the total renal blood flow. Additionally, local differences are described for the outer and inner medulla, with the latter being less perfused. Vasoactive regulatory factors have different effects on cortical and medullary blood flow. The medulla is relative insensitive to vasoconstriction.³² Therefore, local increased blood velocity could be present in the medulla in cats with CKD. However, further studies are needed to confirm this finding and further investigate the underlying pathophysiology.

Significant correlations were found between time-based perfusion parameters and sCr, IRIS stage, USG, UPC and renal size in this study. However, correlation coefficients were low and did even not exceed 0.50 in most cases. The highest correlated coefficient was observed for the UPC and TTP for the renal medulla. Similarly low, but significant correlation coefficients are described in 2 human studies. Tsuruoka et al. (2010), observed a correlation between the slope of the ascending and descending parts of the time-intensity curve and sCr-based estimated GFR (correlation coefficients ranging from 0.26 – 0.40). Additionally, a significant correlation was present between PE and estimated GFR ($r = 0.27$).²⁷ Similarly, a correlation ($r = 0.47$) between AUC and GFR measured by radionuclide clearance techniques has been described in people with diabetic nephropathy.²⁸ Moreover, the correlations calculated in our feline study are only based on a small number of subjects and should therefore be interpreted with caution.

In conclusion, our findings in a small cohort of cats with CKD are encouraging to use CEUS to evaluate renal perfusion in cats. A decrease in blood velocity was detected for the renal cortex whereas an increased blood velocity was present for the renal medulla. The enhancement of the renal cortex was found to be of shorter duration in cats with CKD (decreased mTT). However, no significant changes could be detected in parameters representing the blood volume. Further studies are necessary to evaluate the added value of CEUS to diagnose early, non-azotemic CKD.

Acknowledgements

The authors want to thank Bracco Suisse SA (Geneva, Switzerland) for their scientific support on the use of VueBox® and Medvet (Antwerp, Belgium) for the laboratory analyses.

6. References

1. Lund EM, Armstrong PJ, Kirk CA, Kolar LM, Klausner JS. Health status and population characteristics of dogs and cats examined at private veterinary practices in the United States. *Journal of the American Veterinary Medical Association*. 1999;214: 1336-1341.
2. Lulich JP, Osborne CA, O'Brien TD, Polzin DJ. Feline Renal-Failure - Questions, Answers, Questions. *Compendium on Continuing Education for the Practicing Veterinarian*. 1992;14: 127-152.
3. Polzin DJ. Chronic kidney disease. In: Ettinger SJ, Feldman EC (eds): *Textbook of veterinary internal medicine: diseases of the dog and the cat* Missouri: Saunders Elsevier, 2010;1990 - 2020.
4. O'Neill DG, Church DB, McGreevy PD, Thomson PC, Brodbelt DC. Longevity and mortality of cats attending primary care veterinary practices in England. *Journal of Feline Medicine and Surgery*. 2015;17: 125-133.
5. Jepson RE. Current Understanding of the Pathogenesis of Progressive Chronic Kidney Disease in Cats. *Veterinary Clinics of North America: Small Animal Practice*. 2016;46: 1015-1048.
6. Brown CA, Elliott J, Schmiedt CW, Brown SA. Chronic Kidney Disease in Aged Cats: Clinical Features, Morphology, and Proposed Pathogeneses. *Veterinary Pathology*. 2016;53: 309-326.
7. Paepe D, Daminet S. Feline CKD: Diagnosis, staging and screening - what is recommended? *Journal of Feline Medicine and Surgery*. 2013;15 Suppl 1: 15-27.
8. Paepe D, Lefebvre HP, Concordet D, van Hoek I, Croubels S, Daminet S. Simplified methods for estimating glomerular filtration rate in cats and for detection of cats with low or borderline glomerular filtration rate. *Journal of Feline Medicine and Surgery*. 2015;17: 889-900.
9. Finco DR, Brown SA, Vaden SL, Ferguson DC. Relationship between plasma creatinine concentration and glomerular filtration rate in dogs. *Journal of Veterinary Pharmacology and Therapeutics*. 1995;18: 418-421.
10. Herget-Rosenthal S. Imaging Techniques in the Management of Chronic Kidney Disease: Current Developments and Future Perspectives. *Seminars in Nephrology*. 2011;31: 283-290.
11. Daniel GB, Mitchell SK, Mawby D, Sackman JE, Schmidt D. Renal nuclear medicine: A review. *Veterinary Radiology & Ultrasound*. 1999;40: 572-587.
12. d'Anjou MA, Penninck D. Kidneys and ureters. In: Penninck D, M.A. dA (eds): *Atlas of small animal ultrasonography*. Oxford: Wiley Blackwell, 2015;331-362.

13. Tipisca V, Murino C, Cortese L, Mennonna G, Auletta L, Vulpe V, et al. Resistive index for kidney evaluation in normal and diseased cats. *Journal of Feline Medicine and Surgery*. 2015;18: 471-475.
14. Novellas R, de Gopegui RR, Espada Y. Increased renal vascular resistance in dogs with hepatic disease. *Veterinary Journal*. 2008;178: 257-262.
15. Dong Y, Wang WP, Cao J, Fan P, Lin X. Early assessment of chronic kidney dysfunction using contrast-enhanced ultrasound: a pilot study. *British Journal of Radiology*. 2014;87: 1-7.
16. Hosotani Y, Takahashi N, Kiyomoto H, Ohmori K, Hitomi H, Fujioka H, et al. A new method for evaluation of split renal cortical blood flow with contrast echography. *Hypertension Research*. 2002;25: 77-83.
17. Ghys LF, Paepe D, Duchateau L, Taffin ER, Marynissen S, Delanghe J, et al. Biological validation of feline serum cystatin C: The effect of breed, age and sex and establishment of a reference interval. *Veterinary Journal*. 2015;204: 168-173.
18. IRIS kidney. 2017 [cited; Available from: <http://www.iris-kidney.com>]
19. Baldwin K, Bartges J, Buffington T, Freeman LM, Grabow M, Legred J, et al. AAHA Nutritional Assessment Guidelines for Dogs and Cats. *Journal of the American Animal Hospital Association*. 2010;46: 285-296.
20. Boretti FS, Sieber-Ruckstuhl NS, Gerber B, Laluha P, Baumgartner C, Lutz H, et al. Thyroid enlargement and its relationship to clinicopathological parameters and T-4 status in suspected hyperthyroid cats. *Journal of Feline Medicine and Surgery*. 2009;11: 286-292.
21. Paepe D, Verjans G, Duchateau L, Piron K, Ghys L, Daminet S. Routine health screening: findings in apparently healthy middle-aged and old cats. *Journal of Feline Medicine and Surgery*. 2013;15: 8-19.
22. Stock E, Vanderperren K, Haers H, Duchateau L, Hesta M, Saunders JH. Quantitative differences between the first and second injection of contrast agent in contrast-enhanced ultrasonography of feline kidneys and spleen. *Ultrasound in Medicine and Biology*. 2017;43: 500-504.
23. Nangaku M. Chronic hypoxia and tubulointerstitial injury: a final common pathway to end-stage renal failure. *Journal of the American Society of Nephrology*. 2006;17: 17-25.
24. Basile DP, Donohoe D, Roethe K, Osborn JL. Renal ischemic injury results in permanent damage to peritubular capillaries and influences long-term function. *American Journal of Physiology Renal Physiology*. 2001;281: F887-899.

25. Horbelt M, Lee SY, Mang HE, Knipe NL, Sado Y, Kribben A, et al. Acute and chronic microvascular alterations in a mouse model of ischemic acute kidney injury. *American Journal of Physiology Renal Physiology*. 2007;293: F688-695.
26. von Stillfried S, Apitzsch JC, Ehling J, Penzkofer T, Mahnken AH, Knuchel R, et al. Contrast-enhanced CT imaging in patients with chronic kidney disease. *Angiogenesis*. 2016;19: 525-535.
27. Tsuruoka K, Yasuda T, Koitabashi K, Yazawa M, Shimazaki M, Sakurada T, et al. Evaluation of renal microcirculation by contrast-enhanced ultrasound with sonazoid (TM) as a contrast agent. *International Heart Journal*. 2010;51: 176-182.
28. Ma F, Cang YQ, Zhao BZ, Liu YY, Wang CQ, Liu B, et al. Contrast-enhanced ultrasound with SonoVue could accurately assess the renal microvascular perfusion in diabetic kidney damage. *Nephrology Dialysis Transplantation*. 2012;27: 2891-2898.
29. Dong Y, Wang WP, Cao JY, Fan PL, Lin XY. Quantitative evaluation of contrast-enhanced ultrasonography in the diagnosis of chronic ischemic renal disease in a dog model. *Plos One*. 2013;8: e70377.
30. Tang MX, Mulvana H, Gauthier T, Lim AKP, Cosgrove DO, Eckersley RJ, et al. Quantitative contrast-enhanced ultrasound imaging: a review of sources of variability. *Interface Focus*. 2011;1: 520-539.
31. Hyvelin JM, Tardy I, Arbogast C, Costa M, Emmel P, Helbert A, et al. Use of Ultrasound Contrast Agent Microbubbles in Preclinical Research Recommendations for Small Animal Imaging. *Investigative Radiology*. 2013;48: 570-583.
32. Evans RG, Eppel GA, Anderson WP, Denton KM. Mechanisms underlying the differential control of blood flow in the renal medulla and cortex. *Journal of Hypertension*. 2004;22: 1439-1451.

CHAPTER X

GENERAL DISCUSSION

1. Introduction

One of the most important health issues in cats, and more importantly in older cats, is chronic kidney disease (CKD).^{1,2} The diagnosis is based on a combination of clinical signs, a blood test showing an increased serum creatinine and urinalysis demonstrating a decreased urine specific gravity. Unfortunately, this only allows diagnosis in a relatively late stage of the disease process, as approximately two-thirds to three-quarters of functional renal mass must be lost before these abnormalities will develop.^{3,4} Therefore, the search for non-invasive, safe and clinical applicable methods allowing early diagnosis of chronic renal disease in cats, is still of great interest.

The underlying cause of feline renal disease is poorly understood and is likely to be influenced by several genetic, individual and environmental factors.⁵ The diagnosis of feline CKD is hence not based on identifying the primary cause, but rather on detecting early changes indicative for progressive renal damage. Renal function is closely related to renal perfusion, moreover changes in renal perfusion are believed to play a key role in the pathophysiology of renal disease.^{6,7} Consequently, assessment of renal perfusion could deliver important new insights in feline CKD and its diagnosis.

Contrast-enhanced ultrasound (CEUS) is an emerging technique in veterinary medicine. The unique nature of the contrast agents used in CEUS provides real-time and quantitative imaging of the vasculature. CEUS has many favorable characteristics for its use in clinical practice: it is very safe, non-invasive, relatively fast and cost-effective, and does not involve the use of ionizing radiation.^{8,9} Studies in human medicine and preliminary studies in dogs have shown great promise for the use of CEUS in the diagnosis of diffuse renal diseases.¹⁰⁻¹⁴ However, studies in cats are currently limited to description of the normal perfusion pattern in healthy cats.¹⁵⁻¹⁷ An overview of the current knowledge on CEUS in human and veterinary medicine is provided in **Chapter I**.

The main objective of this thesis was to establish the potential value of CEUS in the evaluation of feline renal perfusion.

Contrast-enhanced ultrasound is a relatively new technique, hence no uniform, standardized protocols are currently available. Nevertheless, the reliability and reproducibility of the technique strongly relies on a well-designed and punctually executed protocol.¹⁸ Contrast-enhanced ultrasound is a fast-growing imaging modality, consequently, new literature and software tools

are being developed continuously. Therefore, the protocols used in this thesis were adapted as knowledge increased and as new software programs became available. The main study design (bolus-kinetics) and technical parameters (low mechanical index, gain setting, focus setting), as explained in **Chapter I**, remained constant during this thesis.

The first study (**Chapter III**) was performed using a MyLab 30CV ultrasound machine (Esaote), equipped with a linear probe. Subsequent quantitative analysis was performed with ImageJ. Analysis was labor intensive; moreover only log-compressed data could be analyzed. However, it was revealed that log compression leads to loss of linearity between local contrast agent concentrations and the resulting signal intensity.¹⁸⁻²⁰ Therefore, the study in **Chapter V** was performed on an iU22xMATRIX system (Philips), allowing us to export native radio-frequency data, which overcomes the problem of log compression. These data were analyzed using a more user-friendly software program (QLab®, Philips). After this study (**Chapters IV, VI, VII, VIII and IX**), we were able to use the recently developed quantification software VueBox® (Bracco Suisse SA). This system- and user-independent application allows standardized perfusion quantification across different users and systems, thereby improving reproducibility of results across several research centers. The software allows linearization of all video data, a reliable tool to overcome the problems encountered with log compression, moreover, a motion compensation tool allows reduction of breathing artifact. Automatic curve fitting is applied to the time-intensity curve allowing to extract multiple perfusion parameters.

For the first studies (**Chapters III and V**) a typical clinical dynamic range setting of 38 dB was used, whereas a high dynamic range (50 dB) was used for the later studies (**Chapters IV, VI, VII, VIII and IX**). Signal saturation may occur with lower dynamic range setting, which can prevent proper linearization of log-compressed data.²⁰

The contrast agent dose has also evolved: a fixed dose of contrast agent (0.15 mL per cat) was used in most studies on experimental animals (**Chapters III, V, VII**), whereas a dose per kg of bodyweight (0.05 mL/kg) was used in studies on clinical patients (**Chapters VI, VIII, and IX**). The experimental cats were within the same weight category and the dose corresponded approximately to the dose per kg used in patients. In contrary, the clinical patients showed more variability in weight, and therefore we decided to adapt the dose to their body weight, as this would be more correct. Moreover, in **Chapter VIII**, an increase in body weight was noticed for the cats after 131-I treatment. In general, the dosage of contrast agent used in our studies was judged

to be appropriate, since a good signal-to-noise ratio was obtained with uniform enhancement in most cats, eliminating attenuation artifacts.

The major consequence of the slight modifications of the study protocol is that the absolute values of the perfusion parameters cannot be compared between studies with a different protocol. However, this has no influence on the results of the separate studies neither on the final conclusions of this thesis.

In **Chapters III, V and VII** only the left kidney was studied. This is justified since the response of renal perfusion in healthy individuals is similar in both kidneys.⁶ However in disease states, the left and right kidneys can be affected in a different degree and therefore CEUS of both kidneys was performed (**Chapters VI, VIII, and IX**). The left kidney is located more caudal compared to the right kidney²¹, resulting in an easier accessibility, even more since linear transducers were used. Linear transducers were chosen given their superior image resolution compared to curvilinear transducers. However, the larger footprint of linear transducers complicates visualization of organs (partially) located under the rib cage, as the right kidney. In **Chapter IV**, we found that the extra variation added by studying a different kidney in the same cats, was minimal. Nevertheless, few clips of the right kidney of clinical patients in **Chapters VI, VIII and IX** could not be analyzed due to difficult visualizing of this kidney which was never noticed for the left kidney.

2. Quantitative differences between sequential injections

In this thesis, manual bolus injections of ultrasound contrast agent (USCA) were used. Manual bolus injections are the most common way of contrast administration in veterinary CEUS, mainly because no special equipment is needed to perform the injection. In theory, a single injection per studied organ should be sufficient. However, some authors have previously described unsatisfactory enhancement after the first injection of USCA²²⁻²⁵, whereas this is not mentioned in multiple other publications. Subjectively we had the impression that the first injection often leads to poor enhancement. Performing an additional injection increases the imaging time and total administered dose of USCA, and could thereby increase the costs. However, image quality and reliability of quantification are always of superior importance. Therefore, in **Chapter III**, we assessed if quantitative differences were present between the first and second injection of USCA. Perfusion parameters for the left kidney and spleen, imaged simultaneously, for the first and second injection of USCA, of 7 healthy cats were compared.

In our study, higher peak enhancement (PE) and area-under-the-curve (AUC) were present for the second injection compared to the first injection. This was significant for the renal cortex and spleen, whereas a tendency was noted for the PE for the renal medulla. Additionally, for the renal cortex, the time-intensity curve was flatter for the first injection. This was reflected by lower wash-in (W_{in}) and wash-out (W_{out}) values. Moreover, additional quantifications on data of other studies in this thesis learned that no significant differences were present between the second and third injection, nor between the right and left kidney (unpublished results).

The underlying mechanism remains still unclear and it was beyond the scope of this thesis to investigate this further. The presence and extent of quantitative differences between the first and second injection of USCA is likely to be influenced by several factors and several explanations are proposed.

Microbubbles have a tendency to adhere to the catheter, three-way stopcock and even vessel walls. A part of the microbubbles in the first injection may thereby be 'lost' for imaging. The second injection may cause propagation of these bubbles in the systemic circulation or, alternatively, the bulk of subsequent injections may arrive in the circulation since the multiple adherence sites are occupied by contrast agent of the first injection.²⁵

Microbubbles may be captured in capillaries and sinusoids of the organs of the reticuloendothelial system as the liver and spleen. Microbubble destruction in-between the injections is believed to clean the majority of the captured contrast agent, however it cannot be excluded that some microbubbles remain lodged in capillaries. Haers et al. (2012) assumed that remnant microbubbles may be propelled into the systemic circulation following the second injection, thereby causing a relative increase in the dose of contrast agent for the second injection.²² In mice, short-term saturation of the hepatic and splenic sinusoids is described. Consequently, a lower amount of microbubbles will be captured by these organs upon the second injection, leaving relatively more microbubbles available to circulate.²⁶ However, injection of 1.2 – 1.4 mL USCA in people did not cause liver saturation.²⁷ It is unclear if the dose used in this study, 0.15 mL, could cause liver saturation in cats. Similarly, saturation of pulmonary macrophages may occur.²⁸ This would allow more microbubbles to pass the lung and finally reach the systemic circulation.

The composition of the USCA, mainly microbubble shell composition, also affects the degree phagocytosis by the reticuloendothelial system.²⁰ Moreover, it is assumed that species- and even individual-specific responses to microbubbles exist. The organ studied may be another factor influencing the presence and degree of this phenomenon.

Because our study proved that quantitative differences were present between the first and second injection of contrast agent, the first injection was not used for further analysis in the following studies.

3. Repeatability

Contrast ultrasound is known to suffer from an inherent relatively high variability.²⁰ Nevertheless, the repeatability of CEUS for the kidney in a clinical setting has not been described, neither in human medicine, nor in veterinary medicine. In **Chapter IV** we assessed the repeatability of CEUS of the kidneys in 12 healthy cats. To determine and compare the repeatability of the different perfusion parameters, the coefficient of variation (CV) was calculated.

The lowest CV, and thus best repeatability, was present for the time-to-peak (TTP) for the renal cortex. This was followed by rise time (RT), fall time (FT) and mean transit time (mTT) for the renal cortex. The CV values of these parameters were < 25% and even < 10% for the TTP, this may be judged as good to moderate repeatability. The injection technique is crucial for the variation in these time-related parameters. The manual bolus injection used in our studies is more susceptible to variation compared to controlled injections performed using specialized equipment.²⁰ Nevertheless, all efforts were made to standardize the injection procedure as the injection was always performed by the same person, not only for this study, but also for all studies in this thesis. Recently, a commercial bolus-injection system has become available.²⁹ Using this system might lead to a further improvement in the repeatability of the TTP, mTT, WiR and WoR, whereas no improvement is expected for PE and AUC.²⁹

Repeatability for the perfusion parameters related to the intensity (and thus concentration of contrast agent) and shape of the time-intensity curve was low. These parameters are susceptible to several sources of variation. The first source of variation encountered is the contrast agent. It may be assumed that the contrast agent itself is one of the most important sources of variation as the CV for PE and AUC was 33-36% in an in vitro study³⁰, eliminating variation related to the patient. The manual shaking of the vials for reconstitution prior to use may already introduce significant variations in size and concentration of the USCA. Moreover, significant differences exist between the shell compositions of the microbubbles of the same contrast agent, leading to different responses to ultrasound waves.²⁰ Further variation is caused by administration and the physical and physiological conditions in the immediate environment. Different degrees of

sedimentation in the syringe and catheter will result in different microbubbles doses. Patient-related factors will cause some additional variation. The acoustic window and several uncontrollable patient factors such as blood pressure, heart rate, filtration of microbubbles by the lungs and phagocytosis by the reticuloendothelial system will influence quantification of CEUS.²⁰ Normalization of areas of interest with neighboring normal tissue may reduce variation.²⁰ This method is extremely useful in the evaluation of abnormal tissue surrounded by normal tissues as focal liver lesions. It is more difficult to accomplish in the diagnosis of diffuse renal disease, in which the entire kidney is involved. Choosing reference tissue outside the kidney seems most appropriate, however this interferes with the imaging of the kidney itself. Obtaining a standardized, longitudinal plane of the kidney is of major importance, as suboptimal and inconsistent imaging planes will induce extra variation. Therefore, after multiple attempts by experienced persons, we decided that combining standardized imaging of the kidney with simultaneous imaging of normal reference tissue is not feasible. In several studies we tested normalization to the interlobar arteries. However, in **Chapter IV**, the variance in PE was higher for the interlobar artery compared to the PE for the renal cortex or medulla. Therefore, normalization to the interlobar artery did not reduce variation but in contrast, higher CV was found for the normalized PE values. Moreover, in **Chapter VII**, significant changes in PE were obtained after angiotensin II (AT II) infusion, whereas this difference was no longer seen if the parameters were normalized to those of the interlobar artery. Nevertheless, in **Chapter VIII**, a significant decrease in normalized PE for the renal medulla was found after treatment for hyperthyroidism, whereas the change in PE did not reach significance. Interlobar arteries are tiny structures and are therefore very susceptible to motion artifact, resulting in inconsistent imaging and therefore difficult placement of regions-of-interest (ROI). Moreover, the flow in the interlobar artery could also be influenced by a renal condition.

For the last patients of the clinical studies described in **Chapters VI, and VIII** an attempt was made to use the caudal abdominal aorta as reference tissue. The major drawback was that this was accomplished by imaging the aorta separately, thus acquiring an additional clip. Therefore, it could not correct for variation induced by the imaging plane. Moreover, an additional injection of USCA is subject to its own sources of variability, which may slightly differ from those of the previous injections. A proper repeatability study could not be performed on the data normalized to the aorta, however the variability seems similar to those obtained after normalization to the interlobar artery.

Flash-replenishment kinetics may be less susceptible to variation, but no supporting data are currently available. Therefore, it would be interesting to test this hypothesis in a prospective, randomized crossover study.

4. Influence of sedation and anesthesia

In **Chapter V** the influence of a commonly used sedative agent and an anesthetic agent on quantitative CEUS was assessed. Although CEUS is a relatively short procedure, it is very important that the animal remains immobile during the acquisition of the CEUS clip, lasting approximately 90 s to be able to perform accurate quantification. As this is not possible for all cats, we aimed to investigate the influence of 2 commonly used sedative/anesthetic protocols: intramuscular (IM) administration of 0.4 mg/kg butorphanol and intravenous (IV) boluses of propofol on effect. This was accomplished by enrolling 6 healthy cats in a randomized crossover design. No significant effect of butorphanol was observed for any of the perfusion parameters. In contrast, increases in TTP and AT, and a decrease in W_{in} , were observed after using propofol, indicating a decrease in blood velocity. This is explained by the well-known cardiovascular effects of propofol, namely decreased cardiac output and systemic vascular resistance, resulting in depression of the systolic and diastolic blood pressure.³¹

Therefore, we concluded that butorphanol could be used for CEUS studies, however the sedative effect is often inadequate in anxious or nervous cats. Propofol is a favorable anesthetic to use in cats: it is safe in older patients and cats with various diseases and induces a superficial anesthesia of short duration. However, the CEUS parameters are influenced by the use of propofol, hence cannot be compared with those from conscious animals. Consequently, at the start of every study we needed to decide whether anesthesia would be used in all patients or in none of them. Propofol anesthesia was used in all experimental cats in the studies in **Chapter III and IV** in order to reduce stress for the animals and facilitate the ease of performing CEUS. Moreover, we assume that the cardiovascular effects of stress could also induce extra variation. Propofol was also used in the hyperthyroid cats (**Chapter VIII**), before and after treatment. Hyperthyroid cats often suffer from hyperactivity, stress intolerance and aggressiveness³², justifying the use of anesthesia. Inhalation anesthesia was used in the angiotensin-study (**Chapter VII**) because of the longer imaging times related to the combination of CEUS and renal scintigraphy. The effects of general anesthesia were not investigated in this thesis as it was only used in one study; moreover there was no need to

compare these results with those of conscious animals. Beside cardiovascular effects, inhalation anesthetics can influence perfusion parameters through their direct effect on the microbubbles. The inhaled gasses change the local blood gas concentration and hence gas diffusion between the bubbles and environment.^{18,20}

For the healthy client-owned cats and the cats suffering from renal disease (**Chapters VI and IX**), we decided to perform CEUS on conscious animals. Cat owners are often reluctant to allow their cat to participate in a study if sedation or anesthesia is involved. Some cats had to be excluded because of uncooperative behavior, however CEUS could be performed relatively easy in the majority of the cats.

5. Influence of aging in healthy cats

In humans, aging has a degenerative effect on the kidney: both functional and morphological changes are present in elderly people.³³ The prevalence of feline CKD, increases with age.^{1, 2} However, information on age-related variations in feline renal perfusion is currently lacking. Therefore, in **Chapter VI**, we assessed the influence of age on renal perfusion parameters in healthy cats. Forty-three client-owned cats aging from 1 year to 16 years and 6 months were enrolled in the study and divided into 4 age groups: group 1: 1-3 years, group 2: 3-6 years, group 3: 6-10 years and group 4: > 10 years. No significant differences in any of the perfusion parameters were observed among the age groups. Still, a tendency towards a lower PE and WiAUC was present when comparing cats > 10 years with the cats between 1 and 3 years. This suggests a reduction in renal blood volume as ageing progresses. A lower renal plasma flow, measured by para-aminohippurate (PAH) clearance, has been reported in elderly people.^{33,34} Similarly, in a large study on 331 people monitoring the transit of radioxenon through the kidney, a significant age-associated reduction in mean renal blood flow was observed.³⁵ Moreover, the blood flow reduction exceeded the reduction in GFR and renal mass, and is hence believed to be primary.³⁵ Age-related changes in humans were found to be most prominent in the renal cortex, corresponding to the findings in our study in cats.³⁵

Age-related increase in renal resistance and loss of intrarenal arterial compliance results in higher resistive index measured with Doppler in elderly people.^{36,37} However, an age-related increase in resistive index could not be detected in cats.³⁸ A higher renal resistance is likely to cause changes in time-based perfusion parameters and contribute to a lower PE and AUC. However, significant

changes in time-based parameters were not observed in this study. It remains unclear if they could not be detected with CEUS or if age-related renal changes in cats are less pronounced compared to people.

Several studies report a higher sCr in aging cats.³⁹⁻⁴¹ In dogs, an age-effect on GFR has only been reported in small breed dogs, whereas it was not present in large breed dogs.⁴¹ Moreover, vascular morphological changes as reported in humans (decreased luminal area and hyalinization of afferent arterioles, loss of peritubular capillaries) are not detected in dogs.^{33,42-44} Therefore, more studies should be performed in dogs and cats to clarify the existence and extent of the effect of aging on renal morphology and function.

In this study (**Chapter VI**) we have shown that no significant age-effect was present on the renal perfusion parameters obtained with CEUS. Moreover, no linear correlation between age and the renal perfusion parameters was detected. Nevertheless, a tendency towards lower PE and WiAUC in cats > 10 years was present. Therefore, we decided to incorporate age as categorical fixed effect in the statistical analysis of the study performed on cats with chronic kidney disease in **Chapter IX**.

6. Perfusion changes induced by angiotensin-II infusion

In **Chapter VII**, we performed an exploratory study to determine the ability of CEUS to detect changes in renal perfusion and correlated them with perfusion parameters obtained with renal scintigraphy. This study makes the link between the studies in healthy cats in **Chapters III, IV, V and VI** and the studies in cats with naturally occurring renal disease (**Chapter IX**) and hyperthyroid cats (**Chapter VIII**).

CEUS and ^{99m}Tc-mercaptoacetyl triglycerine (MAG₃) scintigraphy were performed in 11 healthy cats, at baseline and during infusion of AT II. AT II is a potent vasoconstrictor that is often upregulated in patients with CKD and in cats with hyperthyroidism.^{45,46}

AT II-induced perfusion changes could be detected with CEUS, whereas no significant changes were detected using renal scintigraphy. Ang-II infusion caused a lower PE and a tendency towards a lower WiAUC, corresponding with a decrease in global renal blood volume. Moreover, WiPI and WoR for the entire kidney decreased significantly after AT II-infusion, indicating a slower in- and outflow of contrast medium and thus slower renal blood velocity. These changes were expected knowing the physiologic effects of AT II: AT II is a potent vasoconstrictor, causing systemic but even more pronounced renal vasoconstriction, thereby decreasing total and renal blood flow.^{47,48} In a human

study, a decrease in perfusion index (calculated as renal blood volume divided by mean transit time) was detected after AT II infusion. Moreover, the changes in perfusion index paralleled those in estimated renal plasma flow.⁴⁹ In a similar study in sheep, a very heterogeneous and inconsistent response on CEUS parameters was noticed after AT II infusion. Only an increase in mean transit time was present after infusion of high dose AT II. CEUS-derived perfusion indices did not parallel changes in renal blood flow measured with invasive flow probes.⁵⁰ In both the sheep and the human study, CEUS was performed using a completely different technique compared to the one used in this thesis. They used a continuous infusion of contrast agent followed by consecutive destruction-refilling sequences (as explained in **Chapter I**). Consequently, other perfusion parameters were calculated, thereby strict comparison between our results and the results from these 2 studies is not possible.

We did not observe AT II-induced changes in perfusion parameters of the renal medulla. A variable response of the medullary blood flow on AT II has been reported in experimental animals.^{48, 51, 52} Moreover, the renal medulla is inherently less sensitive to vasoconstriction compared to the cortex.⁵³

To our knowledge, this is the first study using AT II infusion in cats; therefore it was difficult to determine an optimal dose. The aim was to give the lowest dose inducing renal vasoconstriction without causing significant systemic effects. We chose to administer 2 ng/kg/min, which is intermediate between the low (1 ng/kg/min) and high (3 ng/kg/min) dose used in the human study of Schneider et al. (2012).⁴⁹ This dose was believed safe in cats, by extrapolation from a study using boluses of AT II in healthy cats. Boluses between 0.02 ng/kg and 500 ng/kg did not cause important side effects and effects were transient. Significant increase in blood pressure were observed for boluses > 20 ng/kg.⁵⁴ The total duration of AT II infusion was about 30 min in our study, thereby corresponding to a total dose of 60 ng/kg. However, we expected the effect of a continuous infusion to be less pronounced compared to a bolus. It would have been interesting to test several dosages of AT II infusion and evaluate the change in response in perfusion parameters.

A major problem in this study is the absence of a golden standard to evaluate renal perfusion. To validate CEUS as a technique for the evaluation of renal perfusion it would be mandatory to compare the results to those of a golden standard. To our knowledge there is currently no standardized technique available to measure renal perfusion. Flow probes that are directly inserted into renal vascularization are used in experimental settings. However, these probes can only assess perfusion in larger vessels and hence do not evaluate microperfusion.^{48, 50, 51} Moreover,

their use has not been described in cats, and would be unethical since their invasiveness. PAH clearance techniques are considered the gold standard to evaluate global renal perfusion in humans. The technique is poorly described in cats and is not applicable in a clinical setting due to the requirement for specific equipment and multiple sampling strategies.⁵⁵ Additionally, comparison between CEUS and PAH clearance cannot be strict since these techniques actually compare different parameters, regional microvascularisation and total renal blood flow respectively.⁴⁹ Nevertheless, significant correlations between CEUS parameters and PAH clearance have been described in humans.^{10, 49, 56} In this study, we chose to compare CEUS parameters to perfusion parameters obtained with MAG₃ scintigraphy. MAG₃ has a similar chemical structure to PAH and good correlation between MAG₃ and PAH clearance has been described in humans and dogs, however no information is available in cats.^{57, 58} One study in people found a significant correlation between effective renal plasma flow calculated based on MAG₃ and decline ratio obtained with CEUS.¹⁰ We did not observe a correlation between the CEUS parameters and the ratio's calculated with MAG₃. Important differences are present between our study and the human study of Hosotani et al. (2002). In the latter study, CEUS was performed using a different technique hence resulting in different parameters. Moreover, in humans, formulas are available to calculate effective renal plasma flow from data obtained with MAG₃, whereas these formulas are not validated in cats. Therefore, we used ratios to assess renal perfusion with MAG₃.

This study proved the potential of CEUS to detect renal perfusion changes, thereby encouraging further research in patients (**Chapters VIII and IX**)

7. Renal perfusion evaluation in treatment of hyperthyroid cats

In **Chapter VIII** we assessed renal perfusion changes in cats occurring 1 month after radioiodine treatment for hyperthyroidism. The complex relationship between the kidney and thyroid gland has been extensively described.^{45, 59, 60} It is known that hyperthyroidism causes an increase in GFR, whereas GFR will normalize again 1 month after treatment.^{61, 62} Changes in renal blood flow are believed to underlie the changes in renal function.^{59, 60} Nevertheless, only 1 study has investigated renal perfusion in iatrogenic hyperthyroidism.⁶³ Therefore, a prospective study was performed to evaluate renal perfusion in hyperthyroid cats, before and 1 month after treatment of hyperthyroidism. The RT, mTT, TTP and FT for the renal cortex significantly increased after resolution of the hyperthyroid state. In parallel with these findings, WiR and WoR decreased, and

WiAUC, WoAUC and total AUC for the cortex increased. Similarly for the renal medulla, RT and TTP increased and WiR decreased. The combination of these findings indicates a slower renal blood velocity in both renal cortex and medulla after treatment of hyperthyroidism. Additionally, a decrease in normalized PE was present for the renal medulla, suggesting a decrease in medullary blood volume. This was not noticed for the renal cortex.

Increased total T4 levels will lead to an increased renal blood flow caused by a combination of decreased systemic and intrarenal vascular resistance and increased cardiac output.^{59, 60} Additionally, a significant decrease in heart rate was noticed post-treatment. As the contrast agent relies on the systemic circulation to reach the kidney, changes in cardiovascular parameters may influence renal perfusion parameters. Therefore, the post-treatment decrease in heart rate likely contributed to the changes in time-based parameters in our study.

An increased renal blood flow, measured by clearance of ¹³¹I-orthoiodohippuric acid, was present in one study with iatrogenically induced hyperthyroidism.⁶³ Our study is the first to evaluate the response of renal perfusion to treatment of hyperthyroidism. The renal perfusion is expected to parallel the changes in GFR and thus decrease 1 month after treatment as noticed in our study.^{61, 62} Moreover, as the changes in GFR occur within the first month after treatment, and not anymore thereafter, we would expect the same for renal perfusion.^{61, 62} However, this was not evaluated in our study, since only a short follow-up of 1 month was performed. Nevertheless, it would be interesting to test this hypothesis in a longer follow-up study.

An unexpected low number of cats (4.8%) developed post-treatment azotemia in our study. Therefore, we were not able to evaluate the predictive value in CEUS for the development of post-treatment azotemia.

8. Cats with chronic kidney disease

Finally in **Chapter IX** we aimed to assess renal perfusion in cats diagnosed with CKD. In humans and experimental animals, there is increasing evidence that renal hemodynamic changes underlie functional and morphological changes in chronic kidney disease.⁶⁴⁻⁶⁷ Loss of peritubular capillaries is a prominent feature in CKD and seems to be independent of the underlying cause. Moreover, renal capillary rarefaction is considered a central mechanism in the initiation and progression of CKD.^{64, 65} Therefore, evaluation of renal microvascularization might deliver important insights in the pathophysiology of CKD, and its diagnosis.

CEUS was performed in 14 cats with CKD and 43 healthy control cats. In cats with CKD, a longer TTP for the renal cortex, indicating slower blood flow, was present. Moreover, a shorter mTT suggested shorter cortical contrast enhancement in CKD cats. In contrast, a shorter TTP and RT, and hence higher blood velocity was present for the renal medulla.

The changes in the renal cortex were expected and are likely to be caused by an increased vascular resistance occurring secondary to the loss of peritubular capillaries and activation of the renin-angiotensin system.^{66, 67}

Comparison of our results to those obtained in literature is complicated since different CEUS methods often used, thereby obtaining other perfusion parameters. The human study of Dong et al. 2014, had a comparable study design to ours. They performed a bolus injection of Sonovue® in 41 patients with CKD and 45 healthy controls. A lower AUC, lower PE and lower inflow slope was present in people with CKD, a longer TTP was detected but did not reach statistical significance.¹¹ Another human study used bolus kinetics to study renal perfusion in patients suffering from CKD, a different contrast agent was used and different parameters were calculated. A decreased intensity and decreased steepness of the time-intensity curve was present in patients with renal disease in the latter study.¹⁴ In a study using continuous infusion, a lower enhancement was seen in CKD patients.¹⁰ Delayed arrival time and TTP were seen in humans with early stage diabetic nephropathy, PE and AUC only decreased in advanced diabetic nephropathy.⁶⁸ It is striking that a decreased intensity, corresponding to a lower renal blood volume, is a rather consistent finding in human studies. A lower PE was also present in the CKD cats in our study, however no statistical significance was reached. As described in **Chapter IV**, this parameter suffers from a high degree of variability, thereby complicating interpretation. Nevertheless, Dong et al. (2014) assumed that PE has the best diagnostic accuracy in the detection of CKD in people, whereas the opposite is proven in both our study in CKD cats (**Chapter IX**) and the repeatability study in healthy cats (**Chapter IV**). The reason for this discrepancy between our study and the human study remains unclear, since broad reference intervals and overlap between values of people with renal disease and healthy individuals is also present in the human study.¹¹

The decreased TTP and RT for the renal medulla in CKD cats, where rather unexpected. Medullary perfusion is less extensively studied compared to the renal cortex. Only 1 study has described CEUS parameters for the renal medulla in people with CKD. In this study, the changes in medullary perfusion parameters paralleled those of the renal cortex.¹⁴ The renal medulla only receives about 10% of the total renal blood flow and the medullary circulation diverges from the cortical

circulation.⁵³ Nevertheless, it is known that the medullary blood flow is controlled differently compared to the cortical blood flow, moreover the medullary circulation is relatively insensitive to vasoconstrictive factors.⁵³ In a study using CT angiography to assess renal perfusion in people with CKD, medullary blood flow was found to be very variable and did not correlate with GFR.⁶⁹ More studies are necessary to confirm the increased medullary blood velocity in cats with CKD and further investigate the underlying pathophysiology.

9. Future perspectives

Our results show that CEUS is capable of detecting perfusion changes in cats and thus holds promise for further use in the evaluation of renal perfusion in cats, however considerable challenges need to be addressed before wider clinical use of quantitative CEUS can be achieved. These are largely related to the high degree of variability resulting in diagnostic uncertainty as described in **Chapter IV**. Continuous development in the areas of contrast agent composition, ultrasound systems, transducer design and signal processing may allow more reliable quantification of CEUS studies in the future. Moreover, there is a strong need for international standards in study design of CEUS procedures. Currently, multiple different experiments set-ups are used, resulting in a large variety of perfusion parameters, complicating comparison. Well-powered (clinical) trials are needed to compare the different experimental designs and assess the variability and reliability of the perfusion parameters they deliver. Results of these trials should be used to build strong uniform guidelines in performing CEUS studies. Given the diagnostic and even therapeutic potential (not discussed in this thesis), we believe CEUS is likely to grow in prominence over the coming decade.

Additionally, veterinary science could also follow other pathways in the evaluation of renal perfusion. Interesting results have recently been obtained with the use of quantitative CT angiography in people and experimental animals.⁷⁰ In contrast to CEUS, CT angiography has a low inter-individual variability. However, the clinical application is currently limited by the potential risk of contrast agent nephropathy and use of ionizing radiation. Nevertheless, efforts are made to produce iodine free contrast with reduced toxicity and novel reno-protective imaging protocols.^{69,70} Similarly, Blood Oxygen Level Dependency (BOLD) and Diffusion-weighted (DW) MRI techniques,

which can be used to study renal perfusion without requiring contrast agent, are likely to develop within the next years ^{71,72}

10. General conclusion

In this thesis, we have investigated the use of contrast-enhanced ultrasound for the evaluation of renal perfusion in cats. Encouraging results were obtained in the study using AT II infusion in experimental cats (**Chapter VII**), as well in the clinical studies in CKD cats (**Chapter IX**) and cats with hyperthyroidism (**Chapter VIII**). The time-based perfusion parameters, TTP, mTT, RT and FT hold the most promise as they showed significant results in the clinical studies in **Chapters VIII and IX**, moreover they suffer from the least variability (**Chapter IV**). However, PE, an important parameter for the blood volume currently suffers from very high variability.

In conclusion, renal perfusion quantification with CEUS has been shown to be a promising but yet not validated method. The large variability currently limits the application of CEUS in a clinical setting. Despite these limitations, CEUS is still a promising method for renal microvascular evaluation and further technical advances are likely to improve repeatability.

11. References

1. Lulich JP, Osborne CA, O'Brien TD, Polzin DJ. Feline Renal-Failure - Questions, Answers, Questions. *Compendium on Continuing Education for the Practicing Veterinarian*. 1992;14: 127-152.
2. Marino CL, Lascelles BDX, Vaden SL, Gruen ME, Marks SL. Prevalence and classification of chronic kidney disease in cats randomly selected from four age groups and in cats recruited for degenerative joint disease studies. *Journal of Feline Medicine and Surgery*. 2014;16: 465-472.
3. Polzin JP. Chronic kidney disease. In: Bartges J, Polzin JP (eds): *Nephrology and Urology of Small Animals*. Chichester: Wiley-Blackwell, 2011;433-471.
4. Finco DR, Brown SA, Vaden SL, Ferguson DC. Relationship between plasma creatinine concentration and glomerular filtration rate in dogs. *Journal of Veterinary Pharmacology and Therapeutics*. 1995;18: 418-421.
5. Jepson RE. Current Understanding of the Pathogenesis of Progressive Chronic Kidney Disease in Cats. *Veterinary Clinics of North America: Small Animal Practice*. 2016;46: 1015-1048.
6. Regan MC, Young LS, Geraghty J, Fitzpatrick JM. Regional renal blood flow in normal and disease states. *Urological Research*. 1995;23: 1-10.
7. Schmiedt CW, Brainard BM, Hinson W, Brown SA, Brown CA. Unilateral Renal Ischemia as a Model of Acute Kidney Injury and Renal Fibrosis in Cats. *Veterinary Pathology*. 2016;53: 87-101.
8. Seiler GS, Brown JC, Reetz JA, Taeymans O, Bucknoff M, Rossi F, et al. Safety of contrast-enhanced ultrasonography in dogs and cats: 488 cases (2002-2011). *Journal of the American Veterinary Medical Association*. 2013;242: 1255-1259.
9. Dietrich CF, Ignee A, Hocke M, Schreiber-Dietrich D, Greis C. Pitfalls and Artefacts using Contrast Enhanced Ultrasound. *Zeitschrift Fur Gastroenterologie*. 2011;49: 350-356.
10. Hosotani Y, Takahashi N, Kiyomoto H, Ohmori K, Hitomi H, Fujioka H, et al. A new method for evaluation of split renal cortical blood flow with contrast echography. *Hypertension Research*. 2002;25: 77-83.
11. Dong Y, Wang WP, Cao J, Fan P, Lin X. Early assessment of chronic kidney dysfunction using contrast-enhanced ultrasound: a pilot study. *British Journal of Radiology*. 2014;87: 1-7.
12. Dong Y, Wang WP, Cao JY, Fan PL, Lin XY. Quantitative evaluation of contrast-enhanced ultrasonography in the diagnosis of chronic ischemic renal disease in a dog model. *Plos One*. 2013;8: e70377.

13. Haers H, Daminet S, Smets PMY, Duchateau L, Aresu L, Saunders JH. Use of quantitative contrast-enhanced ultrasonography to detect diffuse renal changes in Beagles with iatrogenic hypercortisolism. *American Journal of Veterinary Research*. 2013;74: 70-77.
14. Tsuruoka K, Yasuda T, Koitabashi K, Yazawa M, Shimazaki M, Sakurada T, et al. Evaluation of renal microcirculation by contrast-enhanced ultrasound with sonazoid (TM) as a contrast agent. *International Heart Journal*. 2010;51: 176-182.
15. Kinns J, Aronson L, Hauptman J, Seiler G. Contrast-enhanced ultrasound of the feline kidney. *Veterinary Radiology & Ultrasound*. 2010;51: 168-172.
16. Leinonen MR, Raekallio MR, Vainio OM, Ruohoniemi MO, Biller DS, O'Brien RT. Quantitative contrast-enhanced ultrasonographic analysis of perfusion in the kidneys, liver, pancreas, small intestine, and mesenteric lymph nodes in healthy cats. *American Journal of Veterinary Research*. 2010;71: 1305-1311.
17. Schweiger H, Ohlerth S, Gerber B. Contrast-enhanced ultrasound of both kidneys in healthy, non-anaesthetized cats. *Acta Veterinaria Scandinavica*. 2015;57: 57-80.
18. Hyvelin JM, Tardy I, Arbogast C, Costa M, Emmel P, Helbert A, et al. Use of Ultrasound Contrast Agent Microbubbles in Preclinical Research Recommendations for Small Animal Imaging. *Investigative Radiology*. 2013;48: 570-583.
19. Tranquart F, Mercier L, Frinking P, Gaud E, Arditi M. Perfusion Quantification in Contrast-Enhanced Ultrasound (CEUS) - Ready for Research Projects and Routine Clinical Use. *Ultraschall in Der Medizin*. 2012;33: S31-S38.
20. Tang MX, Mulvana H, Gauthier T, Lim AKP, Cosgrove DO, Eckersley RJ, et al. Quantitative contrast-enhanced ultrasound imaging: a review of sources of variability. *Interface Focus*. 2011;1: 520-539.
21. Budras KD, McCarthy PH, Fricke W, Richter R. *Anatomy of the dog*. Hannover, Germany: Schlütersche, 2007.
22. Haers H. Contrast-enhanced ultrasonography of canine kidneys. Ghent University, Merelbeke, 2012 (thesis).
23. Pey P, Vignoli M, Haers H, Duchateau L, Rossi F, Saunders JH. Contrast-enhanced ultrasonography of the normal canine adrenal gland. *Veterinary Radiology & Ultrasound*. 2011;52: 560-567.

24. Salwei RM, O'Brien RT, Matheson JS. Characterization of lymphomatous lymph nodes in dogs using contrast harmonic and power Doppler ultrasound. *Veterinary Radiology & Ultrasound*. 2005;46: 411-416.
25. O'Brien R, Seiler G. Clinical applications of contrast ultrasound In: Penninck D, d'Anjou MA (eds): *Atlas of small animal ultrasonography* Oxford, UK: John Wiley and Sons, 2015;481 - 493.
26. Rix A, Palmowski M, Gremse F, Palmowski K, Lederle W, Kiessling F, et al. Influence of Repetitive Contrast Agent Injections on Functional and Molecular Ultrasound Measurements. *Ultrasound in Medicine and Biology*. 2014;40: 2468-2475.
27. Weskott HP. Emerging roles for contrast-enhanced ultrasound. *Clinical Hemorheology and Microcirculation*. 2008;40: 51-71.
28. Skrok J. Markedly increased signal enhancement after the second injection of Sonovue compared to the first - a quantitative normal volunteer study. 12th European symposium on ultrasound contrast imaging. Rotterdam, the Netherlands, 2007.
29. Dizeux A, Payen T, Barrois G, Le Guillou Buffello D, Bridal SL. Reproducibility of Contrast-Enhanced Ultrasound in Mice with Controlled Injection. *Molecular Imaging Biology*. 2016;18: 651-658.
30. Gauthier TP, Averkiou MA, Leen EL. Perfusion quantification using dynamic contrast-enhanced ultrasound: the impact of dynamic range and gain on time-intensity curves. *Ultrasonics*. 2011;51: 102-106.
31. Short CE, Bufalari A. Propofol anesthesia. *Veterinary Clinics of North America: Small Animal Practice*. 1999;29: 747-778.
32. Scott-Moncrieff JC. Feline hyperthyroidism. In: Feldman EC, Nelson RW, Reusch C, Scott-Moncrieff JC, Behrend E (eds): *Canine and feline endocrinology*. St Louis, Missouri, USA: Saunders Elsevier, 2015;136-195.
33. Esposito C, Plati A, Mazzullo T, Fasoli G, De Mauri A, Grosjean F, et al. Renal function and functional reserve in healthy elderly individuals. *Journal of Nephrology*. 2007;20: 617-625.
34. Fliser D, Zeier M, Nowack R, Ritz E. Renal functional reserve in healthy elderly subjects. *Journal of the American Society of Nephrology*. 1993;3: 1371-1377.
35. Hollenberg NK, Adams DF, Solomon HS, Rashid A, Abrams HL, Merrill JP. Senescence and the renal vasculature in normal man. *Circulation Research*. 1974;34: 309-316.

36. Pontremoli R, Viazzi F, Martinoli C, Ravera M, Nicoletta C, Berruti V, et al. Increased renal resistive index in patients with essential hypertension: a marker of target organ damage. *Nephrology Dialysis Transplantation*. 1999;14: 360-365.
37. Terry JD, Rysavy JA, Frick MP. Intrarenal Doppler: characteristics of aging kidneys. *Journal of Ultrasound in Medicine*. 1992;11: 647-651.
38. Tipisca V, Murino C, Cortese L, Mennonna G, Auletta L, Vulpe V, et al. Resistive index for kidney evaluation in normal and diseased cats. *Journal of Feline Medicine and Surgery*. 2015;18: 471-475.
39. Paepe D, Bavegems V, Combes A, Saunders JH, Daminet S. Prospective evaluation of healthy Ragdoll cats for chronic kidney disease by routine laboratory parameters and ultrasonography. *Journal of Feline Medicine and Surgery*. 2013;15: 849-857.
40. Ghys LF, Paepe D, Duchateau L, Taffin ER, Marynissen S, Delanghe J, et al. Biological validation of feline serum cystatin C: The effect of breed, age and sex and establishment of a reference interval. *Veterinary Journal*. 2015;204: 168-173.
41. Miyagawa Y, Takemura N, Hirose H. Assessments of factors that affect glomerular filtration rate and indirect markers of renal function in dogs and cats. *Journal of Veterinary Medical Science*. 2010;72: 1129-1136.
42. Cianciolo RE, Benali SL, Aresu L. Aging in the canine Kidney. *Veterinary Pathology*. 2016;53: 299-308.
43. Yoon HE, Choi BS. The renin-angiotensin system and aging in the kidney. *The Korean Journal of Internal Medicine*. 2014;29: 291-295.
44. Smets PM, Lefebvre HP, Aresu L, Croubels S, Haers H, Piron K, et al. Renal function and morphology in aged Beagle dogs before and after hydrocortisone administration. *Plos One*. 2012;7: e31702.
45. Langston CE, Reine NJ. Hyperthyroidism and the kidney. *Clinical Techniques in Small Animal Practice*. 2006;21: 17-21.
46. Klein BG. *Cunningham's textbook of veterinary physiology* St Louis, Missouri: Elsevier Saunders, 2013.
47. Evans RG, Head GA, Eppel GA, Burke SL, Rajapakse NW. Angiotensin II and neurohumoral control of the renal medullary circulation. *Clinical and Experimental Pharmacology and Physiology*. 2010;37: e58-69.

Chapter X General discussion

48. Badzyska B, Grzelec-Mojzesowicz M, Dobrowolski L, Sadowski J. Differential effect of angiotensin II on blood circulation in the renal medulla and cortex of anaesthetised rats. *Journal of Physiology*. 2002;538: 159-166.
49. Schneider AG, Hofmann L, Wuerzner G, Glatz N, Maillard M, Meuwly JY, et al. Renal perfusion evaluation with contrast-enhanced ultrasonography. *Nephrology Dialysis Transplantation*. 2012;27: 674-681.
50. Schneider AG, Calzavacca P, Schelleman A, Huynh T, Bailey M, May C, et al. Contrast-enhanced ultrasound evaluation of renal microcirculation in sheep. *Intensive Care Medicine Experimental*. 2014;2: 33.
51. Nobes MS, Harris PJ, Yamada H, Mendelsohn FAO. Effects of angiotensin on renal cortical and papillary blood flows measured by laser-Doppler flowmetry. *American Journal of Physiology*. 1991;261: F998-F1006.
52. Walker LL, Rajaratne AA, Blair-West JR, Harris PJ. The effects of angiotensin II on blood perfusion in the rat renal papilla. *Journal of Physiology*. 1999;519 Pt 1: 273-278.
53. Evans RG, Eppel GA, Anderson WP, Denton KM. Mechanisms underlying the differential control of blood flow in the renal medulla and cortex. *Journal of Hypertension*. 2004;22: 1439-1451.
54. Coleman AE, Schmiedt CW, Jenkins TL, Garber ED, Reno LR, Brown SA. Evaluation of a rapid pressor response test in healthy cats. *American Journal of Veterinary Research*. 2013;74: 1392-1399.
55. Osbaldiston GW, Fuhrman W. The clearance of creatinine, inulin, para-aminohippurate and phenosulphothalein in the cat. *The Canadian Journal of Comparative Medicine*. 1970;34: 138-141.
56. Kishimoto N, Mori Y, Nishiue T, Nose A, Kijima Y, Tokoro T, et al. Ultrasound evaluation of valsartan therapy for renal cortical perfusion. *Hypertension Research*. 2004;27: 345-349.
57. Itkin RJ, Krawiec DR, Twardock AR, Gelberg HB, Koritz GD. Evaluation of the Single-Injection Plasma Disappearance of Tc-99m Mercaptoacetyltriglycine Method for Determination of Effective Renal Plasma-Flow in Dogs with Normal or Abnormal Renal-Function. *American Journal of Veterinary Research*. 1994;55: 1652-1659.
58. Daniel GB, Mitchell SK, Mawby D, Sackman JE, Schmidt D. Renal nuclear medicine: A review. *Veterinary Radiology & Ultrasound*. 1999;40: 572-587.
59. van Hoek I, Daminet S. Interactions between thyroid and kidney function in pathological conditions of these organ systems: A review. *General and Comparative Endocrinology*. 2009;160: 205-215.

60. Vaske HH, Schermerhorn T, Grauer GF. Effects of feline hyperthyroidism on kidney function: a review. *Journal of Feline Medicine and Surgery*. 2015.
61. van Hoek I, Lefebvre HP, Peremans K, Meyer E, Croubels S, Vandermeulen E, et al. Short- and long-term follow-up of glomerular and tubular renal markers of kidney function in hyperthyroid cats after treatment with radioiodine. *Domestic Animal Endocrinology*. 2009;36: 45-56.
62. Boag AK, Neiger R, Slater L, Stevens KB, Haller M, Church DB. Changes in the glomerular filtration rate of 27 cats with hyperthyroidism after treatment with radioactive iodine. *Veterinary Record*. 2007;161: 711-715.
63. Adams WH, Daniel GB, Legendre AM. Investigation of the effects of hyperthyroidism on renal function in the cat. *Canadian Journal of Veterinary Research*. 1997;61: 53-56.
64. Ballermann BJ, Obeidat M. Tipping the balance from angiogenesis to fibrosis in CKD. *Kidney International Supplements*. 2014;4: 45-52.
65. Babickova J, Klinkhammer BM, Buhl EM, Djurdjaj S, Hoss M, Heymann F, et al. Regardless of etiology, progressive renal disease causes ultrastructural and functional alterations of peritubular capillaries. *Kidney International*. 2017;91: 70-85.
66. Nangaku M. Chronic hypoxia and tubulointerstitial injury: a final common pathway to end-stage renal failure. *Journal of the American Society of Nephrology*. 2006;17: 17-25.
67. Basile DP, Donohoe D, Roethe K, Osborn JL. Renal ischemic injury results in permanent damage to peritubular capillaries and influences long-term function. *American Journal of Physiology Renal Physiology*. 2001;281: F887-899.
68. Ma F, Cang YQ, Zhao BZ, Liu YY, Wang CQ, Liu B, et al. Contrast-enhanced ultrasound with SonoVue could accurately assess the renal microvascular perfusion in diabetic kidney damage. *Nephrology Dialysis Transplantation*. 2012;27: 2891-2898.
69. von Stillfried S, Apitzsch JC, Ehling J, Penzkofer T, Mahnken AH, Knuchel R, et al. Contrast-enhanced CT imaging in patients with chronic kidney disease. *Angiogenesis*. 2016;19: 525-535.
70. Ehling J, Babickova J, Gremse F, Klinkhammer BM, Baetke S, Knuechel R, et al. Quantitative Micro-Computed Tomography Imaging of Vascular Dysfunction in Progressive Kidney Diseases. *Journal of the American Society of Nephrology*. 2016;27: 520-532.
71. Herget-Rosenthal S. Imaging Techniques in the Management of Chronic Kidney Disease: Current Developments and Future Perspectives. *Seminars in Nephrology*. 2011;31: 283-290.

72. Grenier N, Merville P, Combe C. Radiologic imaging of the renal parenchyma structure and function. *Nature Reviews Nephrology*. 2016;12: 348-359.

SUMMARY

Chronic kidney disease (CKD) is a common pathology in elderly cats. Early treatment is important as it may improve prognosis and quality of life, nevertheless timely detection remains challenging in current veterinary practice. Changes in renal perfusion play an important role in the pathophysiology of CKD. Therefore, evaluation of renal perfusion may serve as a sensitive diagnostic tool, potentially allowing diagnosis in the first stages of the disease process. Contrast-enhanced ultrasound (CEUS) is an emerging functional imaging technique allowing non-invasive assessment of renal perfusion.

In **Chapter I**, the anatomy and physiology of the kidneys, focusing on the renal vascularization, are explained. A summary on the commonly used medical imaging techniques to visualize the kidneys is provided. Radiography and B-mode ultrasonography are often used in clinical practice, however both techniques only provide morphological information. Renal scintigraphy, CT angiography and MRI may also deliver functional information. However, the practical use of these techniques is limited by equipment availability, costs, long imaging times and use of ionizing radiation or nephrotoxic contrast agents. CEUS does not suffer from these limitations and is thus a promising technique to assess renal perfusion. An overview of the current knowledge of renal CEUS in both human and veterinary medicine is provided in **Chapter I**.

The scientific aims of this thesis are presented in **Chapter II**. The final goal of this work was to assess the value of CEUS in the diagnosis of diffuse renal diseases in cats. In the first part of this thesis, studies on healthy cats were performed to gain more insight in the technique and influencing factors. In the second part, the use of CEUS in the evaluation of renal perfusion in cats with CKD and hyperthyroid cats was evaluated.

Quantitative differences between the first and second injection of contrast agent were investigated in **Chapter III**. Perfusion parameters of the spleen and the left kidney for the first and second injection of SonoVue® were compared in 7 healthy cats. A lower peak enhancement and area-under-the-curve were present for the first injection. This was statistically significant for the renal cortex and splenic parenchyma, whereas a tendency was present for the renal medulla. The time-intensity curve for the renal cortex showed less steep wash-in and wash-out for the first injection. The exact mechanism behind this findings remains unclear, however phagocytosis of the microbubbles in the reticuloendothelial system is believed to play an important role. The findings

of this study proved that significant quantitative differences were present between the first and second injection of contrast agent. Therefore, it is recommended to withdraw the first injection from quantitative analysis.

The repeatability of CEUS in feline kidneys was assessed in Chapter IV to determine the most reliable perfusion parameters in detecting renal perfusion changes. CEUS of both kidneys was performed in 12 healthy cats at 3 time-points with a 7-days interval. Variability was determined on 3 levels: (1) within cat variability for repeated measures on the same cat, (2) the extra variation added by considering both kidneys, and (3) extra variation added by considering observations of different cats. The coefficient of variation (CV) was also determined. The CEUS parameters with the lowest variation were time-to-peak (CV 5.7%), rise time (CV 13.1%), fall time (CV 19.0%) and mean transit time (CV 24.4%) for the renal cortex. Intensity-related parameters and parameters related to the slope of the time intensity curve suffered from high variability (CV 36.6 – 56.0%). For the renal medulla, only the time-to-peak (CV 12.9%) and rise time (CV 26.3%) showed reasonable variability, whereas high coefficients of variation were present for all other parameters (CV 37.7 – 83.4%). The extra variation added by studying different kidneys was minimal. The variation added by considering different cats was moderate in respect to relatively high within-cat variability. In summary, time-related parameters for the renal cortex and, in a lesser extent for the renal medulla, show good to moderate repeatability, whereas poor repeatability is present for intensity-related parameters, and parameters related to the shape of the time-intensity curve. This high degree of variability will complicate diagnosis based on CEUS.

In Chapter V, the effect of sedation with butorphanol and propofol-anesthesia on CEUS perfusion indices of the kidney was investigated. Six healthy cats were enrolled in a randomized crossover design, comparing 3 protocols: (1) awake, (2) butorphanol (0.4 mg/kg IM) and (3) propofol (3.5 – 7.7 mg/kg IV boluses on effect). There was no difference in the subjective enhancement pattern of the kidneys between the 3 protocols. Butorphanol did not cause a significant effect on any of the perfusion parameters, however the sedative effect was minimal. In contrast, anesthesia with propofol resulted in a significant increase in arrival time and time-to-peak, and a slower wash-in phase of the time-intensity curve. These changes indicated a decreased blood velocity, likely caused by propofol-induced decrease in blood pressure by a combination of decreased cardiac output and systemic vascular resistance. In conclusion, propofol is a favorable anesthetic to use in

older cats and cats with CKD, however, its effects on CEUS parameters should be taken into consideration and direct comparison of perfusion parameters obtained in anesthetized cats and awake cats is not possible.

Chapter VI reports the influence of age on CEUS of the kidneys in healthy cats. Forty-three healthy cats, aging 1 to 16.5 years, were included and divided into 4 groups: 1-3 years, 3-6 years, 6-10 years and > 10 years. No significant differences in any of the perfusion parameters were observed among the age groups. Still, a tendency towards a lower PE and WiAUC was noted for the renal cortex when comparing the cats > 10 years to the cats between 1 and 3 years. This corresponds to the findings in people, in whom a progressive age-related reduction in renal blood flow is well known. In conclusion, ageing in cats did not induce significant differences in CEUS renal perfusion parameters. Nevertheless, this study suggests that a mild decreased blood volume might occur in elderly cats.

In Chapter VII, we investigated if CEUS was capable of detecting relatively small perfusion changes induced by angiotensin II infusion. CEUS and renal scintigraphy using ^{99m}Tc -mercaptoacetyltriglycerine were performed in 11 healthy cats, during infusion of angiotensin II (vasoconstriction) and during infusion of 0.9% NaCl (control). Angiotensin II-induced changes were noticed on several perfusion parameters for a region-of-interest on the entire kidney: peak enhancement, wash-in perfusion index and wash-out rate decreased significantly. No significant changes were detected for the medullary or cortical regions of interest. Renal scintigraphy was not capable of detecting significant perfusion changes after angiotensin II-infusion. This study showed that CEUS was able to detect changes in the renal perfusion, suggesting that it is a promising technique for the evaluation of renal perfusion in cats.

After the encouraging results of the angiotensin-study, we aimed to evaluate renal perfusion in hyperthyroid cats, before and after radioiodine therapy. Therefore, in Chapter VIII, 42 hyperthyroid cats were included and CEUS was performed just before radioiodine treatment and at 1-month control. Time-related parameters (time-to-peak and rise time) for the renal cortex and medulla were significantly lower before treatment compared to 1-month control. A higher wash-in rate (cortex and medulla) and wash-out rate (cortex) were also present before treatment. The combination of these findings indicates a higher renal blood velocity during hyperthyroid state. The

mean transit time for cortex was lower during hyperthyroidism, indicating a shorter duration of contrast-enhancement. Additionally, area-under-the-curve for the renal cortex was lower before treatment, resulting from the change in shape of the time-intensity curve due to higher blood velocity. Uniquely for the renal medulla, a higher normalized peak enhancement was present before treatment, suggesting a higher medullary blood volume. The changes in CEUS parameters can be attributed to the decreased systemic and renal vascular resistance typically present in hyperthyroidism. Moreover, higher heart rates in hyperthyroid cats will have reinforced the effect on renal blood velocity. In conclusion, CEUS showed a higher blood velocity and higher medullary blood volume during hyperthyroid state compared to post-treatment control.

Finally, in Chapter IX, the diagnostic capabilities of CEUS were evaluated in cats with CKD (n=14) and compared with healthy control cats (n=43). In cats with CKD, a longer time-to-peak and shorter mean-transit time were observed for the renal cortex. In contrast, a shorter time-to-peak and rise time were seen for the renal medulla. The findings for the cortex indicate a slower renal blood velocity, likely caused by a higher renal vascular resistance in CKD. A higher blood velocity in the renal medulla has not been described before, and may be caused by a different response to regulatory factors. It is known that the renal medulla is less susceptible to vasoconstriction. To conclude, CEUS was capable of detecting perfusion changes in cats suffering from CKD: slower cortical but faster medullary blood velocity were detected.

Chapter X comprises the general discussion and conclusions of this thesis. Throughout the different studies in this work, CEUS has been shown to be a favorable technique for the evaluation of renal perfusion in cats. The large variability currently causes a high degree of diagnostic uncertainty limiting the application of CEUS in a clinical setting. Despite this limitation, CEUS is still a promising method for renal microvascular evaluation and further technical advances may improve repeatability.

SAMENVATTING

Chronische nierziekte (CNZ) is een vaak voorkomende aandoening bij oudere katten. De prognose en levenskwaliteit van de kat kunnen merkelijk verbeteren als de behandeling vroegtijdig ingesteld wordt. Tot op heden blijft het echter moeilijk om de diagnose in een vroeg stadium te stellen omdat de huidige technieken die in de praktijk gebruikt worden (bloed- en urineonderzoek), pas diagnose toelaten wanneer reeds een substantieel deel van de nierfunctie verloren is. Veranderingen in de doorbloeding van de nier spelen een belangrijke rol in het ontstaan en de progressie van CNZ. Evaluatie van de nierperfusie kan daarom nieuwe inzichten geven en ingezet worden voor de vroegtijdige diagnostiek van CNZ. Contrast-echografie (CEUS) is een nieuwe functionele beeldvormingstechniek die toelaat om de doorbloeding van een orgaan te bestuderen.

In het eerste hoofdstuk wordt de anatomie en fysiologie van de nier uitgelegd, de focus ligt op de doorbloeding van de nier. Dit wordt gevolgd door een samenvatting van de meest gebruikte medische beeldvormingstechnieken om de nier in beeld te brengen. Radiografie en klassieke B-mode echografie zijn de meest gebruikte technieken in praktijk. Beiden geven enkel morfologische informatie, maar leren ons niets over de functie van de nier. Scintigrafie, CT angiografie en MRI kunnen wel functionele informatie opleveren. De nadelen van deze technieken zijn hun hoge kosten, beperkte beschikbaarheid van de apparatuur, langere onderzoeksduur, gebruik van ioniserende straling en/of mogelijks nefrotoxische contrast agentia. Contrast echografie is een zeer gebruiksvriendelijke techniek die niet onderhevig is aan de bovenvermelde beperkingen, bijgevolg lijkt het een zeer veelbelovende methode voor de evaluatie van de nierperfusie. In dit hoofdstuk vindt men een overzicht van de huidige kennis omtrent het gebruik van CEUS voor onderzoek van de nieren in de humane geneeskunde en diergeneeskunde.

De doelstellingen van deze thesis worden toegelicht in hoofdstuk II. Het finale doel van dit werk was om het potentieel van CEUS voor de diagnose van CNZ bij de kat te onderzoeken. In het eerste deel van deze thesis werden studies gedaan bij gezonde katten om inzicht te verkrijgen in de techniek en mogelijke factoren die een invloed kunnen hebben op de resultaten. In het tweede deel werd het diagnostisch potentieel van CEUS geëvalueerd bij katten met CNZ en katten met hyperthyroïdie.

Het voorkomen van kwantitatieve verschillen tussen de eerste en tweede injectie van contrast medium werd onderzocht in hoofdstuk III. De perfusieparameters voor de milt en de linker nier

voor de eerste en tweede injectie van SonoVue® werden vergeleken voor 7 gezonde katten. De piekintensiteit en oppervlakte-onder-de-curve waren lager voor de eerste injectie ten opzichte van de tweede. Dit was enkel statistisch significant voor de nierschors en de milt, terwijl er een statistische trend was voor het niermerg. De tijd-intensiteitscurve was vlakker voor de eerste injectie in de nierschors. Het exacte mechanisme achter deze bevinden blijft voorlopig een vraagteken. Er wordt verondersteld dat fagocytose van de 'microbubbles' in het contrast medium door het reticuloendotheliaal systeem een sleutelrol speelt. De bevindingen van deze studie bewijzen dat er significante kwantitatieve verschillen zijn tussen de eerste en tweede injectie van contrast medium. Er wordt daarom geadviseerd om de eerste injectie niet te gebruiken voor verdere analyses.

De herhaalbaarheid van CEUS voor evaluatie van de nierperfusie bij de kat werd bestudeerd in hoofdstuk IV. CEUS van beide nieren werd uitgevoerd bij 12 gezonde katten op 3 tijdstippen met telkens 7 dagen tussenperiode. De variabiliteit werd bestudeerd op 3 niveaus: (1) de variabiliteit binnen eenzelfde kat voor herhaalde metingen op eenzelfde nier, (2) bijkomende variabiliteit wanneer beide nieren in beschouwing genomen werden, (3) bijkomende variabiliteit wanneer observaties van verschillende katten in beschouwing genomen werden. De coëfficiënt van variatie (CV) voor de verschillende perfusie parameters werd eveneens bepaald. De parameters met de laagste variatie en dus hoogste herhaalbaarheid waren tijd-tot-piekintensiteit (CV 5,7%), 'rise time' (CV 13,1%), 'fall time' (CV 19,0%) en de gemiddelde transit tijd ('mean transit time') (CV 24,4%) voor de nierschors. De parameters gerelateerd aan de intensiteit en de helling van de tijds-intensiteitscurve vertoonden een hoge variabiliteit (CV 36,6-56,0%). Voor het niermerg, vertoonden enkel de tijd-tot-piek (CV 19,9%) en 'rise time' (CV 26,3%) een matige coëfficiënt van variatie, terwijl alle andere parameters een hoge coëfficiënt (CV 37,7-83,4%) en dus hoge variabiliteit vertoonden. De bijkomende variabiliteit wanneer beide nieren in beschouwing genomen werden, was laag en zelfs verwaarloosbaar voor de nierschors. Bijkomende variabiliteit door observaties van verschillende katten in rekening te brengen was matig ten opzichte van de hoge variabiliteit binnen eenzelfde kat voor herhaalde metingen. Samenvattend kan er gezegd worden dat de tijd gerelateerde parameters voor de nierschors en, in mindere mate, voor het niermerg een goede tot matige herhaalbaarheid vertonen, terwijl de herhaalbaarheid voor de intensiteit gerelateerde parameters, en de parameters gerelateerd aan de vorm van de tijds-intensiteitscurve laag is. De hoge mate van variabiliteit bemoeilijkt het stellen van een diagnose op basis van CEUS.

In hoofdstuk V werd het effect van sedatie met butorfanol en anesthesie met propofol op de perfusie parameters bestudeerd. Zes gezonde katten werden geïncloseerd in een gerandomiseerde cross-over studie waarin 3 protocollen vergeleken werden: (1) wakker (geen anesthesie of sedatie), (2) sedatie met butorfanol (0,4 mg/kg IM) en (3) anesthesie met propofol (3,5 – 7,7 mg/kg IV bolussen op effect). Er waren geen subjectieve verschillen in het perfusiepatroon tussen de 3 protocollen. Butorfanol veroorzaakte geen significante verschillen in de perfusieparameters, maar het sedatief effect was minimaal. Propofol-anesthesie daarentegen, zorgde voor een significante verlenging van de aankomsttijd ('arrival time') en tijd-tot-piekintensiteit, bovendien was de eerste fase van de tijds-intensiteitscurve minder steil (tragere 'wash-in'). Deze bevindingen wijzen op een tragere bloedsnelheid, meest waarschijnlijk het gevolg van een daling in bloeddruk veroorzaakt door propofol. Deze bloeddrukdaling ontstaat typisch door de combinatie van een gedaald hartminuutvolume en lagere systemische vasculaire weerstand.

Concluderend kunnen we stellen dat propofol een goed anestheticum is voor oudere katten en katten met CNZ, maar er zijn belangrijke kwantitatieve effecten op CEUS van de nieren bij gezonde katten, deze dienen in rekening gebracht te worden. Perfusie parameters bekomen bij wakkere katten kunnen niet vergeleken worden met deze bekomen bij katten die onder anesthesie waren.

In hoofdstuk VI werd de invloed van leeftijd op CEUS van de nieren bij gezonde katten onderzocht. Drieënveertig gezonde katten met een leeftijd tussen 1 en 16,5 jaar werden geïncloseerd en in 4 leeftijdscategorieën onderverdeeld: 1-3 jaar, 3-6 jaar, 6-10 jaar en > 10 jaar. Er waren geen significante verschillen in de perfusieparameters tussen de verschillende leeftijdscategorieën. Er was echter wel een trend tot een lagere piekintensiteit en lagere oppervlakte-onder-de-curve voor het eerste deel van de tijd-intensiteitscurve van de nierschors wanneer de katten tussen 1 en 3 jaar met de katten van meer dan 10 jaar vergeleken werden. Deze bevindingen komen overeen met gegevens bij de mens, waar een progressieve leeftijdgebonden afname in de nierperfusie een goed gekend fenomeen is. Deze studie suggereert voor het eerst een milde daling in bloedvolume voor de nierschors bij oudere katten.

In hoofdstuk VII werd er onderzocht of CEUS in de mogelijkheid was om relatief kleine perfusieveranderingen veroorzaakt door een angiotensine II-infuus, te detecteren. Elf gezonde katten ondergingen CEUS en nierscintigrafie (^{99m}Tc -mercaptoacetyltriglycerine) tijdens infusie van angiotensine II (vasoconstrictie) en 0.9% NaCl (controle). Perfusieveranderingen geïnduceerd door

angiotensine II werden waargenomen in verschillende parameters voor de volledige nier: de piekintensiteit, 'wash-in perfusion index', en 'wash-out rate' daalden significant. Er waren geen significante verschillen tussen controle en angiotensine II-infuus wanneer de nierschors of het niermerg afzonderlijk beschouwd werden. Nierscintigrafie was niet in staat om significant perfusieveranderingen te detecteren. Deze studie toonde aan dat CEUS een zeer veelbelovende techniek is voor de evaluatie van de nierperfusie bij katten, wat verder onderzoek bij patiënten sterk aanmoedigt.

Na de veelbelovende resultaten van de angiotensine-studie, was het volgende doel om de nierperfusie te bestuderen bij hyperthyroïde katten, vóór en na radiojoodbehandeling. Voor de studie in hoofdstuk VIII werden er 42 hyperthyroïde katten geïncubeerd die CEUS ondergingen net voor radiojoodbehandeling en tijdens een controlebezoek 1 maand nadien. Tijd gerelateerde parameters (tijd-tot-piekintensiteit en 'rise time') voor de nierschors en het niermerg waren significant lager vóór behandeling van hyperthyroïdie ten opzichte van het controlebezoek. De 'wash-in rate' (nierschors en medulla) en de 'wash-out rate' (nierschors) waren eveneens hoger vóór de behandeling (steilere tijd-intensiteitscurve). De combinatie van deze bevindingen wijst op een hogere doorbloedingssnelheid ten gevolge van hyperthyroïdie. De gemiddelde transit tijd voor de nierschors was lager vóór behandeling, wat wijst op een kortere verblijfsduur van contrast in de nier. Bovendien was de oppervlakte-onder-de-curve voor de nierschors ook lager vóór de behandeling ten gevolge van de hoger beschreven verandering in vorm van de tijds-intensiteitscurve. Een hogere genormaliseerde piekintensiteit voorafgaand aan de behandeling was een uniek gegeven voor het niermerg, dit suggereert een hoger bloedvolume tijdens de hyperthyroïde status van de kat. De verschillen in CEUS parameters vóór en na de behandeling met radioactief jodium, kunnen toegewezen worden aan een gedaalde systemische en renale vasculaire weerstand tijdens hyperthyroïdie. Hierbij komt nog dat de hogere hartfrequentie bij hyperthyroïde katten het effect of de perfusieparameters van de nier versterkt. Uit deze studie kunnen we afleiden dat CEUS een hogere bloedsnelheid in de nierschors en het niermerg en hoger bloedvolume voor het niermerg aantoont bij katten met hyperthyroïdie, ten opzichte van een controle 1 maand na behandeling.

Tot slot werd in hoofdstuk IX het diagnostisch potentieel van CEUS geëvalueerd bij katten met CNZ (n=14) ten opzichte van gezonde controle katten (n=43). De tijd-tot-piekintensiteit voor de

nierschors was langer en de gemiddelde transit tijd van de nierschors was korter bij katten met CNZ. Voor het niermerg daarentegen was de tijd-tot-piekintensiteit en de 'rise time' korter bij katten met CNZ. Deze bevindingen tonen aan dat de doorbloedingsnelheid van de nierschors daalt bij katten met nierziekte, meest waarschijnlijk veroorzaakt door een hogere vasculaire weerstand in aangetaste nieren. De hogere doorbloedingsnelheid voor het niermerg in deze studie, werd nog niet eerder gerapporteerd. Deze wordt mogelijks veroorzaakt door een niermerg-specifieke respons van de doorbloeding op bepaalde factoren, bovendien is het reeds langer geweten dat het niermerg relatief ongevoelig is aan vasoconstrictie. We kunnen concluderen dat CEUS in staat is om perfusieafwijkingen te detecteren bij katten met CKD: er is een tragere bloedsnelheid in de nierschors, terwijl de bloedsnelheid in het niermerg toeneemt.

Hoofdstuk X omvat de algemene discussie en de conclusies van dit doctoraatsonderzoek. Doorheen de verschillende studies in deze thesis bleek dat CEUS een beloftevolle techniek is voor de evaluatie van de nierperfusie bij katten. De hoge variabiliteit en dus lage reproduceerbaarheid waarmee de techniek momenteel te kampen heeft, leiden echter tot een grote mate van diagnostische onzekerheid wat het gebruik in de praktijk momenteel beperkt. Desondanks deze beperking blijft CEUS een veelbelovende techniek om de microvascularisatie van de nier te beoordelen, bovendien zal de technologische vooruitgang in de toekomst hoogstwaarschijnlijk zorgen voor merkelijke verbeteringen in de herhaalbaarheid.

DANKWOORD

Het einde is in zicht, het is tijd geworden voor het allerlaatste hoofdstuk, waarschijnlijk ook het belangrijkste. Enerzijds is het dé kans om iedereen te bedanken die mij geholpen en gesteund heeft om dit doctoraat tot een goed einde te brengen, anderzijds is het ook het meest gelezen deel van een doctoraat.

In de eerste plaats wil ik mijn promotoren, Prof. Jimmy Saunders en Prof. Katrien Vanderperren, bedanken voor alle kansen die ik gekregen heb. Zonder hen was er geen sprake geweest van dit doctoraat. Jimmy, Katrien, jullie hebben me begeleid van de eerste beursaanvraag tot het printen van dit boekje. Jullie hebben me steeds veel vrijheid gegund, maar op hetzelfde moment hebben jullie me bijgestuurd en afgeremd waar nodig. Gelukkig maar, anders was ik nu waarschijnlijk nog steeds katjes aan het rekruteren. Katrien, bedankt voor alle steun, het luisterende oor en om mij op te peppen als ik het even minder zag zitten. Je hebt mij altijd net dat ene stapje meer laten bereiken. Dankzij jou waren er af en toe interessante nevenprojectjes, waar ik steeds met plezier aan meegewerkt heb. Ik koester ook goede herinneringen aan de congressen in Rotterdam of het congres in Barcelona, waar we de avond steevast afsloten bij de 'Font màgica'.

Mijn volgende woordje van dank richt ik graag tot de leden van de lees- en examencommissie. Bedankt voor alle tijd die jullie in dit werk gestoken hebben, jullie opbouwende commentaar was van onschatbare waarde om het finale werk te verbeteren. Prof. Duchateau, bedankt om de taak van voorzitter op u te nemen en daarmee alles in goede banen te leiden, net zoals u doorheen mijn ganse doctoraat gedaan hebt. U was steeds beschikbaar om een optimaal studiedesign uit te werken, om gegevens statistisch te verwerken, en, het allerlastigste, om mij nadien wegwijs te maken in die statistiek. Bedankt voor al uw geduld, ik hoop alvast dat ik vandaag geen statistische flaters sla. Prof. Paepe, beste Dominique, reeds van voor de start van mijn doctoraat speelde u een belangrijke rol. Het begint allemaal in het laatste jaar van mijn studies, met een masterproef omtrent idiopathische hypercalcemie bij de kat. U ligt aan de basis van mijn interesse in nierziekte bij de kat, tevens heeft u mij aangespoord om mijn eerste artikels te schrijven, het prille begin van dit alles. Toen ik later aan mijn doctoraat begon, stond u steeds klaar met goede raad, bovendien kon ik altijd op u rekenen als ik hulp nodig had met patiëntjes (je bent kampioen in het bloednemen van springerige Ragdolls met kleine bloedvaatjes!). Artikels nalezen (en nog eens nalezen), het was u nooit teveel, uw suggesties en correcties waren steeds zeer waardevol.

Bedankt voor alles! Prof. Vanhove, bedankt om in de examencommissie te willen zetelen. Een eindje geleden, kreeg ik de kans om enkele introductielessen in 'translational biomedical in vivo imaging' van u te volgen. Een boeiende lessenreeks over beeldvorming in al zijn aspecten. U leidt een fantastische onderzoeksgroep, misschien zit er ooit wel eens een samenwerking in? Prof. Bolen, nous nous sommes rencontrées la première fois en Pologne, pendant les conférences EVDI. Nous avons parlé de votre chat, Chaminou, alors hyperthyroïdien. Quelques semaines plus tard, Chaminou, est venue à Merelbeke pour un traitement avec l'iode radioactive et a été incluse dans mon étude. Un grand merci pour votre confiance et un gros câlin pour Chaminou, elle a été formidable. Dr. Smets, Pascale, bedankt om met veel enthousiasme mee te stappen in de studie met de hyperthyroïde katjes. Het was altijd fijn om op maandagochtend bij u langs te komen voor de echocardio's. Uw enthousiasme in cardiologie werkt aanstekelijk, ik kom binnenkort nog wel eens meevolgen. Dr. Broeckx, bedankt voor de gezellige babbels tussendoor, om mij even bij te sturen als ik, zelfs na de uitgebreide uitleg van Prof. Duchateau, toch nog wat meer achtergrond nodig had bij een of andere statistische analyse. Bedankt ook om mij te introduceren in de wondere wereld van de HD screening, ik kijk alvast uit naar meer. Dr. Raes, Els, bedankt om de voorbije jaren zo'n fijne geduldige collega te zijn. Ik kijk naar je op, desondanks je iets wat warrige levensstijl, slaag je er toch maar in om alles te combineren. Die diplomate-titel is meer dan verdiend. Binnenkort kom ik jullie nog af en toe eens vergezellen op paard, ik kan zoveel van je leren. Nu Frits en Nova toch beslist hebben om vriendjes te worden, zullen we elkaar ook tijdens de middag wel eens vergezellen voor een wandelingetje.

Prof. Daminet, uw bijdrage aan dit doctoraat is groot. U heeft geholpen in de uitwerking van de protocollen van de klinische studies en u stond steeds klaar met advies. Bedankt dat ik u steeds mocht lastigvallen voor vragen ivm 'de hyperthyroïdjes'. Uw endocrinologische kennis is onuitputtelijk. Bedankt ook om de artikels steeds met zorg te lezen en altijd opnieuw naar een hoger niveau te tillen.

Hendrik, ook zonder jou was dit doctoraat er niet geweest. Je bent wat op de achtergrond geraakt, ontrecht! Jouw doctoraat was het eerste doctoraat dat ik ooit bijgewoond heb, wat een introductie in 'het universitaire wereldje'! Ik probeer mijn verdediging iets korter te houden (al is het een efficiënte manier om te vragenronde in te korten), maar om aan jouw kennis van microbubbles en contrast-echografie te geraken, zal ik serieus mijn best moeten doen. Je hebt mij de basis van

contrast-echografie bijgebracht, geholpen met het opstellen van protocols, en geleerd hoe je een goede contrast-echografie van een nier doet. Het was altijd aangenaam werken met jou, het filosoferen achteraf niet te vergeten. Onze gans is momenteel aan het broeden, hopelijk zijn er binnenkort kleintjes, dan kunnen we een ruil organiseren (een gansje tegen een kalkoentje?). Als je eens in de buurt van Melden bent, ben je zeker welkom. Dan kan je 'onzen hof' eens inspecteren en tips geven.

'De mensen van de farmacie', Ine en Heleen, ik ben blij dat ik jullie tijdens mijn doctoraat heb mogen ontmoeten. Jullie zijn fantastische madammen. Dankzij jullie heb ik een geheel andere kant van het microbubble onderzoek leren kennen. Bedankt ook om ons te introduceren op het microbubble symposium in Rotterdam. Hopelijk mogen er nog heel wat gemeenschappelijke projecten volgen.

During the last years, the faculty has been my second home. I would like to thank all the colleagues for creating a nice working environment. The colleagues of the medical imaging department, thanks for all your help and patience with me and my patients (the first one is probably the worst). I'm sorry for my impatience in the ultrasound room when I wanted to 'steal' the machine for a contrast-ultrasound while you were very busy running the clinic. Laure, I'm so happy you are staying some more months with us, thanks for teaching me; you make me a better imager. Blandine, Olivia, Tibor, Lise, Mileva, you are a great team of residents, I'm so lucky to be part of that. Good luck with everything in the future. Elke, thank you for guiding and teaching me. I hope you can finalize your own PhD soon. Kim, a small talk with you can cheer up my day. Thanks for listening when I needed someone. The equine department wouldn't be the same without you. I'm looking forward to spent some more time at equine imaging soon. Veerle and Ines, you both left the faculty, nevertheless you kept on supporting me from the UK and Swiss. I've greatly enjoyed working with you; you've thought me so much. We keep in touch and we'll meet again. Many other current and previous colleagues, Caroline, Olga, Eva, Kaatje, Walter, Daisy, Annemie, Aqui, Ingrid, Prof. van Bree, Prof. Dik, Kathelijne, Robrecht, Marnix, Claudine, Sandra, less words, but not less gratitude for you.

The orthopaedics team, Prof. Van Ryssen, Yves, Evelien dB en B, Eva, Tine, Stijn, thanks for being who you are, contributing to a nice working environment. Special thanks (woef!) to Vita, Wilson, Soda and Isa for being friends with my little monster, Fritske.

The team of the small animal department thanks for contributing each in your own way. The internal medicine team, Lisa, Eva, Gonçalo, Femke, Sofie, Annelies, thanks for the nice collaboration in clinics and your professional advice on some of the patients in my study. Eva, a special word for you, thanks for your contribution in the hyperthyroid study. We spent several Sundays together performing GFR's, I think we can say, we are a superb cat-GFR team by now. The cardiology team, Veronique, Dominique, Valérie, Iris, thanks for all the help with the hyperthyroid cats. I have enjoyed attending the echocardiography exams and the small talks in-between; it felt like a nice refreshing break in the Monday morning rush. The people from anaesthesia, you are a top-team, thanks for your help. Prof. de Rooster, Sophie, Eline and Laetitia, I'm so happy our research topics crossed at some point. I have always enjoyed working with you. Several teams of cheerful interns have passed by during my PhD, thanks for assisting me with patients in the weekends. Nausikaa, thanks to **Juno** and Frits we started our (almost) daily walks around the faculty, you have become a friend in that period. Thanks for listening to me, for the small breaks in-between, it makes the working day so much more fun.

De mensen van diervoeding, Prof. Hesta, Veerle Vandendriesche, Amy en Isolde, bedankt voor jullie bijdrage aan de studies met proefkatjes.

Alle katjes, katteneigenaars en doorverwijzende dierenartsen, zonder jullie was dit uiteraard niet mogelijk geweest. Bedankt voor jullie enthousiasme om deel te nemen aan mijn studies. Jullie kunnen niet geloven hoeveel plezier de mailtjes met updates en foto's mij doen.

Gelukkig waren er naast het werk ook **vrienden** om de weekends en avonden op te fleuren. Bedankt voor de leuke intermezzo's, maar even naar mijn werk gerelateerde verzuchtingen te luisteren en het dan moeiteloos over een andere, vrolijke boeg te gooien. Zonder jullie steun was dit niet haalbaar geweest. Ine en Kristof, ik kijk al uit naar onze volgende 'date', bowlen, een etentje, bootje varen of één of andere workshop, zolang we elkaar maar af en toe eens zien. Ik kijk toch wel uit naar het moment dat jullie terug wat dichterbij komen wonen, misschien kunnen we onze squash-avonden dan weer opnemen? Hanne en Wim, bedankt om alle voorbijgegaan bbq'tjes op jullie te nemen, binnenkort nemen wij terug over (beloofd!). Hanne, je wordt nog een echte kippendierenarts. Ken en Astrid, jullie hebben een prachtig gezinnetje. Ik sta er altijd van versteld hoe jullie alles voor elkaar krijgen. Een bezoekje bij jullie is altijd gezellig. Lieze en Gwij, het spijt

me verschrikkelijk dat ik jullie meermaals heb laten zitten met de ingrediënten voor Tajine. Ik beloof dat ik het binnenkort goed maak. **Rebecca**, dinsdag is onze vaste afspraak geworden. Je bent altijd welkom, ook als we binnenkort wat verder wonen. De fantastische bende van **Stal ten Legenbos**, allemaal totaal verschillend maar samen de gezelligste stal van het land. Ik ben altijd blij als ik zie dat er auto's staan als ik 's avonds laat nog langskom: samen poetsen, babbelen tijdens het instappen, ... een uurtje op stal, en ik kan terug alles aan. **Peter en Hilde**, jullie verdienen toch een speciaal woordje van dank om zo goed voor ons mannetje te zorgen. Het is ongelooflijk wat jullie allemaal doen voor de paarden en de baasjes, chapeau!

Als ons huisje binnenkort voorzien is van alle comfort (lees: ramen, deuren, elektriciteit en water), zijn jullie allemaal welkom!

Mama, papa, bedankt om mij alle kansen te geven om te studeren en om me te ondersteunen in alles wat ik doe. **Papa**, op het moment dat ik dit aan het schrijven ben, is het onduidelijk of je er zal kunnen bij zijn vandaag. Hou de moed erin, binnenkort heb je een nieuwe aorta en nieuwe klep, dan zal het ongetwijfeld beter gaan dan ooit tevoren. **Mama**, bedankt om er altijd te zijn voor mij, om mij de kans te geven naar **Admiral** te gaan als ik wil, maar even goed voor hem te zorgen als het te druk is. **Bomma, bompa, oma en opa**, jullie zijn er niet meer, maar ik ben zeker dat jullie trots zouden geweest zijn. Je ziet maar, het heeft geloond om mijn West-Vlaams accent te proberen 'afleren' en mij te stimuleren om flink te studeren, ik ben toch op 'den unif' geraakt.

Mama en papa van Roel, Yves en Daniëlla, jullie zijn mijn 2^{de} ouders geworden. Het is jullie nooit te veel om de was of strijk te doen, of te helpen bij de verbouwingen. **Moeke, Peter, Marleen en Jan, Lore, Janne, Lien en Kris**, bedankt om mij in de familie op te nemen. Ik probeer om in de toekomst wat meer familiefeestjes en etentjes bij de wonen. **Broertje en Tara**, jullie zijn een prachtig koppel. Jullie trouwfeest was het beste ooit, zo wil ik ook wel trouwen... Bedankt voor de leuke babbels. Ik zal het toch wat missen als je binnenkort ietsje verder wonen. Veel succes in alles wat jullie doen, er staat jullie nog zoveel moois te wachten.

Mijn mannen, Admiral, Frits, Florian en Gaudi (om alle verwarring te vermijden: paard, hond en katten respectievelijk), jullie maken alles zoveel mooier. **Admiraltje**, je bent mijn mateke, bedankt om je energie af en toe wat te temperen als ik op je rug zit, het wordt geapprecieerd. Ik probeer binnenkort wat meer tijd voor je te maken. **Fritske**, jouw werkvreugde valt in een aparte categorie, je bent al uitzinnig van blijdschap als de faculteit vanaf het rondpunt in zicht komt. De korte

wandelingetjes zijn vaak een deugdoende verfrissing tussendoor, bovendien heeft het gezorgd dat collega's, vrienden zijn geworden. Florian en Gaudi, voor jullie toch een kleine opmerking: jullie hebben niet willen deelnemen aan mijn studie (foei). Toegegeven, het was het veiligste voor iedereen. Thuis zijn jullie wel , gelukkig, de allerliefste en allerschattigste katjes.

Roel, woorden schieten te kort om jou te bedanken. Je hebt mij altijd gesteund, hoe onhaalbaar mijn plannen ook leken, jij stond altijd achter mij. Je hebt jezelf dikwijls weggecijferd zodat ik mijn dromen kon waarmaken. Zonder jou was dit allemaal niet gelukt. Ik zie je graag! Ik kijk uit naar onze toekomst samen.

Emmelie

CURRICULUM VITAE

Emmelie Stock werd geboren op 23 oktober 1988 te Kortrijk. Na het behalen van het diploma hoger secundair onderwijs, richting wetenschappen-wiskunde aan het Koninklijk Atheneum te Kortrijk, startte ze in 2006 met de studies Diergeneeskunde aan de universiteit Gent. In 2012 behaalde ze het diploma van Master in de diergeneeskunde, afstudeerrichting gezelschapsdieren, met grote onderscheiding.

Aansluitend startte ze een internship bij de dienst medische beeldvorming van de vakgroep Medische beeldvorming van de huisdieren en Orthopedie van de kleine huisdieren, faculteit diergeneeskunde van de universiteit Gent. Geboeid door de mogelijkheden die het wetenschappelijk onderzoek kan bieden voor de kliniek, startte ze in 2013 een doctoraatsstudie naar contrast-echografie voor de evaluatie van de nierperfusie bij katten. Dit onderzoek werd gefinancierd door het Bijzonder Onderzoeksfonds van de universiteit Gent. Tevens vervulde ze het trainingsprogramma van de Doctoral School of Life Science and Medicine van de Universiteit Gent.

Emmelie Stock is auteur en medeauteur van verschillende wetenschappelijke publicaties en nam actief deel aan verschillende nationale en internationale congressen.

BIBLIOGRAPHY

Publications in peer-reviewed scientific journals

Stock E., Paepe D., Daminet S., Duchateau L., Saunders J.H.*, Vanderperren K.* Influence of ageing on quantitative contrast-enhanced ultrasound of the kidneys in healthy cats. *Veterinary Record*, *under revision*. [* shared senior authorship]

Stock E., Daminet S., Paepe D., Buresova E., Vandermeulen E., Smets P., Duchateau L., Saunders J.H.*, Vanderperren K.* Evaluation of renal perfusion in hyperthyroid cats before and after radioiodine treatment. *Journal of Veterinary Internal Medicine*, *under revision*. [* shared senior authorship]

Stock E., Paepe D., Daminet S., Vandermeulen E., Duchateau L., Saunders J.H.*, Vanderperren K.* Contrast-enhanced ultrasound for the assessment of renal perfusion in cats with chronic kidney disease. *Journal of Veterinary Internal Medicine*, *under revision*. [* shared senior authorship]

Stock E., Duchateau L., Volckaert V., Polis I., Saunders J.H.*, Vanderperren K.* Repeatability of contrast-enhanced ultrasonography of the kidneys in healthy cats. *Ultrasound in Medicine and Biology*, *under revision*. [* shared senior authorship]

Broeckx B.J.G., Vezzoni A., Bogaerts E., Bertal M., **Stock E.**, Deforce D., Peelman L., Saunders J.H. Comparison of three methods to quantify laxity in the canine hip joint. *Veterinary Comparative Orthopaedics and Traumatology*, *under revision*.

Van Hoof K.J.M., Van der Vekens E., Samoy Y., de Bakker E., **Stock E.** Fysaire dysplasia van de femurkop bij een jonge Golden Retriever. *Vlaams diergeneeskundig tijdschrift* 2017; 86: 35-39.

Vanderperren K., **Stock E.**, Pardon B., Saunders J. Contrast-enhanced ultrasound in sheep. *Small Ruminant Research* 2017. *In press*

Stock E., Vanderperren K., Haers H., Duchateau L., Hesta M., Saunders J. Quantitative differences between the first and second injection of contrast agent in contrast-enhanced ultrasonography of feline kidneys and spleen. *Ultrasound in Medicine and Biology* 2017; 43: 500-504.

Ciccelero L, Denies S, Vanderperren K, **Stock E.**, Van Brantegem L, de Rooster H, Sanders N. Immunological, anti-angiogenic and clinical effects of intratumoral interleukin 12 electrogene therapy combined with metronomic cyclophosphamide in dogs with spontaneous cancer: a pilot study. *Cancer Letters* 2016; S0304-3835: 1-14.

Rossi F.*, Fina C.*, **Stock E.**, Vanderperren K, Duchateau L, Saunders J.H. Effect of sedation on contrast-enhanced ultrasonography of the spleen in healthy dogs. *Veterinary Radiology and Ultrasound* 2016; 57: 276-81. (*Contributed equally)

Ciccelero L, Denies S, Haers H, Vanderperren K, **Stock E.**, Van Brantegem L, de Rooster H.*, Sanders N.N*. Intratumoral interleukin 12-gene therapy stimulates the immune system and decreases angiogenesis in dogs with spontaneous cancer. *Veterinary and Comparative Oncology* 2016.

Stammeleer L, de Bakker E., **Stock E.**, Dehuysser V., Gielen I., Van Ryssen B. Flexor tenosynovitis bij een Italiaanse Cane Corso: diagnostische bevindingen en resultaat na behandeling. *Vlaams diergeneeskundig tijdschrift* 2016; 85: 215-20.

Stock E., Vanderperren K, Bosmans T, Dobbeleir A, Hesta M, Lybaert L, Peremans K, Vandermeulen E, Saunders J. Evaluation of feline renal perfusion with contrast-enhanced ultrasonography and scintigraphy. *Plos One* 2016; 11: e0164488.

Dewitte H, Vanderperren K, Haers H, **Stock E.**, Duchateau L, Hesta M, Saunders JH, De Smedt SC, Lentacker I. Theranostic mRNA-loaded Microbubbles in the Lymphatics of Dogs: Implications for Drug Delivery. *Theranostics* 2015; 5: 97-109.

Abma E., Kitshoff A., Vandenabeele S., Bosmans T., **Stock E.**, de Rooster H. Treatment of necrotizing fasciitis using negative wound therapy in a puppy. *Vlaams diergeneeskundig tijdschrift* 2015; 84: 147-153.

Stock E., Vanderperren K., Van der Vekens E., Haers H., Duchateau L., Polis I., Hesta M., Saunders J.H. The effect of anaesthesia with propofol and sedation with butorphanol on quantitative contrast-enhanced ultrasonography of the healthy feline kidney. *Veterinary Journal* 2014; 202: 637-639.

Vanderperren, K., Haers, H., Van der Vekens, E., **Stock, E.**, Paepe, D., Daminet, S., Saunders, J.H. Description of the use of contrast-enhanced ultrasonography in 4 dogs with pancreatic tumors. *Journal of Small Animal Practice* 2014; 55: 164–169.

Combes A., **Stock E.**, Van der Vekens E., Duchateau L., Van Ryssen B., Saunders J. Ultrasonographical examination of feline adrenal glands: intra- and inter-observer variability. *Journal of Feline Medicine and Surgery* 2014; 16: 937-42.

Raes E., Bergman E., Vanderperren K., **Stock E.**, Van Ryssen B., Saunders J. Computed tomographic features of lesions detected in horses with tarsal lameness. *Equine Veterinary Journal* 2014; 46: 189-93.

Stock E., Paepe D., Daminet S. Clinical approach of feline hypercalcemia. *Vlaams diergeneeskundig tijdschrift* 2013; 82: 3-10.

Stock E., Paepe D., Verhaert L., Van de Maele I., Daminet S. Casereport – Idiopathic hypercalcemia in a Persian cat. *Vlaams diergeneeskundig tijdschrift* 2013; 82: 11-16.

Abma E., Vandenabeele S., Campos M., Bosmans T., **Stock E.**, de Rooster H. Necrotizing fasciitis: a case report in a dog. *Vlaams diergeneeskundig tijdschrift* 2013; 82: 134-42.

Research communications/abstracts presented during scientific meetings

Stock E., Daminet S., Vanderperren K., Paepe D., Saunders J.H. Contrast-echografie voor de diagnose van diffuse nieraandoeningen bij de kat. SAVAB najaarsmeeting: work in progress, 10 december, 2016, Gijzenzele (Belgium). Oral presentation.

Stock E., Vanderperren K., Bosmans T., Duchateau L., Hesta M., Lybaert L., Vandermeulen E., Saunders J. Evaluation of feline renal perfusion using contrast-enhanced ultrasound and scintigraphy. ECVDI Annual congress, August 31 – September 3, 2016, Wroclaw (Poland). Oral presentation.

Vanderperren K., **Stock E.**, Van der Vekens E., de Rooster H., Duchateau L., Saunders J. Contrast-enhanced ultrasound of normal canine mammary glands during the estrus cycle. ECVDI Annual congress, August 31 – September 3, 2016, Wroclaw (Poland). Oral presentation.

Dewitte H., Van Lint S., Vanderperren K., **Stock E.**, De Smedt S.C., Breckpot K., Lentacker I. Microbubbles as magic bullets in cancer immunotherapy. LKI Symposium “Tumor Immunology & Immunotherapy: harnessing the immune system to fight cancer”, September 12-14, 2016, Leuven (Belgium). Poster presentation.

Stock E., Vanderperren K., Haers H., Duchateau L., Hesta M., Saunders J. Quantitative differences are present between the first and second injection of contrast agent in contrast-enhanced ultrasonography of feline kidneys. Ultrasound contrast imaging symposium, January 21-22, 2016, Rotterdam (the Netherlands). Oral poster presentation.

Cicchelero L., Vanderperren K., Denies S., **Stock E.**, Haers H., Van Brantegem L., de Rooster H., Sanders N. Contrast-enhanced ultrasound imaging of the anti-angiogenic effects of interleukin-12 in pet dogs with spontaneous malignant tumors. Ultrasound contrast imaging symposium, January 21-22, 2016, Rotterdam (the Netherlands). Oral presentation.

Stock E., Vanderperren K., Van der Vekens E., Haers H., Duchateau L., Polis I., Hesta M., Saunders J. Assessment of the influence of propofol and butorphanol on contrast-enhanced ultrasonography of the feline kidney. Ultrasound contrast imaging symposium, January 22-23, 2015, Rotterdam (the Netherlands). Oral presentation.

Stock E., Vanderperren K., Van der Vekens E., Haers H., Duchateau L., Polis I., Hesta M., Saunders J. Assessment of the influence of propofol and butorphanol on contrast-enhanced ultrasonography of

the feline kidney. Southern European Veterinary Conference, October 16-18, 2014, Barcelona (Spain).
Poster presentation.

Stock E., Vanderperren K., Moeremans I., Van der Vekens E., de Rooster H., Hermans K., Saunders J.
Use of contrast-enhanced ultrasonography in the diagnosis of liver lobe torsion in a rabbit: case
report. Southern European Veterinary Conference, October 16-18, 2014, Barcelona (Spain). Poster
presentation.

Fina C., Rossi F., **Stock E.**, Vanderperren K., Duchateau L., Saunders J. Effect of sedation on contrast-
enhanced ultrasonography of the spleen in healthy dogs. ECVDI Annual congress, August 27-30,
2014, Utrecht (the Netherlands). Oral presentation.

Stock E., Vanderperren K., Van der Vekens E., Haers H., Duchateau L., Polis I., Hesta M., Saunders. The
effect of anesthesia and sedation on contrast-enhanced ultrasound of the feline kidney. European
Veterinary Conference: Voorjaardsdagen, April 17-19, 2014, Amsterdam (the Netherlands). Oral
presentation. *Awarded with the 2nd prize in the Boehringer research award.*

Vanderperren K., Cool S., Haers H., **Stock E.**, Fina C., Sanders N., Saunders J. The use of unloaded
self-made microbubbles for contrast-enhanced ultrasound imaging in dogs: potential for image-
guided drug delivery in vivo. Annual scientific meeting of the British Medical Ultrasound Society,
December 9-11, 2013, Gateshead (United Kingdom). Poster presentation.

Stock E., Quist-Rybachuk G., Paes G., Hesta M. Treatment of canine acute renal failure with omega-
3 fatty acids and fermentable fiber supplementation of commercial adult diet. AAVN Clinical
Nutrition and Research Annual Symposium, May 30, 2012, New Orleans (United States of America).
Abstract. *Awarded with the 1st prize in the AAVN case writing contest.*

